HIGHWAY RESEARCH RECORD

Number 291

Design, Evaluation, and Performance of Pavement Systems

19 Reports

Subject Area

25 Pavement Design
26 Pavement Performance

HIGHWAY RESEARCH BOARD
DIVISION OF ENGINEERING NATIONAL RESEARCH COUNCIL
NATIONAL ACADEMY OF SCIENCES—NATIONAL ACADEMY OF ENGINEERING

Washington, D. C., 1969 Publication 1669

Price: $6.00

Available from

Highway Research Board
National Academy of Sciences
2101 Constitution Avenue
Washington, D.C. 20418

Department of Design

W. B. Drake, Chairman
Kentucky Department of Highways, Lexington

HIGHWAY RESEARCH BOARD STAFF

L. F. Spaine

PAVEMENT DIVISION

Milton E. Harr, Chairman
Purdue University, Lafayette, Indiana

COMMITTEE ON RIGID PAVEMENT DESIGN
(As of December 31, 1968)

F. H. Scrivner, Chairman
Texas Transportation Institute
Texas A & M University, College Station

W. Ronald, Hudson, Secretary
University of Texas, Austin

Henry Aaron
Phillip P. Brown
John E. Burke
B. E. Colley
E. A. Finney
Phil Fordyce
W. S. Housel
F. N. Hveem
W. H. Jacobs
Wallace J. Liddle
Franklin B. McCullough
Phillip L. Melville
Thomas J. Pasko, Jr.
Ernest T. Perkins
Thomas B. Pringle
Emery L. Shaw
M. D. Shelby
W. T. Spencer
William Van Breemen
K. B. Woods

COMMITTEE ON FLEXIBLE PAVEMENT DESIGN
(As of December 31, 1968)

Stuart Williams, Chairman
Bureau of Public Roads, Washington, D. C.

A. C. Benkelman
John A. Bishop
W. H. Campen
Bonner S. Coffman
Robert A. Crawford
James M. Desmond
W. B. Drake
Charles R. Foster
John M. Griffith
Frank B. Hennion
Raymond C. Herner
W. S. Housel
Wallace J. Liddle
R. E. Livingston
Alfred W. Maner
Chester McDowell
C. E. Minor
Carl L. Monismith
Frank P. Nichols, Jr.
R. L. Peyton
E. Guy Robbins
Donald R. Schwartz
Emery L. Shaw
George B. Sherman
Eugene L. Skok, Jr.
John H. Swanberg
B. A. Vallerga

COMMITTEE ON COMPOSITE PAVEMENT DESIGN

(As of December 31, 1968)

James H. Havens, Chairman
Kentucky Department of Highways, Lexington

Edward L. Kawala, Secretary
Portland Cement Association, Skokie, Illinois

Ernest J. Barenberg
Richard D. Barksdale
Karl H. Dunn
R. Ian Kingham
R. E. Livingston
Thomas B. Pringle
George W. Ring, III
Robert L. Schiffman
Donald R. Schwartz
F. H. Scrivner
Russell N. Sharpe
John H. Swanberg
William Van Breemen
Eldon J. Yoder
Ernest Zube

COMMITTEE ON SURFACE PROPERTIES-VEHICLE INTERACTION

(As of December 31, 1968)

David C. Mahone, Chairman
Virginia Highway Research Council, Charlottesville

M. D. Armstrong
Glenn G. Balmer
Joseph E. Bell
A. D. Brickman
W. F. R. Briscoe
John E. Burke
William C. Burnett
A. Y. Casanova, III
John H. Cox
Blaine R. Englund
E. A. Finney
William Gartner, Jr.
Douglas I. Hanson
B. G. Hutchinson
Robert N. Janeway
B. Franklin McCullough
Robert B. McGough
W. E. Meyer
A. B. Moore
Desmond F. Moore
Ralph A. Moyer
F. William Petring
Bayard E. Quinn
John J. Quinn
F. A. Renninger
Rolands L. Rizenbergs
Hollis B. Rushing
Richard K. Shaffer
Elson B. Spangler
Sam Spinner
W. E. Teske
E. A. Whitehurst
Ross G. Wilcox
Dillard D. Woodson

COMMITTEE ON THEORY OF PAVEMENT DESIGN

(As of December 31, 1968)

Aleksandar S. Vesic, Chairman
Duke University, Durham, North Carolina

W. F. Abercrombie
Richard G. Ahlvin
Ernest J. Barenberg
Richard D. Barksdale
Eugene Y. Huang
W. Ronald Hudson
William J. Kenis, Sr.
Carl L. Monismith
Thomas D. Moreland
R. G. Packard
William H. Perloff
Robert L. Schiffman
G. Y. Sebastyan
James F. Shook
Ernest B. Wilkins
Nai C. Yang

Foreword

In the entire realm of highway design, probably no other area has received so much attention as has the structural design of pavements systems, and probably in no other area have acceptable solutions been so elusive. This can be attributed to numerous factors, including the wide variety of materials used and the criticality of their mechanical properties, extreme and varying environmental conditions, difficulty with quality control of on-site production, variability of magnitude and application of loads, inadequacy in projecting traffic and predicting cumulative damage, economic aspects, and inability to devise theory to adequately analyze the structural system. This RECORD contains 19 papers devoted to several of these subjects. They have been included in a single volume to emphasize the fragmented yet significant approach to the design of acceptable pavement systems.

General grouping of papers has been attempted, the first of which deals with continuously reinforced concrete pavements. The need to upgrade existing rigid pavements is recognized by McCullough and Boedecker in their development of an acceptable model for designing continuously reinforced concrete overlays. The model is derived using linear elastic theory and is validated by comparing derived values of mechanical stress, strain, and deflection with corresponding values from the Westergaard interior equation and field measurements. Performance of field test sections are reported by Dougan of Connecticut and Treybig of Texas. The former documents a four-year history of the performance of an experimental reinforced concrete pavement that was self-stressed by use of expansive cement, while the latter provides an evaluation of continuously reinforced concrete pavement test sections in terms of steel strain, deflection, crack pattern, pumping, and traffic. Finally, Persson and Friberg show that substantial savings in steel quantities are possible in continuously reinforced concrete pavements designed with elastic joints. Continuity of the pavement system can be assured across joints by transferring the low-temperature joint movements to elastic deformation in short unbonded segments of the continuous steel.

Composite pavement performance is treated in a single paper by Zube, Gates, Shirley, and Munday. The paper contains performance evaluation and ratings of 175 pavements constructed in California between 1950 and 1962.

A second major grouping of papers encompasses various aspects of flexible pavement design and performance. Kersten and Skok's investigation covers the evaluation of 50 test sections in Minnesota that were designed using AASHO concepts. A second paper by Skok used traffic data from each of the 50 sections to develop a method for calculating the 20-year summation of equivalent 18,000-lb axle loads represented by the present Minnesota categories. These studies led to suggestions for modification of Minnesota flexible pavement design procedures. Vaswani presents two design methods for flexible pavements in Virginia. These are based on the performance of 54 satellite projects, analysis of 74 newly recommended projects, and a comparison of the two methods with present designs. A study by Southgate and Deen resulted in the development of a method of estimating the temperature distribution within flexible pavements that can be used to analyze deflection data at any time if the hour of day and surface temperature are included in the recorded data. The final contribution to this group of papers is a report by Moore, Scrivner, Poehl, and Phillips on a method of detecting seasonal change in load-carrying capabilities of flexible pavements by use of the Dynaflect instrument. Warrants for establishing seasonal load limits are suggested.

Two papers relating to determination of equivalent axle loads for pavement design are included. Deacon and Deen report on the development of a relatively

simple and accurate methodology for determining equivalent axle loads for design of pavements for rural highways in Kentucky. Huang uses the elastic-layered theory to develop a method for determining equivalent single-wheel loads for multiple wheels.

Another logical grouping of papers includes those relating to new theories and concepts. Vesic and Saxena present a critical review of existing theories of structural behavior of rigid pavements and study the behavior of the rigid pavements of the AASHO Road Test. A simple expression is presented relating the ultimate number of axle load applications to flexural strength of pavement material, thickness of pavement slab, and the magnitude of axle load. Kasianchuk and Monismith present a working model for a subsystem to consider the fatigue mode of stress for asphalt concrete pavements. The subsystem can be extended to consider loading conditions and material characteristics for which experience is not now available. The object of the Lemer and Moavenzadeh paper is to provide a more rational pavement design base to promote technological growth and innovation. It discusses general engineering design in terms of goal formulation, search, and selection and relates the pavement design process to this logical framework. Lewis and Harr present a theory whereby stresses and deflections can be calculated for a series of rectangular slabs lying on a viscoelastic foundation and subjected to a moving load. Stresses and deflections are caused by weight of slab, moving concentrated load, and linear temperature (or moisture) variations that cause sufficient warping so that the slab is only partially supported by its foundation. Niu and Pickett consider a cracked Westergaard pavement supported on a Winkler foundation and subjected to a normal load applied near the crack. Their study shows that increasing efficiency of moment and shear transfer across a crack reduces maximum deflection and moments in pavements due to applied loads.

The final two papers report on the use of pavement roughness instruments. The purpose of the report by Holbrook is to show the relationship between rapid travel profile parameters, roughometer values, and subjective response. Phillips and Swift use statistical methods to evaluate and rank the CHLOE profilometer, BPR roughometer, PCA roadmeter, and Mays Road Meter.

Contents

Use of Linear-Elastic Layered Theory for the Design of CRCP Overlays

B. F. McCULLOUGH, University of Texas; and
K. J. BOEDECKER, United States Steel Corporation

The design of overlay pavements for upgrading existing pavements, especially rigid pavements, has presented a formidable task for engineers in the past due to the lack of a rational design procedure. This paper justifies the use of linear-elastic layered theory for the design of continuously reinforced concrete pavements (CRCP) overlays of existing pavements. The background rationale for selecting layered theory instead of conventional concrete pavement design procedures from plate theory is presented. A comparison is made of the mechanical state of stress, strain, and deflection derived from layered theory and the Westergaard interior equation with field measurements of pavement deflection and strain. This comparison indicates that layered theory is an acceptable model for the design of CRCP overlays. Techniques such as increasing the subgrade stiffness with depth beneath a pavement structure are presented for developing a reasonable correlation between predicted and measured deflection. Layered theory is applied to the design of a CRCP overlay of an existing jointed concrete airport pavement for a series of jumbo jets. Also discussed are the effects on design of an intermediate asphalt concrete stress-relieving layer between concrete pavements.

•THE DESIGN of overlays for existing pavements, especially rigid pavements, has presented a formidable task for engineers in the past due to the lack of a rational design procedure. In recent years, continuously reinforced concrete pavements have been used to overlay existing highway and airport pavements, but the thickness design for these projects has largely been based on engineering judgment.

The purpose of this paper is to select a mathematical model and to develop techniques that may be used for rationally designing continuously reinforced concrete overlays to upgrade existing pavement structures.

The mathematical models considered are restricted to those satisfying the following conditions: (a) the mathematical models presently exist, and (b) the loading conditions are static. The reason for the first condition is apparent in the context of this study because its purpose is to place overlay design on a more rational basis than that of most current procedures. The nature of the first condition, in part, limits the mathematical model to static conditions because the development of models for dynamic loading is in the early stages. Only limited data, such as those developed by Lee (1) and at the AASHO Road Test (2), are available as to the nature of dynamic loading for vehicles.

REVIEW OF AVAILABLE THEORIES

Mathematical models used in the highway field to predict the state of stress in a multilayered pavement structure fall into two basic categories: plate theory and layered theory.

Paper sponsored by Committee on Rigid Pavement Design and presented at the 48th Annual Meeting.

Figure 1 shows the features of plate theory—a plate of finite thickness resting on a semi-infinite half-space of another material. Stresses may be computed for the various positions of load placement shown, e.g., edge, corner, interior, and joint. Some of the models will even allow varying conditions of support, such as a void beneath the slab (3). The theory will give considerable information pertaining to the state of stress in the plate, but none pertaining to the supporting media.

In most applications of the layered theory, a uniform circular load is applied to a half-space of infinite dimensions in a horizontal direction and to several layers of finite thickness and one of infinite depth in the vertical direction. The state of stress may then be predicted at any point in the half-space. Any one mathematical model within each of the categories may give the most appropriate solution, depending on the type of information sought.

Plate Theory

The existing plate theory solutions assume that the supporting foundation material is either a dense liquid or a linear-elastic half-space. Most of the solutions used in the highway field are based on the dense-liquid assumption. Boundary-value problems have been solved assuming that the supporting material is a linear-elastic material, but these solutions have not been fully developed and utilized.

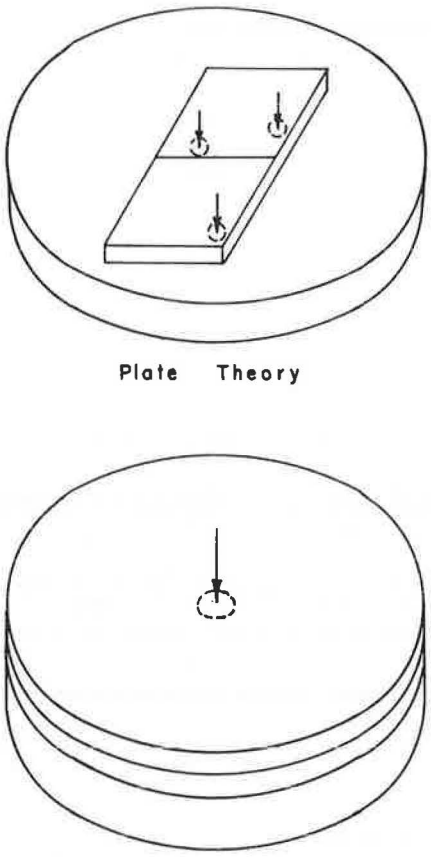

Figure 1. Conceptual diagram for comparing and contrasting plate and layered theory.

Dense-Liquid Foundation—The primary implications of using a dense liquid or Winkler-Zimmerman's assumption are shown in Figure 2. First, there are no shear stresses in the foundation material; therefore, a force applied over an area develops an equal and opposite force that is equal to the deflection times a modulus of reaction value (generally defined as k). This assumption implies that, if a block were pushed into the foundation, the deflection pattern would take a rectangular shape rather than a more realistic basin shape. Of course, when the concrete slab is placed on the simulated soil, the computed shape is a basin; Figure 2 illustrates the nature of the assumption. A popular physical interpretation of this model, shown in Figure 3, indicates that the foundation acts as a bed of springs or as a dense liquid with a density equal to k times the deflection of a given load.

The most widely known and generally accepted plate theory development, using a dense-liquid foundation, is Westergaard's work in 1926 (4). Westergaard presented solutions for the following three conditions of load placement: (a) the corner of a large rectangular plate, (b) the slab edge at a considerable distance from the corner, and (c) the interior area away from the edge. Kelley (5) and Spangler (6) later revised the corner formula on the basis of field measurements to provide for curling stresses and load transfer at the joint.

Pickett (7) noted that the equations for corner stress developed by previous investigators had poor boundary conditions, giving zero stress with certain load radii and pavement properties. Using mathematical techniques, Pickett developed a formula that had the shape and characteristics of Westergaard's corner equations, but with a more rational boundary condition. The Pickett

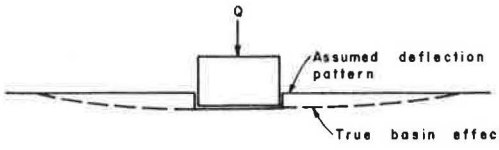

Figure 2. Implications of using a dense-liquid assumption for the foundation material.

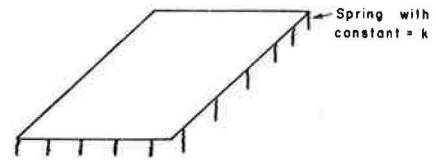

Figure 3. Generally accepted physical interpretation of the dense-liquid foundation.

equation also provides for varying degrees of load transfer between slabs, as does the Spangler equation.

All of these equations produce closed-form solutions, and they can be solved for a given set of conditions. For this reason they have been applied widely because of the relative ease of solution. Recently, Hudson (3) developed an open-form solution of a plate problem on a dense-liquid subgrade that provides special capabilities not available with the previous equations. This solution has the advantage of being able to handle the special problems of nonuniform support, special loadings, and discontinuities such as cracks.

Linear-Elastic Foundation—The use of a linear-elastic foundation with plate theory has not been extensive in the highway and airport field, possibly because of the momentum previously developed by the dense-liquid approach. The use of an elastic foundation is probably a more realistic assumption and would permit laboratory measurements of elastic properties, i.e., modulus of elasticity and Poisson's ratio, rather than the more difficult and impractical measurement of modulus of subgrade reaction required with the dense-liquid approach. The complex mathematics required with these solutions have tended to impede their use.

Layered Theory

The boundary-value problems for layered theory have been solved through the use of both conventional numerical techniques and finite-element techniques. The full development of the solutions was not feasible until the computer age. Before then, the solution of the problem was impractical for any pavement with two or more layers. In contrast to plate theory, layered theory permits the complete state of stress to be determined at any point in the pavement structure.

Burmister (8) laid much of the groundwork for solution of elastic layers on a semi-infinite elastic subgrade. He first solved the boundary-value problem for two layers, assuming a continuous interface, and conceptually established the solutions for three-layered problems. The assumption of full continuity implies that there is no slippage between the layers; hence, the strain in the bottom of one layer is equal to the strain in the top of the next layer, but the stress levels in the two layers will differ as a function of the modulus of elasticity for each layer.

Hank and Scrivner (9), Peattie and Jones (10), and others extended Burmister's solution to three-layered pavements and also solved for the complete stress and strain in the pavement structure. In addition, Hank and Scrivner presented solutions for full continuity and zero continuity between layers. Their solutions indicate that the stresses in layer one for the frictionless case (zero continuity) are larger than the stresses predicted for full continuity. The increase in stress between the two continuity conditions depends on the dimensions and material properties of the layer. In general, the error increases as the ratio of the stiffness of the lower layer to the stiffness of the upper layer increases.

From the Hank and Scrivner data, it may be concluded that where there is a large relative difference in stiffness between the layers, the question as to full, zero, or intermediate continuity is partially nullified because the error of assuming full continuity is small. As the material properties of the two layers become equal, the continuity condition becomes more important. In an actual pavement, the layers are very likely to

develop full continuity; hence, the assumption of full continuity between layers is probably a realistic one.

Recently the Chevron Research Corporation (11) and the Shell Oil Company (12) developed multilayered pavement programs that permit the determination of the complete state of stress and strain at any point in a pavement structure. The modulus of elasticity, Poisson's ratio, and thickness of each layer are treated as variables. Furthermore, the effect of multiple loads may be taken into account.

The use of layered theory will allow the development of design curves for subbase layers as well as normal design curves for concrete layers. Curves derived in this manner will provide design compatibility among layers. Hence, design manuals may be developed for the pavement and subbase that allow the designer to select adequate thicknesses based on the material properties of each layer.

THEORY SELECTION

The use of plate theory has an initial advantage with concrete pavements because it has been associated with this pavement type for approximately 40 years. Its use for overlay design, however, is eliminated in favor of layered theory for the following reasons:

1. Only the state of stress in the surface layer of the pavement structure can be predicted; therefore, the subsurface layers cannot be rationally designed without applying empirical procedures.
2. The complete state of stress cannot be predicted because the vertical stress is assumed to be zero with plate theory. The vertical stresses and strains in the subgrade may be an important factor in design; hence, a prediction is required.
3. Layered theory will permit the use of elastic constants that can be measured in the laboratory. Although the subgrade materials are not linear-elastic in a puristic sense, they may be characterized by using tests such as the resilient modulus, which simulates dynamic loading conditions and has given good correlation with field measurements (13). A valid criticism of plate theory is that the k value cannot be measured in the laboratory; hence, elaborate field tests are required. Rather than resort to impractical techniques, most agencies either assume a k value or correlate with their standard soil tests (14, 15, 16).

Although a departure from the conventional approach, the use of layered theory with concrete pavements is felt to be sound, and its possibilities were recognized as early as 1948 by Hank and Scrivner (9). It is felt that the layered theory offers the greatest flexibility and possibility for developing an overlay design procedure for existing rigid and flexible pavements. The theory is especially applicable to continuously reinforced concrete pavements because the commonly accepted interior loading condition is similar to the axisymmetric loading condition of layered theory. This choice will also allow one theory to be used, thereby avoiding the presently accepted schism, which has evolved over the years, of using two different mathematical models for rigid and flexible pavements.

VERIFICATION OF EXISTING THEORY

It was considered necessary to compare solutions of typical pavement-structure problems obtained from using conventional layered theory with solutions obtained from using the Westergaard equation, because the Westergaard equation, with subsequent modifications, has been used with confidence in concrete pavement design for approximately 40 years. If a favorable comparison were established, it would provide an initial confidence in the design of overlays developed from layered theory. The Westergaard interior equation was selected for comparison because its boundary conditions are very similar to the axisymmetric boundary condition of layered theory and its use in the design of CRCP is established (17, 18).

The applicability of layered theory is checked by comparing the stresses in concrete pavement at the interface of the pavement and subbase layers directly beneath the wheel load (Fig. 4). This is the only permissible point of comparison because stresses at

other depths in concrete pavement cannot be predicted with the Westergaard formula. The deflection comparison is at the surface of the concrete layer directly beneath the wheel load.

One problem in comparing Westergaard's formula and layered theory mathematical models is how to assign to subbase and subgrade materials elastic constants that are representative of the k values used with the Westergaard analysis. For the comparisons, k values were obtained from deflections predicted by loading various layered systems with a 10-psi load on a 30-in. diameter plate (Fig. 4). The pressure and plate dimensions are those recommended by several agencies performing the test (19, 20). Figure 5 shows the relationship between k value and subgrade modulus of elasticity derived from these computations. It is realized that k values from field tests vary with the rate of loading, plate dimensions, and pressure (21), but these variations are not a factor when comparing theories. The k values obtained by this procedure are equivalent to those that would be obtained with flexible-plate measurements. To convert to rigid-plate k values, the flexible-plate values have to be increased by approximately 27 percent (13). All comparisons are made on the basis of flexible-plate k values; if rigid-plate k values were used, the stresses obtained by the Westergaard interior equation would be less than those shown.

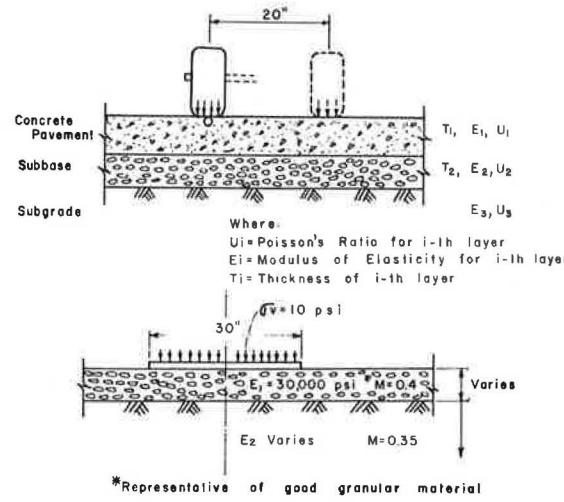

Figure 4. Method of determining k value using a two-layered analysis and points in pavement structure where deflection and stress predicted from layered theory and Westergaard's Interior Equation are compared.

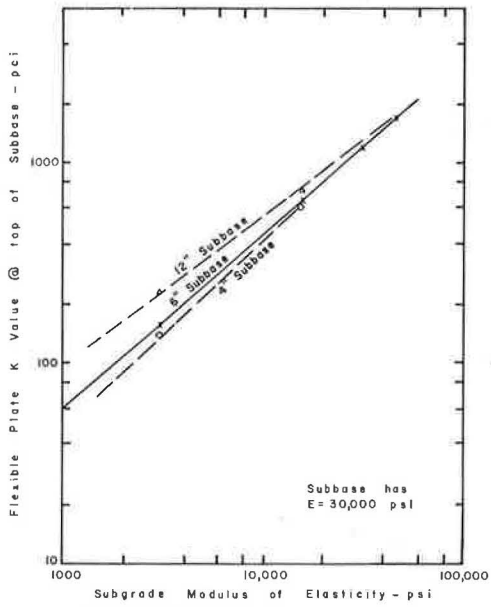

Figure 5. Relationship between subgrade modulus of elasticity and the flexible-plate k value derived by layered theory.

Comparison of Predicted Stress

Figures 6 and 7 compare pavement stresses at the pavement-subbase interface for varying wheel loads, subgrade modulus, and pavement thickness for single and dual wheel loads. Figure 8 shows the same types of data as Figure 6, except that the modulus of the concrete pavement is 1,000,000 psi rather than 4,000,000 psi. All stresses in this comparison are tensile because the lower face of concrete pavement is always in tension in the immediate area of the wheel load.

Subgrade Modulus—For both single and dual wheels, the line equating layered theory and Westergaard stresses varies with the subgrade modulus. As the subgrade modulus increases, the relationship between the two approaches the line of equality, i. e., a slope of 45 deg. When the subgrade modulus is approximately equal to 30,000 psi, the stresses estimated by the two methods are equal.

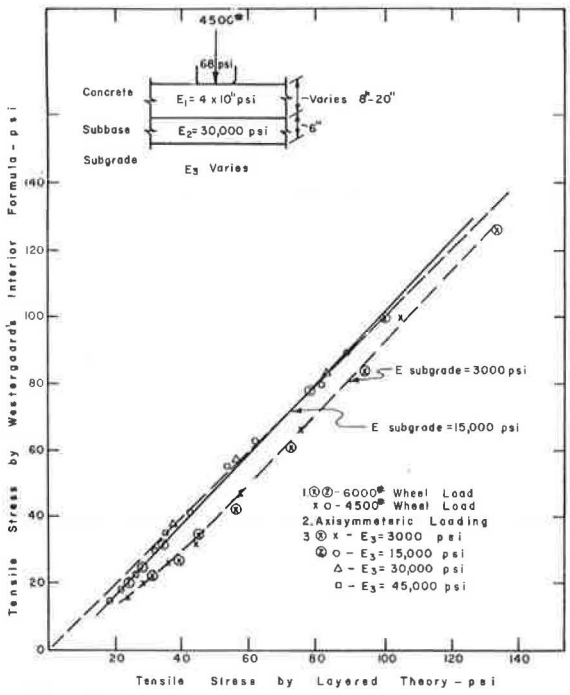

Figure 6. Comparison of pavement stresses at the pavement-subbase interface computed by Westergaard and layered theory for varying wheel load, subgrade modulus, and pavement thicknesses—single wheel load.

Wheel Load—The stresses for two different wheel loads (4,500 lb and 6,000 lb in Fig. 6) fall along the same line of equality for a given value of subgrade modulus. The observation indicates that the stresses for different wheel loads vary in a linear fashion, as would be expected from examining mathematical models for Westergaard and layered theory.

Concrete Modulus of Elasticity—Figure 8 shows that the Westergaard and layered theory stresses vary less with the subgrade modulus when the concrete modulus of elasticity equals 1,000,000 psi than when it equals 4,000,000 (Fig. 6). These stresses predicted by the two mathematical models approach equality for the lower range of modulus of elasticity used in concrete pavements.

Comparison of Predicted Deflection

Figure 9 compares pavement-surface deflection on the line of axisymmetry for varying wheel loads, subgrade modulus, and pavement thickness for dual wheel loads only.

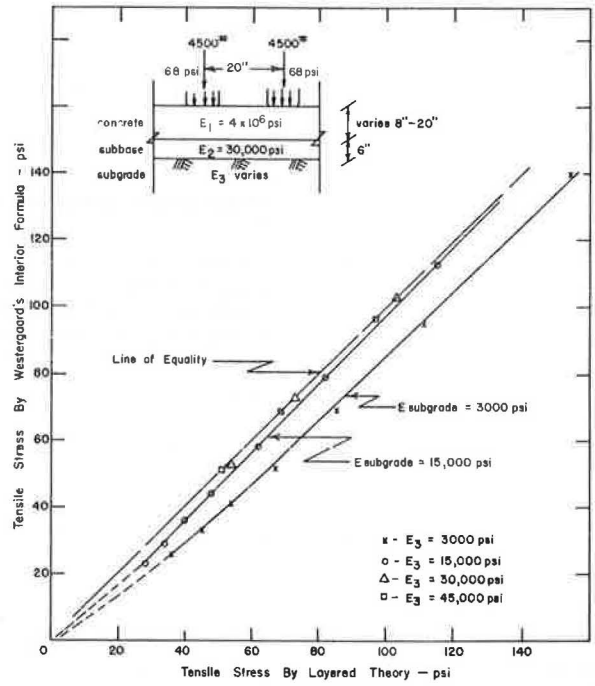

Figure 7. Comparison of pavement stresses at the pavement-subbase interface computed by Westergaard and layered theory for varying wheel loads, subgrade modulus, and pavement thicknesses—dual wheel load.

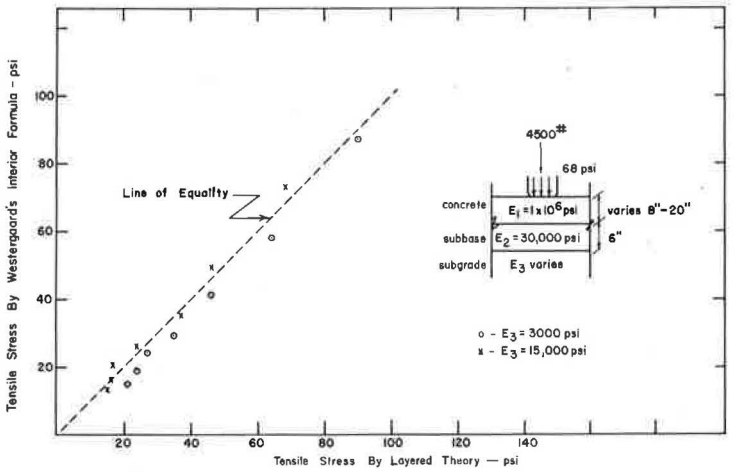

Figure 8. Comparison of stresses at the pavement-subbase interface computed by Westergaard and layered theory for concrete pavement with E value of 1,000,000 psi.

In general, layered theory predicts a deflection two to four times greater than that predicted by Westergaard.

The line equating deflections predicted by layered theory and Westergaard varies with the subgrade modulus as did the line equating predicted stress, but with a much more pronounced effect. As the subgrade modulus increases, the deflections predicted by the two mathematical models approach one another. For a subgrade modulus of 45,000 psi, the layered theory deflection is still two orders of magnitude greater than that predicted by the Westergaard equation. The 45,000-psi figure represents an excellent soil; hence, the two mathematical models are not equal at any point over the range of subgrade moduli generally found applicable to soils.

This study indicates that the stresses predicted by layered theory are somewhat higher than those predicted by the Westergaard interior equation. This observation may be interpreted to mean that layered theory gives more influence to a variation in subgrade

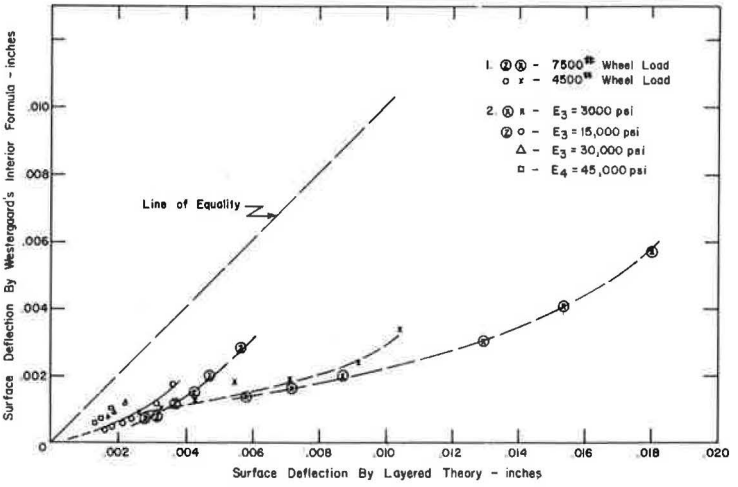

Figure 9. Comparison of pavement surface deflection predicted by Westergaard and layered theory for varying wheel loads, subgrade modulus, and pavement thicknesses—dual wheel loads.

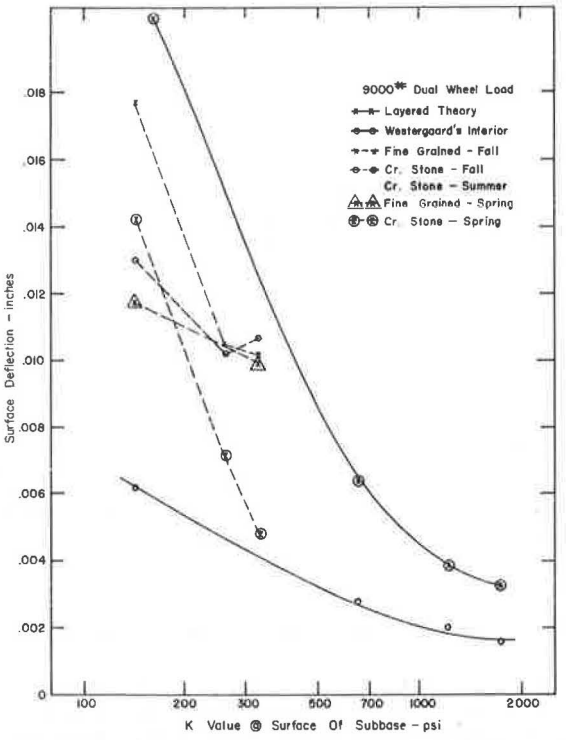

Figure 10. Comparison of predicted deflection and measured deflection considering subgrade support.

support than does the Westergaard equation. The deflections predicted by the two mathematical models differ considerably, especially for poor subgrade soils. Despite this discrepancy, the comparison does indicate that the two mathematical models may be used interchangeably with approximately the same degree of confidence. Hence, layered theory may be used in lieu of plate theory for interior loading conditions.

VERIFICATION WITH FIELD OBSERVATIONS

For practicing engineers to gain a degree of confidence in the layered theory mathematical model, they must compare predicted values of deflection and stress with field data if possible. The AASHO Road Test is an excellent source of data for investigating the effect of wheel load and pavement thickness on deflection and strain (2). Following are the statistically derived empirical models from the AASHO Road Test for predicting pavement deflection and strain.

$$d = \frac{0.00883 \times L}{10^{0.0075T} \times D^{1.178}} \quad (1)$$

$$\epsilon = \frac{20.54 \times L}{10^{0.0031T} \times D^{1.278}} \quad (2)$$

where

d = deflection at the pavement edge, in inches;
ϵ = strain at the pavement edge;
L = axle load, in pounds;
T = difference in pavement temperature between the top and the bottom of the slab, in degrees Fahrenheit; and
D = pavement thickness, in inches.

Equations 1 and 2 are for edge deflection and strain, which are different from the interior condition assumed for the two mathematical models being studied. This fact should be recalled when comparing the predicted deflection to measured deflection in later sections. Another factor peculiar to these equations and relative to the mathematical model being considered is the inclusion of a pavement temperature differential value. Although warping and curling stresses due to pavement temperature differential have long been considered in computing stresses, their effect on deflection has generally been ignored in mathematical modeling. All comparisons of deflection in this report are made at zero temperature differential to eliminate this factor.

Soil Support

The effect of soil support on deflection and stress cannot be ascertained from the AASHO Road Test data because only one subgrade soil type was present. Therefore, one must resort to other sources. The Texas Highway Department has recently completed a study of concrete pavement deflection in which the effect of soil support on

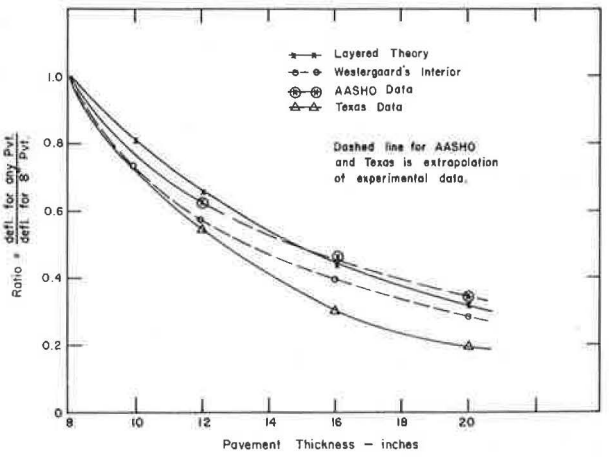

Figure 11. Comparison of predicted deflection and measured deflection considering pavement thickness.

deflection was investigated using the techniques developed at the AASHO Road Test (22).

The Texas soil data are expressed in terms of the Texas triaxial test, which was correlated with the k value (22) to develop soil support values compatible with those used in the mathematical models. Figure 10 compares deflections measured from in-service projects with those computed from the layered theory and Westergaard formula. The data are for 8-in. concrete pavements resting on a 6-in. subbase of fine-grained sandy or limestone materials. These two materials are unstabilized and represent the range of subbase materials normally used in construction.

The deflection predicted by the layered theory is considerably higher than that measured in the field, but Figure 10 shows that the shapes of the data lines are very similar. Therefore, it may be stated that, although the layered theory predicts somewhat higher deflections, its response to the influence of the soil support value is much more representative of actual conditions than is that of the Westergaard equation. Therefore, layered theory is somewhat more conservative.

Figure 11 compares the effect of pavement thickness on deflection derived from the experimental data with the same type relationships developed from the two mathematical

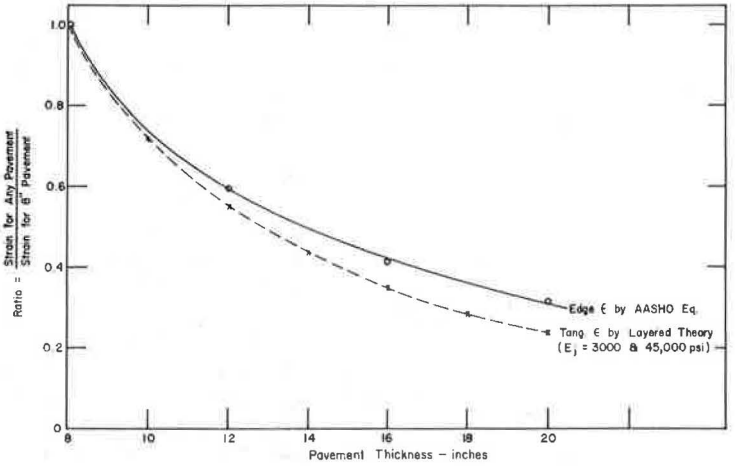

Figure 12. Comparison of predicted strain and measured strain considering pavement thickness.

models. The deflection data have been normalized to the deflection for an 8-in. thick pavement. Both of the mathematical models agree favorably with experimental data from the two different sources, especially within the limits of the data for which the experimental models were derived.

Figure 12 compares the relationship between pavement thickness and pavement strain derived from the AASHO equation and the layered theory mathematical model. The strain predicted from the layered theory mathematical model agrees reasonably with that measured on experimental projects.

Subgrade Thickness

Figure 10 indicates that the deflection predicted by layered theory is considerably larger than that measured. This is partly because layered theory assumes that the subgrade is of infinite depth. The assumption can be partially erroneous because most soil deposits generally increase in stiffness with depth below the surface. Therefore, in order to make the predictions from layered theory more realistic relative to real pavements, it is generally necessary to assume that a very stiff layer is present at some depth below the surface. Figure 13 shows the effect of thickness of subgrade material overlying a very stiff layer. For this particular graph, the stiff layer is assumed to have an E value of 300,000 psi. Another study was also conducted assuming an E value of 2,000,000 psi for the stiff layer, but the data from the latter study did not portray a relationship significantly different from that in Figure 13.

Figure 13 shows that variations in subgrade thickness between 0 and 12 feet have a significant effect on the deflection, especially for the lower soil-support values. The difference in deflection between a subgrade layer 4 ft thick and one with an infinite thickness may vary 150 percent on poor soils and up to 50 percent on good soils. A few of the data points from Texas highways previously shown in Figure 10 are shown as dashed lines in Figure 13. It may be hypothesized from Figure 13 that, to simulate the deflection as measured by the Texas study, it is necessary to increase the soil stiffness at depths of 6 to 10 feet below the surface.

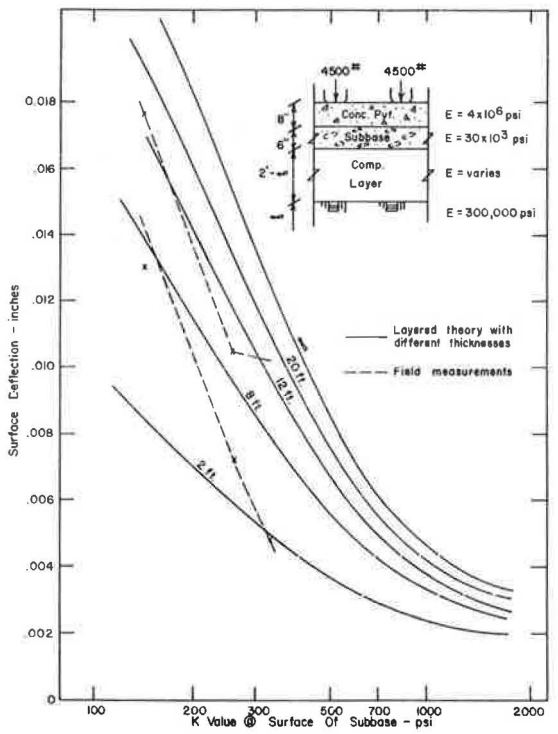

Figure 13. Influence of subgrade-layer thickness on pavement surface deflection.

Figure 14 is similar to Figure 13 except that the effects of the subgrade thickness on the tensile stress in the pavement are shown for different subgrade soils. The deep rigid layer is assumed to have an E value of 300,000 psi. A similar study, in which the rigid layer was assumed to have an E value of 2,000,000 psi, gives essentially the same answers as those in Figure 14. When the thickness of the subgrade layer above the deep rigid layer ranges from 0 to 12 ft it has an effect on the tensile stress in the pavement. If the subgrade layer is greater than 20 ft, then the stress in the pavement remains constant. The stress difference with a layer 4 ft thick compared to one of infinite thickness is approximately 14 percent with poor soils and approximately 1 percent with good subgrade soils. This indicates that the stresses in the pavement are not as sensitive to thicknesses of the subgrade soil and the stiff-

ness of the rigid layer as are deflections. Therefore, it may be concluded that the stresses in the pavement may be predicted with a fair degree of accuracy whenever the subgrade soil layer is greater than 12 ft in thickness.

PROBLEMS ADAPTABLE TO SOLUTION BY LAYERED THEORY

Layered theory may be applied to the design of CRCP overlays of existing pavement, flexible or rigid. The layered theory application to airport or highway pavements will give the designer a rational method of examining the stress level in any layer of the pavement structure that was heretofore impossible. In addition, the designer may confidently investigate the effect of unusual designs on the stress state, e.g., use of a cushion course, rather than resorting to empirical methods or impractical test sections. Furthermore, the effect of the reinforcing steel related to an increase in slab stiffness may also be taken into account. This may be of special interest with regard to overlay design.

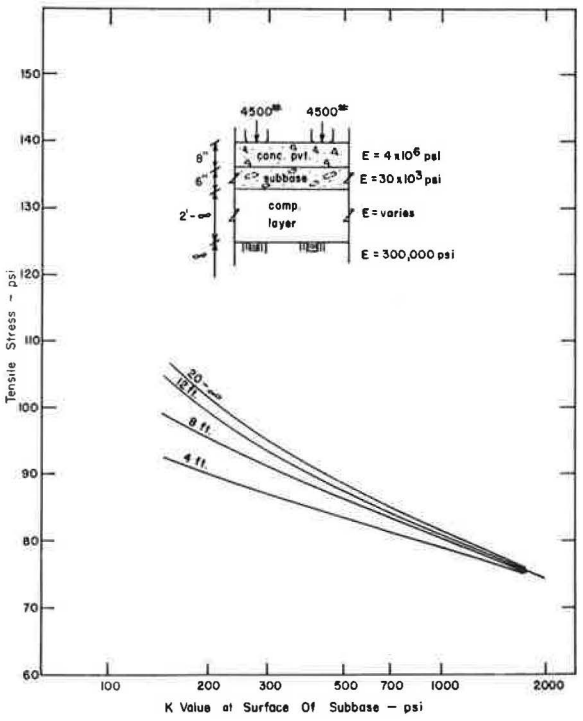

Figure 14. Influence of subgrade-layer thickness on pavement stress.

Figure 15 shows a series of design curves for a CRCP overlay of an existing jointed concrete pavement for several different aircraft and design conditions recently used at a U.S. Air Force facility (23). The predicted stresses are the combinations of multiple wheel loads for complex gear configurations, e.g., the Boeing 747 gear configuration consisting of sixteen 42,334-lb wheel loads. The effect of a stress-

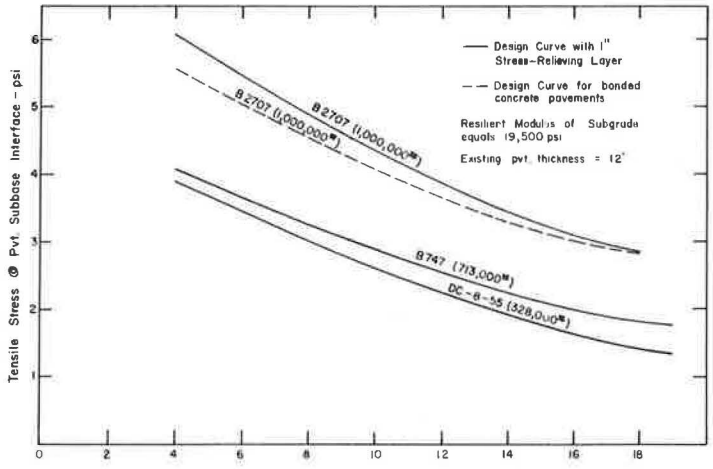

Figure 15. Design curves for a CRCP overlay of existing 12-in. jointed concrete pavement.

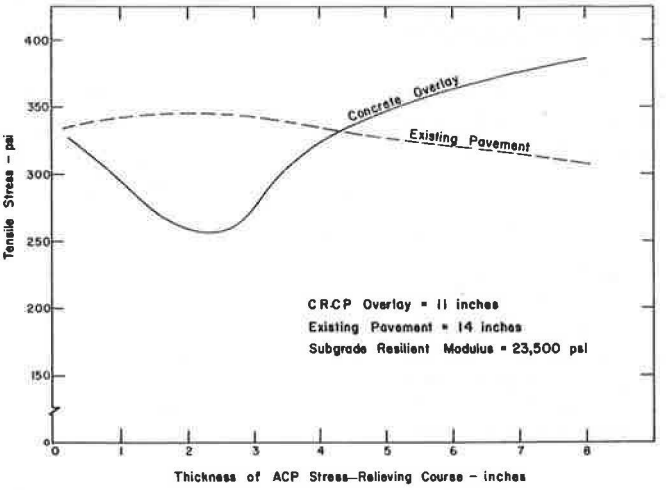

Figure 16. Effect of stress-relieving course on the stress in CRCP overlay and existing concrete pavement.

relieving course between the existing jointed pavement and the CRCP is illustrated. Many designers feel the use of an asphalt concrete stress-relieving course is necessary with this type of condition to prevent the volume-change movements of the existing pavement from overstressing the longitudinal steel in the CRCP overlay. Figure 15 shows the increase in overlay thicknesses required when the stress-relieving course is used. For this particular design example, the stress in the existing concrete pavement at the subgrade interface gives the maximum stress level for all cases. For other combinations of thicknesses and material properties, other points in the pavement structure may give the controlling design conditions.

Figure 16 shows the effect of various thicknesses of an intermediate asphalt concrete layer on the stress level in the CRCP overlay and the existing concrete pavement. The stress level in the existing pavement controls until the intermediate layer thickness exceeds 4 in., after which the stress in the CRCP overlay controls. This type of analysis is not possible with empirical procedures or with the plate theory. Furthermore, the material properties used for the subgrade (i. e., resilient modulus) can be determined in the laboratory and are not dependent on impractical plate theory load tests.

CONCLUSIONS AND RECOMMENDATIONS

On the basis of this study, the following conclusions and recommendations are warranted:

1. The application of layered theory to the design of CRCP overlays meets the criteria of reasonableness, and its use is recommended.
2. The material properties used in the analysis may be measured in the laboratory. This eliminates the need for the impractical plate theory load tests in the field as well as allows for a better statistical sampling to be achieved.
3. Special loading conditions and layered combinations for CRCP overlays may be analyzed with layered theory that are beyond the scope of empirical methods or presently used theories.
4. The stress level of every layer in the pavement structure may be taken into account during design.
5. The thickness of subgrade and its general increase in stiffness with depth should be taken into account in pavement structure computations, although the effect on stress is nominal relative to the effect on deflection.

REFERENCES

1. Lee, Clyde E. A Portable Electronic Scale for Weighing Vehicles in Motion. Highway Research Record 127, pp. 22-33, 1966.
2. The AASHO Road Test: Report 5—Pavement Research. HRB Spec. Rept. 61E, 1962.
3. Hudson, W. R. Discontinuous Orthotropic Plates and Pavement Slabs. PhD Dissertation, Univ. of Texas, Austin, 1965.
4. Westergaard, H. M. Stresses in Concrete Pavements Computed by Theoretical Analyses. Public Roads, Vol. 7, No. 2, April 1926.
5. Kelley, E. F. Application of Results of Research to Structural Design of Concrete Pavements. Public Roads, Vol. 20, No. 5, July 1939.
6. Spangler, M. G. Stresses in the Corner Region of Concrete Pavements. Iowa State Univ., Eng. Expt. Sta. Bull. 157, 1942.
7. Concrete Pavement Design. Portland Cement Association, Chicago, 1951.
8. Burmister, D. M. The Theory of Stresses and Displacements in Layered Systems and Applications to the Design of Airport Runways. HRB Proc., Vol. 23, pp. 126-148, 1943.
9. Hank, R. J., and Scrivner, F. H. Some Numerical Solutions of Stresses in Two- and Three-Layered Systems. HRB Proc., Vol. 28, pp. 457-468, 1948.
10. Peattie, K. R., and Jones, A. Surface Deflection of Road Structures. Symposium on Road Test for Pavement Design, Proc., Lisbon, 1962.
11. Warren, H., and Eieckmann, W. L. Numerical Computations of Stresses and Strains in a Multiple-Layer Asphalt Pavement System. Chevron Research Company, Sept. 1963 (unpublished).
12. Peutz, M. G. F., Jones, A., and Van Kempen, H. P. M. Layered Systems Under Normal Surface Loads. Highway Research Record 228, pp. 34-45, 1968.
13. Seed, H. B., Mitry, F. G., Monismith, C. L., and Chan, C. K. Prediction of Flexible Pavement Deflection From Laboratory Repeated-Load Tests. NCHRP Report 35, 1967.
14. Airport Paving. AC-150/5320-6, Federal Aviation Agency, June 1964.
15. The United Soil Classification System. Corps of Engineers, Waterways Expt. Sta., Tech. Memo. 3-357, 1953.
16. Design Manual—Airfield Pavements. NAVDOCKS, DM21, U.S. Navy, Bureau of Yards and Docks, 1962.
17. McCullough, B. F., and Ledbetter, W. B. LTS Design of Continuously Reinforced Concrete Pavements. Jour. Highway Div., Proc. ASCE, Vol. 86, No. HW4, Dec. 1960.
18. Design of Continuously Reinforced Concrete Pavements for Highways. Concrete Reinforcing Steel Institute, Committee on Continuously Reinforced Concrete Pavement, Bull. 1, Dec. 1960.
19. Thickness Design for Concrete Pavements. Concrete Information, HB 35, Portland Cement Association, 1966.
20. Engineering and Design—Rigid Airfield Pavement. AM-1110-45-303, Corps of Engineers, Feb. 3, 1958.
21. Symposium on Load Test for Bearing Capacity of Soils. ASTM Spec. Tech. Publ. 79, 1947.
22. McCullough, B. F., and Treybig, H. J. A Deflection Study of Continuously Reinforced Concrete Pavement in Texas. Highway Research Record 239, pp. 150-174, 1968.
23. McCullough, B. F., and Fredrick, J. B. Pavement Evaluation Study—Runway 7-25. U.S. Air Force Plan No. 42, Palmdale, Calif., 1968.

An Experimental Self-Stressing Concrete Pavement: II. Four-Year Pavement Evaluation

CHARLES E. DOUGAN, Division of Research and Development,
Connecticut State Highway Department

During the 1963 paving season, an experimental reinforced concrete pavement was constructed in which an expansive cement was used to produce thin prestressed slabs. The experimental section contains three slabs 24 ft wide, 6 in. thick, and approximately 490 ft long. The conventional pavement, of 40-ft contraction joint design, is placed 9 in. thick in two 12-ft lanes.

This report is devoted to the 4-year, post-construction performance of this pavement. Slab movement data, crack observation, and other information are presented, as well as suggestions for the future application of this self-stressing technique.

Early construction difficulties and pavement distress appear to have significantly affected the pavement performance to date. Transverse cracking that has developed in the test section is probably related to insufficient prestress in the concrete slabs.

•IN 1963, the Connecticut State Highway Department constructed an experimental expansive cement concrete pavement. The feasibility of the test installation was explored in early meetings with Bureau of Public Roads personnel and other interested parties (1), and a pilot installation was made in June 1963. Final plans for the test section were completed after the pilot installation, and the test pavement was placed in September 1963.

The 1500-ft test area is in the southbound roadway of Route 2 in Glastonbury. The facility is a four-lane divided highway with fully controlled access. The test area starts in a gravel fill at the northern end and runs into a reddish-brown clay cut that continues throughout the test section. The southbound roadway at the test site is a tangent section with a +1.5 percent grade that enters a superelevated horizontal curve to the right about 150 ft from the southern end of the test area (Figs. 1 and 2).

DESIGN AND CONSTRUCTION

The following design features were included in the test section. To minimize subgrade friction, two layers of polyethylene sheeting were placed on a 1-in. depth of dense-graded bituminous concrete for the subbase. To avoid difficulties with keyway formation, 24-ft paving with no longitudinal joint was required. Reinforced concrete sleeper blocks were placed flush with the surface of the bituminous concrete at the end of each experimental slab (a) to provide anchorage for the longitudinal reinforcement, and (b) to provide anchorage for devices to restrain the slab ends from curling and restrain vertical displacement.

Paper sponsored by Committee on Rigid Pavement Design and presented at the 48th Annual Meeting.

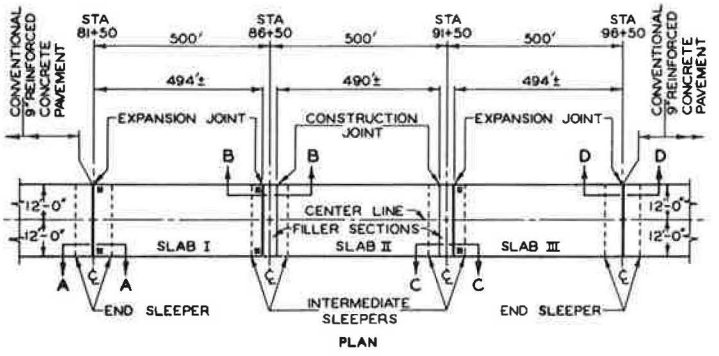

Figure 1. Self-stressing concrete pavement.

Longitudinal reinforcement for the test slabs was with a ½-in. diameter, 7-wire strand prestressing cable (ASTM 416), spaced 14 in. on centers with outside strands 4 in. from the edge of pavement. The cables were continuous throughout the slab length and were initially tensioned to a load of approximately 1,000 pounds. Transverse reinforcement was provided by No. 7 deformed steel bars (ASTM A 432 and ASTM A 305) spaced 2 ft on centers, and alternating above and below the longitudinal strands. The ends of the deformed bars were bent 90 deg to form hooks of 8-diameter length and laid flat to clear the forms by 1½ in. Transverse bars were tied to the longitudinal cables and all steel was supported by chairs.

To restrain the slab ends from curling, a device, which was anchored in the sleeper block and the experimental slab and allowed free end movement of the test pavement, was used at the ends of slab I and the northern end of slab III. The other end of slab III was restrained by using the downward component of the resultant pavement stress. Slab II was restrained by tying concrete filler blocks to the slab ends (1, p. 58).

Mix design for the project required an 8½-bag mix that included an expansive component conforming to State Highway Department specifications. Concrete was to be placed with a 1½-in. slump and fog-spray cured for a minimum period of 24 hours after placement.

Early difficulties with consistency control, and consequently with the finishing operations, were lessened by field changes in the mix design. The difficulties encountered were caused by the cement's affinity to water, resulting in slab growth that was less than anticipated. The resultant longitudinal stress in the pavement was approximately 70 to 90 psi at the slab ends, 30 psi at the mid-length, and about 140 psi transversely. In addition, the slab surface was very rough and wavy because of the finishing of the

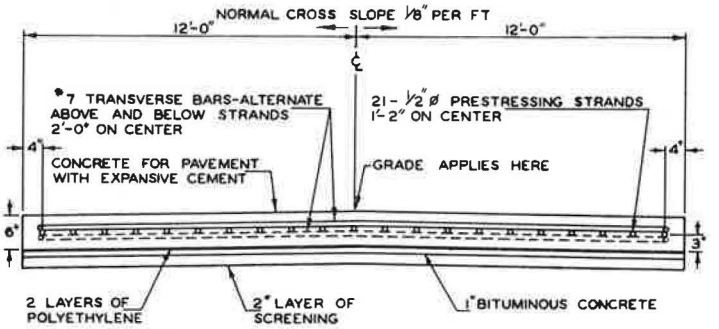

Figure 2. Typical cross section of pavement.

stiff concrete. Further details on the design and construction were given by Dougan (1).

SIGNIFICANT FINDINGS

Two types of transverse cracking have developed in the test area. They are full-width transverse cracks, greater than 12 ft in length, and partial transverse cracks less than 12 ft in length. Both types of cracking are attributed to inadequate tensile strength in the pavement slabs. Insufficient prestress is believed to be a major factor contributing to the cracking. The relative vertical position of the transverse reinforcement does not affect the full-width cracks except by reducing the cross-sectional area of the concrete slabs. The partial cracks start at the hooked ends of the transverse bars and progress toward the centerline of the roadway. The vertical position of the transverse steel does not affect the occurrence of partial transverse cracks.

The transverse joints in the test area are closing. The transverse cracks in the "self-stressed" slabs have opened, resulting in permanent end displacements. Resistance to movement at the filler blocks at the ends of slab II is also contributing to the closure at joints 2 and 3. The adjacent conventional design also shows a permanent end displacement, which is to be expected from a contraction-joint design pavement.

Slab end curling has not been detected. Slab hold-down devices (1) could probably be eliminated and cost savings achieved. If the filler blocks are used to prevent curling, further research on the amount of steel required to hold the filler blocks to the ends is needed. It appears feasible to use the downward component of the self-stress as a hold-down mechanism, but data are limited on this aspect of the project. To utilize the self-stress it is necessary to lower the longitudinal reinforcement below the neutral axis. As the pavement grows longitudinally, a downward component of the resultant prestress would be developed and, in conjunction with the weight of the slab, would act as a vertical restraint.

The daily and seasonal joint movements indicate a fairly uniform unit change in length per unit change in temperature. These data do, however, indicate a slight decrease in magnitude with time. The decrease is probably related to the end displacements at the transverse joints. Estimates of the coefficient of expansion indicate that there may be a seasonal variation in the expansion characteristics of the test slabs.

The compression joint seal is working well. Minor humps have been created by the slab end displacements, but to date the seal has adhered well to the joint faces and has undergone upward displacement in only joint 1.

The surface of the test area shows large areas of surface wear or abrasion and development of spalls at some full-width transverse cracks. The following abnormalities were detected by the Materials Division of the Bureau of Public Roads and they could well be a basis for the development of the previously mentioned defects: (a) calcium sulfoaluminate, a weak component in portland cement, was present; (b) large air voids were found that indicate insufficient compaction, i.e., consolidation of the concrete; and (c) the entrained air content of the test slabs was quite low.

TRANSVERSE JOINTS

In mid-July 1964, the transverse joints between the test slabs were sealed with an extruded neoprene joint seal. The four transverse joints in the test area are designated joints 1 through 4 from north to south respectively (joints 1 and 4 at the termini of the test area and joints 2 and 3 within the test area).

The joints were prepared for sealing by cleaning out the joint cavity and sawing the joint faces to a $2\frac{1}{2}$-in. width for joints 1 and 4, and a $4\frac{1}{2}$- to 5-in. width for joints 2 and 3 (Figs. 3, 4, 5, 6, 7). While sawing the end of slab III, it was noted that the steel collars used in the tensioning of the longitudinal reinforcement had not been removed after construction (Fig. 3).

The seals were placed in the joints and recessed $\frac{1}{4}$ to $\frac{1}{2}$ in. below the surface of the pavement. All seals were continuous for the 24-ft pavement width, and the ends of the seals were butted against a steel plate to prevent infiltration of materials from the side.

Figure 3. Joint 3—sawed face of slab III showing the steel collars.

Figure 4. Placing seal in joint 1.

Joints 1 and 4 required a 4-in. wide seal. For joints 2 and 3, two 3-in. wide seals were bonded together in the field and placed in the joint. To compensate for the lack of depth in the 3-in. seals, redwood strips were placed in the bottom of the joint groove for support (Fig. 6).

Joint Seal Performance

To date, the joint seal appears to be effectively embedded in the transverse joints. Unfortunately, maintenance forces placed hot-poured liquid joint seal on the upper surface of the neoprene seals. It was felt that the liquid sealer would compensate for the recess of the neoprene seal and thus minimize the thump at the transverse joints.

The neoprene seals have maintained their compressed position throughout the winter. In the summer months the compression seals form a slight bump because of the pavement expansion. Figure 8 shows the only area in which the joint seal has been forced out of the joint. The seal is about $1\frac{1}{4}$ in. (maximum) above the pavement for a distance

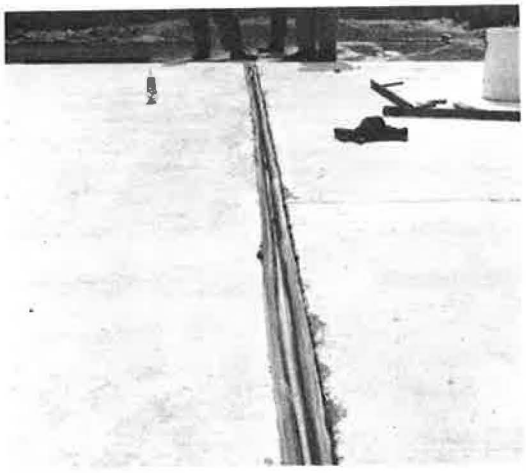

Figure 5. Joint 1—seal in place.

Figure 6. Joint 3—seal ready for placement; note the redwood strips used for support.

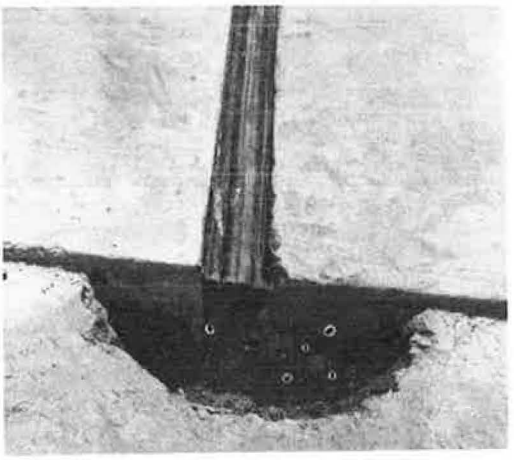

Figure 7. Joint 3—seal in place.

Figure 8. Transverse joint 1—seal above pavement surface for a distance of 4 ft.

of 4 ft. Permanent end displacements are cited as primary factors in causing this extrusion. The rest of the seal appears to be performing well.

CONDITION OBSERVATIONS

Pavement Cracking

Pavement distress in the form of longitudinal edge cracks was noted immediately after the paving operation was completed (1). Since that time, the number of these cracks has doubled in slabs II and III and tripled in slab I. A few of these cracks have caused edge spalls that required maintenance (Figs. 9 through 11), but most of the cracks have been confined to the area above the hooked ends of the transverse reinforcement.

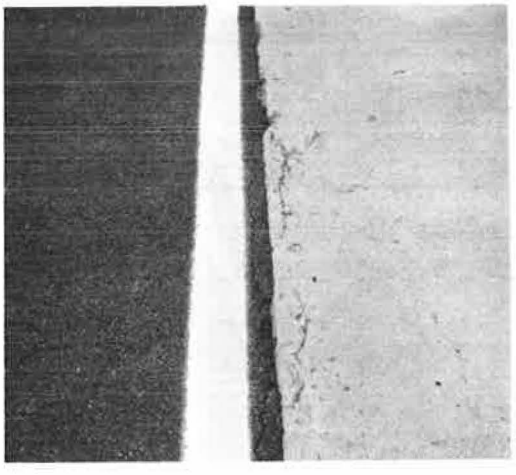

Figure 9. Slab II—longitudinal edge cracks near mid-length of slab; crack width approximately $\frac{1}{8}$ in., August 1965.

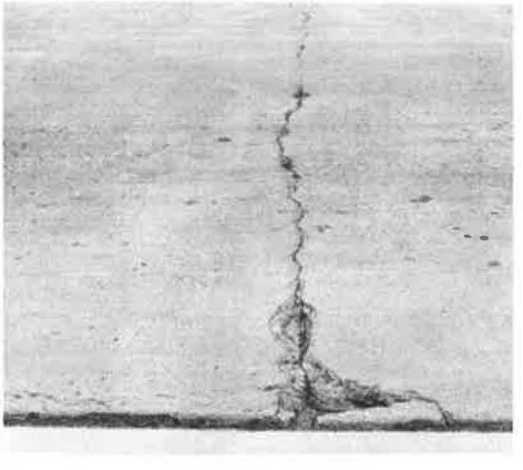

Figure 10. Slab II—distress at longitudinal edge crack, mid-length of slab; transverse crack open $\frac{1}{8}$ in., August 1965.

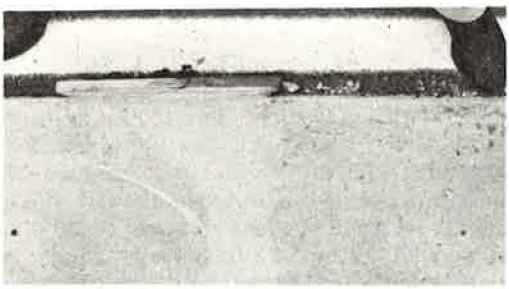

Figure 11. Slab II—completed repairs at area of distress shown in Figure 10; epoxy resin patching material used, August 1965.

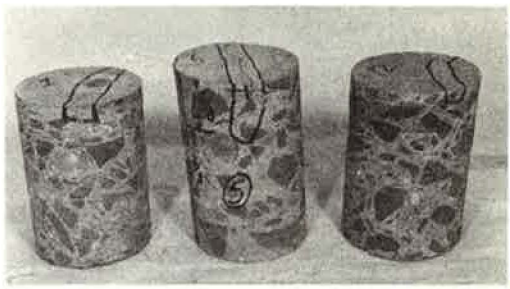

Figure 12. Cores taken at partial transverse cracks; core numbers 1, 5, and 12 taken in slabs I, II, and III respectively, January 1966.

About a year after paving, partial transverse cracks originating at the longitudinal cracks were noted. These cracks, generally 1 to 3 ft in length, are very narrow. Tables 1 and 2 summarize data obtained from pavement cores. The data show that these partial transverse cracks occur over the transverse reinforcement. The data indicate that these cracks can penetrate to the transverse bars but do not extend the full pavement depth, as can be seen in Figure 12. Crack widths measured at the surface of the core with a hand microscope range from 0.010 to 0.002 in. and they decrease to approximately 0.002 in. about ¼ in. below the surface.

Figure 13 summarizes the total amount of cracking with time. The figure indicates that the partial transverse cracking is still developing in the test area, but the rate of occurrence is decreasing with time.

These cracks are attributed to the plane of weakness created by the hooked ends of the transverse reinforcement. It is quite possible that this cracking will stop when most of the longitudinal edge cracks have developed a partial transverse crack. The greatest dangers from this failure are the development of full-width transverse cracks and the development of spalls along the crack faces and the edge of the pavement. Presently, the only areas that show adverse effects from the partial cracks are those in which construction difficulties were encountered, particularly the shoulder edge of slab II.

TABLE 1

SUMMARY OF CRACK DATA FROM PAVEMENT CORES

Slab No.	Core No.	Type of Crack	Depth of Core (in.)	Depth of Cover (in.)	Depth of Crack (in.)	Crack Width (in.)		Date Crack First Noted
						Top	Bottom	
I	1	Partial	5¾	1⅜	½ to ⅝	0.005	0.002 0.001	Dec. 1965
	2	Full	6 1/16	3 5/16	Full			Feb. 1964
	3	None	6 3/16					
	4	None	6¼					
II	5	Partial	6⅜	1⅝	1⅝	0.010	0.010 0.002	Sept. 1964
	6	None	6⅞					
	7	None	—					
	8	Full	6⅛	3 3/16	Full			Feb. 1964
III	9	Full	6 7/16	2	Full			Feb. 1964
	10	None	6 3/16					
	11	None	6⅛					
	12	Partial	5⅞	1½	3/16	0.003 0.001	0.001	Sept. 1964

TABLE 2

SUMMARY OF COMPRESSIVE STRENGTH OF CONCRETE CORES

Slab No.	Core No.	Strength[a] (psi)	Density (pcf)
I	3	5870	137.0
	4	5670	135.8
II	6	6190	139.7
	7	4980	136.2
III	10	5400	135.6
	11	4790	135.4

[a]All cores corrected to L/D = 2. Cores soaked in water for 48 hours prior to test and tested in moist condition.

Full-Width Transverse Cracks

In late November 1963, full-width transverse cracks appeared in the test slabs. The cracking was located at about the mid-length of the slabs, but has progressed toward the slab ends with time. Figure 14 is a plan view of the test site showing the present location of these cracks. There are now 38, 32, and 22 full-width cracks in slabs I, II, and III respectively. This cracking occurred before the pavement was 2 years old and there has been no appreciable increase in cracking of this nature since September 1965.

Cores taken over full-width cracks show that the cracks extend through the entire depth of slab, and that the location of the transverse reinforcement (above or below the longitudinal cables) has no effect on the cracks (Figs. 15, 16, 17). Inspection of the core holes gives no indication that the cracking has extended into the bituminous concrete

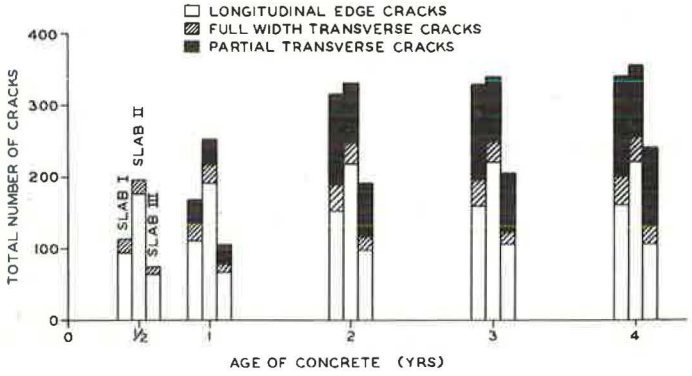

Figure 13. Summary of total cracking with time.

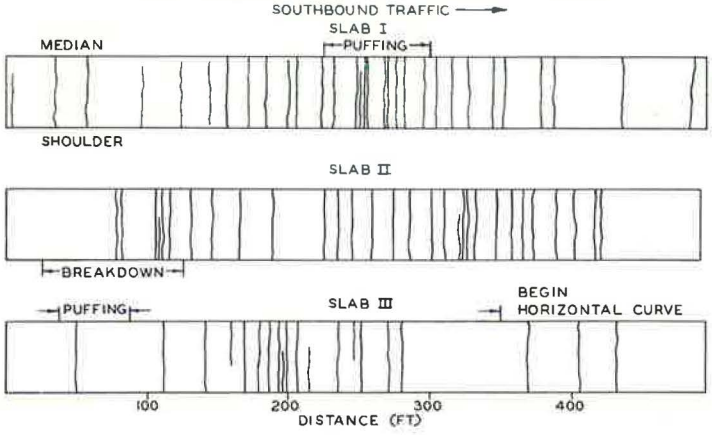

Figure 14. Plan view of test area locating full-width transverse cracks: age of concrete, 3 years.

Figure 15. Cores from slab I, January 1966.

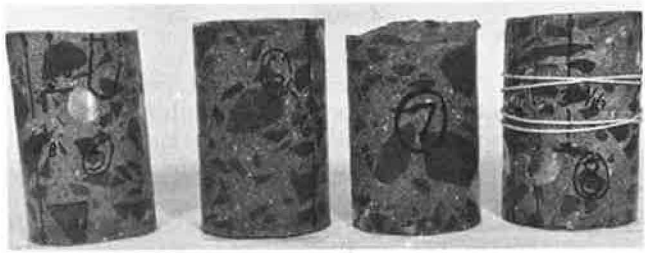

Figure 16. Cores from slab II, January 1966.

Figure 17. Cores from slab III, January 1966.

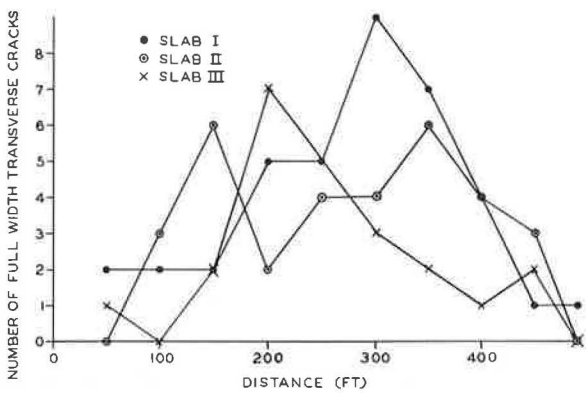

Figure 18. Longitudinal distribution of full-width transverse cracks: age of concrete, 4 years.

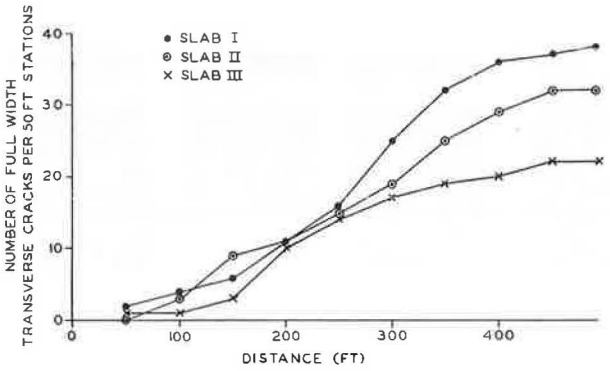

Figure 19. Cumulative distribution of full-width transverse cracks per 50-ft stations: age of concrete, 4 years.

subgrade. Crack widths from full-width cracks are not available; however, visual inspection of the cores shows that silt and fine sand particles have penetrated the crack to the depth of the transverse steel. Corrosion of the transverse steel has begun on the circumference of the bar. The corrosion is spotty and usually occurs on the surface of the bar closest to the surface of the pavement.

The full-width cracks are attributed to tensile stresses developed from subgrade friction. Figures 18 and 19 show the longitudinal and cumulative distribution of the cracks respectively. Note the high frequency of cracks in the central 200 ft of the slabs. Undoubtedly the low value of prestress (30 psi) at the mid-length of the slabs and construction difficulties have contributed greatly to this type of failure. Had the slabs attained sufficient growth to induce a uniform prestress of 300 psi, and had we assumed the tensile strength of the concrete to be 500 psi, then the concrete would have had 60 percent more resistance to the tensile stresses.

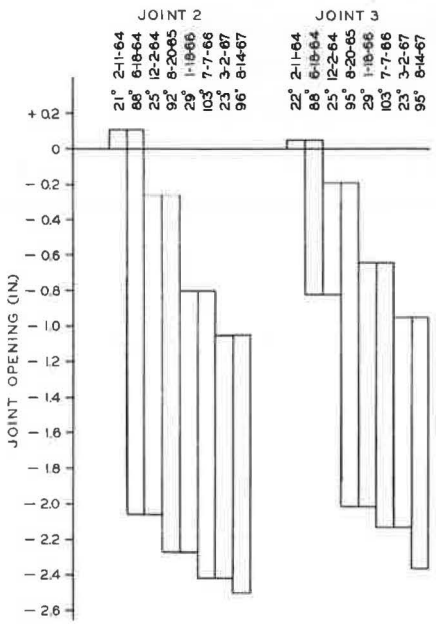

Figure 20. Seasonal joint movement for joints 2 and 3.

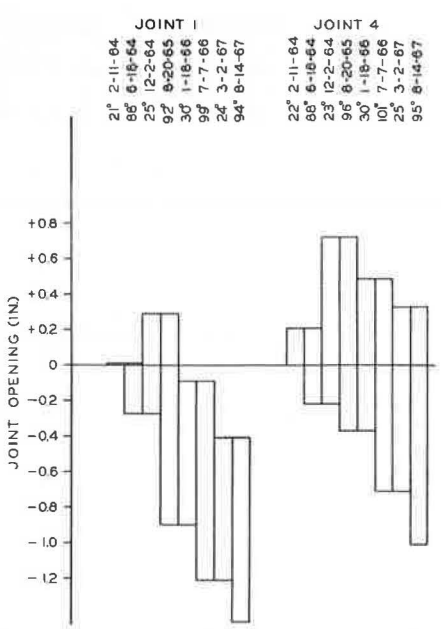

Figure 21. Seasonal joint movement for joints 1 and 4.

Figure 14 shows the approximate locations of the major difficulties encountered during construction. In slabs I and II, the high frequency of cracking in the areas indicated has been caused or been affected by discontinuities in paving operations experienced on the project. The highest frequency of cracking in slab III is about 200 ft south of joint 3. Although no breakdowns were encountered in this area, this is the approximate location of the start of the transition section that results in full superelevation at the south end of the test area. It is possible that the additional sand used in the concrete on this day and the stops required to adjust the screeds for the superelevation have caused a reduction in concrete strength sufficient to cause the high crack frequency.

In all probability the full-width transverse cracks are contributing to the development of compressive stresses within the test slabs by creating strains on the longitudinal reinforcement. This is supported by the core data. Unfortunately, the areas of slab II in which the strain instrumentation was located were filled with concrete shortly after paving the test site. This oversight precludes estimates of current slab stresses. However, data presented hereafter on joint closure reinforce the foregoing theory on slab stresses.

Joint Movement

Joint movement at the transverse joints in the test area is measured by instrumentation placed in the pavement during construction. All readings are obtained with a vernier gage and each set of readings is checked against highly probable limits established for the joint under observation. Figures 20 and 21 show the seasonal joint movement for the transverse joints. The data in these figures show the average seasonal movement indicated by four individual gage readings per joint. The base temperature for all joints is 54 F. Linear regression equations, which show change in joint opening as a function of change in temperature, are summarized in Figure 22. The equations were obtained using data from the time of construction up to and including June 1967. In all of the figures it is evident that the transverse joints are now closing. Joints 2 and 3 presently show a closure of 1.33 and 0.93 in. respectively, which has been gradually increasing in magnitude since construction. Joints 1 and 4 began to close about two years after construction and are still closing. Figure 23 shows the increase in joint closure with time.

Undoubtedly, their closure is owing in large part to slab end displacements resulting from the full-width transverse cracks in the test area. This is reflected in the increase in slope of Figure 23 between 1½ and 2½ years of age, which is the time period when the greatest number of full-width cracks were recorded.

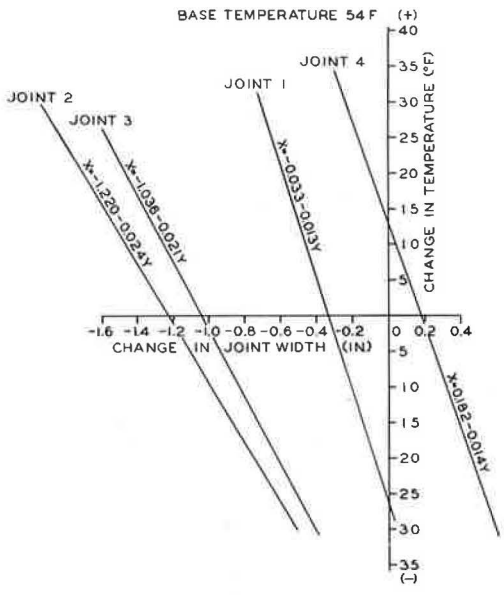

Figure 22. Regression equations, change in temperature vs change in joint width.

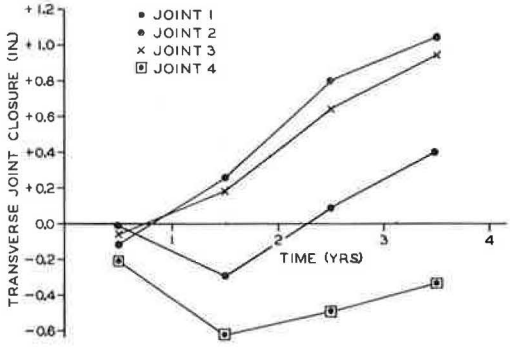

Figure 23. Decrease in joint opening with time.

The fact that the terminal joints and the central joints have, during the early stage, opposite slopes in Figure 23 is attributed to an obstacle to movement that developed at the filler blocks early in the pavement life. During the first winter, the interface between the filler blocks and the slab ends opened. Subsequently, longitudinal and then semicircular cracks developed over or extending from the tiebars, and a full-width transverse crack appeared at about the mid-length of the filler blocks. These defects are shown in Figures 24 through 27. The sequence in which the distress appeared suggests that the restricted movement is caused by frictional resistance. It was pointed out (1) that the steel I-beam used in tensioning the longitudinal reinforcement was to be burned off "reasonably flush" with the surface of the sleeper slab. Experience with this type of operation indicates that it is nearly impossible to remove the I-beam flush with the surface of a supporting concrete block. Furthermore, pieces of blown glass were set on top of the web sections that extended above the sleeper slab. Therefore, it is highly probable that early resistance to movement developed as a result of the filler block being forced to slide over pieces of the I-beam that protruded from the sleeper slab. At present no cores are available to support this theory, but in the future they could easily be obtained for confirmation.

Pavement Cross Sections

Elevations were obtained at the slab ends, 50 ft from the ends, and at the midpoint of each slab to measure slab curling or frost effects in the test area. Base readings were obtained after construction and the measurements continued each winter. To date, no curling of the slab ends or frost effects have been detected.

These data and the few full-width transverse cracks adjacent to the slab ends suggest that the means used to prevent curling show promise. The uniform movement at the transverse joints also supports this statement. At this time, it is not known what influence, if any, the full-width transverse cracks have on slab curling. Possibly the subdivision of the slabs by the cracks has offset any failure caused by curling stresses.

Data presented herein show that further research is required if the filler blocks are to be used for vertical restraint. The special hold-down devices (1) could be eliminated because of economic considerations. The resultant downward component of the self-stress is judged to be, presently, the most practical method of slab tie-down. The downward resistance to vertical displacement can easily be achieved in the field with no added construction cost.

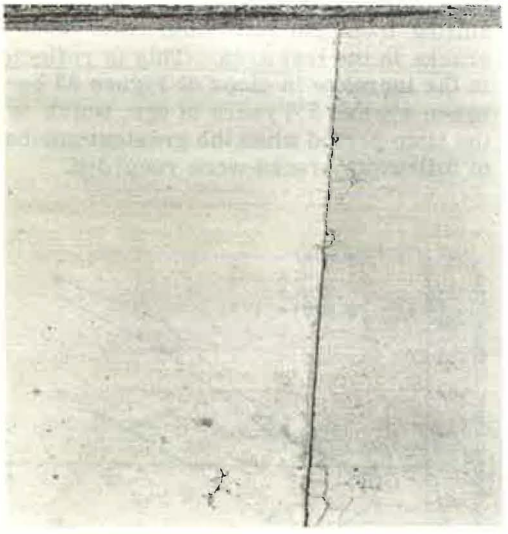

Figure 24. Interface at filler block between slabs II and III; crack width approximately ¼ in., April 1964.

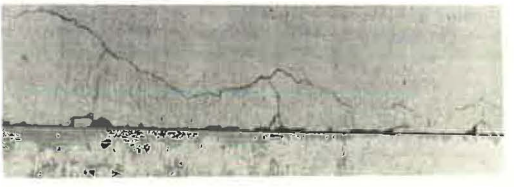

Figure 25. Longitudinal and semicircular cracks, same location as Figure 24, April 1964.

Figure 26. Close-up of cracking in Figure 25, April 1964.

Figure 27. Filler block between slabs I and II, faulted at median side $\frac{5}{8}$ to $\frac{3}{4}$ in., April 1964.

Figure 28. Slab I—gage plug instrumentation at a partial transverse crack, mid-length of slab; longitudinal edge crack in upper center of photo.

Surface Condition Observations

The present surface condition of the test area is shown in Figures 27 through 34. Large areas of surface wear as well as spalls have developed at transverse cracks. Cores removed from the test slabs indicate that the concrete is fairly homogeneous despite construction difficulties. A general examination of cores showed the following:

Figure 29. Distressed area of slab; width of spall, 3 to 6 in.; at median edge, 12-in. steel not visible.

Figure 30. Transverse crack 15 ft south of distress in Figure 29; minor spalling, crack tight.

Figure 31. Close-up of area in Figure 30 showing longitudinal edge crack.

Figure 32. Transverse crack in slab II; rust spots on surface of pavement at crack.

Figure 33. Cracking at interface between slab II and filler block 3.

Figure 34. Transverse crack in filler block 3 approximately at mid-length of the block.

1. Calcium sulfoaluminate was present, but this is to be expected because it is the normal product of an expansive reaction in portland cement.
2. Numerous large air voids were encountered. These indicate insufficient compaction of the plastic concrete, and are probably related to early construction difficulties.
3. The air content of the test slabs is quite low. The air content of slabs I, II, and III is 2.6, 2.6, and 3.2 percent respectively, as determined by the high-pressure method. Bureau of Public Roads comments on the marginal air content of the cores indicated a good probability of developing surface scale.

The author believes that the wear in the test area probably results from insufficient entrained air, coupled with the use of de-icing chemicals. Furthermore, the presence of calcium sulfoaluminate, which is a relatively weak crystalline structure in a cement paste, would tend to make the slab surface more susceptible to abrasion.

Present thinking is that the occurrence of spalling in the test slabs is affected by the presence of the large air voids and calcium sulfoaluminate. The wide, full-width transverse cracks that have developed have no load transfer mechanism; therefore, the reduced strength of the mortar could aggravate spalling in the test area.

SUPPLEMENTARY DATA AND INSTRUMENTATION

In March 1965, additional measurements on the end displacements of each test slab and the adjacent conventional concrete were started. The data are obtained by establishing a reference line at each transverse joint using monuments installed prior to paving. The slab end movements are then measured with a hand rule and recorded to the nearest $\frac{1}{32}$ in. Two sets of readings are taken at each joint at each edge of pavement. The average movement of each slab end is then reported as the average of four readings. All measurements are statistically analyzed.

Figures 35 and 36 show the slab displacements at each transverse joint. The total movement is the sum of the measured individual slab displacements at the joint. The

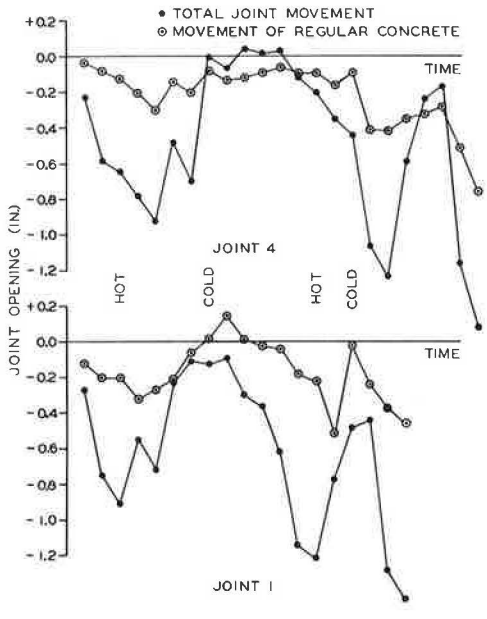

Figure 35. Thermal end movement of regular concrete.

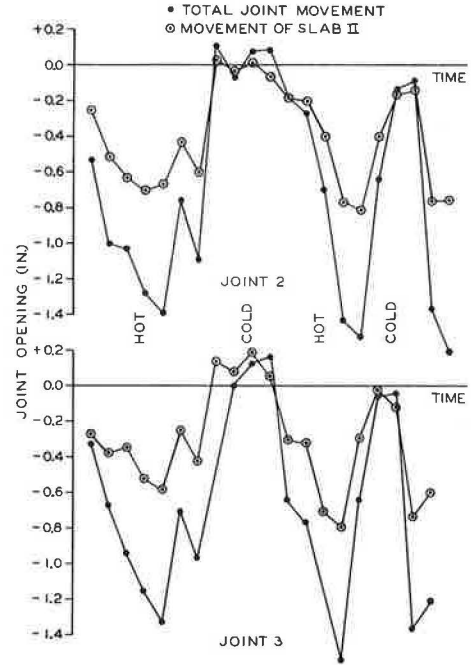

Figure 36. Thermal movement of slab II.

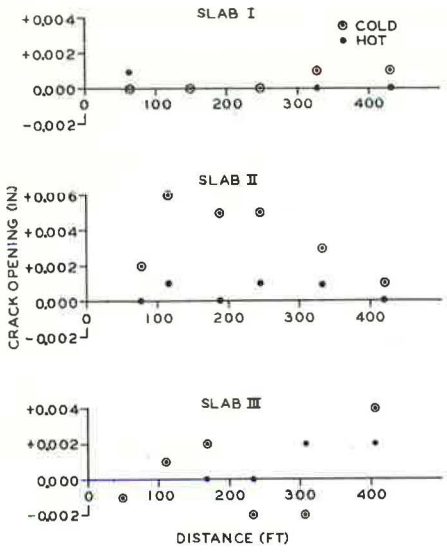

Figure 37. Width of full-width transverse cracks.

movement of slab II is shown and the movement of the opposite slab end is the algebraic difference between the total movement and the movement of slab II. The data are not corrected to the original base readings for the joint movements, but the total joint movement measured at the slab ends is comparable to that measured with the vernier gage.

In July 1966, additional gage plugs were installed in the test area at selected cracks, in the interface between the filler block and the ends of slab II, and at a full-width crack in the filler block. Figure 37 shows the increase in crack width from summer to winter for the full-width transverse cracks. Recognizing the fact that the additional gage plugs would have been more valuable if they had been installed at an earlier date, it is felt that the data support the observation that the full-width transverse cracking in the test area is contributing to the joint closure. This can be seen in the data for slab II in Figure 20.

The partial transverse cracks show a seasonal movement of 0.003 to 0.007 in. The cold-weather data indicate that these cracks are open more than the full-width cracks. It is quite probable that the smaller amount of movement at the full-width cracks results from the intrusion of incompressible material into the cracks that creates localized compressive stresses in the test slabs.

Figure 38 shows the change in crack width at the interfaces of slab II and the filler blocks. In Figure 36 there is about $\frac{1}{10}$ in. difference in the end displacement of slab II and the adjacent slabs. The difference in end displacements is probably owing to the excess movement of the filler blocks at the ends of slab II. This condition results from a combination of factors, the primary causes being insufficient steel tiebars and the resistance to movement cited previously. Initially, it was thought that the difference in end displacements might be caused by the difference in thermal characteristics resulting from changes in mix design. This theory was abandoned because of the error involved in measuring the end displacements and the fact that the unit change in joint width with respect to change in temperature is fairly constant for all three test slabs (Fig. 39).

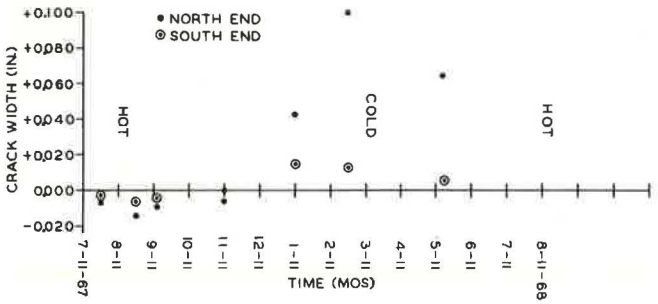

Figure 38. Crack width of interface between slab II and concrete filler blocks.

Estimated Coefficient of Expansion

Estimates of the coefficient of expansion were obtained from the daily joint movement data of joints 2 and 3. Computed values for the joints are 0.0000037 0.0000041 in. per in. per degree Fahrenheit respectively. These estimates are obtained by using an assumed length of 500 ft and the average joint movement measured over a 10 F or greater rise in temperature. No data are available on the amount of daily contraction in the test slabs. An estimate of the seasonal coefficient of expansion and contraction can be obtained from the data in Figure 20 by dividing the seasonal movement by 6,000 in.

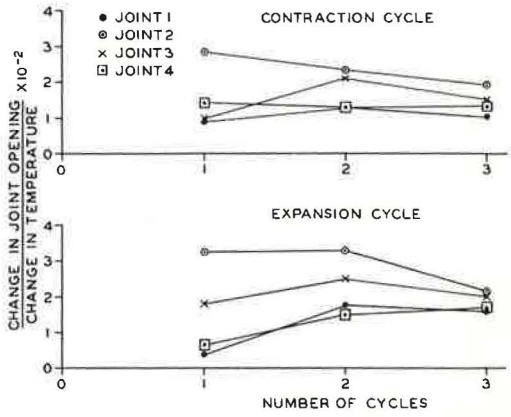

Figure 39. Decrease in joint movement per unit change in temperature.

Table 3 gives data on the daily change in length used to calculate the coefficient of expansion. Note the wide dispersion of data. There appears to be cause to suspect that the amount of expansion will vary with the season of the year—that is, the amount or rate of expansion is greater in the summer than it is in the winter. Figure 23 indicates a decrease in joint opening with time. The amount of influence this has on the expansion and contraction characteristics of the slabs is not known at this time. Presently, it is felt that more data are required to determine if significant differences can be detected in the daily and seasonal coefficients of expansion.

PAVEMENT SERVICEABILITY

Based on the minimum number of cracks and pavement surface wear, slab III has performed best. The cracks in slab III are tight and only minor spalling has occurred. This again reflects improved paving technology over that used in paving slabs I and II.

TABLE 3

DAILY CHANGE IN LENGTH MEASURED AT JOINTS 2 AND 3

Joint 2					Joint 3				
Temperature		T (F)	Length (in.)	L/T	Temperature		T (F)	Length (in.)	L/T
a.m.	p.m.				a.m.	p.m.			
77	92	15	0.3350	0.0223	77	95	18	0.4723	0.0262
77	92	15	0.4828	0.0322	71	85	14	0.3785	0.0270
60	70	10	0.1748	0.0175	39	52	13	0.2993	0.0230
69	84	15	0.4048	0.0270	45	56	11	0.2610	0.0238
36	52	16	0.3163	0.0198	81	93	12	0.2853	0.0238
43	57	14	0.3025	0.0216	75	87	12	0.3705	0.0309
80	94	14	0.2990	0.0214	75	88	13	0.2725	0.0210
89	103	14	0.2760	0.0197	77	95	18	0.3830	0.0213
70	87	17	0.4170	0.0245					x 0.1970
53	64	11	0.2708	0.0246					$\bar{x}$ 0.0246
72	87	15	0.2658	0.0177					e = 0.0000041
76	96	20	0.4070	0.0204					
				x 0.2687					
				$\bar{x}$ 0.0224					
				e = 0.0000037					

TABLE 4

SUMMARY OF TRAFFIC DATA
(Percent of ADT)

Year	ADT	Passenger Cars	Single-Unit Trucks			Combination Trucks			Buses
			4 Tire	6 Tire	10 Tire	3 Axle	4 Axle	5 Axle	
1965	4,900	88.7	5.7	2.4	0.1	0.5	2.0	0.5	0.1
1966	6,100	86.7	7.0	3.0	0.1	0.5	1.9	0.6	0.2

The present pavement condition of the test area is shown in Figures 27 through 34. The cracks in Figures 30 and 32 are typical of those in slab III.

Tables 4 and 5 summarize the traffic data and the estimated PSI and equivalent 18-kip axle loads respectively. In Table 4 it is evident that the test area has not been subjected to a heavy traffic load. This is supported by the estimated equivalent 18-kip axle loads shown in Table 5.

In Table 5 two values of D were used to compute the 18-kip equivalencies. This was done because it was not known to what extent the steel reinforcement has influenced the pavement stiffness. In other words, is D = 6 in. equal to D = 9 in.? Because the sums of the equivalent 18-kip loads, by both assumed values of D, differ by roughly 4 percent, the value of D = 6 in. will be used hereafter.

The PSI (2.98) of the test area is also shown in Table 5, and is based on pavement roughness determined by a BPR-type roughometer (7). The roughness readings, which are the average values from all wheelpaths in the 1,500-ft test section, indicate a decrease in roughness with time. This is inconsistent with condition observations of the test slabs. Supplementary calculations of the PSI, incorporating estimates of cracking and patching per 1,000 sq ft of pavement surface, show that the PSI of the test area is reduced by about 0.6 for the 1966 value and slightly less than 0.6 for the 1965 value. However, the decrease in pavement roughness from 1965 to 1966, when used in the PSI formula, indicates that the PSI has increased from 1965 to 1966. These data suggest that some other measure of pavement serviceability is needed for this project.

SUGGESTED FUTURE RESEARCH

Based on data from the test installation, the following suggestions are submitted for consideration in future research on expansive concretes:

1. To attain uniform longitudinal prestress in the pavement slabs, some type of positive anchorage should be provided along the reinforcing wires. Professor Alex Klein suggested attaching slotted washers at various intervals on the longitudinal reinforcement. Klein also thought that there should be a better distribution of steel in the cross-sectional area of the pavement, with more strands used to achieve a given area.

To fully utilize the potential of an expansive cement to develop prestress, additional data are needed on type and percentage of reinforcement, bond strength of the resultant

TABLE 5

ESTIMATED PAVEMENT SERVICEABILITY INDEX AND EQUIVALENT 18-KIP AXLE LOADS

Year	PSI*	Pavement Roughness (in./mi)	Estimated Equivalent 18-Kip Loads**		18-Kip Loads	
			D = 6 in.	D = 9 in.	D = 6 in.	D = 9 in.
1963	2.81	182	—	—	—	—
1965	2.84	177	97,400	92,600	—	—
1966	2.98	162	95,900	87,900	193,300	185,500

*PSI = 5.34 - 1.70 (2.16 log R - 3.39). R = pavement roughness (in./mi, BPR-type roughometer).
**p = 2.5.

concrete, optimum spacing of intermediate anchorages, and accurate information on the percentage of expansion and rate of gain of strength under field conditions.

2. Slab lengths of 500 ft are too long. Klein indicated a preference for slab lengths of 175 to 225 ft with filler sections placed between adjacent prestressed sections. The difficulties encountered in this test installation do not permit an evaluation of the optimum slab length, but the full-width transverse cracking that developed indicates that the most effective slab length is less than 500 ft. It could be anticipated that economic considerations would be of primary importance in determining an optimum slab length.

3. This project has provided field experience with expansive cement concrete highway construction. The data in this report suggest that the test slabs are now performing in a manner similar to continuously reinforced concrete pavements. However, the following questions have not been answered: (a) Will the transverse cracks in the test area, which have caused the joints to close prematurely, create sufficient strain in the longitudinal cables to stabilize the joint closure? or (b) Will the increase in crack width create localized compressive failures in the test slabs? It is the intent of future observations on this project to answer these questions.

REFERENCES

1. Dougan, Charles E. An Experimental Self-Stressing Concrete Pavement: I. Construction Report. Highway Research Record 112, pp. 55-81, 1966.
2. Gustaferro, A. H., et al. Expansive Concrete—Laboratory Tests of Freeze-Thaw and Surface Scaling Resistance. Jour. PCA Research and Development Laboratories, Vol. 8, No. 1, pp. 10-36, Jan. 1966.
3. Monfore, G. E. Properties of Expansive Cement Made With Portland Cement, Gypsum, and Calcium Aluminate Cement. Jour. PCA Research and Development Laboratories, Vol. 6, No. 2, pp. 2-9, May 1964.
4. Instructional Memorandum 50-1-65. U. S. Bureau of Public Roads.
5. AASHO Recommended Guide for Design of Flexible Pavement Structures. AASHO Committee on Design, Oct. 1960.
6. Irick, Paul E. An Introduction to Guidelines for Satellite Studies of Pavement Performance. NCHRP Rept. 2, 1964.
7. Irick, Paul E., and Hudson, W. Ronald. Guidelines for Satellite Studies of Pavement Performance. NCHRP Rept. 2A, 1964.
8. Yoder, Eldon J., and Milhous, R. T. Comparison of Different Methods of Measuring Pavement Condition: Interim Report. NCHRP Rept. 7, 1964.
9. The AASHO Road Test: Report 5—Pavement Research. HRB Spec. Rept. 61E, 1962.
10. The AASHO Road Test: Proceedings of a Conference Held May 16-18, 1962, St. Louis, Missouri. HRB Spec. Rept. 73, 1962.
11. Zevin, Israel. Lane Distribution of Traffic on 4-Lane Divided Highways in Connecticut. Connecticut State Highway Department, Oct. 1961.
12. Timms, Albert G. Friction Reducing Mediums for Rigid Pavement Subbases. Public Roads, Vol. 33, No. 6, Feb. 1965.

Performance of Continuously Reinforced Concrete Pavement in Texas

HARVEY J. TREYBIG, Highway Design Division, Texas Highway Department

This is a summary of the performance of continuously reinforced concrete pavement in Texas. The performance of pavement test sections with varying subbase, subgrade, and slab thickness characteristics is evaluated in terms of steel strain, deflection, crack pattern, pumping, and traffic. Data collection and analysis techniques were essentially the same as those used at the AASHO Road Test but with appropriate modifications for the continuously reinforced concrete pavement. Empirical equations developed by using regression techniques are modified for use as design tools.

Results indicate that each of the parameters mentioned affects the performance of continuously reinforced concrete pavement in some way. Pavement type, pavement thickness, subbase type, and subgrade were all found to affect deflection. Pavements with 0.5 percent longitudinal steel perform satisfactorily as true continuous pavements, i.e., good load transfer is obtained.

The crack pattern development is related to pavement age, subbase friction, concrete flexural strength, and curing temperature. Crack distribution in a given pavement length indicates performance. A normal distribution reflects satisfactory performance while a skewed distribution reflects unsatisfactory performance.

Based on percentage evaluation, twice as many jointed pavements as continuous pavements were found pumping. If not protected, lime-stabilized subbases may pump. Asphaltic concretes with high asphalt content or good surface treatments will protect stabilized subbases. Signs of pumping are not always proof that the subbase is being eroded.

The present serviceability indexes of CRC pavements in Texas follow the trend of the AASHO equations but with a somewhat lower initial PSI. CRC pavements are performing with a significantly higher PSI than are jointed concrete pavements with the same number of equivalent 18-kip axle applications.

•THE FIRST continuously reinforced concrete pavement (CRCP) was built in Texas in 1951. At the time, it was in use in several other states on a small scale, and more was built as the Interstate Highway System got under way.

By 1960 research studies were started to evaluate the performance of continuously reinforced concrete pavement. One of these studies was initiated in 1963 by the Texas Highway Department in cooperation with the Bureau of Public Roads. In very general terms, the objective of this research effort was to determine the performance characteristics of continuously reinforced pavement under varying conditions of subbase support, subgrade, and pavement thickness.

In addition to this final report, seven others have been published on some portion of the research. The first report (1) gave a detailed account of equipment and procedures developed for the large research study. A later report was on an experimental pavement built in 1964 (2). A deflection study of two pavements (3) reported the response

Paper sponsored by Committee on Rigid Pavement Design and presented at the 48th Annual Meeting.

of the pavements as measured by deflection and radius of curvature and compared the effects of percent steel, load, concrete modulus of elasticity and crack spacing. A detailed analysis of deflection in terms of slab temperature differential, crack spacing, crack width, and soil support (4) was based on data taken from three different pavements recorded around-the-clock to get all effects of temperature. The climax to the performance study of CRCP in terms of load-deflection studies contained deflection data gathered from 45 different pavements located throughout the state (5). A 1966 report on a laboratory study of the relationship of deflection and modulus of elasticity found that the relationship of deflection to modulus of elasticity under certain conditions was not always consistent with accepted theory. Finally, a recent report (7) compared data collected and analyzed on this project with theoretical methods of slab analysis now being developed at the University of Texas (8).

PERFORMANCE

The performance of a pavement is a measure of its accumulated service or the adequacy with which it serves its purpose. Pavement performance in its most general sense is usually measured or specified with an index value as suggested by Carey and Irick (9). In this research study pavement test sections were evaluated and pavements of varying designs were studied for their relative performance and their performance in terms of the present serviceability index (PSI). Relative performance was measured or indicated by steel strain, deflection, crack pattern, pumping, and traffic.

Steel Strain

Based on a very limited amount of steel-strain data collected in this investigation, no significant relationship was found between performance and the amount of longitudinal reinforcing steel in pavements of similar design (2). Investigations prior to this one indicated extremely high stresses in the longitudinal steel when Type III cement is used (11). Specifications now also limit the fineness of cement.

Deflection

Pavement deflection or response to load indicates the relative performance of pavements of different design. Different subgrades were evaluated in terms of deflection (5). In Figure 1 the relative performance of poor, fair, and good subgrades is shown in terms of deflection. Also indicated in Figure 1 is the relative performance of the three subbases shown. The low deflection of the fine-grain subbase on the fair subgrade was a case where the subgrade was stabilized with lime. Lime stabilization of the subgrade was not part of the experiment factorial. Stabilization of the subgrade with lime is a widely used technique for developing a construction platform in areas of the state where subgrades are very wet.

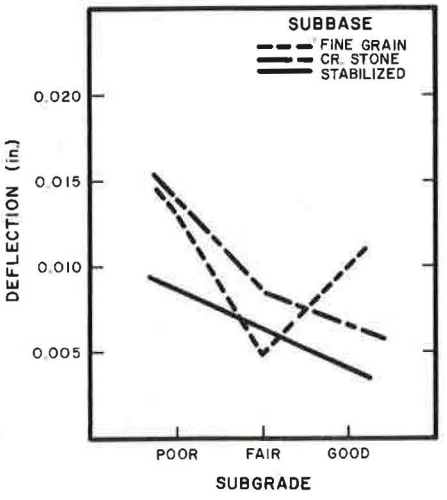

Figure 1. Relative performance of subbases and subgrades.

Because of results with lime-stabilized subgrades, it is believed that the lime-treated subgrade actually performs like an additional subbase layer in terms of response to static load. Therefore, a soil support term was formulated to correlate deflections on different foundations (4). It is defined as follows:

$$SS = \frac{U_1 + U_2}{T_{sg}}$$

where

SS = soil support,
U_1 = seven-day unconfined compressive strength of subbase,

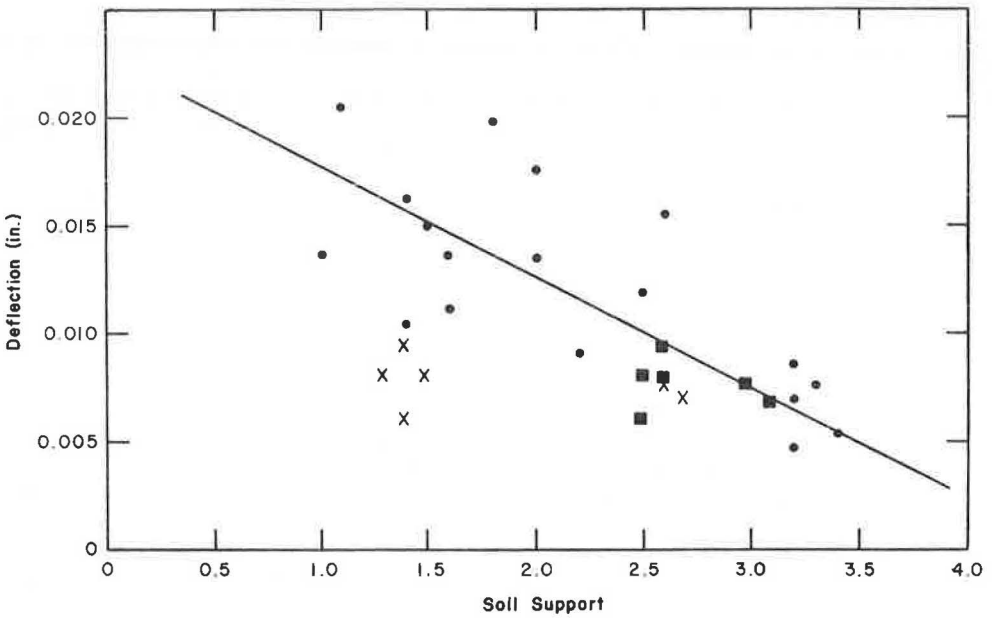

Figure 2. Deflection as a function of soil support.

U_2 = seven-day unconfined compressive strength of lime-stabilized subgrade, and
T_{sg} = Texas triaxial classification of subgrade material.

In Figure 2 the X data points represent pavements that have lime-treated subgrades. The soil-support value for these pavements was modified to include the treated subgrade layer as a second subbase. After inclusion in the soil support, the X data points moved to the positions shown as squares. Now the squares and circles form the data set that displays the relation of deflection to soil support shown. Thus, the lime-treated subgrade layers do strengthen the pavement system. However, this additional strength is usually not considered in the design stage. Usually the stabilization with lime is primarily for developing a workable subgrade or a construction platform.

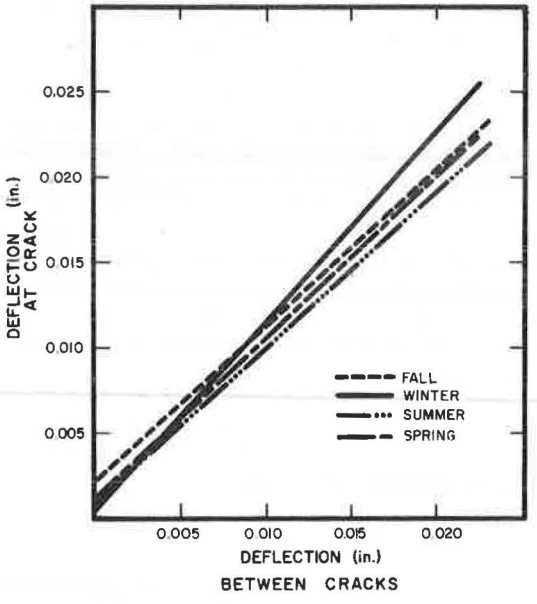

Figure 3. Comparison of deflection at and between cracks.

Deflection measurements were also used to compare measured responses at cracks and at midpoints between cracks on the continuously reinforced concrete pavement. The continuity in the CRCP or load transfer across the volume-change cracks is measured by the comparison shown in Figure 3. The lines in Figure 3 are regression lines for data taken at and between volume-change cracks. Each of the four lines represents data recorded in one of the four seasons of the year (5). Note that the lines are nearly 45 deg and that the intercept is very small—smaller than the resolution of

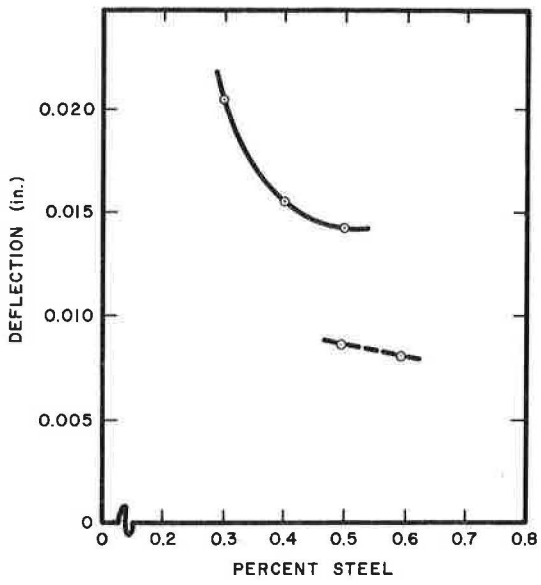

Figure 4. Relationship of percent steel to deflection.

the Benkelman beam. The design of the longitudinal reinforcing steel was identical in all of the pavements from which the data in Figure 3 were gathered. It is apparent from a deflection standpoint that the 0.5 percent steel design was performing satisfactorily at the time of this investigation.

The deflection-percent steel relationship has been investigated on two experimental paving projects where more than one steel design was used. Figure 4 shows the relationship of steel percentage to deflection on two projects. The subbases and subgrades for these two projects were entirely different. This accounts for the vertical placement of the two data sets, i.e., data from two different populations. From Figure 4 it is believed that increases beyond 0.5 percent steel will probably not decrease deflection a significant amount. Thus, a design with more than 0.5 percent steel will have a small amount of built-in insurance.

The response of pavements with different slab thickness was measured by deflection. As expected, thinner slabs deflected more than thicker ones (5). Data in Figure 5, collected from pavements of identical design except for the slab thickness compare satisfactorily with other research and theory.

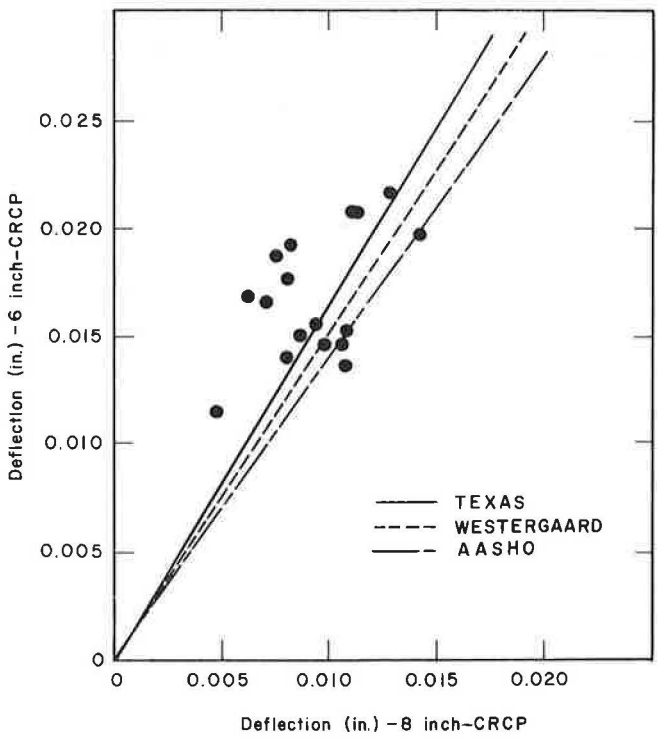

Figure 5. Comparison of deflection of 6- and 8-in. CRCP.

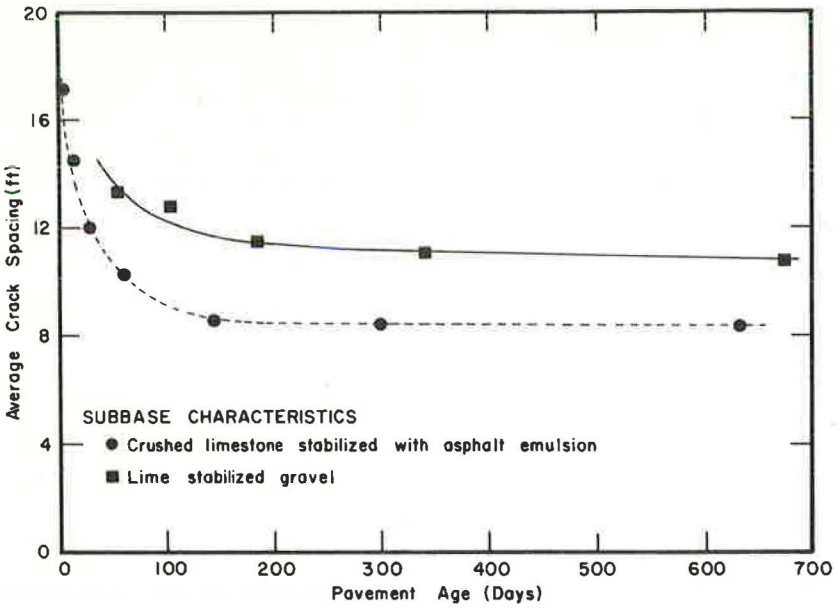

Figure 6. Relationship of pavement age to average crack spacing.

Crack Pattern

The development of the random crack pattern in CRCP is very complex. It is affected by the tensile strength of the concrete, percent steel shrinkage, curing temperature, friction between concrete and subbase, and the uniformity and homogeneity of the paving concrete.

Crack pattern development with time is shown in Figure 6. The two pavements shown are identical in design except for the subbases. Both pavements were built under the same contract and are adjacent to one another. The solid line represents a CRCP with 0.4 percent longitudinal steel (deformed wire mat) on a lime-stabilized gravel subbase. The dashed line shows the same pavement on a subbase of crushed limestone stabilized

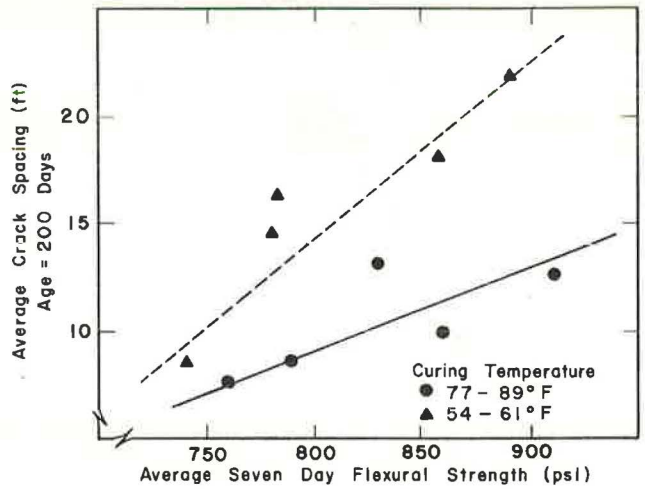

Figure 7. Relationship of flexural strength to crack spacing.

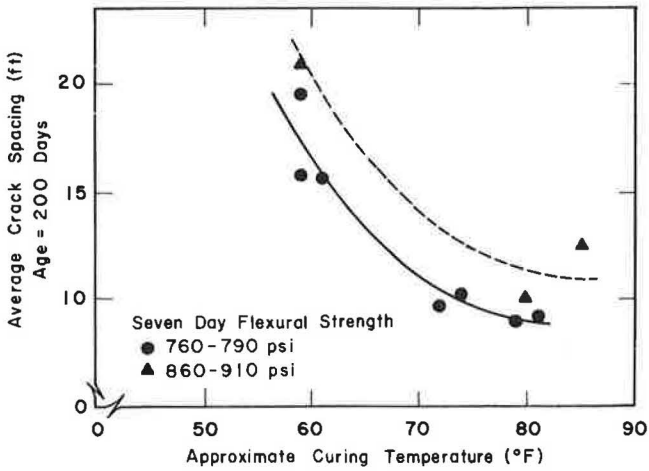

Figure 8. Relationship of curing temperature to crack spacing.

with asphalt emulsion. At 600 days, the pavement on the asphalt-treated subbase had a crack spacing 23 percent less than that of the pavement on the lime-stabilized gravel. This difference in crack spacing can be attributed to the difference in subbase friction or resistance to movement.

The concrete tensile strength also affects the cracking pattern. A tensile test is not used for job control in Texas. Midpoint-loading flexural strengths are determined, however, because there is a correlation between the tensile and flexural strengths of concrete. Thus, in Figure 7 for two different curing conditions, the seven-day flexural strength is related to the average crack spacing at a pavement age of 200 days (12).

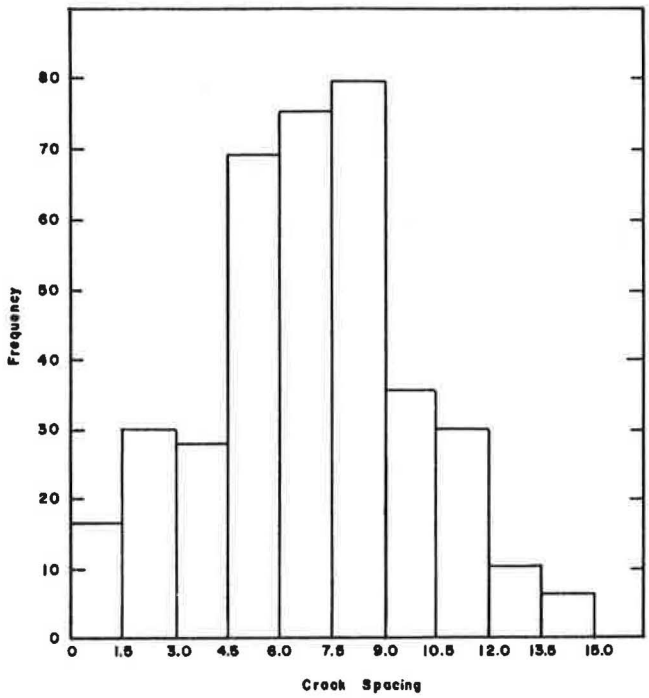

Figure 9. Distribution of crack spacings in a pavement with satisfactory performance.

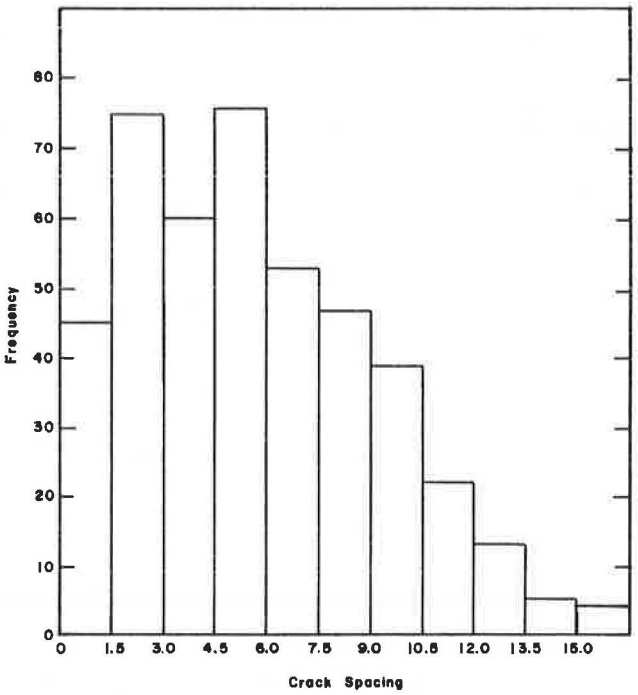

Figure 10. Distribution of crack spacings in a pavement with unsatisfactory performance.

C- CRCP
J- JCP

Numbers indicate degree of pumping: 1-heavy 3-trace 5 - no pumping
2-moderate 4-clear water

SUBGRADE SUPPORT	SUBBASE TYPE	SUBBASE MATERIAL	3,500,000 PSI CONCRETE FLEXURAL STRENGTH			5,500,000 PSI CONCRETE FLEXURAL STRENGTH		
			LOW 580 PSI(-)	MEDIUM 580-690 PSI	HIGH 690 PSI(+)	LOW 580 PSI(-)	MEDIUM 580-690 PSI	HIGH 690 PSI(+)
POOR 5.5+	NON-STABILIZED	FINE GRAIN		C-5 J10-2			C-2	
		CRUSHED STONE		C-2, C-2 J9-3, J10-5			C-5 J8-1, J9-5, J10-3	C-2
	STABILIZED	CEMENT					C-2 , C-5	C-3
		ASPHALT		C-3				
		LIME	C-5	C-5				
FAIR 5.0-5.5	NON-STABILIZED	FINE GRAIN		C-5			C-5 J8-1	
		CRUSHED STONE		C-5 J10-3			J9-3, J10-1	
	STABILIZED	CEMENT					C-5 , C-5	
		ASPHALT		C-5				
		LIME		C-5				
GOOD 4.0-5.0	NON-STABILIZED	FINE GRAIN		C-1 J10-3			C-2, C-2 J9-5	
		CRUSHED STONE		C-3 J9-5, J10-1			C-5 J8-1, J9-5	C-2
	STABILIZED	CEMENT		C-5			C-5, C-5 J9-3, J10-2	C-5
		ASPHALT		C-5				
		LIME		C-5				

Figure 11. Pumping data from concrete pavement.

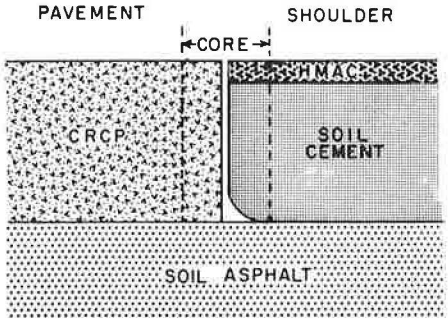

Figure 12. Cross section of pavement-shoulder joint.

As concrete strengths go up and curing temperatures go down, wider crack spacings result.

The ambient temperature, i.e., curing temperature of the pavement, also affects the crack spacing significantly, as shown in Figure 7 where the slope of the lines is a measure of the curing temperature. Figure 8 shows that as the temperature of pavement reduces, the crack spacing approaches infinity, i.e., spacings much larger than the optimum of 5 to 8 feet. Data in Figures 7 and 8 are from one construction project.

The distribution of crack spacings in a given length of pavement is a good indicator of performance. Crack-spacing data shown in Figure 9 approach a normal distribution and reflect satisfactory performance. Cracking patterns such as these are representative of the random crack pattern desired in CRCP. The data are from a pavement test section 2,500 ft long. A distribution like this can only be obtained with uniform, homogenous, well-consolidated concrete. Figure 10 shows a crack-spacing distribution on a pavement test section also 2,500 ft long where the concrete was neither uniform, homogenous, nor well consolidated. Extensive areas of unconsolidation were present, and most of the cracks formed over the transverse steel, which is spaced on 2-ft centers. This is reflected in the skewed distribution. The frequency is very high for the range from 1.5 to 3.0 ft. In general, the normal distribution indicates satisfactory performance, and the skewed distribution reflects unsatisfactory performance.

Pumping

Loss of uniform support under a rigid pavement usually causes distress in a pavement slab when heavily loaded. A survey of test sections selected for this investigation indicated that pumping was not a problem on pavements with stabilized subbase layers. Figure 11 shows a qualitative evaluation of the pumping found on some of the test pavements selected for the overall experiment, both jointed and continuously reinforced.

Other experience in Texas with lime-stabilized subbases directly under CRCP has been somewhat unsatisfactory. Lime-treated soil apparently loses some of its integrity when it becomes wet. After wetting it erodes and pumps like a fine-grained material.

Signs of pumping, such as water movement and material deposited on a paved shoulder, do not always indicate true pumping, i.e., removal of foundation from beneath the portland cement concrete pavement slab. Some pavements with sound, stabilized subbases have shown signs of pumping. For example, an 8-in. CRC pavement with an asphalt-stabilized subbase showed severe signs of pumping. The pavement had cement-stabilized shoulders with shoulder surfacing of 1-in. asphaltic concrete. The pavement edge was cored. It was found that when the shoulder base material was stabilized with cement, a small portion in the corner between the blanket subbase and the edge of the slab was either not mixed with cement or not compacted. It was this material that was being forced out by the pumping action of water in the joint between the shoulder and the slab. Figure 12 shows what was found. A careful examination of the core holes showed the small channel where the loose material had all been removed.

Traffic

Since the test sections for this project were selected at the inception of the project, the traffic load applications have been estimated several times. Data were collected for one direction only from the date of completion to the time of data collection.

The total data for one direction in reality forced all traffic into one lane as far as the number of 18-kip applications is concerned. This may be reasonable because

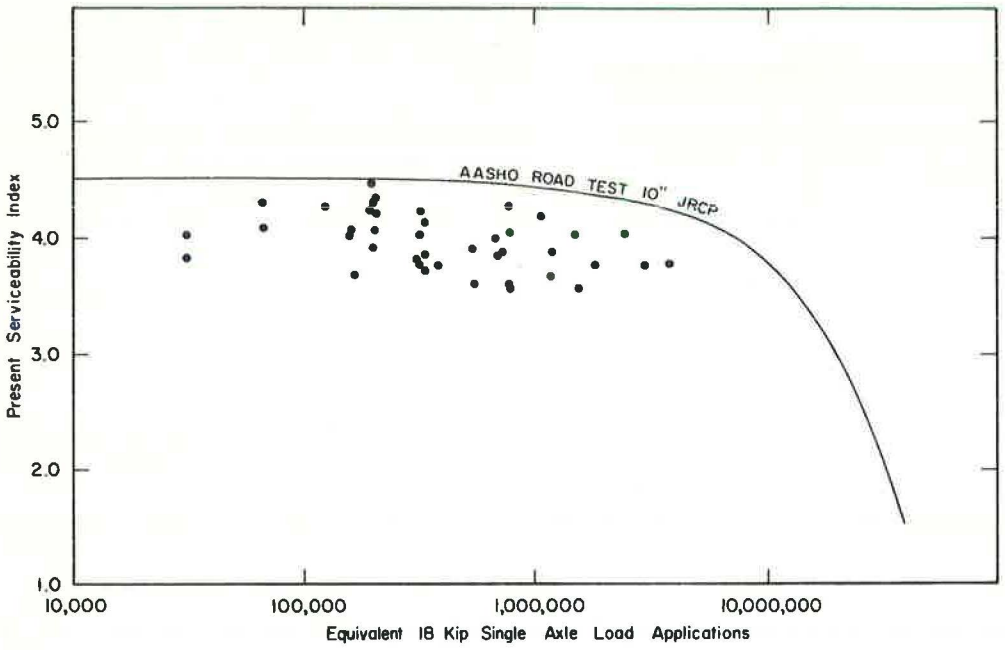

Figure 13. Comparison of performance of 8-in. CRCP with AASHO performance equation for 10-in. jointed rigid pavement.

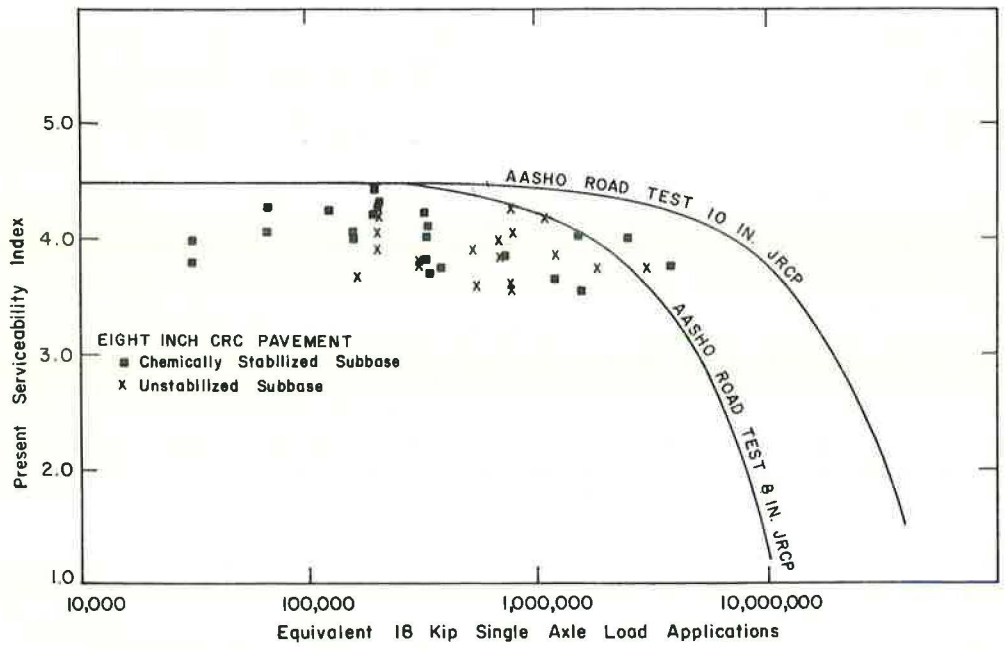

Figure 14. Comparison of performance of pavements with stabilized and unstabilized subbases with AASHO performance equations.

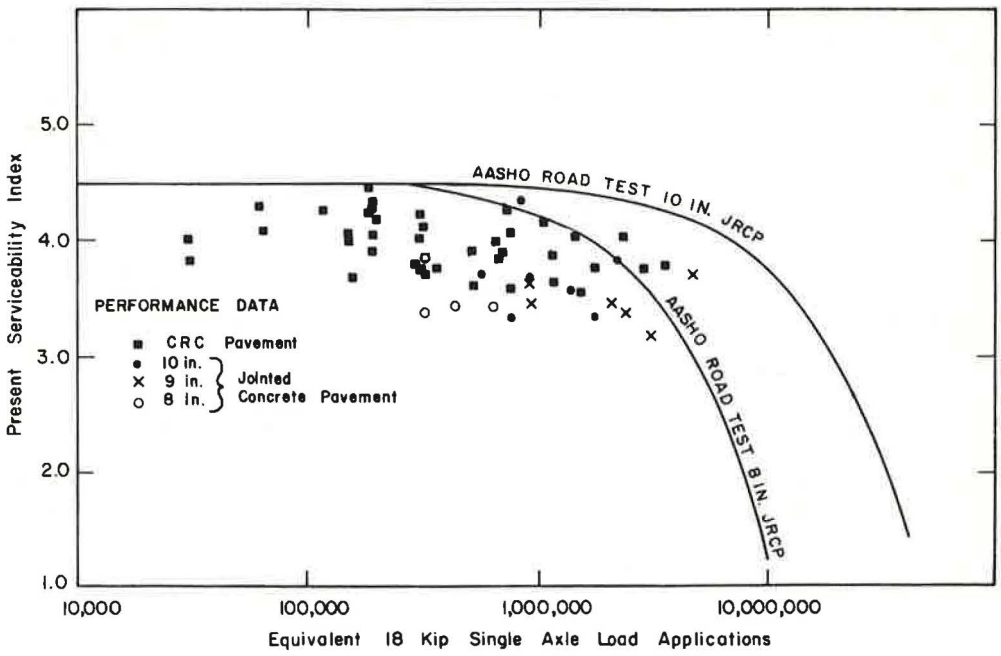

Figure 15. Comparison of performance of jointed and continuous pavements with AASHO performance equations.

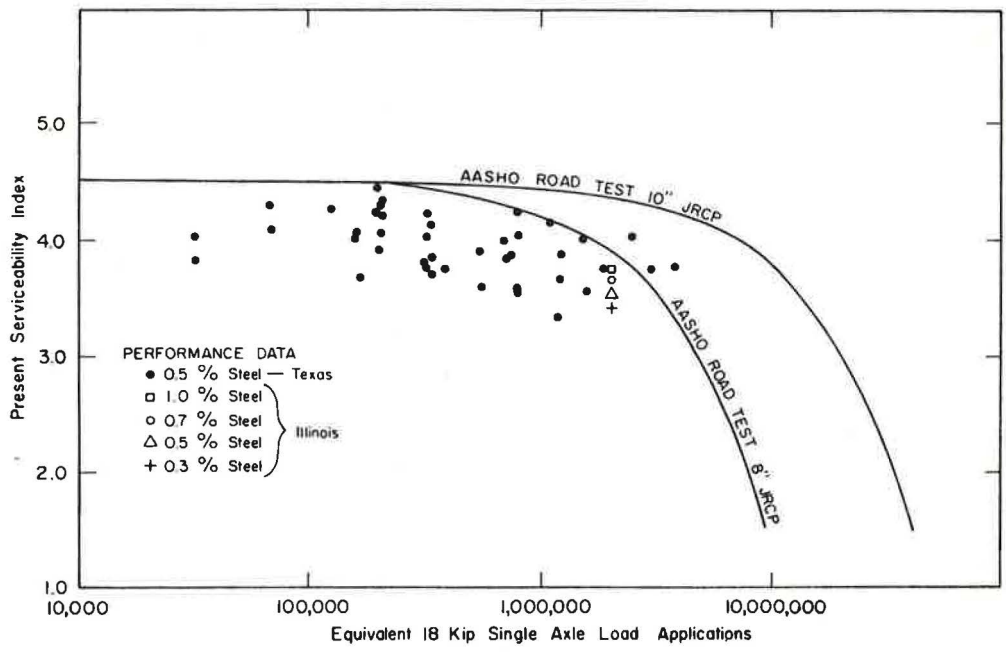

Figure 16. Comparison of performance of 8-in. CRCP in Texas and Illinois with AASHO performance equations.

almost all the test sections were on roadways with two traffic lanes in each direction, and heavily loaded vehicles usually travel the outside lane where all test sections are located.

The pavement serviceability-performance concept developed at the AASHO Road Test relates the traffic load application to a performance index known as the present serviceability index (13). The CHLOE profilometer was used to determine the PSI of each test section in the experiment. Only one value of PSI was obtained for each section; the PSI's immediately after construction were unknown.

Because the test sections are all about the same age, a relative comparison of PSI's is reasonably valid. The limited data indicate that the average relationship of PSI to traffic for the sections was in the range of 4.0 to 4.2. These pavements were all three to six years old at the time of measurement. Even so, this does indicate the ability of continuously reinforced concrete pavement to maintain a high level of serviceability.

For the test sections in this experiment, corresponding PSI and traffic data were assembled and are shown in Figure 13. All pavements in the experiment factorial are shown with no attempt to differentiate between pavements of different design. The line represents the AASHO equation that related the PSI of a 10-in. jointed reinforced concrete pavement to traffic. The initial PSI of rigid pavements at the AASHO Road Tests was 4.5, and thus the line passes through 4.5 on the vertical axis on the semilog graph of PSI and traffic.

Figure 14 shows similar data except that a differentiation is made between pavements with stabilized subbases and pavements with unstabilized subbases. Data are inconclusive.

Figure 15 compares the performance of jointed and continuously reinforced pavements. The sample of jointed pavements is smaller than that of the continuously reinforced. The observations do indicate that in Texas the continuously reinforced pavement is performing with a higher serviceability index than is the jointed concrete pavement. The lines on this figure again represent the AASHO correlation of traffic to serviceability index for 8- and 10-in. jointed reinforced concrete pavements.

Figure 16 compares the performance of 8-in. continuously reinforced concrete pavements in Texas and Illinois (14). The Illinois data are from pavements having a range of 0.3 to 1.0 percent longitudinal steel.

These four figures indicate that the AASHO equations cannot be applied directly because they predict a higher level of performance than that determined from in-service pavements. This was also the finding of an investigation on pavements in Illinois (14). The trend of loss in serviceability with increased traffic is correct and valid. However, the PSI's measured for this investigation indicate that the average initial PSI after construction is something less than the 4.5 measured at the AASHO Road Test.

DESIGN

The research in this study led to the development of several empirical equations. In each case the equations were statistical models that correlate the parameters involved. The symbols used in these equations are defined as follows:

- S = stress in longitudinal steel (plus is tension);
- E_c = compressive modulus of elasticity of concrete;
- α_c = coefficient of thermal expansion for concrete;
- ΔT = change in slab temperature from time in question to time of concrete placement;
- $\overline{X}$ = average crack spacing, ft;
- P = percent longitudinal steel;
- Z_c = shrinkage, in./in.;
- ΔZ = change in shrinkage, in./in.;
- ΔX = crack width in concrete, in.;
- K_1 = constant equal to 1.468;
- K_2 = constant equal to 2.553;
- D_c = edge deflection at a crack in CRCP, in.;

D = slab thickness, in.;
T = slab temperature differential, deg F;
T_{sg} = Texas triaxial classification of subgrade material;
L = 18-kip single axle load;
SS = soil support;
U_1 = seven-day, unconfined compressive strength of subbase, psi; and
U_2 = seven-day, unconfined compressive strength of lime-stabilized subgrade, psi.

From the study of steel strain the following model was developed for stress in the longitudinal steel (2):

$$S = A_1 + A_2E_cZ_c + A_3E_cZ_c\left(\frac{1}{P}\right)^2 + A_4E_c\alpha_c\Delta T + A_cE_c\alpha_c\Delta T\left(\frac{\bar{X}}{P}\right)^2 \quad (1)$$

where A_1, A_2, A_3, A_4, and A_5 are constants that were determined from the data.

Equation 1 can be solved for P, the percent longitudinal steel. Thus it takes the form

$$P = \left[\frac{A_3E_cZ_c + A_5E_c\alpha_c\Delta T\bar{X}^2}{S - (A_1 + A_2E_cZ_c + A_4E_c\alpha_c\Delta T)}\right]^{0.5} \quad (2)$$

An additional result of the stress and concrete movement investigation was an empirical equation for crack width in the concrete (2). Model number DK1 has been selected for this exhibit. It follows as

$$\Delta X = \frac{\bar{X}(\Delta Z + \alpha_c\Delta T)}{e^{K_1P}} \quad (3)$$

where K_1 is a constant determined from the data.

From the analysis of the load-deflection data collected in this research study, the final result was an empirical equation or model that correlated the parameters in the study to the deflections measured in the field (4, 5).

The first study evaluated the effects of temperature and crack spacing, and the second, a statewide investigation, determined the effect of subbase, subgrade, and materials properties. The final model for predicting the edge deflection of a CRC pavement was

$$D_c = \frac{A_0L\ 10^{B_5\Delta X}\ \bar{X}^{B_4}\ T_{sg}^{0.25B_3}}{D^{1.75}\ E^{B_2}\ U^{0.25B_3}\ 10^{0.0147T}} \quad (4)$$

where A_0, B_2, B_3, B_4, and B_5 are constants determined from the data.

Equation 4 could be rearranged so that a solution for D, slab thickness, could be obtained. Thus the equation would take the form

$$D = \left(\frac{A_0L\ 10^{B_5\Delta X}\ \bar{X}^{B_4}\ U^{0.25B_3}\ T_{sg}^{0.25B_3}}{D_c\ E^{B_2}\ U^{0.25B_3}\ 10^{0.0147T}}\right)^{0.571} \quad (5)$$

Thus two empirical equations have been formulated that may serve as design aids. First, Eq. 2 displays the percent of longitudinal steel in terms of the material properties of the concrete, environment, and stress. The values for the constants are as follows:

$$P = \left\{\frac{E_c(2.46\ Z_c - 0.002\ \alpha_c\Delta T\ \bar{X}^2)}{S - [3{,}400 - E_c(18.22\ Z_c + 27.79\ \alpha_c\Delta T)]}\right\}^{0.5}$$

By having the concrete modulus of elasticity, coefficient of thermal expansion for concrete, range of temperature from construction to extreme cold temperature, shrinkage

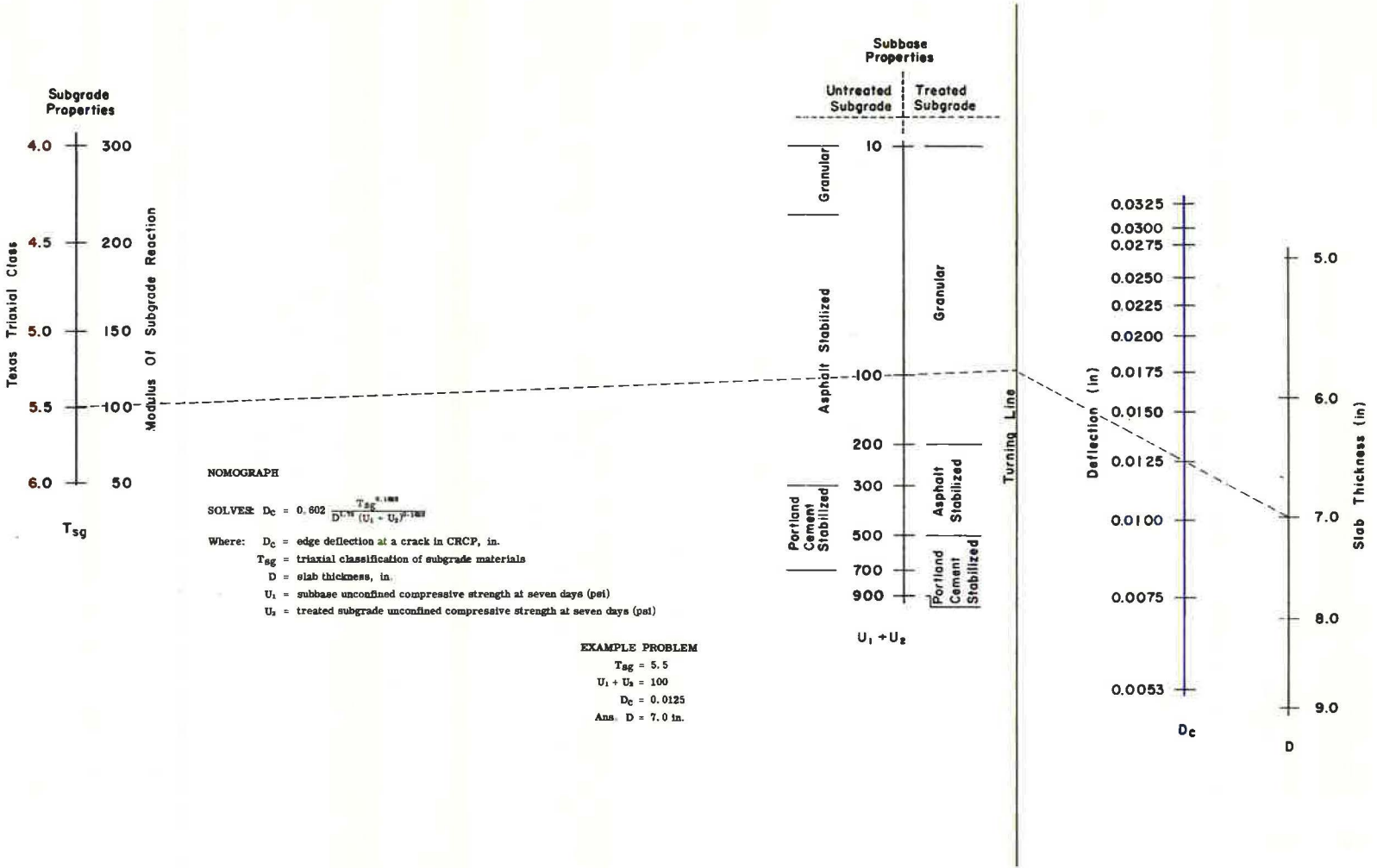

Figure 17. Design chart for CRC pavement.

of concrete, and desired crack spacing, the necessary percentage of steel can be computed. An example problem is solved in the Appendix.

Slab thickness may be determined from Eq. 5. The slab thickness would be based on a static load condition and a maximum allowable edge deflection. Equation 7 is Eq. 5 with constants substituted:

$$D = \left(\frac{0.378L \ 10^{6.341\Delta X} \ \overline{X}^{0.027} \ T_{sg}^{0.163}}{D_c \ E^{0.168} \ U^{0.163} \ 10^{0.0147T}} \right)^{0.571} \tag{7}$$

The value of crack width, ΔX, may be computed from Eq. 3, rewritten here as Eq. 8:

$$\Delta X = \frac{-X(\Delta Z + \alpha_c \Delta T)}{e^{1.468P}} \tag{8}$$

or it may be computed from the following equation, which was also developed along with Eq. 8:

$$\Delta X = \frac{-\overline{X}(Z + \alpha_c \Delta T)}{1 + K_2 P} \tag{9}$$

where $K_2 = 2.553$.

Either Eq. 8 or Eq. 9 will give a satisfactory answer; however, Eq. 8 is recommended.

Axle load, L, in Eq. 7 was replaced by 18 since the load used in the experiment was 18 kips. For design it may be desirable to use a temperature differential, T, equal to zero. Thus, other than the allowable deflection, only strength parameters need to be determined.

The allowable deflection, D_c, is a subject that may be conjectured. A deflection of 0.012 in. has been suggested for design purposes where the average of the single axle loads is in the neighborhood of 15,000 lb (15). Based on the AASHO Road Test, a reinforced jointed concrete pavement after being fatigued with 7,000,000 18-kip equivalencies should have an edge deflection of about 0.014 in. at PSI of 2.5. It is believed that CRCP performs equally well and better than JCP in Texas; thus, based on the fatigue relationship, the 0.014 in. may be considered for CRC pavement (13).

For design purposes a maximum allowable deflection of 0.012 in. is recommended at this time. This is the most conservative figure in the available literature. The 0.012 in. is also satisfactory from the standpoint of experience in having measured deflections on many CRC pavements of varying design and service level.

Figure 17 is a graphical solution of Eq. 4. The nomograph may be used to solve for slab thickness with the following parameters being known: subgrade triaxial classification, subbase unconfined compressive strength at seven days, and maximum allowable deflection. In the development of the nomograph in Figure 17 the parameters in Eq. 4 were assigned the following values:

$X = 5.0$ ft
$\Delta X = 0.010$ in.
$T = 0$
$L = 18$ kips
$E = 5.5 \times 10^6$ psi

SUMMARY

This performance study of continuously reinforced concrete pavement encompassed a wide variety of environmental elements. The pavements studied were located throughout the state. This research effort was conducted over a period of five years, during which much data were collected, many analyses made, and numerous reports written.

The following conclusions are for the entire research study and include some that are repeated from earlier reports on this project. In general they summarize the relative performance of continuously reinforced concrete pavement as evaluated in this investigation.

1. Steel Strain—Temperature stresses are a direct function of the concrete's modulus of elasticity and coefficient of thermal expansion. Stress is an inverse function of percent longitudinal steel. It is a direct function of the spacing of volume change cracks and of concrete shrinkage.
2. Deflection—Pavements with good subgrades deflected less than those with poor subgrades. Pavements with lime-stabilized subgrades performed better than identical pavements with no subgrade treatment. In pavements with 0.5 percent steel and having a wide variation of support and environmental conditions, the transverse cracks were small enough to retain sufficient aggregate interlock to maintain approximately 100 percent load transfer. Pavements with more steel respond more favorably; however, beyond the 0.5 or 0.6 percent point, additional steel will not decrease deflection significantly. The relationship of slab thickness to deflection determined from this research is in agreement with accepted theory and other research. Pavements with stabilized subbases are superior to those with unstabilized subbases.
3. Crack Pattern—There is a relationship between pavement age and crack pattern on an individual project basis. The flexural strength of the concrete has a direct effect on the crack spacing; it is also affected by the subbase friction and is related to the curing temperature. The distribution of crack spacings in a known length of pavement is an indicator of performance.
4. Pumping—Based on percentages, twice as many jointed concrete pavements as CRC pavements with similar subbases were found pumping. Lime-stabilized subbases will pump if they are not protected with a nonerosive surface. Signs of pumping are not always proof that a pavement's subbase is being eroded.
5. Traffic—The performance data show the trend set forth by the AASHO equations, but with a somewhat lower initial serviceability index. In Texas, CRC pavements show a significantly higher serviceability index than jointed concrete pavements. CRC pavements in Texas are performing well compared to others in this country.

ACKNOWLEDGMENTS

This research was conducted under the general supervision of T. S. Huff, former Chief Engineer of Highway Design, M. D. Shelby, former Research Engineer, Robert L. Lewis, former Research Engineer, now Chief Engineer of Highway Design, and John F. Nixon, Engineer of Research. The first three years of the research study were under the immediate direction of B. F. McCullough, former Supervising Design Research Engineer.

The author extends his thanks to the numerous District Engineers, Laboratory Engineers, and Resident Engineers who assisted and cooperated to make this endeavor possible.

REFERENCES

1. McCullough, B. F. Development of Equipment and Techniques for a Statewide Rigid Pavement Deflection Study. Research Rept. No. 46-1, Texas Highway Department, Jan. 1965.
2. McCullough, B. F., and Treybig, Harvey J. Analysis of Steel Stress and Concrete Movement on an Experimental Continuously Reinforced Concrete Pavement. Research Rept. No. 46-2, Texas Highway Department, May 1968.
3. McCullough, B. F. Evaluation of Single Axle Load Response on an Experimental Continuously Reinforced Concrete Pavement. Research Rept. No. 46-3, Texas Highway Department, April 1965.
4. McCullough, B. F., and Treybig, Harvey J. Determining the Relationship of Variables in Deflection of Continuously Reinforced Concrete Pavement. Highway Research Record 131, pp. 65-86, 1966.

5. McCullough, B. F., and Treybig, Harvey J. A Statewide Deflection Study of Continuously Reinforced Concrete Pavement in Texas. Highway Research Record 239, pp. 150-174, 1968.
6. McCullough, B. F., and Mays, Ivan K. A Laboratory Study of the Variables That Affect Pavement Deflection. Research Rept. No. 46-6, Texas Highway Department, Aug. 1966.
7. Treybig, Harvey J. Observation and Analysis of Continuously Reinforced Concrete Pavement. Research Rept. No. 46-7, Texas Highway Department, April 1968.
8. Stelzer, C. F., and Hudson, W. R. A Direct Computer Solution for Plates and Pavement Slabs. Research Rept. 56-9, Center for Highway Research, University of Texas, Austin, Oct. 1967.
9. Carey, W. N., Jr., and Irick, P. E. The Pavement Serviceability-Performance Concept. HRB Bull. 250, pp. 40-58, 1960.
10. Hudson, W. R., Finn, F. N., McCullough, B. F., Nair, K., and Vallerga, B. A. Systems Approach to Pavement Design. Unpublished report, NCHRP Project 1-10, March 1968.
11. Shelby, M. D., and McCullough, B. F. Determining and Evaluating the Stresses in an In-Service Continuously Reinforced Concrete Pavement. Highway Research Record 5, pp. 1-49, 1963.
12. Shelby, M. D., and McCullough, B. F. Experience in Texas With Continuously Reinforced Concrete Pavements. HRB Bull. 274, pp. 1-29, 1960.
13. The AASHO Road Test: Report No. 5—Pavement Research. HRB Spec. Rept. 61E, 1962.
14. The AASHO Road Test: St. Louis Conference Proceedings. HRB Spec. Rept. 73, 1962.
15. Hveem, F. N. Pavement Deflections and Fatigue Failures. HRB Bull. 114, pp. 43-87, 1955.

Appendix

EXAMPLE PROBLEM—SOLUTION FOR PERCENT STEEL

The percent steel for a given set of conditions can be completed by using the empirically developed Eq. 6:

$$P = \left\{ \frac{E_C(2.46\ Z_C - 0.002\ \alpha_C\ \Delta T\ \overline{X}^2)}{S - [3{,}400 - E_C(18.22 Z_C + 27.79\ \alpha_C\ \Delta T)]} \right\}^{0.5}$$

For the following set of conditions the required longitudinal steel percentage is computed:

$E_C = 4.0 \times 10^6$ psi,
$Z_C = 100.0 \times 0^{-6}$ in./in.,
$\alpha_C = 5.0 \times 10^{-6}$,
$\Delta T = 50$ F,
$\overline{X} = 10$ ft, and
$S = 33{,}000$.

Substituting these values,

$$P = \left(\frac{4.0 \times 10^6 [2.46\ (100 \times 10^{-6}) - 0.002(5.0 \times 10^{-6})(-50)\ 10^2]}{33{,}000 - \{3{,}400 - 4.0 \times 10^6 [18.22\ (100 \times 10^{-6}) + 27.79(5.0 \times 10^{-6})(-50)]\}} \right)^{0.5}$$

Simplifying,

$$P = \left[\frac{4.0 \times 10^6\ (296 \times 10^{-6})}{33{,}000 - 3{,}400 + 20{,}504} \right]^{0.5} = \left[\frac{1{,}184}{9{,}096} \right]^{0.5} = 0.4 \text{ percent} \qquad \text{(Answer)}$$

Concrete Pavements With Continuous Reinforcement and Elastic Joints

BENGT O. E. PERSSON, Consulting Engineer, Täby, Sweden; and
BENGT F. FRIBERG, Consulting Engineer, St. Louis, Mo.

Attempts have been made to obtain the benefits of continuous pavement designs without the large amounts of steel in continuously reinforced and randomly cracked roads. The designs use weakened plane joints with steel ties crossing the joints (here called elastic joints) to form transverse hinges across the pavement. In common practice, contraction joints have been used intermittently as every fourth or fifth joint to avoid excessive stresses in the continuous steel in between.

Continuous pavements using elastic joints exclusively have been explored in Sweden. Controlled slab tension tests and joint-width measurements have given data on joint-cracking forces and movements and on full-section cracking. The effectiveness of different bar bond breakers and corresponding elastic joint forces was observed. An initial short highway installation indicated that 0.2 percent continuous steel and elastic joints could be used, with the bars coated with asphalt to prevent bond for a short distance under the elastic joints.

The highway installation was inspected after three years of use and found to be in excellent condition. No random cracks or other deterioration could be seen. Although traffic was light compared to that on American divided highways, a large percentage was trucks.

•CONTINUOUSLY reinforced concrete pavements have demonstrated that transverse cracks need not be detrimental to pavement performance. As usually built, the continuous steel is depended upon to cause closely spaced transverse cracks in pavement portions away from free ends. The tension forces transmitted by the steel across the cracks to the concrete must exceed the concrete tension strength to be effective for cracking at some critical early age; over 0.5 percent of steel section has been found to be necessary.

Some continuity across cracks is necessary, especially with respect to shear transfer, for satisfactory highway pavement performance. If cracks, or joints, become too wide, aggregate interlock may be lost, and faulting is a common and objectionable result in jointed pavements without doweling. In continuously reinforced pavements, a reasonably equal width of all cracks is assured by the uniformity of steel tension forces at adjacent cracks.

Continuous reinforcement, as generally used, maintains even crack widths because it has tension force capacity many times greater than the small forces needed to overcome variations in subgrade friction and crack-face tensions between short pavement elements. Any continuing functions of the large amounts of continuous steel are insignificant compared to its initial early-age objective—to promote cracking across the pavement section. In the mature pavement, crack widths at different temperatures appear

Paper sponsored by Committee on Rigid Pavement Design and presented at the 48th Annual Meeting.

to be directly related to crack spacing and temperature but not to the amount of steel. This indicates that cracks might be caused by less steel through the use of weakened planes across the pavement, resulting in substantial savings in steel quantities and possibly equally satisfactory performance. Elastic joint pavements are intended to meet this design objective.

ELASTIC JOINT PAVEMENTS

The term "elastic joint", as used in this report, refers to transverse joints across which steel ties connect the two pavement elements. As the elastic joint opens on decreasing temperature, the ties are strained in tension. Overstressing the steel at low temperatures is avoided by treating the parts nearest the joint to prevent bonding to the concrete. The steel then serves as an elastic tie across the joint.

Limited applications of elastic joint pavements have appeared in the United States, Switzerland, and Germany; in each case, free-moving contraction joints are employed at intervals. In Sweden elastic joint pavements have been investigated and applied to highway construction as fully continuous construction.

Limited forms of elastic joint pavements have been used in highway pavements in the United States. The Arkansas standard pavement design, in use since about 1955, consists of 45-ft reinforced pavement slabs between contraction joints, with two intermediate weakened-plane joints forming three 15-ft panels tied together by continuous wire mesh for the full 45-ft slab length. Examination of many miles of this pavement shows nearly complete absence of cracking and excellent performance.

A similar design used on Connecticut highways during the 1950's was less successful. It consisted of 100-ft mesh reinforced pavement slabs between expansion joints, with three intermediate weakened-plane elastic joints forming four 25-ft panels tied together by the continuous wire mesh. Some of the elastic joints have opened wide due to tension failure of the steel wires. The reason was determined to be increasing resistance to pavement contraction at the expansion joints as a result of dowels that rusted after some 5 to 10 years, and induced excessive tension in the longitudinal pavement reinforcement when temperatures decreased. Many expansion joints were immobilized at the narrow joint widths during summer temperatures, and the contraction and expansion functions were transferred to the failed elastic joints, which thereafter performed as undoweled expansion joints.

Elastic-joint pavements have been built as standard construction in Switzerland since about 1960, and in 1961 a test road using the design was laid in West Germany near Offenburg, between Karlsruhe and Baden-Baden. The pavements consist of 30-m (99-ft) slabs between contraction joints with three intermediate elastic joints forming four 7.5-m (25-ft) elements. All the joints are formed by a narrow strip of corrugated asbestos board on edge as base and a vibrated-in fiberboard joint crack guide at the top surface, including a 45-deg surface kerf cut. The elastic joints are tied across with 12-mm (½-in.) plain bars 1m (40 in.) long with end hooks spaced 40 cm (16 in.); the 70 cm (28 in.) at the center of each tie bar are coated with asphalt cutback. On the German test road of similar design, the observed maximum elastic joint openings were 0.8 mm (0.03 in.) average and 1.5 mm (0.06 in.) extreme width. The observed residual elastic joint openings averaged 0.02 mm (0.008 in.). The observed maximum openings at the contraction joints were 10 mm (0.40 in.).

CONTINUOUSLY REINFORCED PAVEMENTS WITH ELASTIC JOINTS

The investigations in Sweden are of particular interest because their objective is the development of fully continuous pavements (1, 2, 3). The investigations covered:

1. Pullout bond tests of plain bars with different treatments;
2. Controlled tension tests of narrow slabs on subgrades, with different dimensions of weakened-plane crack starters to determine the joint-cracking and slab-cracking forces and the relationship between tension forces and crack openings for bars variously treated at the elastic joints; and

3. Performance of an exploratory highway pavement installation after two years of use, consisting of 340 ft of 6.3-in. thick pavement with elastic joints spaced 13.5 to 20 ft and reinforced with 0.2 to 0.4 percent of continuous plain bars, including joint width measurements of the elastic joints.

The controlled tension tests were made at a site near Stockholm. The exploratory highway was installed in 1964 on European expressway E4/E6 in southern Sweden. A second longer test road is in the planning stage. The tests were made from 1964 to 1966. All work is financed by the State Research Council.

PULLOUT TESTS

Initial data on slip resistance of plain round steel bars with different coatings were obtained from pullout tests on 32 concrete specimens with embedded bars, tested in tension. Concrete specimens 16 by 16 cm (6 by 6 in.) in cross section and 1 cm (40 in.) long were used. The 12-mm or 16-mm bar (0.47 in. or 0.63 in.) to be tested was embedded 50 cm (20 in.) in the center of the cross section and was pulled from one end. The concrete specimen was anchored by a heavy deformed bar similarly embedded and extended from the opposite end. Loads were observed for beginning slip, maximum slip resistance, and continuing sliding. The tests included bars uncoated and bars coated with cutback asphalt (RMA 15), epoxy, epoxy and sand, and an epoxy-tar formulation. Table 1 gives the test results in summary. Bar stress is given for initial slip and maximum resistance; bond stress for continuing slip is based on 50-cm (20-in.) embedment.

TENSION TESTS ON JOINTED SLABS ON SUBGRADE

An extensive series of applied-tension tests was performed on narrow slabs reinforced with continuous steel and provided with weakened-plane type joints placed on prepared subgrade. The slabs were 16 cm (6.3 in.) thick and 50 cm (19.7 in.) wide; 46 slabs were 5 m (16.4 ft) long with one weakened plane at midlength of most, and 6 slabs were 20 m (65.6 ft) long with three weakened planes at the quarter points. All slabs were placed on a sand base covered with a thin plastic film. The slabs were enclosed under temporary shelters as protection against weather and frost and were tested after about one-half year.

The continuous reinforcement consisted of two plain bars at a center depth of 12.5 cm (4.9 in.) from the sides, with diameters of 12, 16, and 19 mm (0.47, 0.63, and 0.75 in.), equivalent to 0.27, 0.47, and 0.67 percent reinforcement. In a majority of the slabs, the bars were coated with RMA 15 asphalt over a distance of 75 or 150 cm (29 or 59 in.)

TABLE 1

SUMMARY OF PULLOUT TESTS ON PLAIN BARS
(Average Values)

Coating and Bar Size	Initial Slip		Maximum Resistance		Continuing Slip			
	Bar Stress		Bar Stress		Bar Stress		Bond Stress	
	kp/cm²	psi	kp/cm²	psi	kp/cm²	psi	kp/cm²	psi
Uncoated bars								
12-mm (0.47 in.)	2,580	36,700	3,600	51,200	2,170	30,800	13	180
16-mm (0.63 in.)	1,390	19,800	2,760	39,200	2,140	30,400	17	240
Asphalt coated, RMA 15								
12-mm	150	2,130	450	6,400	300	4,720	1.8	26
16-mm	140	2,000	580	8,250	460	6,550	3.7	52
Various epoxy coatings (average)[a]								
12-mm	2,950	42,000	3,780	53,800	2,740	39,000	16	230
16-mm	1,860	26,500	2,850	40,500	2,320	33,000	19	260

[a]Two bars, which were coated with epoxy tar, are not included. They had bond values about one-half of the values for uncoated bars.

centered under the weakened planes. Other details in some tests, such as deformed bars, wire mesh between the joints, and other coatings, did not provide sufficient information for appraisal.

The weakened-plane joints consisted of 3-mm (⅛-in.) Masonite strips as crack starters, vibrated into place at the midlength of the 5-m slabs and at the three-quarter points in the 20-m slabs. In most slabs the crack-starter depth was 5 cm (2 in.). Different depths and shapes from 1.9 to 8 cm (¾ to 3 in.) were tried; the ¾-in. depth was insufficient to localize the crack, and the ¾-in. crack starters were deepened by saw cuts. In 14 slabs no crack starters were used; instead, coating on the continuous bars was varied to serve as crack localizers. Results of these tests proved inconclusive and are not included in the discussion.

Longitudinal tension on the slabs was applied through header beams beyond both ends. Four deformed bars were embedded in each slab end and protruded through holes in the steel header beams where they were anchored by wedges. Force against the header beams was applied by two hydraulic jacks, one on each side of the slab, bearing against 6 by 6-in. timbers as reaction columns that extended between the header beams. Changes in joint width and subsequent full-section cracks were measured for increasing jack loads with a 10-in. Huggenberg gage between points on the top surface. The longitudinal tension force was centered at middepth of the 16-cm slabs.

Cracking at the joints below the crack starters was visible at the sides of the slabs. Cracked joints were observed before tension application in only two 5-m slabs; however, such initial cracks were observed at most of the joints in the 20-m slabs. A distinct increase in the rate of extension across the joint with increasing tension force was considered as a joint-cracking load. Figure 1 shows typical joint cracking for the three joints in a 20-m slab. Figure 1 also shows cracking at joints in two 5-m slabs that showed no indications of cracks at the sides of the slabs before testing.

Figure 2, prepared from tabulated data, shows the relationship between joint opening (as measured by extension on the 10-in. gage length) at cracking and the average stress on the joint net section below the crack starter for slabs reinforced with 12-, 16-, and 19-mm bars. The data show two groupings of the cracking or joint activation: group 1, averaging below 0.002-in. extension, apparently applicable to joints uncracked before tension application, and group 2, averaging above 0.005-in. extension, believed to apply for joints cracked before tension application, even if not visible. In the latter group the change in rate of extension, rated as cracking, might be due to bond slip. With reference to Figure 2, the force at which a substantial rate of joint widening began increased with bar size, from 6.1 to 9.4 to 11.8 kp/cm^2 average stress on the joint net section for 12-, 16-, and 19-mm bars. Table 2 gives average net section stress and extension at cracking for the two groups with typical joint behavior. The joint cracking force was lower for the joints with 150-cm coated bars, but the joint cracking width was nearly the same for 75- and 150-cm coatings with the cutback asphalt.

Full-section cracks occurred in nearly all slabs tested. The force required for cracking away from the joints averaged 3.8, 2.7, and 2.3 times that required for joint activation for the slabs reinforced with 12-, 16-, and 19-mm bars respectively. The even stress distribution on the concrete section, as well as bars in bond, would account for the great increase in force necessary for full-section cracks. The use of crack starters of different depths in some slabs with 16-mm bars caused the relationship between cracking at the weakened plane and full section, as shown in Figure 3. The effect of eccentric loading on the joint net section is apparent in the disproportionate decrease in cracking force for the net section.

Longitudinal deformation measurements in connection with the tension tests (3) show the value of asphalt coatings on the bars for keeping steel stresses at elastic joints within limits. Typical relationships between steel stress and joint opening are shown in Figure 4 for 12-mm and 16-mm bars. For example, asphalt coating of 29 in. at the elastic joint resulted in steel stress of 55 and 35 ksi respectively for a 1.5-mm joint opening.

Without asphalt coating the steel stress in 12-mm bars reached yield-point stress of about 85 ksi at a joint opening of 0.05 in. Residual joint openings after tension removal are shown on the left side of Figure 4. They increased linearly in proportion to joint

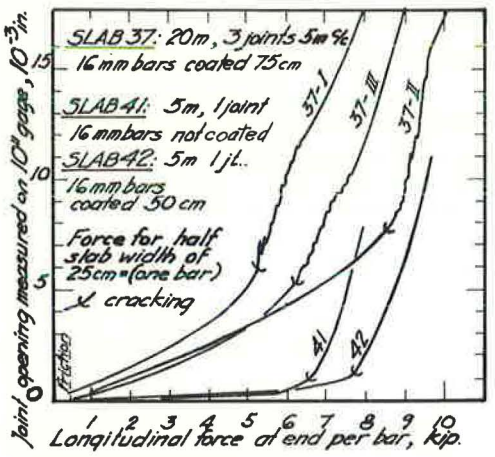

Figure 1. Relationship between tension force and length change across elastic joints for typical conditions. The joint was apparently uncracked before tensioning in slabs 41 and 42. The three joints in slab 37 were apparently cracked before tension application at the two ends of the slab.

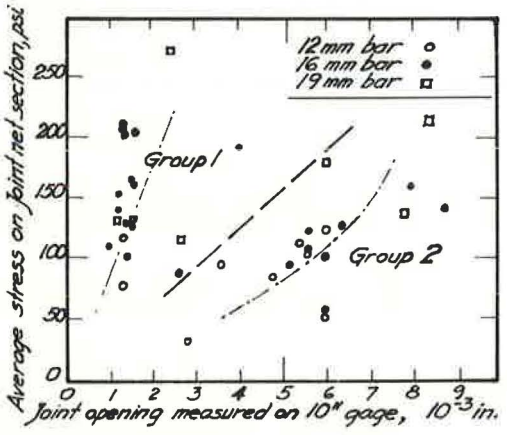

Figure 2. Average stress on the joint net section at which a large increase in the rate of joint opening took place, as measured on the 10-in. gage length across the crack starter, for different slabs. The results on different slabs fall into two groups (separated by the dashed line). Activation of the joint in the slabs of group 1 apparently coincided with cracking of the concrete below the crack starter. The joints in group 2 slabs apparently were cracked before tension application, and the change in rate of joint widening with tension was related to extended bond slip.

TABLE 2

STRESSES AND EXTENSION ACROSS JOINTS AT JOINT CRACKING

Plain Bar Size, mm	Coated Bar Length, cm	Group 1 Small Extension Across Joint			Group 2 Large Extension Across Joint		
		No. of Tests	Net Section Stress, kp/cm²	Ext. Across Joint at Cracking, mm	No. of Test	Net Section Stress, kp/cm²	Ext. Across Joint at Cracking, mm
12	75	1	9.1	0.035	7	5.4	0.121
	150	2	6.9	0.033			
16	75	5	11.0	0.031	7	8.6	0.165
	150	3	8.4	0.046			
19	75	2	14.1	0.049	2	13.8	0.180
	150	2	8.7	0.049	1	9.7	0.196

Data are from Table 6 of Persson (1).
Extension values are for 10-in. gage length across joint.
Net section stress is the total force, deducting friction between the slab end and the joint, divided by the joint net section area below the crack starter, without consideration of transformed steel area. It is an average value.

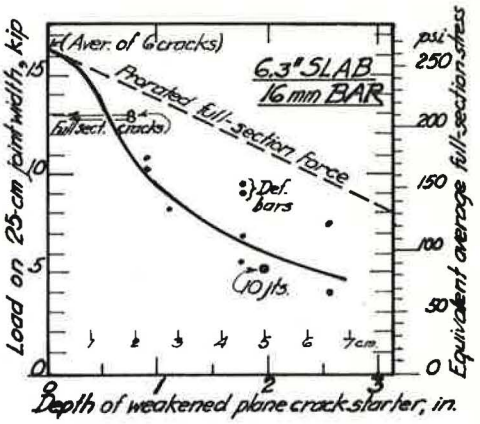

Figure 3. Cracking force on the weakened-plane joints in relation to the depth of the crack starters. Cracking stress lower than that prorated from full-section cracking stress can be explained by eccentric force on the joint net section.

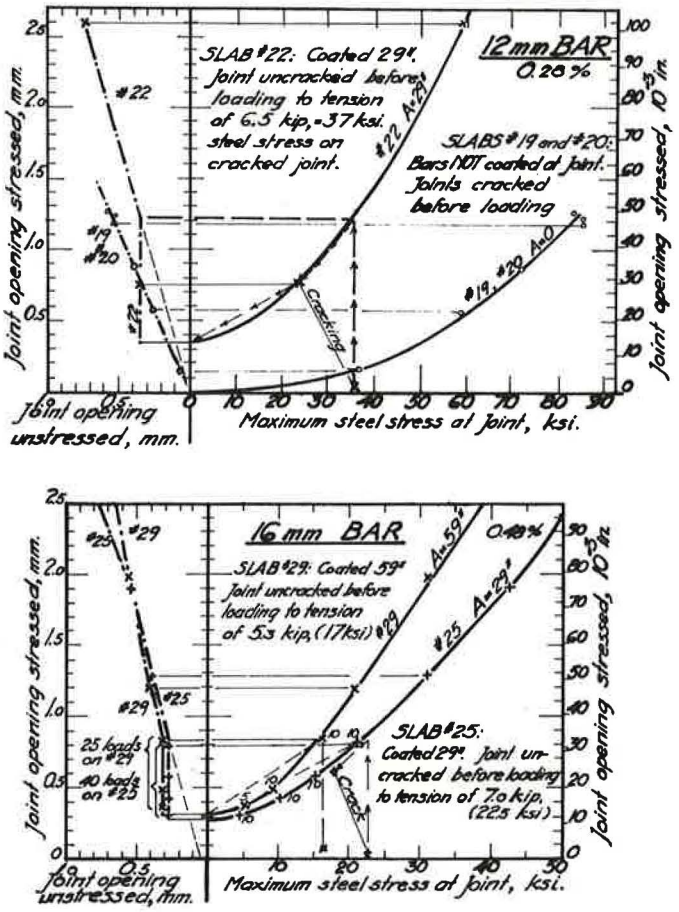

Figure 4. Relationship between joint opening and increasing bar stress in the continuous steel with asphalt coating. Data reveal the joint widening incident to joint cracking under tension stress as a permanent set joint width.

openings under tension; however, joints that cracked during tension testing assumed a constant residual opening, that did not change, even for many repeated tension applications, until the tension force exceeded the cracking force.

EXPLORATORY PAVEMENT AT HOFTERUP AFTER TWO YEARS OF USE

The exploratory concrete pavement (2) was placed on September 29, 1964, on the divided highway E4/E6 in the southern part of Sweden about 30 km north of the city of Malmö. It is 8 m (26 ft) wide and 103 m (340 ft) long, and consists of eight 4-m, seven 5-m, and six 6-m slabs (13.2 ft, 16.5 ft, and 19.7 ft), all 16 cm (6.3 in.) thick. The continuous reinforcement was 16-mm (5/8-in.) plain bars of 75,000-psi yield strength steel, spaced 40 cm (16 in.) in the 4- and 5-m slabs and 30 cm (12 in.) in the 6-m slabs, giving 0.31 and 0.42 percent steel, except that four of the 4-m slabs had 12-mm (0.47-in.) bars spaced 35-cm (14-in.) or 0.2 percent steel. Fifteen of the 19 slabs also were individually reinforced with wire mesh with from 0.04 to 0.16 percent longitudinal steel which stopped back from the transverse joints. The experimental pavement was placed on 15 cm (6 in.) of open-graded granular base and was separated at both ends from the 8-in. thick conventional pavement of 33-ft slabs on cement-treated base by contraction joints with 5/8-in. dowels spaced 16 in. center-to-center. Construction temperatures averaged 15 C(60 F).

The continuous bars were at middepth and were coated with RMA cutback asphalt of low viscosity for a distance of 1.4, 1.7, and 2.0 m (55, 67, and 79 in.) centered at the elastic joint locations between the 4-, 5-, and 6-m slabs respectively. The joints consisted of 1/8-in. bitumen-coated hard Masonite crack starters 5 cm (2 in.) deep, placed in cut grooves and troweled smooth. At three weeks of age a 5-mm (0.2-in.) deep 45-deg kerf was sawed in the surface at each transverse joint line. Construction details are shown in Figure 7.

Points for joint-width measurements with a 10-in. Huggenberg gage were set in the plastic concrete. Figure 6 shows joint widening at 3 and 20 days as measured with the gage. Of the 20 joints, 9 showed clear crack indications at 3 days. At 20 days all joints appeared to be working except the first three joints between 4-m slabs, at which the bars were displaced by the paving operations, partially locking those joints.

Figure 7 shows joint movements from the lowest to the highest observed temperatures, February to July 1966, in relationship to joint widths at one year, September 1965. The extreme air temperatures, -11 C (12 F) and 38 C (100 F) correspond to a change of approximately 70 F in average slab temperature, equivalent to unrestrained

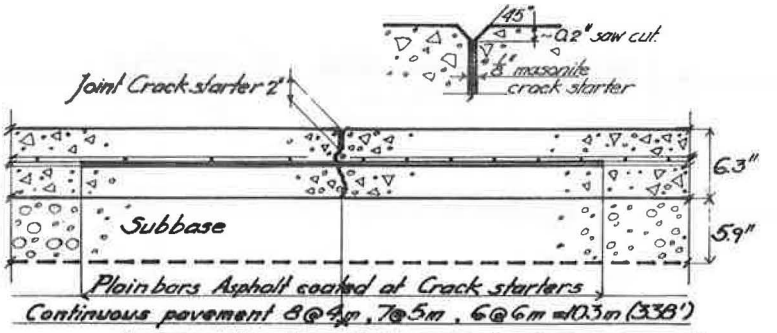

Group	Slabs No.	Slabs Length	Reinforcement Size	Reinforcement Spac.	Reinforcement %	Reinforcement Coated	
I	4	13'-2"	.63"	15.8"	.31	55"	Light mesh of varied size and spacing between joints
	4	-"-	.47"	13.8"	.20	55"	
II	7	16'-5"	.63"	15.8"	.31	67"	
III	6	19'-8"	.63"	11.8"	.42	79"	

Figure 5. Design details of joints in the exploratory pavement with elastic joints and continuous reinforcement, built in 1964, with 0.20 to 0.42 percent steel and 13- to 20-ft joint spacing.

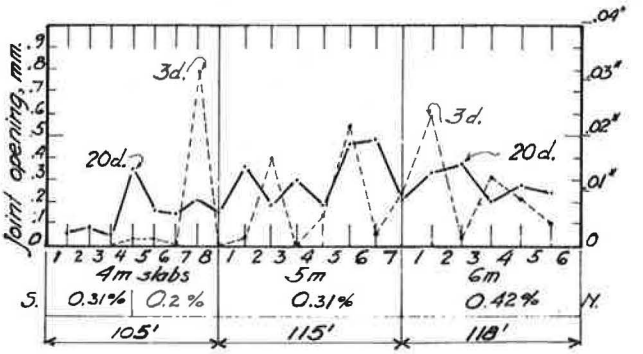

Figure 6. Elastic joint widths at 3 and 20 days of age. Air temperature at construction 59 F, at 20 days 50 F. About half of the joints were uncracked at 3 days; at 20 days, all joints appeared to be working as intended, except the first three joints at the south end, where the continuous bars were misaligned by paving operations.

length changes and average observed length changes as follows (coefficient of thermal expansion 0.0000055 in./in./deg F):

Slab	Unrestrained Change	Observed Change
4-m (13.2 ft)	0.060 in.	0.03 in.
5-m (16.5 ft)	0.075 in.	0.03 in.
6-m (19.7 ft)	0.090 in.	0.02 in.

No observations were made of width changes of the joints at both ends where large compensating movements may have taken place during seasonal temperature changes.

The measurements of joint openings on the test road show maximum joint opening at low temperatures of about 0.9 mm for slabs reinforced with 12- and 16-mm continuous bars coated at the joints for distances of 1.4 m (55 in.) and 1.7 m (67 in.) respectively. Assuming steel stress and joint opening relationships on the test road to be

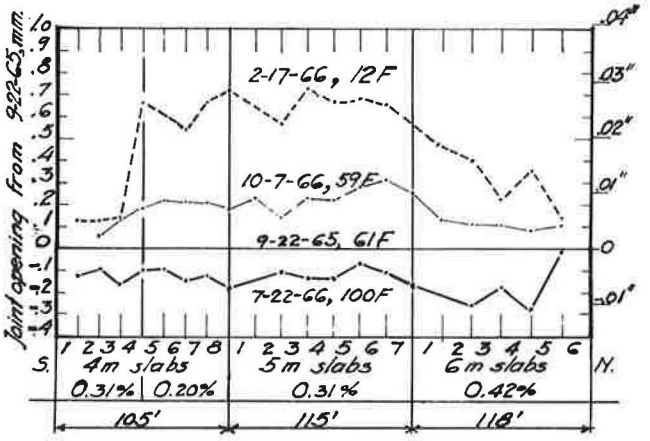

Figure 7. Changes in elastic joint widths on the exploratory pavement from one to two years of age. The measurements include the low and high air temperatures, 12 and 100 F. Gage points set on the day of construction were lost during the first year.

the same as illustrated for the tension tests in Figure 4, the maximum tension stress in the 12-mm bars (0.47 in.) would have been at most 25,000 psi, and in the 16-mm bars (⅝ in.), perhaps 15,000 psi. The approximate corresponding concrete stresses away from the joints, based on 0.20 and 0.31 percent reinforcement, would be 50 and 45 psi respectively maximum at the extreme low temperature. The increase in the low-temperature joint widths from the north end toward midlength according to Figure 7 indicates that subgrade friction was a primary stress-producing factor. At midlength, about 150 ft from each end, a concrete stress of 45 psi would correspond to an average friction coefficient of about 0.3 (assuming a concrete weight of 1 lb/ft length per in^2 cross section).

Steel stresses in the continuous reinforcement in the test road were quite low for the largest observed joint width, in accordance with the indicated stresses for up to 1-mm joint openings in Figure 4. The joints were even; 0.2 percent steel was apparently sufficient to provide uniform joint movements. The bond prevention by asphalt coating of the continuous bars through the joints worked as intended and limited steel stresses effectively to very low maximums.

No random cracks have occurred to date in the test road. Traffic is heavy, including continental traffic to Norway and to central Sweden. The surface of the test road, as of adjacent conventional pavement, is excellent.

REFERENCES

1. Persson, B. O. E. Concrete Pavements With Continuous Reinforcement and Elastic Joints: Pullout Tests and Study of Crack Formation and Joint Opening. Cement och Betong, No. 2, pp. 3-29, 1967.
2. Persson, B. O. E. Concrete Pavements With Continuous Reinforcement and Elastic Joints: Test Road at Hofterup After Two Years Traffic. Cement och Betong, No. 2, pp. 1-16, 1967.
3. Persson, B. O. E. Concrete Pavements With Continuous Reinforcement and Elastic Joints: Longitudinal Deformation Measurements. Cement och Betong, No. 3, pp. 1-24, 1967.

Service Performance of Cement-Treated Bases as Used in Composite Pavements

ERNEST ZUBE, C. G. GATES, E. C. SHIRLEY, and H. A. MUNDAY, JR.,
Materials and Research Department, California Division of Highways

One hundred seventy-five cement-treated base (CTB) composite pavements with varying cement contents built between 1950 and 1962 were evaluated; 64 percent are giving excellent service, 17 percent were rated good, 8 percent were rated fair, and 11 percent required extensive maintenance early in their design lives. The main causes of failure appeared to be insufficient cement content, poor mixing of cement, excessive trimming of the compacted CTB, insufficient CTB thickness, inadequate CTB compaction, or deficiencies in the asphalt concrete surfacing thickness or quality.

A significant improvement in the performance of CTB composite pavements was attributed to extending the CTB at least 1 ft into the shoulder; plant-mixing the CTB; building the project in a temperate climate; increasing the thickness of the asphalt concrete surfacing; limiting the compacted thickness of any one layer of CTB to 0.50 ft; using type II rather than type I cement, using a minimum CTB thickness of 0.50 ft; and providing a minimum in-place CTB compressive strength of 500 psi.

•SEVERAL HUNDRED miles of roads using cement-treated base (CTB) were built in California prior to 1950. Between 1950 and 1962 over 700 miles of California highways were built with either class A or class B cement-treated base, which was surfaced with asphalt concrete (AC). Table 1 gives the various quality requirements specified for these cement-treated bases.

With this substantial amount of CTB composite pavement construction completed, we felt that a comprehensive evaluation should be made of this type of construction. The scope of the investigation was limited to include only classes A and B CTB. Because the 1949, 1954, and 1960 Standard Specifications were not too radically different from one another, we further limited the investigation to include only those projects built between 1950 and 1962. Projects built after 1962 were considered too new for a valid performance rating.

PROJECT EXAMINATION AND SELECTION

The performance of the projects was evaluated by a visual examination in which the amount and type of cracking and the amount and type of maintenance performed were noted. Physical characteristics of the terrain were also observed. On projects with four or more lanes, only the outside truck travel lane was evaluated. Visual observations were made by driving along the shoulder of the road at a slow speed (approximately 5 mph), using the odometer of the vehicle to measure the extent of distressed areas. A description of the type of distress and photographs of typical cracking were made for

Paper sponsored by Committee on Composite Pavement Design and presented at the 48th Annual Meeting.

TABLE 1

VARIATION OF CTB QUALITY REQUIREMENTS DUE TO SPECIFICATION CHANGES

Standard Specs.	Class of CTB	Minimum Compressive Strength at 7 Days (psi)	Cement Content (percent of dry wt. of aggr.)
1949	A	650	4 to 7
1954	A	650	3½ to 6
	B	300	2½ to 3½
1960	A	750	3½ to 6
	B	400	2½ to 4½

each project. The amount of block cracking (normally caused by excessive deflection under traffic) and pumping for each project was established by totaling the length of each type of distress, dividing this value by the length of the travel lanes, and then converting the resulting value to a percentage.

Longitudinal and transverse cracking (normally caused by thermal shrinkage of the CTB) was classified as normal, greater than normal, or less than normal. An average CTB roadway was considered to have narrow transverse cracks at a spacing of about 20 ft and to have a small amount of intermittent longitudinal cracking throughout the length of the project. These ratings are strongly influenced by the rater's judgment but, because the same rater reviewed all the projects, they provide fairly valid comparative values. There was such a small amount of alligator cracking observed on these CTB projects that it was combined with the block cracking, and no separate evaluation was made. Patched areas were considered to have been block-cracked and were included in that rating unless the patching was obviously necessitated by something other than a failure of the structural section, such as fill settlement. The field review of these projects was completed in the summer of 1966.

Contract files for all the projects investigated were searched for all pertinent information on construction equipment, construction methods, control test values, and structural section design criteria. Questionnaires were sent to district maintenance personnel requesting information concerning the amount of maintenance performed on each project and the time at which the first significant amount of maintenance was necessary.

Upon completion of the visual survey, 35 projects were selected for field sampling. In most cases, 2 projects that performed well and 2 projects that performed poorly were chosen from each district. A few districts had used little or no CTB that met the conditions established for this evaluation and could not provide 4 projects for sampling. A completely random selection of projects was sacrificed to ensure that projects were evaluated from as many parts of the state as possible.

Dynaflect deflection measurements (1) were made in February 1966, on each of the 35 projects. The data were obtained at 25-ft intervals for a distance of 200 ft for 2 locations on each project.

The Dynaflect deflection data were used as an aid in locating the specific areas for coring. One sampling location was selected to be representative of the better portions of the project and the other was chosen to be representative of the poorer portions. One large core, ranging from 6 to 12 in. in diameter, and two 4-in. diameter cores were cut at each sampling location. The larger cores were used to check the extent of cracking, and the small cores were used for compressive strength and density determinations.

DATA ANALYSIS

In order to simplify the data analysis for this project, an optical coincidence method was used. Numbered cards with a printed coordinate system, shown in Figure 1, were used. Holes were punched in these cards at a specific set of coordinates for each project. The use of a different card to represent a specified range of each variable made it possible to compare a number of different variables by lining up the cards representing the variables and counting the number of holes that coincided. This number could then be divided by the total number of holes in the independent variable card to determine the ratio of all the projects within the range of the independent variable that were also within the ranges of the other variables being considered. This procedure provided a fairly rapid means of comparing a large number of different variables.

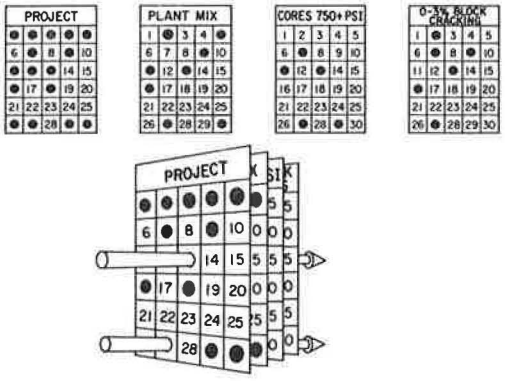

Figure 1. Optical coincidence system.

TABLE 2

CTB SHOULDER EXTENSION VS BLOCK CRACKING ON PROJECTS HAVING GREATER THAN 5 MILLION EWL

Extension of CTB into Shoulder (ft)	Percent of Length Affected by Block Cracking			Number of Projects
	0-3	3-31	31-100	
0 through 0.5	53	24	23	38
1.0 or more	70	28	2	38

Dependent at 98 percent confidence.

After the various relationships were established by the optical coincidence method, each was then tested for statistical independence by comparing it to the chi square distribution (2).

A 95 percent level of confidence was chosen to establish significance. When the data indicated a definite trend toward dependency and were above a confidence level of 85 percent, we indicated the data tended to be dependent. All data showing a statistical dependency at less than a confidence level of 85 percent were considered to be totally independent.

Tables 2 through 13 give comparisons of the many variables that were considered likely to affect the service life of CTB projects. All of these tables have the independent variable in the left column. Three columns are used to show the percentage of projects falling within the selected ranges of the dependent variables. The right column lists the total number of projects or sample locations that were within each class of the independent variable. Below each table is a statement as to whether or not the variables considered in the table are statistically dependent and, if so, at what degree of confidence they are dependent.

Data in Table 2 indicate that block cracking is significantly reduced by extending the CTB 1 ft or more into the shoulder. The 0 to 3 percent range of block cracking is representative of good to excellent performance, the 3 to 31 percent range is representative of fair to good performance, and the 31 to 100 percent range is representative of poor performance. The reduction in block cracking is very likely caused by the additional lateral support that develops in the outer wheelpath when the CTB is extended 1 ft or more into the shoulder. Projects experiencing less than 5 million equivalent 5,000-lb wheel loads (EWL) were excluded from this comparison to eliminate projects that had obviously failed prematurely (3).

Data in Tables 3 and 4 show that plant-mixed CTB material is more effective in preventing both block cracking and longitudinal and transverse cracking than is road-mixed material. This is probably because better control of the cement and moisture content and more thorough mixing are possible in a plant-mixed operation.

CTB projects that were built along the coast had much less longitudinal and transverse cracking than did projects built in inland valleys (Table 5). The temperature

TABLE 3

TYPE OF MIXING OF CTB MATERIAL VS BLOCK CRACKING

Type of Mixing	Percent of Length Affected by Block Cracking			Number of Projects
	0-3	3-31	31-100	
Plant	72	16	12	67
Road	48	30	22	83

Dependent at 98 percent confidence.

TABLE 4

TYPE OF MIXING OF CTB MATERIAL VS LONGITUDINAL AND TRANSVERSE CRACKING

Type of Mixing	Longitudinal and Transverse Cracking (percent)			Number of Projects
	Less Than Normal	Normal	More Than Normal	
Plant	60	13	27	60
Road	40	22	38	76

Dependent at 95 percent confidence.

TABLE 5

GEOGRAPHIC LOCATION VS LONGITUDINAL AND TRANSVERSE CRACKING

Geographic Location	Longitudinal and Transverse Cracking (percent)			Number of Projects
	Less Than Normal	Normal	More Than Normal	
Coastal	63	21	16	81
Inland	29	15	56	55

Dependent at 99.5 percent confidence.

TABLE 6

CTB CORE COMPRESSIVE STRENGTH VS BLOCK CRACKING

CTB Core Compressive Strength (psi)	Percent of Length Affected by Block Cracking			Number of Sample Locations
	0-3	3-31	31-100	
200 to 500	42	11	47	19
500 to 750	87	7	6	15
Over 750	91	6	3	33

Dependent at 99.5 percent confidence.

along the coast is not subject to nearly the degree of change as that in the inland valleys. The higher humidity could also be a factor.

Block cracking was not significantly affected by the geographical location of the project.

Drainage had no statistically significant effect on either pumping or block cracking, but there was a tendency for both to be greater when the drainage was rated poor. A significant relationship would probably have developed if these projects had been inspected during the wet season when the drainage characteristics would have been more obvious.

Comparisons of the cement content used on the various projects with the amount of both longitudinal and transverse cracking and block cracking produced statistically independent relationships. This implies that our CTB design method has been producing structural sections of comparable strength throughout the full range of cement content used on these projects (2.2 through 7.0 percent).

Longitudinal and transverse cracking was not significantly affected by an increase in the compressive strength of the CTB. Block cracking was significantly reduced by increasing the compressive strength of the CTB (Table 6).

The data in Table 6 are based on the 35 projects that were sampled during this study. The compressive strength values were based on 4-in. diameter specimens that were cut with a surface set diamond core barrel. The CTB in locations in which the core disintegrated during the coring process was given an arbitrary compressive strength of 200 psi. This value was chosen because at one location we were able to retrieve a core that had a compressive strength as low as 232 psi, and it is unlikely that the CTB at all of the uncoreable locations had absolutely no compressive strength.

Longitudinal and transverse cracking was greatly reduced by using an AC thickness of 0.29 ft or greater (Table 7). The projects that were less than 7 years old were eliminated from this comparison to reduce the effect of age on the longitudinal and transverse cracking rating.

A comparison of AC thickness and block cracking was found to be statistically independent, but there appeared to be a trend for the amount of block cracking to be reduced as the AC surfacing thickness was increased. The type of terrain in which the project was built had no significant effect on the amount of either longitudinal and transverse cracking or block cracking. The amount of commercial traffic and quality of the basement soil also had no significant effect on the amount of cracking. This implies that our design method (3) has been successful in overcoming the effects of variations in heavy truck traffic and in basement-soil quality.

TABLE 7

AC THICKNESS VS LONGITUDINAL AND TRANSVERSE CRACKING ON PROJECTS 7 TO 16 YEARS OLD

AC Design Thickness (ft)	Longitudinal and Transverse Cracking (percent)			Number of Projects
	Less Than Normal	Normal	More Than Normal	
0.15 to 0.25	28	20	52	25
0.25	28	24	48	50
0.29[a] to 0.51	73	11	16	19

Dependent at 98 percent confidence.

[a]Only 2 of the 19 projects had AC thicknesses of less than 0.33 feet.

TABLE 8

NUMBER AND THICKNESS OF CTB LIFTS VS BLOCK CRACKING

Number of Lifts	Thickness of Lifts (ft)	Percent of Length Affected by Block Cracking			Number of Projects
		0-3	3-31	31-100	
1	0.67	35	38	27	29
2	0.33	62	23	15	66

Dependent at 95 percent confidence.

Within a 20 to 80 range, the sand equivalent of the CTB aggregate had no significant effect on the amount of cracking and pumping or on the compressive strength of the CTB construction control samples. The sand equivalent is a relative measure of the amount of clay-like material in an aggregate mixture.

Data in Tables 8 and 9 show that both block cracking and longitudinal and transverse cracking are significantly reduced by compacting the CTB in two 0.33-ft thicknesses rather than one 0.67-ft thickness. The reason for this, undoubtedly, is that it is more difficult to achieve adequate compaction in the lower portion of a single lift of CTB 0.67 ft thick. Also, it is more difficult to achieve adequate cement distribution in heavier road-mixed lifts. A number of the thicker CTB core samples were cut in half, and the top and bottom portions were tested separately. Some of these samples showed a significantly lower density for the bottom half of the core, and the majority of the cores had a lesser compressive strength in the bottom half than in the top half.

A CTB 0.67 ft thick was no more effective than a CTB 0.50 ft thick in preventing block cracking. This also attests to the adequacy of our design formula, in that a comparable overall structural strength was provided when either thickness of CTB was used.

Table 10 data show that the compressive strength of contract control samples increased as the CTB aggregate grading moved from the fine to the coarse side of Talbot's optimum density grading limits (4). As is often the case, however, an adjustment that improves one characteristic adversely affects another. Using a coarse grading in order to improve the compressive strength makes the CTB more difficult to compact. The difficulty in achieving adequate compaction caused the grading variations to have no significant effect on the amount of either longitudinal and transverse cracking or block cracking. The season of the year in which the CTB was placed had no significant effect on cracking.

Sections with the highest CTB compressive strength had the longest maintenance-free service life (Table 11). In this report, maintenance-free service life is defined as the project's life to the point at which major repair of the roadway is necessary. Minor repairs, such as crack sealing and patching of a limited amount of localized failures, are disregarded. Also, the maintenance-free service life of projects that had not reached the point of requiring extensive maintenance was estimated to be in one of the three tabulated ranges of service life based on their condition at the time of the field survey. In most cases this amounted to a projection of service life by no more than three years, which is felt to be a reasonable extrapolation of the data.

According to Table 12, type II cement is better than type I cement in preventing block cracking. Longitudinal and transverse cracking was unaffected by the type of cement that was used. California's present specifications require the use of type II cement for all CTB construction.

When a minimum of 92 percent relative compaction was maintained, cracking was unaffected by variations in relative compaction. Only 3 of the 32 projects that were available for this comparison had relative compactions of less than 95 percent.

TABLE 9

NUMBER AND THICKNESS OF CTB LIFTS VS LONGITUDINAL AND TRANSVERSE CRACKING

Number of Lifts	Thickness of Lifts (ft)	Longitudinal and Transverse Cracking (percent)			Number of Projects
		Less Than Normal	Normal	More Than Normal	
1	0.67	20	24	56	25
2	0.33	59	18	23	60

Dependent at 97.5 percent confidence.

TABLE 10

CTB AGGREGATE GRADATION VS CTB COMPRESSIVE STRENGTH OF CONTRACT CONTROL SAMPLES

Grading	Compressive Strength (psi) Percentage			Number of Projects
	200-500	500-750	750-1450	
Coarser	3	36	61	33
Talbot's optimum density	9	37	54	78
Finer	21	58	21	47

Dependent at 99 percent confidence.

TABLE 11

CTB CORE COMPRESSIVE STRENGTH VS MAINTENANCE-FREE SERVICE LIFE

CTB Core Compressive Strength (psi)	Percent Maintenance-Free Life		Number of Sample Locations
	Less Than 10 Years	More Than 10 Years	
200 to 500	50	50	20
500 to 750	40	60	20
Over 750	10	90	30

Dependent at 99.5 percent confidence.

Projects that were in very good condition but not 10 or more years old were assumed to be 10 or more years old.

TABLE 12

TYPE OF CEMENT VS BLOCK CRACKING

Type of Cement	Percent of Length Affected by Block Cracking			Number of Projects
	0-3	3-31	31-100	
I	41	26	33	27
II	66	22	12	82

Dependent at 95 percent confidence.

Eleven percent of the 175 projects evaluated required extensive maintenance within 3 years after they were built. Over half of these projects were in Shasta and Siskiyou Counties, and were built with a maximum cement content of 3 percent; one used as little as 2.2 percent. When such low cement contents are used, small variations in cement distribution and mixing can cause serious reductions in the compressive strength of the CTB.

Our present specifications allow a variation in cement content of ±0.6 percent for road-mixed CTB material and ±0.4 percent for plant-mixed. One of our recent investigations showed that, for plant-mixed operations using good to excellent equipment and operating procedures, approximately 3 to 8 percent of the CTB material placed on each of three projects was shy of the planned cement content by more than the allowable deviation of -0.4 percent (5). These percentages were based on the calculated standard deviation and the assumption that the material was normally distributed. It is easy to see, therefore, how projects built under less than ideal conditions with a minimal cement content could develop many areas that require extensive maintenance. This is particularly true for plant-mixed material in which the equipment was not in perfect operating condition and for most road-mixed projects.

Shasta and Siskiyou Counties are in mountainous areas that are subject to freezing winter weather. In a laboratory and field test of the effect of cement content on the durability of CTB when subjected to freezing and thawing action, Abrams found that a minimum of 3 percent cement was necessary to insure that the CTB would withstand freezing and thawing conditions (6). Admittedly his tests were on materials quite

TABLE 13

CTB CONDITION VS DEVIATIONS FROM THE CTB DESIGN THICKNESS (CORED PROJECTS)

CTB Condition in Vicinity of Sample Location	Percent CTB Design Thickness Deviations			Number of Sample Locations
	Thinner	± 0.04 ft	Thicker	
Block-cracked	55	45	0	20
Extensive shrinkage cracking	20	60	20	10
Uncracked or slight to moderate shrinkage cracking	21	42	37	38

Dependent at 99 percent confidence.

different from those found in the Shasta-Siskiyou area, but there is still a strong possibility that some of the distress that developed on these projects was caused by a freezing and thawing action.

According to Table 13, 55 percent of the 20 sample locations where the CTB was block-cracked were shy of their CTB design thickness by more than 0.04 ft, and none of the sample locations was block-cracked when the CTB exceeded its design thickness by more than 0.04 ft. It is readily seen that shrinkage cracking is unaffected by CTB thickness variations. Only 21 percent of the locations with no block cracking were shy of their design thicknesses by more than 0.04 ft. The majority of the locations that were deficient in CTB thickness were badly cracked.

The CTB was badly cracked at every location where it was less than 0.46 ft thick. These data indicate that many of our past CTB designs should have required increased thickness in order to protect against thickness deficiencies resulting from normal construction and that, in some cases, closer control should have been maintained over the construction operations. The increased thickness of CTB, which is presently added to our structural section designs as a safety factor, should reduce the amount of future pavement failures caused by slight deviations from the design thickness. We emphasize strongly, however, that it is important to inspect the construction operations to insure that the structural section is built within the tolerences specified for the project.

Only 4 of the 175 projects that were included in this study had a design CTB thickness that was less than 0.50 ft: 2 were 0.42 ft thick and 2 were 0.33 ft thick. None of these projects was successful. All required major repairs before they were 7 years old, and the 0.33-ft thick CTB projects required major repairs within 5 years after they were completed.

From a total of 32 coring locations in which the CTB had been placed in two compacted lifts, only 2 locations produced cores that were bonded together at the interface of the two lifts. Both of these coring locations were on the same project, which had used a volcanic tuff material as the CTB aggregate.

Figure 2 shows an example of a situation that was observed on several of the sampled projects. The upper layer of class A CTB had a transverse crack that did not extend through the lower layer of class B CTB, indicating that the two layers were definitely acting independently.

The value of having the CTB layers well bonded together is self evident, and it is imperative that some means of achieving this bond be developed. Arman and Dantin

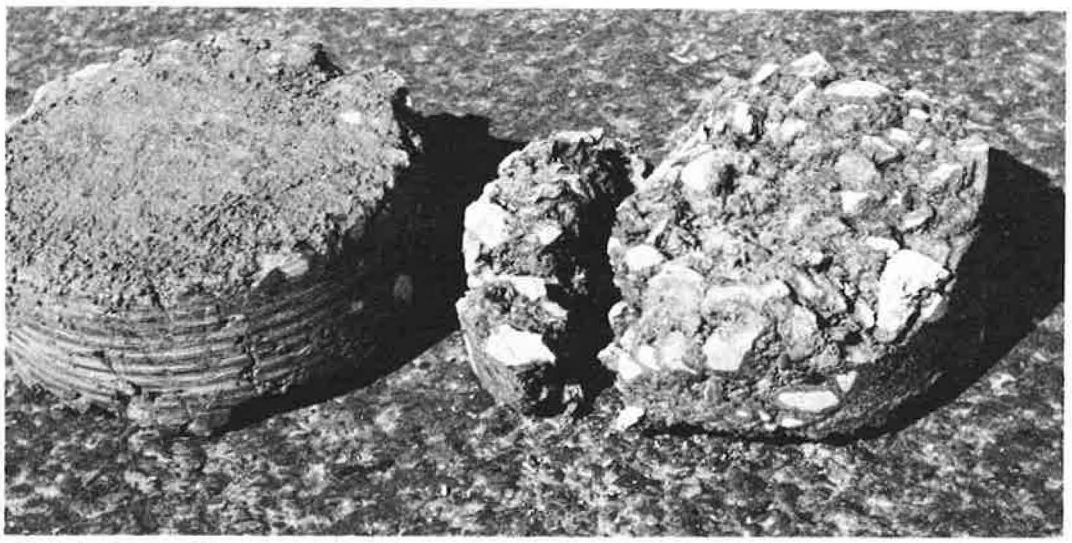

Figure 2. Class A and class B CTB cores.

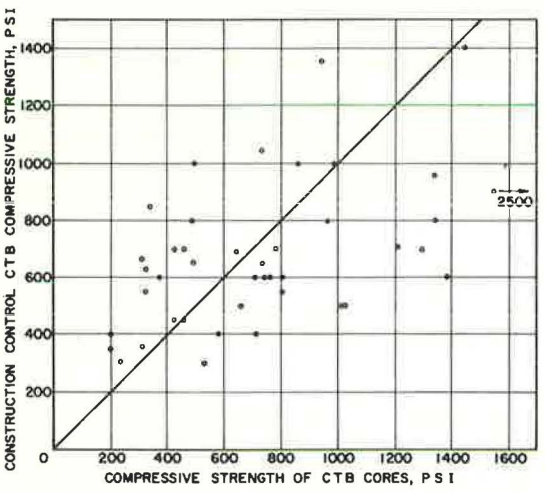

Figure 3. Compaction of compressive strength of construction control samples with that of the field cores: Each point represents the average compressive strength of four 4-in. diameter cores.

found set-retarding agents to be effective in producing bond between CTB lifts in laboratory tests with up to 7 hours time lag between placement of the two lifts (7). Set-retarding agents could also be of value in achieving better compaction when the contractor is slow in achieving compaction. Use of an asphaltic bonding agent could also be an effective solution to the CTB bonding problem.

The asphalt concrete surfacing was well bonded to the CTB at 57 out of 66 sample locations. This bond is undoubtedly caused by the asphalt curing seal used on the CTB.

Figure 3 shows a comparison of the average construction control compressive strength for each sampled project vs the average compressive strength of the field cores from each of these projects. The points appear to be randomly distributed about the line of perfect correlation with about 50 percent having a strength less than that obtained from the construction control samples. This implies that there has been about an even chance that the strength indicated by the CTB construction control samples would never be reached by the CTB in the structural section. About one-third of the CTB cores never even reached 75 percent of the strength indicated by the construction control samples. It would appear to be advisable, therefore, to design new cement-treated

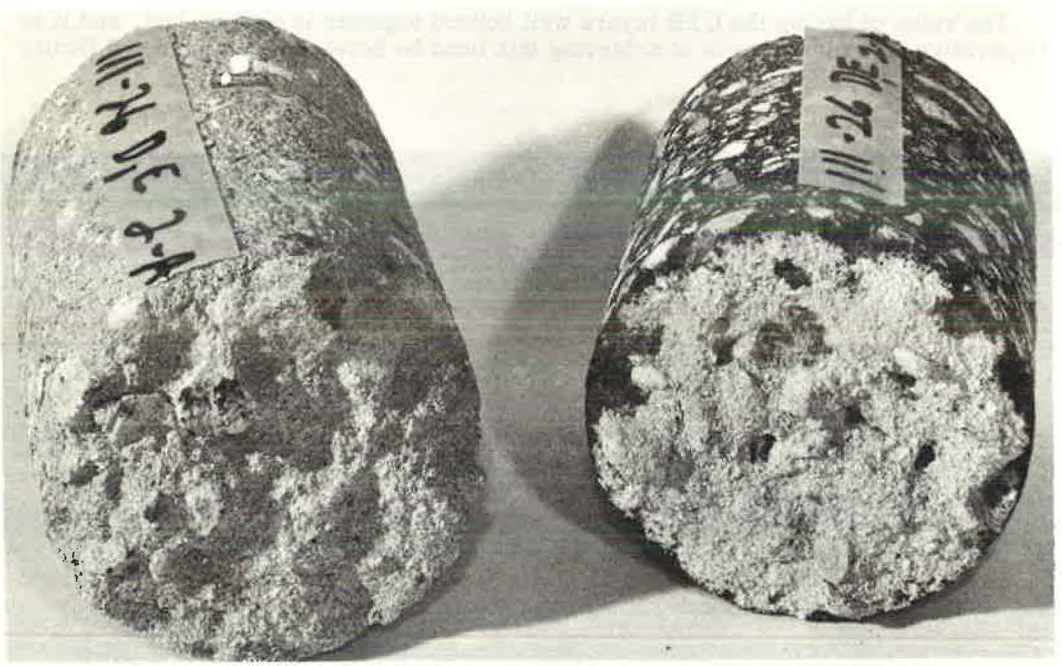

Figure 4. Shear plane in class A CTB.

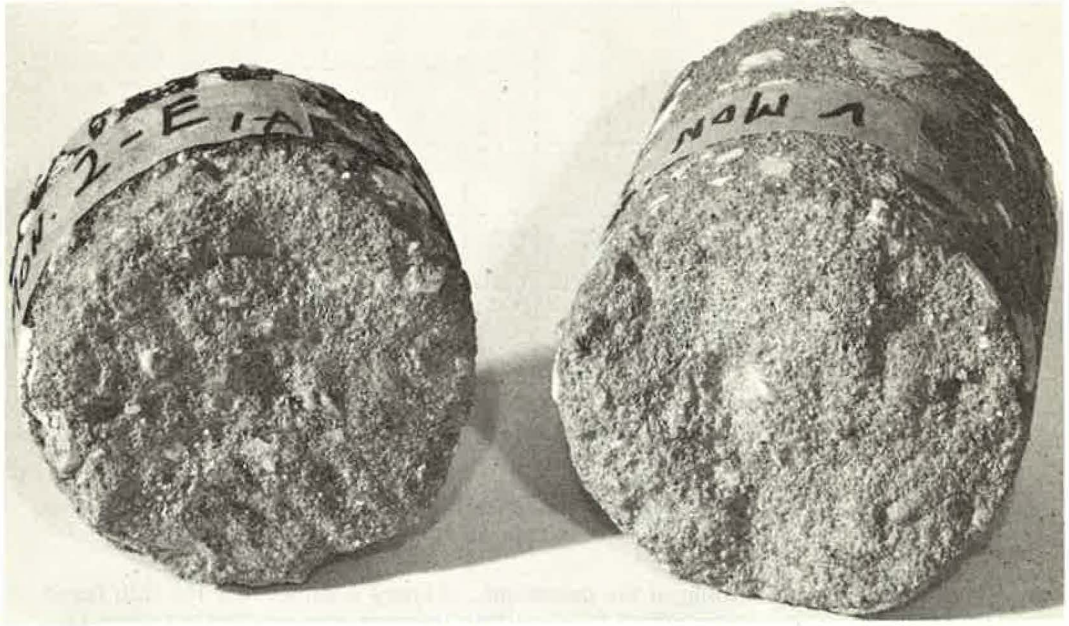

Figure 5. Compaction plane between two lifts of class B CTB.

bases for a strength about 25 to 30 percent higher than that considered necessary in the completed CTB. The Washington State Department of Highways is presently doing just that (8). Experience there indicates that an in situ minimum 7-day compressive strength of 650 psi is necessary for a CTB to be successful on Washington highways. Because the compaction specifications allow acceptance with only 95 percent of the density upon which the design cement content is based, Washington's highway department has increased the minimum design compressive strength to 850 psi at 7 days to compensate for the lesser field densities.

Four of the 35 projects that were sampled had thin layers of disintegrated CTB about 0.04 to 0.08 ft thick at the top surface of the CTB while the lower portions remained sound. This situation has also been noted on projects other than those investigated during this study. In nearly every case, this condition has led to block cracking and pumping early in the design life of the project even though the underlying CTB remained sound. One of these four projects appeared to have been trimmed excessively to reduce the thickness of the partially cured CTB. This process undoubtedly weakens the upper surface of the CTB. Figure 4 shows how the CTB sheared off in this weakened portion just below the surfacing while being cored.

Figure 6. Core hole with void under AC surfacing.

A thin layer of CTB was known to have been placed on another of these projects in order to bring it to design grade. Figure 5 shows the smooth separation of these two layers of CTB and the thin layer that remained bonded to the AC surfacing. This core was cut from the center of the lane. The thin layer of CTB was pulverized in the wheel tracks at this location and had caused

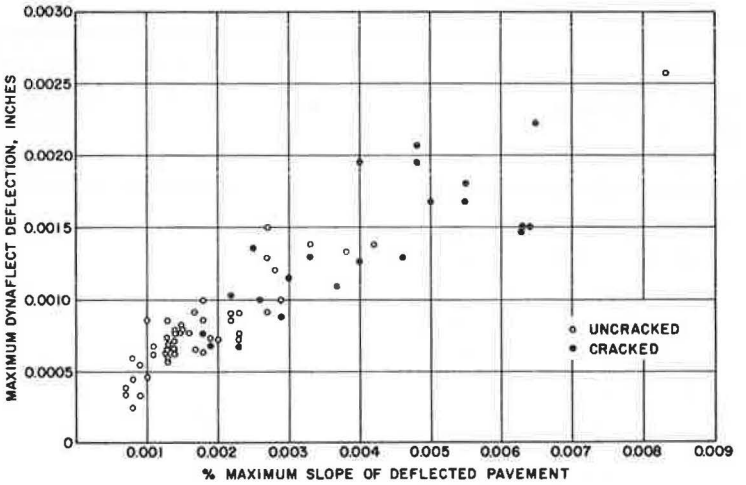

Figure 7. Maximum deflection vs maximum slope of deflected pavement from Dynaflect readings.

extensive cracking and pumping of the pavement. Figure 6 shows how the thin layer of disintegrated CTB in the outer wheel track at this location was washed out from beneath the AC by the drill water. It is difficult to spread and compact a thin layer of CTB, and it is unlikely that this layer would bond to the underlying CTB. It is easy to see, therefore, how the thin layer between the underlying CTB and the AC surfacing could be pulverized by the action of heavy wheel loads.

These projects point out the disadvantages of placing extremely thin CTB layers or trying to manipulate the surface of the CTB after it has been compacted.

Figure 7 shows the maximum deflection vs the maximum slope of the deflected pavement between any 2 of the 5 geophones of the Dynaflect for both cracked and uncracked locations. Both deflection and slope seem to indicate a maximum tolerable value. However, it is apparent that the maximum slope of the deflected pavement provides a more sensitive break between cracked and uncracked locations than does the maximum deflection. These data indicate the maximum tolerable slope to be about 0.002 percent; 59 percent of the locations with a greater slope had already block-cracked, and many

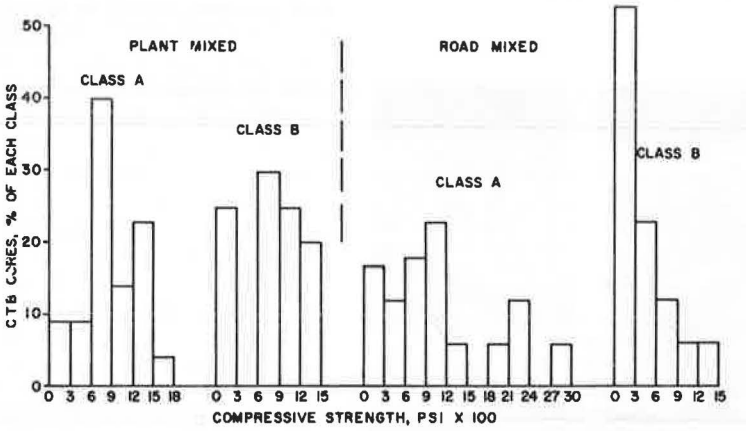

Figure 8. Compressive strength frequency distribution of CTB cores by class of CTB and type of mixing (uncoreable locations were grouped in the 0- to 300-psi range of compressive strength).

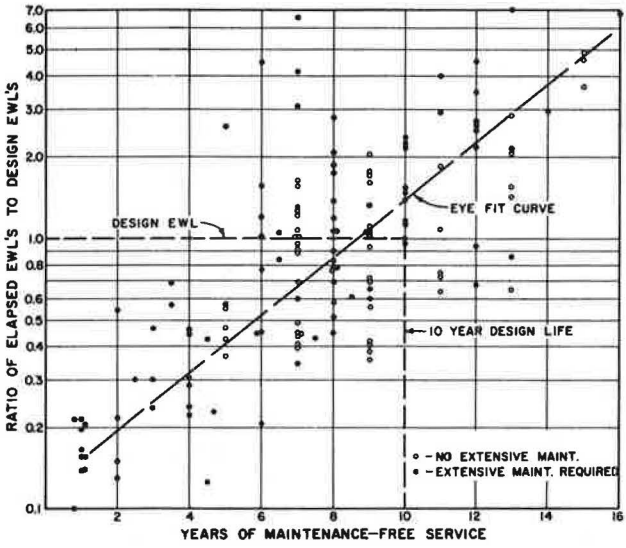

Figure 9. Ratio of design wheel loads elapsed vs years of maintenance-free service.

that had not will probably do so before their design lives are exceeded.

Figure 8 shows the compressive strength frequency distribution of the CTB cores for each type of mixing and class of CTB. Plant-mixing produces more of a normal frequency distribution, whereas road-mixing produces a distribution that is skewed toward the low range. Also, the broad range of compressive strengths produced by class A road-mixed CTB cores indicates poor uniformity that was very likely caused by a poor distribution of cement; 25 percent of the class B plant-mixed projects had CTB compressive strengths of less than 300 psi whereas 53 percent of the class B road-mixed projects were in that range of compressive strength, and 18 percent of the class A plant-mixed projects had CTB compressive strengths of less than 600 psi whereas 29 percent of the class A road-mixed projects were in that range of compressive strength. These data clearly demonstrate the superiority of plant-mixing over road-mixing and the disadvantage of specifying a cement content that is too low.

Figure 9 shows the ratio of the number of elapsed equivalent 5,000-lb wheel loads to the number for which the structural section was designed vs the number of years of relatively maintenance-free service life. The majority of the projects requiring extensive maintenance were less than 5 years old, and over half of these projects had experienced less than 25 percent of their design traffic loading. Of the 25 projects requiring extensive maintenance before they were 5 years old, 18 were built with class B CTB and had low cement contents. Five of the remaining seven projects were built by the road-mixed method of construction, which is much more likely to produce an inferior CTB (Fig. 8).

A straight line would appear to best fit the data in Figure 9, but this line would pass a year or two to the left of a point that represents the end of a ten-year design life. This indicates that we have been slightly underestimating the design wheel loads on most of our projects.

SUMMARY AND CONCLUSIONS

1. Block cracking is reduced by extending the CTB at least 1 ft into the shoulder. Longitudinal and transverse cracking is not similarly affected.
2. Plant-mixed CTB projects have less cracking of all types than do road-mixed CTB projects.
3. CTB projects along the coast have much less longitudinal and transverse cracking than projects built inland. This is likely due to the more uniform temperatures that are found along the coast. There is no significant effect on the amount of block cracking.
4. Block cracking is significantly less when the in situ CTB compressive strength exceeds 500 psi. Longitudinal and transverse cracking is not significantly affected by the compressive strength of the CTB.

5. Increasing the AC surfacing thickness is very effective in reducing the amount of longitudinal and transverse cracking but has no statistically significant effect on block cracking. There is a trend toward a reduction in block cracking as the AC surfacing thickness is increased.

6. The number of heavy wheel loads and the stability of the basement soil, as measured by the R-value test, have no significant effect on the amount of either longitudinal and transverse cracking or block cracking. This implies that our design method adequately accounts for these variables.

7. CTB compacted in one 0.67-ft thickness does not perform as well as CTB compacted in two 0.33-ft thicknesses.

8. When the CTB is placed in two compacted layers, there is generally very little bond between these layers. The asphalt concrete surfacing was well bonded to the CTB at most sampling locations, however. This bond is undoubtedly produced by the asphaltic curing seal used on the CTB.

9. The season of the year in which the CTB is placed has no significant effect on the amount of either block cracking or longitudinal and transverse cracking.

10. CTB projects built with type II cement have less block cracking than those built with type I cement. The type of cement has no significant effect on the amount of longitudinal and transverse cracking.

11. The average compressive strength of CTB cores from about half of the projects sampled during this investigation did not exceed that of their respective construction control samples, and the average compressive strength of about a third of the CTB cores did not reach 75 percent of the strength indicated by the construction control samples. These lower strengths undoubtedly occur because only 95 percent relative compaction is required during construction.

12. The structural sections with the greatest CTB compressive strength have the longest maintenance-free service life.

13. The majority of the locations in which the CTB thickness was deficient were badly cracked, and the CTB was badly cracked at every location in which it was less than 0.46 ft thick.

14. From a total of 175 CTB projects, 64 percent performed excellently, 17 percent were rated good, 8 percent were rated fair, and 11 percent performed poorly.

15. Although the comparisons were statistically independent, projects with poor drainage tend to have more block cracking and more pumping of mud fines.

16. The type of terrain in which the CTB projects are built has no significant effect on either block cracking or longtiudinal and transverse cracking.

17. Within a range of 20 to 80, the sand equivalent of the CTB aggregate has no significant effect on block cracking, longitudinal and transverse cracking, pumping, or the compressive strength of the construction control samples.

18. Compressive strengths of contract control samples increased as the CTB aggregate gradings moved from the fine side to the coarse side of the grading specifications, but the coarser gradings were more difficult to compact and this increase in strength was not realized in the cores from the roadway. Therefore, grading has no significant effect on the amount of cracking.

19. The compressive strength of field-cored CTB samples was statistically independent of cement content. However, there is a definite trend toward increased compressive strength with increases in cement content.

20. Relative compaction has no effect on the amount of cracking when a minimum of 92 percent relative compaction is achieved. Only 3 of the 31 projects from which relative compaction data were available had any cores that were below 95 percent relative compaction.

21. The surface of a CTB can be badly damaged by trimming it after it has been compacted.

22. Block cracking did not occur where the maximum tolerable slope of deflected California CTB structural sections between any two geophones of the Dynaflect was found to be approximately 0.002 percent.

ACKNOWLEDGMENT

This paper is based on data collected during a research project financed jointly by the California Division of Highways and the U.S. Bureau of Public Roads. The opinions, conclusions, and findings are those of the authors and not necessarily those of the California Division of Highways or the Bureau of Public Roads; however, their contribution is acknowledged.

REFERENCES

1. Scrivner, F. H., Moore, W. M., and Swift, G. A New Research Tool for Measuring Deflection of Pavements. Highway Research Record 129, pp. 1-11, 1966.
2. Dixon, W. J., and Massey, F. J., Jr. Introduction to Statistical Analysis, 2nd Edition. McGraw-Hill, pp. 221-226, 1957.
3. Structural Design of the Roadbed. Planning Manual, Part 7. California Division of Highways, pp. 7-602.3 and 7-602.4, 1966.
4. Spangler, M. G. Engineering Characteristics of Soils and Soil Testing. In Highway Engineering Handbook, 1st Edition. McGraw-Hill, p. 8-8, 1960.
5. Sherman, G. B., and Watkins, R. O. Control of Cement in Cement Treated Base. Research Rept. 631149, California Division of Highways, Jan. 1968.
6. Abrams, M. S. Laboratory and Field Tests of Granular Soil-Cement Mixtures for Base Courses. ASTM Spec. Tech. Publ. 254, 1959.
7. Arman, A., and Dantin, F. J. The Effect of Admixtures on Layered Systems Constructed With Soil Cement. Eng. Research Bull 86, Louisiana State Univ., 1965.
8. LeClerc, R. V. Cement Treated Bases. Western Construction, Vol. 41, No. 12, pp. 38 and 43, Dec. 1966.
9. Zube, E., Gates, C. G., Shirley, E. C., and Munday, H. A., Jr. Investigation and Appraisal of the Performance of Cement Treated Bases as Used in Composite Pavement in California. California Department of Public Works.
10. Hveem, F. N., and Zube, E. California Mix Design for Cement-Treated Bases. Highway Research Record 36, pp. 11-55, 1963.

Application of AASHO Road Test Results to Design of Flexible Pavements in Minnesota

MILES S. KERSTEN and EUGENE L. SKOK, JR., Civil Engineering Department, University of Minnesota

This paper reports on a study of the design of flexible pavements in Minnesota applying some of the concepts of the AASHO Road Test. The method presently used to design flexible pavements in Minnesota is described; it utilizes ADT and HCADT, a designation of spring axle load, the AASHO soil classification system, and gravel equivalent factors. The design method was studied by measurements on 50 test sections established on in-service highways throughout the state. The program of field plate and Benkelman beam tests and laboratory strength tests on the pavement materials is described. An important aspect was variation in strength throughout the year.

The performance of the sections has been studied by utilizing the roughometer in determining PSI; traffic has been evaluated; performance trends are noted, and predictions have been made. The AASHO Interim Guide and Asphalt Institute design procedures, which are based on the concepts of the AASHO Road Test, are used as a basis of comparison for the performance of the Minnesota test sections. A relationship using the spring Benkelman beam deflection and performance, originally developed at the Road Test, is examined and the Minnesota results thus far are studied for compliance. Modifications of the present Minnesota flexible pavement design are suggested on the basis of the observed performance of the test sections to date.

•FOR THE PAST several years the Minnesota Department of Highways has engaged in a study of its flexible pavement design utilizing some of the concepts developed at the AASHO Road Test. The project is being conducted under the Highway Planning and Research Program financed jointly with federal-aid funds of the U. S. Department of Transportation, Bureau of Public Roads, and with state funds of the Minnesota Department of Highways. A part of this work has been done by personnel of the Civil Engineering Department of the University of Minnesota under a contract with the Department of Highways. This paper is a report based on the work of both the Department of Highways and the University.

The present Minnesota design procedure considers traffic in terms of average daily traffic (ADT) and heavy commercial average daily traffic (HCADT), the AASHO soil classification groups (A-1, A-2, etc.), and gravel equivalencies for various pavement materials. The AASHO Road Test has given relationships that make it possible to predict the number of applications of a given axle load that a given pavement can withstand before being reduced to various levels of serviceability. To use these relationships in a study of the Minnesota design method, it was necessary to collect information on

Paper sponsored by Committee on Flexible Pavement Design and presented at the 48th Annual Meeting.

Minnesota pavements that could be entered into these equations. It was decided that in-service highways would be used in such a study for the following reasons:

1. It is possible to obtain performance information more quickly by using in-service highways;
2. The state can be covered more thoroughly by using individual sections in different areas;
3. A variety of embankment materials can be studied more easily;
4. The effect of various levels of traffic density can be studied as they occur in service; and
5. Using in-service highways is less costly than building a separate test road.

Fifty in-service sections on Minnesota highways were selected for study in 1963 and 1964. Most of these are 1200 ft long and one traffic lane wide. Serviceability tests are made on two 500-ft long sections and a 200-ft section is used for sampling or destructive tests. Plate tests, for example, are run in the 200-ft section. The test sections are located throughout the state and represent a range of soils, climate, and traffic. All are of essentially modern design. The surface thicknesses vary from 1.5 to 9.5 in., the granular bases from 0 to 15 in., and the granular subbases from 0 to 29 in.

The work that has been done on these sections is as follows: (a) the subgrade soils, subbase, base, and surface materials have been sampled and tested in the laboratory both by routine tests and also with special strength tests; (b) field strength tests such as plate bearings and Benkelman beam tests have been made periodically; (c) serviceability determinations have been made yearly; and (d) traffic information has been collected.

Along with the general concept of correlating the performance of Minnesota asphalt pavements to the AASHO Road Test, the establishment of the test sections has made it possible to make various other analyses that when used with Minnesota Department of Highways practice will have immediate use. An example of these programs is the spring recovery program, for which strength tests have been run every week or so on 15 to 20 test sections during the critical spring period. The Benkelman beam deflection test has been established as a useful tool for determining the maximum allowable spring axle load. The use of the R-value for evaluation of soils in the present Minnesota Department of Highways design procedure has also been recommended based on the results of the embankment testing. Methods of using traffic and the serviceability concept (in the present design procedure) have been conceived. A roughometer calibration wheel has also been set up in conjunction with this study. Thus, there already are benefits derived from the investigation.

Using the serviceability determinations and the traffic information, the performance trends of the sections are being studied. Because the history is only a few years old, however, a final evaluation of performance of the sections cannot be made. The performance to date is being studied on the basis of the design procedures in the AASHO Interim Guide and the Asphalt Institute method.

PRESENT MINNESOTA FLEXIBLE PAVEMENT DESIGN PROCEDURE

Since 1954, flexible pavements in Minnesota have been designed essentially using the traffic and the type of embankment soil to determine a design thickness. Also specified for each design is the maximum allowable spring axle load in tons. The thickness specified is in terms of a gravel equivalent that rates the various components of the pavement section.

The traffic loading is considered using allowable spring axle load categories for light traffic, and the ADT and HCADT. The ADT includes all vehicles and the HCADT includes all trucks with six or more tires; thus HCADT does not include small pickup and panel-type trucks. The design makes provision in two cases where the allowable spring axle load can be increased by 2 tons if an additional 2- or 3-in. overlay is added at a later time; thus a 7-ton design can ultimately become a 9-ton design (Table 1).

The ADT and HCADT used for design are values predicted for 20 years in the future. To predict the traffic 20 years from now, it is assumed that the volume increases about

TABLE 1

MINNESOTA FLEXIBLE PAVEMENT DESIGN STANDARDS, 1964[a]

Axle Load	Daily Hvy. Com. (HCADT)	Total Daily Veh. (ADT)	Surface		Bituminous Base		Bituminous Treated Base		Gravel Base, Spec. 3138		Sand-Gravel Subbase, Spec. 3123		Total Base Thickness (in. of G.E.)	Total Pavement Thickness (in. of G.E.)
			Thickness (in.)	Spec.	Thickness (in.)	Spec.	Thickness (in.)	Spec.	Thickness (in.)	Class	Thickness (in.)	Class		
5 ton		Less than 400	1½	2321					3	5	5	4	7	9
7 ton		Less than 400	1½	2331					4	5	6	4	8½	11½
5 ton—ult. 7 ton		400 to 1,000	1½	2331	1	2208			3	5	6	4	9	12
7 ton		400 to 1,000	2	2331	1	2208			3	5	8	4	10½	14½
7 ton—ult. 9 ton	Less than 150	Less than 1,000	2	2208					4	5	9	4	11	14
7 ton—ult. 9 ton	150 to 300	1,000 to 2,000	2	2331	1	2208			5	5	9	4	13½	17½
9 ton	Less than 150	Less than 1,000	2	2331	1	2208			5	5	9	4	13½	17½
9 ton	150 to 300	1,000 to 2,000	3	2341	1	2208			5	5B	10	4	14	20
9 ton	300 to 600	2,000 to 5,000	3	2341	1½	2331	4 Rich	2204			6 6	4A 4	18	24
9 ton	600 to 1,100	5,000 to 10,000	3½	2351	3½	2331	4 Lean	2204			6 6	4A 4	21	28
9 ton	More than 1,100	More than 10,000	3½	2351	4½	2331	4 Lean	2204			6 8	4A 4	24½	31½
9 ton	More than 1,100	More than 10,000	3	2351	8 Concrete				3	5	3	4	—	—

[a]These designs are for use on A-6 subgrade soils; for use on other soils, thicknesses should be adjusted as described in Table 2.

TABLE 2

SOIL FACTORS FOR MINNESOTA DEPARTMENT OF HIGHWAYS FLEXIBLE PAVEMENT DESIGN PROCEDURE

AASHO Classification of Soil	Soil Factor, Percent	AASHO Classification of Soil	Soil Factor, Percent
A-1	50 to 75	A-5	130+
A-2	50 to 75	A-6	100
A-3	50	A-7-5	120
A-4	100 to 130	A-7-6	130

3 percent per year. This is equivalent to multiplying the present values by 1.805. Local conditions are also considered and the projected value may either be increased or decreased, based on the potential use of the road.

The design thicknesses listed in Table 1 are for A-6 type embankment soils, which are the predominant soils in most of Minnesota. The designs are modified for other embankment types using the percentages given in Table 2. These percentages reflect both the strength and the frost susceptibility of these soils relative to the A-6 soils. There are ranges of percents shown for A-1, A-2, and A-4 soils. It is therefore possible to use some judgment relative to capabilities of these soils.

The percentages given in Table 2 are applied to the base plus subbase portion of the gravel equivalents for the A-6 soils. The plus or minus variation in gravel equivalent is applied to the subbase thickness only. For a given set of traffic conditions, the surface and base thicknesses for any type of embankment are the same or greater than the thicknesses shown for the A-6 embankments. If a particular design is calculated to require less gravel equivalent than is provided by the base course, the base thickness shown for the A-6 soils for the given level of traffic is still used. In other words, the surface and base thicknesses shown for A-6 soils in Table 1 are minimum designs for the respective values of traffic.

The gravel equivalent factors used for evaluating the various materials and mixtures in a flexible pavement section are based on a value of 1.00 for gravel base (Spec. 3138, Class 5 or 5B). The factors go as high as 2.25 for plant-mix surface (Spec. 2341 or 2351) and as low as 0.75 for sand-gravel subbase.

PROPERTIES OF PAVEMENT SECTION COMPONENTS AND EMBANKMENTS

All materials of the layers making up the pavements on the 50 test sections have been sampled and tested. Extractions have been made of asphalts from cores of the pavement and such tests as penetration, ductility, and softening point are available for further study.

The tests made on the base and subbase materials include field densities and moisture contents, gradations and plasticity indexes. A study was made to compare the strength of some of the granular materials as determined by three different test procedures. The three tests used were the triaxial test, the California Bearing Ratio (CBR) and the Hveem stabilometer test.

Five base and five subbase materials were selected. Four of the materials represent extremes of T 99 density and of the percent passing the No. 200 sieve. The fifth material chosen represented values between these.

The results of the strength tests run on the 10 samples with the triaxial test, the stabilometer R-value, and the CBR were compared, and the following conclusions are drawn. The angle of internal friction does not vary significantly for any of the granular materials that pass the Minnesota Department of Highways specifications. The CBR results order the granular base materials in a reasonable fashion, but to obtain a design CBR value it is necessary to run a number of tests. The stabilometer R-value has also shown consistent results and it is an easier test to run than either the triaxial or CBR tests. It was, therefore, decided to run R-value determinations on all of the granular base and subbase materials. There were only two base materials with an R-value below 76 and only three subbases below 74.

Extensive testing was also done on the embankment soils, including determination of field density and moisture content, gradation, plasticity index, moisture-density tests, CBR, and stabilometer R-value. The soils range from A-1-b to A-7-6 based on the AASHO classification, and texturally from sands and gravels to heavy clays. The group indexes vary from 0 to 20. The AASHO Road Test embankment was an A-6 soil with a group index of about 8.

The stabilometer R-value test was run using the method outlined by Wolfe (2). This method is essentially the same as that recommended by the California Division of Highways and the Asphalt Institute. An exudation pressure of 240 psi is used to establish the design R-value. It was found that this exudation pressure yielded a specimen with a moisture and density close to what was felt were critical field conditions (2). The distribution of R-values shows a concentration of values below 20. The distribution of these strengths for soils throughout the state are most likely of this same order. The values range from a low of 5 to a high of 77, which indicates about a maximum range based on this test. The R-value of the Road Test embankment has been taken as 12 (3). Correlations are made between the R-value at various exudation pressures and field strength of the embankment based on the plate tests run on the embankment. It was found that the R-value determined at 200- to 240-psi exudation pressure correlated best with the field embankment strength measured with the plate load test.

The CBR test was also run on each of the embankment soils (4, chap. 8). This is essentially the Corps of Engineers CBR test method. Compactive efforts of 26 blows per layer and 55 blows per layer were used for establishing the CBR curves. The design CBR was taken to be the lowest CBR value obtained assuming the embankment was compacted according to Minnesota compaction specifications. The Minnesota specifications state that the top 3 ft of the embankment is to be compacted to maximum T 99 dry density and between 65 and 102 percent of optimum moisture content. The design CBR's range from 1 to 65. The CBR of the AASHO Road Test embankment has been estimated at 2.5 to 4.0, depending on the analysis of the lab data.

FIELD STRENGTH TESTING

The strength of the Minnesota test sections has been evaluated in the field using two strength tests—the plate bearing test and the Benkelman beam deflection test. The plate bearing test has been run using two procedures, the standard Minnesota "quickie" procedure and a repeated load procedure. The quickie method consists of applying loads in several increments to the pavement on a circular 12-in. steel plate and recording deflections. This test has been run on most of the test sections once a year and more often during the critical spring period on test sections selected for spring recovery study. Overall, there has not been a significant change in bearing value from year to year except for the summer of 1965, which had lower values, following the most critical spring thus far observed.

A series of plate load tests, termed "fractional repeated load tests", was run once on every section in 1963 or 1964. In this procedure, repeated load plate tests were run on the surface, the top of the base, the subbase, and the embankment. The test procedure is the same as that used at the AASHO Road Test (1).

The data obtained from a repeated load test consist of total and elastic (rebound) deflections for each application of each load. The first value of total deflection is usually larger than the other two, probably because of seating effects. The rebound deflection does not usually vary by more than 0.01 or 0.02 in. for the three applications of load. E-moduli of the embankments have been calculated using the average elastic deflection for each magnitude of load. The E-modulus is calculated from Boussinesq's equation for a single elastic layer. The E-moduli of the granular embankments tend to increase with increasing pressure, and the E-moduli of the plastic embankments tend to decrease with increasing pressure on the plate.

Repeated load plate tests have been run periodically on the surface of each of the test sections. On all but the spring recovery test sections the tests have been run annually. On the spring recovery sections, repeated load plate tests were run at the same time as the quickie plate tests, which was about every week during the critical spring period.

Benkelman beam deflection tests were run on all test sections in two sets in 1963 and 1964. The summer tests were run in June through August, and the fall tests were run in September and October. In the following years deflection tests were run about once a year in most of the sections. To better define the strength during the critical spring period, deflection tests were run on the spring recovery sections about weekly.

Two procedures for measuring deflections from a 9-ton axle load were used in 1963. The "normal" and "rebound" methods are described in detail elsewhere (1). Also, in 1963, deflections were run in both wheelpaths. In 1964 and following years only the rebound procedure has been used and only in the outer wheelpath. The rebound procedure was used because the effect of the deflection basin on the readings has been found to be less by the Canadian Good Roads Association (6). The outer wheelpath has been used because comparison between the outer and inner wheelpaths showed the outer wheelpath to have higher deflections.

A deflection for a test segment is determined by running deflection tests at 50-ft intervals in each 500-ft segment. The individual values are averaged and a standard deviation is determined.

VARIATION IN PAVEMENT STRENGTH THROUGHOUT THE YEAR

In addition to the annual strength testing on the Minnesota test sections, a number of sections were tested at more frequent intervals and especially during the critical spring period. Pavement strengths determined with the quickie plate load test have been used as criteria for establishing maximum allowable spring axle loads for some 10 to 15 years. A study was run in 1956 and 1957 to establish the variation in pavement strength during the year according to the quickie plate test. The variation in pavement strength was found to be dependent on embankment type and not dependent on pavement section thickness (5).

The more frequent testing on the test sections has been used to check the relationships previously used with the plate test, and to establish spring ratios of Benkelman beam deflections so that the strength measured at any time of the unfrozen portion of the year could be used to predict a spring strength.

The test sections selected have predominantly clayey subgrade soils, which are of greatest interest because this type of soil is most prevalent in Minnesota. Another criterion used in determining the test sections was that the testing crew be able to cover the entire testing circuit in about one week. During 1964 and 1965, 11 test sections were selected to be studied, and in 1966, 1967, and 1968, 15 test sections were included in the program. The spring recovery field testing included the bearing value using the Minnesota quickie plate load test; the Benkelman beam deflection test; moisture contents of the base, subbase, and embankment soil; and air and mat temperatures.

The quickie plate load test was not run in 1968 because it was felt that more information could be obtained faster with the Benkelman beam deflection test. The procedures mentioned previously have been used for the plate load and the Benkelman beam tests. The data studied included climatic variables of temperature and precipitation. These data were considered to give some idea of how critical the years of spring recovery testing were relative to an overall average year. If testing is continued for a number of years on the same sections, it will be possible to estimate the frequency of various critical years in terms of loss of strength.

Both the quickie plate load test and the Benkelman beam deflection test have been used to evaluate bearing capacity of flexible pavements. However, the two methods apparently measure different characteristics of strength. The Benkelman beam test results are more dependent on the upper portion of the pavement, whereas the quickie plate load test results are more dependent on the lower structure. This is reasonable because the quickie plate load test evaluates bearing capacity at a higher deflection than does the Benkelman beam test. It is concluded from the 4 years of spring testing that the Benkelman beam test is easier to run and that more tests can be made in a given length of time. It is felt that the beam devices could be efficiently used in each Department of Highways district to evaluate the roads in the districts, whereas the expenditure involved with providing a plate bearing truck for each district would be prohibitive.

TABLE 3

DEFLECTION RATIOS TO CALCULATE MAXIMUM SPRING DEFLECTIONS FROM DEFLECTIONS TAKEN DURING OTHER NONFROZEN TIMES OF THE YEAR

Asphalt Surface Thickness	Date of Test								
	Sept.	Aug. 16-31	Aug. 1-15	July 16-31	July 1-15	June 16-30	June 1-15	May 16-31	May 1-15
2 in. or less	1.85	1.80	1.75	1.70	1.65	1.60	1.50	1.35	1.15
2½ to 3½ in.	1.80	1.78	1.75	1.70	1.65	1.60	1.50	1.35	1.15
3½ to 5½ in.	1.75	1.70	1.65	1.60	1.55	1.50	1.45	1.30	1.15
5½ to 8 in.	1.45	1.42	1.40	1.37	1.35	1.32	1.30	1.20	1.10
Greater than 8 in.	1.25	1.20	1.15	1.10	1.08	1.05	1.05	1.05	1.00

Ratios given are for clayey embankments. For loam and silt loam embankments, 0.15 higher ratios are recommended from June 15 through September and 0.10 higher from May 1 through June 15. For sand or sand and gravel embankments, a ratio of 1.20 is recommended from June 1 through September, 1.10 from May 15 to June 1, and 1.05 prior to May 15.

With regard to the Benkelman beam deflection test, the following conclusions were drawn:

1. The percent of maximum spring to fall deflection values generally decreases as the surface mat thickness increases.
2. The loss of strength is dependent on the embankment type. A division into three soil-type categories of plastic, semiplastic, and nonplastic is appropriate.
3. One test section with a crushed limestone base material showed high loss of strength. This is evidently because the material had a high percentage of fines.
4. The average percent of maximum spring to fall deflection values compared closely to the value obtained from the CGRA study (6). However, that study does not show deflections to be dependent on surface thickness.
5. The highest average annual Benkelman beam deflection occurred during the spring that showed the highest average moisture content in the subbase and embankment.

The average date of minimum strength occurred 18 days after the end of the freezing season. The longest time period between the end of the freezing season and minimum strength occurred during the year that had the highest freezing index value. These results occurred for both test methods.

Based on the spring recovery study and other information available from previous studies by the Minnesota Department of Highways, three methods have been suggested for the determination of allowable spring axle loads.

The first method uses quickie plate bearing test results and is basically the standard method that had been used by the Department of Highways. Less reduction in spring bearing percentages is recommended for thicker pavements.

The other two methods use the Benkelman beam deflection test to evaluate the strength of the pavement. The first deflection method uses the deflection results to correlate with the plate bearing value and then this value is converted to an allowable spring axle load as presently used. This method is of doubtful value because the correlations between deflection and bearing value are only approximate. The third method uses the Benkelman beam deflection and allowable deflections to establish the allowable spring axle load without a correlation with the plate bearing value. The method requires the determination of three factors to estimate an allowable axle load: (a) the variation of deflections throughout the year for various highway sections; (b) the determination of allowable deflections; and (c) the relationship between load and deflection for appropriate highway sections.

The variation in deflection throughout the year has been determined from the spring recovery study. A deflection measured at any time during the year can be converted to a spring value using the ratios in Table 3. These ratios were developed by plotting deflections for each test section for each year (1). The spring of 1965 was found to be the most critical spring and thus the ratios shown in Table 3 are close to the ratios found for that year. By grouping the sections into various categories of thickness, it was found that the ratios were most dependent on surface thickness. This is reasonable because in the spring the surface mix tends to be harder when cool and thus would tend to decrease the spring deflection. The ratios were also assumed to be dependent on

TABLE 4
SUMMARY OF RECOMMENDED ALLOWABLE SPRING DEFLECTIONS

One-Way Daily $N18^a$	Two-Way ADT	Two-Way HCADT	Allowable Deflection (in.) Where Surface Thickness Is:		
			Less Than 3 in.	3-6 in.	Greater Than 6 in.
25	500	50	0.075	0.065	0.055
25-50	500-1,000	50-100	0.070	0.060	0.050
50-150	1,000-3,000	100-150	0.060	0.050	0.040
150	3,000	150	0.045	0.040	0.035

[a]N18 = Daily equivalent 18,000-lb axle loads.

embankment soil classification. The spring recovery section that had a sand embankment (TS 15) had a very low deflection ratio, which agrees with the previous findings using the plate load test (5). Test Section 41, which has a loam embankment soil, showed very erratic behavior; this had also occurred for this type of soil in previous strength studies. Thus the ratios for this group (semiplastic soils) are the highest.

A number of previous studies (7, 8, 9, 10) along with the AASHO Road Test have been considered to establish allowable spring deflections. The measured maximum spring deflections from the spring recovery study were considered relative to the performance of the sections to help establish allowable deflections. The allowable deflections that result from these considerations are shown in Table 4. The allowable deflections have been assumed to be dependent on the surface thickness and the level of traffic on the road, as indicated in the table. The traffic values in Table 4 are roughly correlated using the relationships developed in the traffic study related to this project and reported elsewhere in this Record (16).

Using the data reported by Huculak (10) and some data from the Minnesota sections plus some load-deflection relationships from the AASHO Road Test, it has been assumed that deflection and load are directly proportional for a relatively well-designed road and loads within the legal axle limit.

With the assumption of a linear relationship between load and deflection used, three quantities are needed to calculate the allowable spring axle load. These are (a) the axle load under which the deflection test is made, (b) the predicted spring deflection, and (c) the allowable spring deflection for that section of road. The allowable spring axle load can then be calculated by

$$L_A = L_D \frac{d_A}{d_s} \quad (1)$$

where

L_A = allowable spring axle load, tons;
L_D = axle load used for deflection testing, tons;
d_A = allowable maximum spring deflection from Table 4, in.; and
d_S = predicted spring deflection for the pavement section, in.

It has been recommended that the spring recovery work be continued so that the relationships thus far developed can be verified.

EVALUATION OF PRESENT CONDITION OF PAVEMENT SECTIONS

The terms of present serviceability rating (PSR) and present serviceability index (PSI) were developed at the AASHO Road Test (15). Equation 2 is the relationship found at the Road Test for flexible pavements:

$$PSI = 5.03 - 1.91 \log (1 + SV) - 1.38 \overline{RD}^2 - 0.01 (C + P)^{1/2} \quad (2)$$

where

PSI = present serviceability index;
SV = slope variance;
RD = rut depth, in.; and
C + P = area of cracking and patching, sq ft per 1,000 sq ft.

These measurements were made every 2 weeks at the Road Test and the rate of decrease of PSI with traffic was used to define performance. Formulas reported from the Road Test define the thickness required to maintain the PSI above a given level for a given number of applications of a particular axle load. The terminal level of PSI for design purposes is usually taken as 2.50 or 1.50. A value of 1.50 was considered failure at the Road Test.

To use the concepts developed at the Road Test it is desirable to establish a serviceability determination for highway pavement sections and study the decrease in value of this serviceability with time. This concept can also be a useful tool for routine evaluation of the condition of highway pavements.

To apply the results of the AASHO Road Test to other areas it is necessary to use the same parameters as were developed in the Road Test. This required, in the case of determination of road condition, that a measure of present serviceability for pavements be devised. A direct correlation is difficult in Minnesota for two reasons. First, a profilometer to measure slope variance was not available. Second, the surface textures on in-service highways differ from those at the AASHO Road Test. A third more basic consideration is that some engineers feel that the present serviceability index, as developed at the Road Test, does not always directly reflect the strength of a pavement structure. An example of this is a case where roughness occurs because transverse cracks have developed and become rough.

A BPR-type roughometer has been used to evaluate roads in Minnesota for about 20 years. Because this device was operational and a reasonably good correlation was found between the roughometer and serviceability at the AASHO Road Test, it was decided to relate roughness measurements to serviceability ratings using the Minnesota Department of Highways roughometer. The correlation has been obtained by special runs made in South Dakota in 1960 through 1962 (11), by a special test between the CHLOE profilometer and the roughometer in Minnesota in 1961 (14), in runs made on sections in Indiana established by Purdue University (12), and in a special study of about 200 half-mile segments selected in Minnesota. The details of all these correlation studies cannot be given here. However, the final equation evolved for determining the present serviceability index is as follows:

$$PSI = 11.03 - 3.98 \log (RI) - 1.38 \overline{RD}^2 - 0.01 (C + P)^{1/2} \qquad (3)$$

RI is the roughometer index in inches per mile and the other items are as noted before. This equation is similar to one developed by the Illinois Division of Highways (13) for their roadometer. To calculate the PSI of the test sections using Eq. 3 it is necessary to determine the roughometer index, the rut depth, and the cracking and patching of the pavement section.

The roughometer electronics may vary somewhat from time to time. A calibration course along TH 96 near Stillwater had been used for calibration of the roughometer. Because this is a typical highway pavement, the surface tends to vary in roughness with time. To establish a more consistent calibration for the roughometer, a 10-ft diameter vertical steel wheel located at the Rosemount Research Center was reactivated during the fall of 1964. A 15-hp AC motor was connected to the existing vari-drive transmission and a set of pulleys so that the wheel runs at 57 rpm, which is equivalent to 20 mph at the circumference. A system has been arranged so that the roughometer truck can be backed up to the wheel and the roughometer wheel placed on the calibration wheel. The calibration wheel is fitted with nine ¼-in. strips on one side, and three ¼-in. strips on the other side. When the wheel of the roughometer is set on the nine-strip side, a roughness of approximately 100 in. per mile results; the three-strip side gives about

60 in. per mile. If the calibration varies by more than 10 percent at any time, the roughness indexes measured in the field must be adjusted.

The other two elements of the serviceability index (rut depth and cracking and patching) have also been determined periodically on the Minnesota test sections. Extreme precision is not necessary because the rut depths usually encountered do not affect the PSI significantly. Cracking and patching values are estimated in square feet per 1000 square feet of pavement area. The structural cracking, or that caused by repeated wheel loads, is the only type considered for serviceability calculations. Shrinkage and contraction cracks that are not load-associated are not included in the area of cracking. Load-associated cracking is divided into three types (15): Class 1 cracking is that which has connected into blocks smaller than about 2 ft in dimension; Class 2 cracking is that which has connected into blocks less than 6 in. in size; and Class 3 cracking is Class 2 cracking with pieces that are loose. Class 2 cracking is also called alligator cracking. Classes 2 and 3 cracking only are included in the C + P term of the PSI formula. This term has only a small effect on the value of the PSI and therefore need be only approximated.

Because the general decreasing trend of the serviceability of the Minnesota test sections is slight, it has only been necessary to determine serviceability once per year. Present serviceability indexes have been determined on each test section in each of the summers of 1963 through 1967 using the roughometer and determinations of rut depth and cracking and patching. The individual values are available for each test segment of each test section and are being used along with the traffic to develop performance trends.

The trends in PSI values for the test segments have been slightly down for the sections that have not been overlaid. The average PSI values for 63 test segments that can be compared for the 5 years are as follows:

Year	Average PSI
1963	3.82
1964	3.76
1965	3.83
1966	3.64
1967	3.63

As can be seen, the general level of PSI has been high and the trend is only very slightly down, which makes a performance analysis based on these concepts somewhat difficult at this time.

Initial PSI values are also necessary for the performance analyses, and they have been obtained from roughometer indexes made when the pavement was constructed. If a roughometer index was not available, an average initial value of 4.10 was used.

DETERMINATION OF A TRAFFIC PARAMETER

To make a performance analysis of flexible pavement sections based on the concepts of the AASHO Road Test, it is desirable to convert the mixed traffic loading on the test sections into a summation of equivalent 18,000-lb single axle loads since the pavement was built. It is also necessary to study the variation in these values on a yearly basis so that equivalent 18,000-lb axle loads can be predicted for the design period of a pavement. A traffic study has been made on the Minnesota test sections to make these determinations possible.

The three purposes of the traffic study can be summarized as follows: (a) to determine the total traffic in terms of the summation of equivalent 18,000-lb axle loads on each of the 50 Minnesota test sections since each was built; (b) to estimate a reasonable growth factor based on the data of the last 12 to 15 years; and (c) to correlate various traffic parameters to equivalent 18,000-lb axle loads for design purposes.

A detailed field traffic study that included weight and volume distributions of vehicles at each test section was made three times throughout 1964 and once during the spring load restriction period in 1965. The data from this study were modified for other years

using statewide data to determine the total equivalent 18,000-lb axle loads on each test section since it was built. The computations were put into a computer program on the CDC 6600 computer.

The rate of increase in equivalent loads has been studied over the last 12 years and it is concluded that a rate of increase of 8 percent per year is reasonable for an overall estimate, but that local conditions can cause a very significant range in growth factor.

The 1964 traffic study was used to correlate ADT, HCADT, and the daily sum of Types 4 and 5 (four-axle and five-axle) trucks to daily equivalent axle loads. The errors in equivalent loads from predicting traffic by these three parameters have been related to gravel equivalent thicknesses. It was found that for design purposes the summation of Type 4 and 5 trucks could best predict equivalent axle loads, but that only a slightly poorer correlation resulted using the HCADT. The error in terms of gravel equivalent is about 1.2 in., which represents about 0.6 in. of asphalt surface.

Using the results of the traffic correlations back to 1956, the correlation between HCADT and daily equivalent loads has been studied and it has been found that the equivalent loads predicted from HCADT over the last 10 years have had an annual increase between 4 and 26 percent, depending on the span of years considered for the increase. Over a 10-year or longer period, an increase of 5 to 8 percent is shown to be appropriate. This increase, along with an annual 3 percent increase in HCADT, yields the growth factor of 8 to 11 percent.

From the results of this study the summation of equivalent 18,000-lb axle loads over a 20-year period represented by the present Minnesota traffic categories shown in Table 1 are calculated (16).

PERFORMANCE TRENDS AND PREDICTIONS

General performance analyses based on the concepts of the AASHO Road Test are made essentially by considering the trend of PSI with the increasing values of summation in equivalent 18,000-lb axle loads. By observing these trends on the test sections it is anticipated that it will be possible to determine how much traffic is required to lower the PSI to a given level (usually 2.5 for primary roads), and to define the shape of the performance curves to aid in the prediction of the number of applications to various levels of serviceability. This can be done by observing the performance trends of the test sections and relating them to the thicknesses and embankment strengths of the sections or to the strength of the sections. At this time the performance of the sections has been compared to the performance predicted by the AASHO Interim Guide and the Asphalt Institute design procedures, which are based on the Road Test concepts. At the Road Test an equation was developed relating spring beam deflections to the number of applications to a PSI of 2.5. Using the measured or predicted spring deflections on the test sections, this relationship is verified for Minnesota conditions. So far there is generally not enough drop in PSI for the test sections to determine thickness or strength requirements absolutely. The relationships shown in this section are the methods that appear to predict performance relationships best from the data available to the present time.

Irick shows a simplified method of predicted log (ΣN18) to a PSI of any level when the original PSI is known and any number of points along the plot are determined (17). A curvature term, B, is calculated and used to make the predictions if more than one point along the line is known. A B-value of 0.5 indicates a curve that is concave down and a B-value of 1.0 indicates a curve that is concave upward.

The equations for this method have been put into a computer program, called PERPRED, that determines the curvature and predicted log (ΣN18) to PSI levels of 2.5 and 1.5. The traffic for the summers of 1963, 1964, 1965, 1966, and 1967 have been used along with the PSI values for those years to enter into the PERPRED program. Most of the test sections had not decreased in PSI enough to yield an accurate estimate of either B or log (ΣN18) to a PSI of 2.5. The B-values generally tend to get higher as the PSI levels decrease. If the initial PSI is high, the B-value tends to be high, indicating upward curvature. At this time it is not possible to establish a well-defined curvature value for the performance trends, but generally it appears that a value close

to 1.0 is appropriate for sections that have lost more than one unit of PSI. For initial estimates of future performance this value can be used.

At the Texas Transportation Institute a method developed at the Asphalt Institute (18) is used to predict performance. For this method the slope of a log (PSI) vs arithmetic $\Sigma N18$ plot is determined and extrapolated to a PSI of 2.5 to predict performance.

Using the same data as used for PERPRED, the last points on the plot are used along with the original point to establish the slope. Again, because of the generally high PSI levels of the sections, the variation in predictions is quite great. Of the 79 test segments for which comparisons were made between PERPRED and this method, only about 21 percent of the predictions were within 50 percent of each other.

Both methods will continue to be used for performance predictions because (a) it is not yet possible to determine which of the models defines the observed performance trends best, and (b) these methods make it possible to predict the applications to a PSI of 2.5 with some degree of accuracy a number of years before the section actually goes to a PSI of 2.5.

The AASHO Interim Guide and Asphalt Institute design procedures are both set up based on the Road Test equations. To check the performance of the Minnesota test sections relative to these, design predictions of life in years left for each test section were made using the traffic level at the time of construction, the thickness of the pavement layers, and the strength of the embankment using the R-value or CBR test value. The number of years of life predicted by these procedures gives an idea of whether a given section is overdesigned or underdesigned according to the procedures.

The following conclusions were made based on a study of these predicted lives:

1. It is not possible to evaluate one of these design procedures against the others because there are not enough test sections that have gone to a PSI of 2.5.
2. The test sections that have nonplastic embankments (high strengths) are generally overdesigned according to these methods. The field performance confirms this because none of those sections are below a PSI of 3.0. Based on this fact, plus the fact that the life predictions are on the order of 40 to 50 years beyond 1967, it has been recommended that a reduction in thickness of pavements on these embankments be made on a trial basis.
3. Some of the sections on plastic soils appear to be overdesigned, as indicated by the long predicted lives, and some others appear to be underdesigned.
4. The parameters necessary to use these design methods can be evaluated in Minnesota and could be used to design flexible pavements in Minnesota.
5. For test sections with granular bases and subbases it is necessary to provide adequate drainage. The three sections that had much less life than would be predicted by these design procedures had poor drainage characteristics primarily because of trench-type constructions. On the other hand, two of the sections that are performing better than anticipated both have good drainage characteristics.
6. Even though the Asphalt Institute design procedure is based on thicknesses that are conservative compared to the AASHO Road Test data, rather than going through the middle of the data, as do the equations of the AASHO Interim Guide, the life predictions using the Asphalt Institute procedures are less conservative (longer). This happens because different types of equations or models have been fitted through the Road Test data.
7. Observation of the test sections should be continued at least until they reach a PSI of 2.5. This can be done adequately by determining the PSI once per year on each test section. The traffic can be updated each year using the statewide traffic report and the traffic program.

Four equations were developed relating Benkelman beam deflection to performance at the AASHO Road Test. The equations relate the number of applications of a given load to a PSI of 2.5 and 1.5 to the fall and spring deflections. The equation for spring deflections predicting equivalent 18,000-lb applications to a PSI of 2.5 is shown as Eq. 4. The equation using spring deflections is considered because the correlation is better than for fall deflections and the standard error is less. This is reasonable because the spring period is the most critical time in Illinois just as in Minnesota.

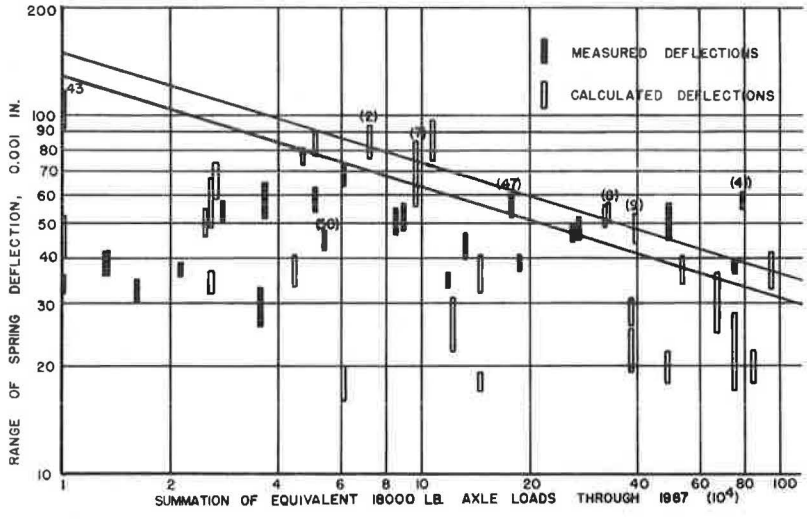

Figure 1. Measured and predicted spring deflection related to equivalent 18,000-lb axle loads sustained by the test section through 1967.

$$\log (\Sigma N18)_{2.5} = 11.06 - 3.25 \log d_S \qquad (4)$$

Squared correlation coefficient = 0.78
Standard error = 0.21

where

$(\Sigma N18)_{2.5}$ = summation of equivalent 18,000-lb axle loads to a PSI level of 2.5; and
d_S = Benkelman beam deflection taken during the spring period, 0.001 in.

At the AASHO Road Test, the normal deflection procedure yielded about the same deflections as the rebound procedure. The rebound procedure is used for determining deflection in Minnesota because this method yields a more accurate deflection on weak pavements. The deflection term in Eq. 4 is therefore assumed to be comparable to rebound deflections measured in Minnesota.

To see how the Road Test equation worked for Minnesota pavement strengths and mixed traffic, plots such as Figure 1 were made. The upper line on the figure is Eq. 4; the lower line represents one standard error conservative from this best-fit line. For each of the test sections a maximum spring deflection level has either been measured directly or estimated from fall deflections for the spring of 1964, 1965, 1966, and 1967. The range of these deflections for the four springs for each of the sections is plotted against the summation of equivalent 18,000-lb axle loads the section has sustained from the time of construction to 1967. The spring deflections have been adjusted to account for the maximum allowable spring axle loads on the test section. In 1967 all of the sections had serviceability levels higher than 2.5 except TS 28, 9, 41, and 50. Test Sections 2, 8, and 41 have been overlaid. In addition to these, only TS 7, 43, and 47 had serviceability levels less than 3.0. The other sections are performing well through 1967 and therefore for the $\Sigma N18$ values indicated for the section on the plot.

The position of the points checks Eq. 4 to some degree at this time because most of the points are to the left of the best-fit line. This means that the equation predicts that the sections can generally withstand more applications of load than have been sustained through 1967.

Unless a test section is overlaid in 1968, it will move to the right on the figure by the increase in log ($\Sigma N18$) represented by the 1968 traffic. If observations of serviceability and determinations of traffic are made in future years until each section reaches

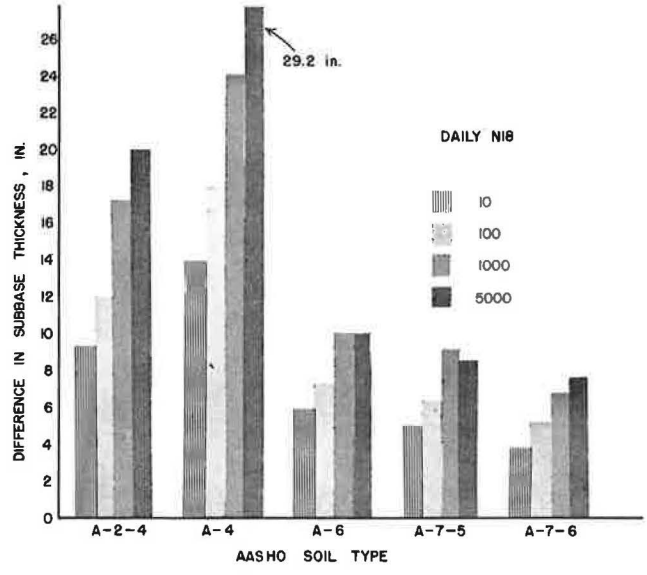

Figure 2. Differences in subbase thickness represented by variation in embankment strength for the AASHO soil classes using the AASHO Interim Guide R-value design procedure.

a serviceability level of 2.5, then a performance line for the Minnesota sections could be established. It may or may not agree with Eq. 4 from the Road Test.

Based on the position of the points in Figure 1 it has been recommended that a line one standard error conservative from the best-fit line from the Road Test be used for the present. This can be represented by Eq. 5, with terms as defined for Eq. 4:

$$\log (\Sigma N18)_{2.5} = 10.85 - 3.25 \log d_s \qquad (5)$$

With additional observations on sections in the future, this recommendation could be changed.

The advantage of using a strength test such as the Benkelman beam deflection to predict performance is that all localized conditions such as drainage, poor quality base material, and the like are evaluated. Using only thickness as an evaluation, this is not possible. These performance predictions with the deflection test are used to develop an overlay design procedure. The deflection test has also been established as a good method for determining allowable maximum spring axle loads.

EVALUATION OF THE PRESENT MINNESOTA FLEXIBLE PAVEMENT DESIGN METHOD

Based on the results of the performance studies on the Minnesota test sections, certain modifications to the present Minnesota design procedure are suggested. Some of these are direct modifications, such as using a strength test for embankment evaluation and changes in thickness requirements, whereas others are relationships developed from the data but that are not presently considered directly in the present procedure, such as an overlay design. In this section the recommendations are outlined and justified.

Embankment Evaluation

At the present time the AASHO classification system is used to evaluate embankments for design in Minnesota. "Standard" sections are given for an A-6 soil and are selected on the basis of the total volume of traffic (ADT) and the volume of heavy com-

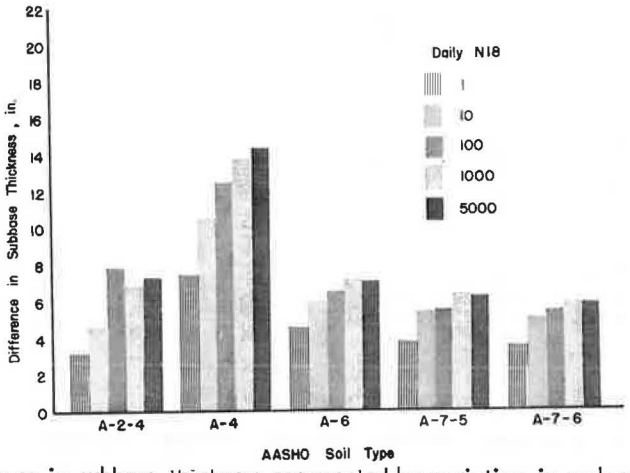

Figure 3. Differences in subbase thickness represented by variation in embankment strength for the AASHO soil classes using the Asphalt Institute R-value design procedure.

mercial trucks (HCADT). It is recommended that strength be used as a criterion for embankment classification based on the experience of a number of other agencies, such as the California Division of Highways (19), the Corps of Engineers (20), the Asphalt Institute (3) and others. For the Minnesota design procedure the recommended thicknesses are constant except for the A-1, A-2, and A-4 soils. However, the variation in strength found within each AASHO classification represents a range in pavement design thicknesses based on design procedures that consider the strength of the embankment. Figure 2 is a plot of the variation in subbase thickness that results if the AASHO Interim Guide is used for design on the weakest and strongest soils according to the R-values found within each AASHO classification. Figure 2 shows that the difference in design thickness in terms of granular subbase ranges from about 5 in. to 29 in., depending on the embankment soil type and the level of traffic. Figure 3 shows the differences in subbase thickness represented by the variation in R-value based on the Asphalt Institute design procedure. These plots show that, even though the AASHO classification generally denotes the strength of a soil, within a given class the variation in strength can be significant. The variation in thickness is shown to be most significant for A-2-4 soils followed by the A-6, A-7-5, and A-7-6 soils in that order. The differences are greatest using the AASHO Guide procedure compared to the Asphalt Institute procedure.

Correlations have been made between the field E-modulus from the plate load test and both the R-value and CBR. For the R-value, correlations were made for R-values obtained at exudation pressures of 100, 200, 240, 300, and 400 psi. The embankment E-moduli have been determined at 5-, 15-, and 25-psi plate pressures. The correlations were best for the R-values relative to the CBR and for the R-value determined at an exudation pressure of 200 psi. Based on these correlations plus the fact that the stabilometer R-value is somewhat easier to run than the laboratory CBR test, the stabilometer R-value has been recommend for evaluating embankment soils in Minnesota.

Evaluation of Materials in the Pavement Structure

The present Minnesota design method uses the gravel equivalent concept to evaluate the relative effect of the pavement layers for design. Ultimately, the relative effect of the layers should be based on the ability of the various layers to improve the performance of a pavement section. The equivalencies from the AASHO Road Test are the only ones based on performance at the present time. The relative effect of the layers has also been determined based on deflections that have also been related to performance. For the Minnesota test sections plus the sections used for Minnesota Investi-

gation 603 (22), equivalencies have been roughly implied based on spring tonnage obtained and deflections. The elastic theory has also been used to predict deflections using appropriate moduli for the layers. The problem with determining equivalencies is that, with variations in field conditions, the equivalencies can vary significantly on a daily and even hourly basis with changes in temperature, moisture content, etc.

Using an equivalency factor of 1.0 for granular-base materials, plant-mix surface equivalency factors have been shown to range from less than 1.0 to 15 depending on the method of evaluation and conditions assumed for evaluation. The greatest percentage of values is in the 2.2 to 3.5 range for critical field conditions. At this time it has therefore been recommended that use of the present factor of 2.25 for hot-mix asphalt concrete surfacing (mixes 2351 and 2341) be continued. A value of 2.00 can be used for the 2331 mix, which has a somewhat more open aggregate gradation requirement. It has also been recommended that the present factors be used for stabilized base courses. These are 1.50 for rich-mixed 2204 mixes and 1.25 for lean bituminous-treated bases. These values compare favorably with the factors determined by Terrel and Monismith for cured mixes using emulsions (23).

It has also been recommended that an equivalency of 1.00 be applied to subbase materials that fail base course specifications only because of material retained on the 1-in. sieve. Also, based on the low R-values found for the base materials on TS 28 and 29, it has been recommended that the gradation and degradation properties of crushed limestone bases be checked carefully. As more performance data are obtained on the test sections it will be possible to determine appropriate equivalencies based on this factor.

Traffic Evaluation

As a result of the study of traffic in this investigation, it has been recommended that the traffic factor in the design method be based on equivalent 18,000-lb loads. With such a factor, changes in the composition of the truck population can be more accurately handled than with a term such as HCADT. It will be possible to take advantage of the trends shown in the last few years that indicate an increase in equivalent 18,000-lb axle loads for a given number of trucks.

Thickness Recommendations

Although the histories of serviceability ratings on the Minnesota sections are still relatively short, it has been possible to make predictions of life by the models discussed and with the Benkelman beam spring deflections. These predictions permit, in effect, a judgment of the present Minnesota design. The results have been studied for various embankment types, R-values of the embankment, and traffic categories. Generally it has been found that the present Minnesota procedure is somewhat conservative for sections with relatively strong embankments. Recommendations are being made for changes in gravel equivalent thicknesses from minus 8 in. to plus 2 in. Continuing observations on the test sections may alter or strengthen these recommendations.

Designing an Asphalt Overlay Using Benkelman Beam Deflections

Benkelman beam deflections have been related to the performance of an asphalt pavement using Eq. 5. Equation 6 was developed for plastic embankment soils from data from a deflection study on Minnesota secondary roads (22) in addition to the data from this satellite study:

$$\log d_S = 2.300 - 0.051 D_1 - 0.022 D_2 \quad (6)$$

where

d_S = spring Benkelman beam deflection, 0.001 in.;
D_1 = asphalt mixture thickness, in.; and
D_2 = granular base plus subbase thickness, in.

With the logarithmic relationship for deflection, the antilogs of the coefficients indicate a percentage reduction in deflection per inch of material. It is stated that this equation should not be used as a design equation (22), but considering all other conditions constant it can be assumed that each inch of asphalt mixture decreases the deflection by about 10 to 12 percent. Using the traffic information developed in this study, it is possible to relate present traffic in terms of a daily number of equivalent loads or

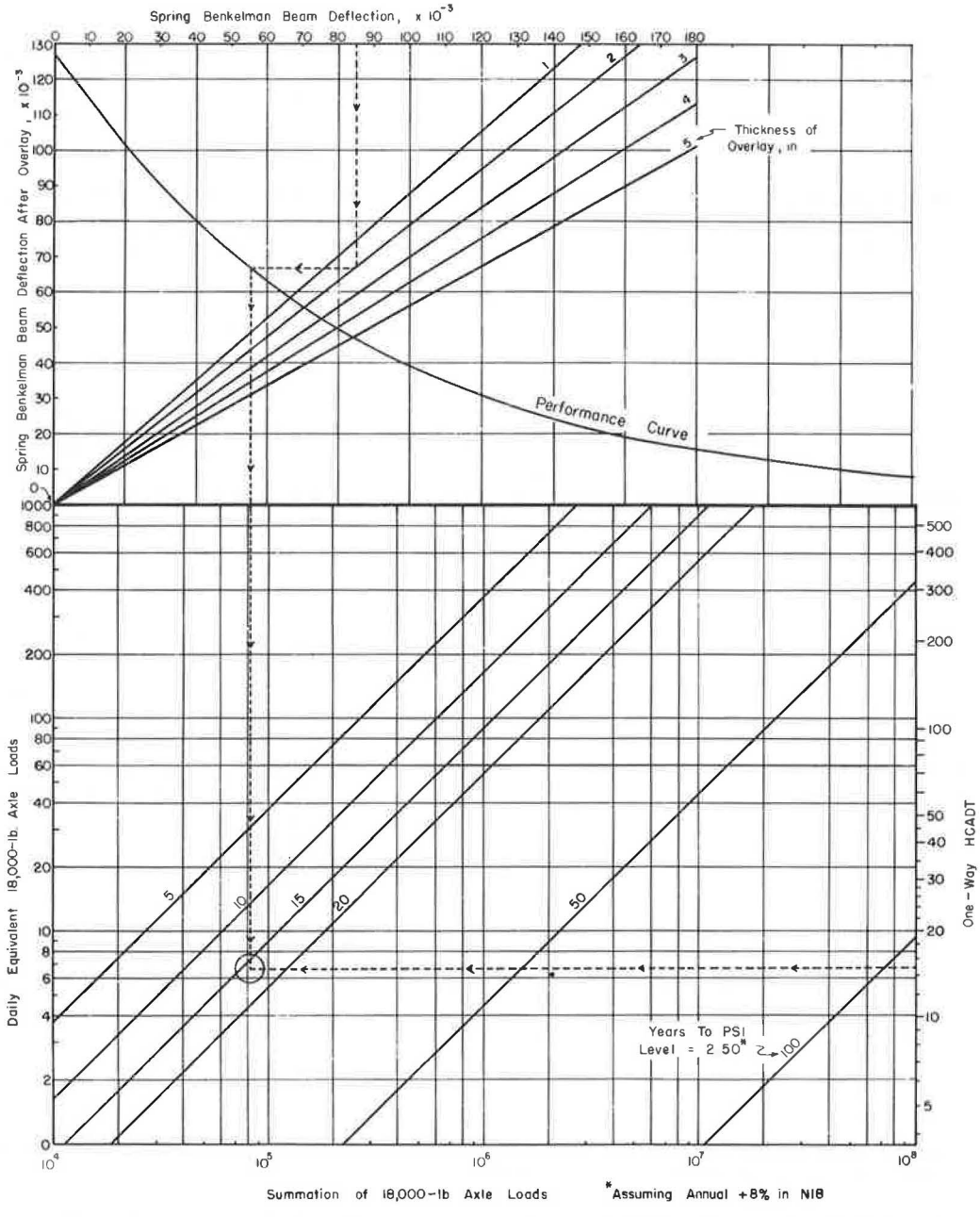

Figure 4. Performance predictions for pavements to be overlaid based on spring Benkelman beam deflections before overlay (for plastic embankments).

HCADT to the number of years it would take to accumulate a given total number of equivalent 18,000-lb axle loads. The number of years to accumulate the loads is, of course, dependent on the annual rate of increase in traffic assumed.

When these relationships are combined, a method such as that shown in Figure 4 could be developed to help estimate the effectiveness of an overlay in extending the life of an asphalt pavement. The upper part of the chart includes both the relationship between spring deflection before overlay and what it can be expected to be after various overlay thicknesses are added to the pavement section, and then how many equivalent 18,000-lb axle loads the pavement can be expected to withstand before the PSI level drops to 2.5 (assuming that the pavement is constructed to a PSI of about 4.0). The total number of equivalent loads is on the bottom axis of the chart. The lower part of the chart shows the relationship between present daily N18, HCADT, and how many years it would take to accumulate the given total number of equivalent axle loads.

The chart is set up for an annual equivalent load increase of 8 percent, but it could easily be modified to another value. The other relationships can also be changed as more information becomes available. It is felt that the present chart is somewhat conservative, which is necessary until more performance data are available from the Minnesota test sections. It is recommended that as many checks as possible be made on the relationships shown in the chart, especially the decrease in deflection observed on a pavement section after it has been overlaid. If possible, some test areas should be established where, on a given job, some ½-mile sections could be overlaid with 1 in. of asphalt, some sections overlaid with 2 in., and so forth, so that both the decrease in deflection and the relative performance of the sections could be observed. This additional information could then be added to the overall system of evaluation of flexible pavements.

This method could also be used as an indicator of an appropriate maximum spring axle load. For instance, if the life of a given overlay was considered too short, the spring deflection could be decreased by limiting the axle load on the pavement during that period. Thus, if a 7-ton axle load were the maximum load rather than a 9-ton load, the spring deflection could be reduced by seven-ninths with a corresponding increase in predicted life of the overlay section.

SUMMARY

By establishing 50 test sections on in-service roads in Minnesota and following a program of measurements—including serviceability determinations, plate tests, Benkelman beam deflections, and traffic—an evaluation of flexible pavements is being made using concepts originally developed at the AASHO Road Test.

A correlation has been developed so that present serviceability indexes can be determined using the Minnesota roughometer. Traffic is being evaluated on the basis of equivalent 18,000-lb axle loads. The performance of the Minnesota test sections for four years has been determined and methods of extending the performance trends are given. A method of utilizing spring Benkelman beam deflections to predict performance shows promise.

Modifications to the present Minnesota flexible pavement design are to be considered on the basis of these findings. Continued observation of the test sections is needed to verify the indicated relationships.

REFERENCES

1. Kersten, M. S., and Skok, E. L., Jr. Application of AASHO Road Test Results to Design of Flexible Pavements in Minnesota. Minnesota Department of Highways, Investigation 183, Summary Report, June 30, 1968.
2. Wolfe, R. E. Resistance R-Value of Embankment Soils and Aggregate for Use as Bases and Subbase. Minnesota Department of Highways, Investigation 176, 1960.
3. Shook, J. F. Development of Asphalt Institute Thickness Design Relationships. Proc. AAPT, 1964.
4. Soils Manual for Design of Asphalt Pavement Structures. The Asphalt Institute, Manual Series 10, April 1963.

5. Load Carrying Capacity of Roads as Affected by Frost Action. Minnesota Department of Highways, Investigation 147, 1947-1958.
6. A Guide to the Structural Design of Flexible and Rigid Pavements in Canada. Pavement Design and Evaluation Committee of Canadian Good Roads Association, CGRA Publ., Sept. 1965.
7. Carneiro, F. Bolivar Lobo. Benkelman Beam—Auxiliary Instrument of the Maintenance Engineer. Highway Research Record 129, pp. 28-59, 1966.
8. Zube, Ernest, and Forsyth, Raymond. Flexible Pavement Maintenance Requirements as Determined by Deflection Measurement. Highway Research Record 129, pp. 60-75, 1966.
9. Benkelman, A. C. General Discussion. Highway Research Record 129, pp. 76-78, 1966.
10. Huculak, N. A. Evaluation of Pavements to Determine Maintenance Requirements. Highway Research Record 129, pp. 12-27, 1966.
11. Crawford, R. A., Anderson, D. W., and Chastain, W. E., Sr. South Dakota Roughometer Comparison Tests—1962. Highway Research Record 28, pp. 63-97, 1963.
12. Yoder, E. J., and Milhaus, R. T. Comparison of Different Methods of Measuring Pavement Condition—Interim Report. NCHRP Rept. 7, 1964.
13. Chastain, W. E., Sr., and Burke, J. E. Experience With a BPR-Type Roadometer in Illinois. HRB Bull. 328, pp. 52-58, 1962.
14. Calibration of the Minnesota Roughometer and the AASHO Profilometer. Minnesota Highway Department Special Study 280, 1963.
15. The AASHO Road Test: Report 5—Pavement Research. HRB Spec. Rept. 61E, 1962.
16. Skok, E. L., Jr. The Development of the Traffic Parameter for the Structural Design of Flexible Pavements in Minnesota. Paper presented at 48th Annual Meeting and included in this Record.
17. Irick, P. E., and Hudson, W. R. Guidelines for Satellite Studies of Pavement Performance. NCHRP Rept. 2A, 1964.
18. Painter, L. J. Analysis of AASHO Road Test Asphalt Pavement Data by the Asphalt Institute. Highway Research Record 71, pp. 15-38, 1965.
19. Materials Manual of Testing and Control Procedures, Vol. I. California Division of Highways, Sacramento.
20. Fergus, S. M. Discussion of "Development of CBR Flexible Pavement Design Method for Airfields." Trans. ASCE, Vol. 115, 1950.
21. AASHO Interim Guide for the Design of Flexible Pavement Structures. American Association of State Highway Officials, Oct. 1961.
22. Skok, E. L., Jr. Load Carrying Capacity of Minnesota Secondary Flexible Pavements. Minnesota Department of Highways, Investigation 603, 1967.
23. Terrel, R. L., and Monismith, C. L. Evaluation of Asphalt-Treated Base Course Materials. Paper presented at AAPT Annual Meeting, Feb. 1968.

Design of Flexible Pavements in Virginia Using AASHO Road Test Results

N. K. VASWANI, Highway Research Engineer,
Virginia Highway Research Council, Charlottesville

A method based on the AASHO Road Test model equation and a theoretical equation for pavement deflection is presented for design of flexible pavements in Virginia. The independent variables evaluated are (a) the thickness of the layers of the pavement, (b) strength equivalencies of the materials in each layer of the pavement, (c) subgrade support value including the soil resiliency and the environmental conditions affecting it, and (d) traffic. The dependent variable is the deflections measured by Dynaflect in the spring of 1967 and 1968.

Thickness equivalencies of the materials used in the construction of flexible pavements in Virginia have been determined. A soil classification map of Virginia, based on about 200 projects (each with 2 to 30 soil samples) throughout the state, has been prepared. This map shows five soil classifications based on resiliency, the AASHO soil classification, and texture of the soils. A design method for Virginia in the form of a nomogram is proposed as a maintenance and design tool. Two additional methods are based on present design conceptions, standards, and practice in Virginia.

•THE MAIN objective of this investigation is to provide a pavement design method for Virginia that is based on the AASHO Road Test results in terms of thickness equivalencies of the materials, soil support values, and traffic and that does not alter the present design concepts in Virginia.

A Dynaflect, which is a dynamic load device for measuring deflections, was used to evaluate the structural performance of pavements. The performance of this equipment was also studied.

The soil support values were determined on the basis of resiliency properties and California bearing ratio (CBR) values.

Fifty-four projects with varying pavement structures throughout Virginia were chosen for a satellite study. All these projects are on primary or Interstate roads. Three design methods are recommended. One of these methods, based on soil support values (SSV), traffic, and thickness index, was further tested on 74 new projects.

A principal purpose of this study is to evaluate the performance of the satellite pavements, to determine the thickness-equivalency values of the different materials in the pavement, and to correlate these values, along with other variables such as soil support and traffic, with the pavement performance.

The climatic and regional factors were considered to affect the subgrade soil, and hence their effects were assumed to have been considered in evaluating the subgrade support value. Strengths of all materials—e.g., asphaltic concrete and stone subbase—are considered to be the same all over Virginia because they are as specified by the Virginia Highway Department. The pavement life before resurfacing was considered in the design.

Paper sponsored by Committee on Flexible Pavement Design.

VARIABLES

Deflections

The Dynaflect records dynamic deflections of a pavement at 5 points at 1-ft intervals along the path of travel. The maximum deflection recorded is midway between its two wheel loads. Dynaflect measurements were made during the spring in 1967 and 1968.

Soil Support Value

Investigations have shown that the subgrade support value depends on two important factors: (a) resistance to a single applied load, and (b) rebound due to soil resiliency. The pavement design recommended herein is based on these two factors.

Traffic

The total traffic up to June 1967 and the average annual daily traffic (AADT) on each project were evaluated.

To determine the 18-kip equivalent the method given in the AASHO Interim Guide (1) was modified. The modified method is given in the first interim report on flexible pavement design (2). This modified method has been accepted by the Virginia Highway Department.

THICKNESS EQUIVALENCY VALUES

The AASHO Road Test report (3) defined the strength of the pavement as

$$D = a_1h_1 + a_2h_2 + \ldots \tag{1}$$

It then equated this strength with pavement deflections. This relationship for a given system of load when converted to thickness equivalencies could be written in the following form:

$$\log d = a_0 + a_1\left(h_1 + \frac{a_2}{a_1}\, h_2 + \frac{a_3}{a_1}\, h_3 + \ldots\right) \tag{2}$$

$$\log d = a_0 + a_1D \tag{3}$$

where

D is the strength or thickness index of the pavement;
a_1, a_2, ..., are strength coefficients;
h_1, h_2, ..., are thicknesses of the respective layers;
$\frac{a_2}{a_1}$, $\frac{a_3}{a_1}$, ..., are the thickness equivalencies; and
d is the Benkelman beam deflection of the pavement.

In this investigation d is taken as the deflection measured by the Dynaflect in the spring. The deflection of a pavement is the sum of the compressions of the different layers of the pavement, including the subgrade. Compression in any layer depends not only on the thickness and the strength of each layer, but also on the following factors: (a) the thickness of the overlying layer, (b) the thickness equivalency of the material of the overlying layers, and (c) the ratio of the strength of the overlying or underlying layer and the strength of the layer itself as given by Burmister's equation (4).

The AASHO equation does not include the effects of these three factors. In this study the effects of factors a and b were investigated to a certain extent. The effect of factor c was not considered because of the lack of data.

To provide for factor a, the thickness of the overlying layers, the following general equation—based on Boussinesq and Westergaard—was adopted. The derivation of the equation is explained in Appendix A.

$$d = \sum A \left[\frac{1}{(1 + cr^a + Ha)b} \right]_{H_1}^{H_2} \quad (4)$$

where

d = deflection of the pavement in inches;
A = deflection modulus, a function of Poisson's ratio, elastic modulus, and a given system of loading;
a, b, and c = constants;
r = horizontal distance of the point where the deflection is to be determined from the load point in inches;
H = vertical distance of the point where the deflection is to be determined from the load point in inches;
H_1 = vertical distance of the top of a layer from the top of the pavement in inches; and
H_2 = vertical distance of the bottom of the same layer from the top of the pavement in inches.

The values of the constants a, b, and c were determined by use of a computer program with different values of H_1 and H_2. The value of r was 10 in. for the Dynaflect. The most suitable values that would give the maximum effect of the thickness of the layer under consideration were adopted. With the values of the constants so determined, Eq. 4 could be written as follows:

$$d = \sum A \left[\frac{1}{(1 + r^2 + H^2)^{0.5}} \right]_{H_1}^{H_2} \quad (5)$$

To provide for factor b, the thickness equivalency of the overlying layers, Eq. 5 was modified. The modification consisted of converting the thickness of any layer of material into the equivalent thickness of asphaltic concrete. Thus, in a multilayered pavement with layered thicknesses h_1, h_2, h_3, ... from the top of the pavement and equivalency values a_1, a_2, a_3, ... respectively, the equation for the pavement deflection will be as follows:

$$d = \left[\frac{1}{(1 + r^2 + H^2)^{0.5}} \right]_{H=0}^{H=a_1h_1} + \left[\frac{1}{(1 + r^2 + H^2)^{0.5}} \right]_{H=a_1h_1}^{H=a_1h_1+a_2h_2} + \ldots \quad (6)$$

EVALUATION OF FACTORS

General Behavior of Pavements

Studies of the satellite pavements in Virginia have shown that in the spring deflections for a given pavement remain almost constant (5), and if any decrease takes place, it is for a short duration immediately after construction. The duration of variation in deflection after construction depends on the pavement components. The satellite projects taken in this investigation were old enough not to provide variations. Deflection data were taken during the springs of 1967 and 1968, and both sets of data gave the same correlation with the structural components of the pavement.

Evaluation of Thickness Equivalencies

A multiple regression analysis of the data from the 54 satellite projects was carried out with a computer to determine the thickness equivalency by means of Eq. 2. Different combinations were tried. Later, the thickness equivalencies of the cement-treated base and cement-treated stone subgrade varied from 0.8 to 1.7 and 0.4 to 0.5, respectively.

The most suitable thickness equivalencies obtained by multiple regression analysis followed by simple regression analysis of these satellite projects are given in Table 1. The values given by the AASHO Committee are also given in the table for comparison.

TABLE 1
THICKNESS EQUIVALENCIES OF THE MATERIALS

Material	Thickness Equivalencies	
	Virginia	AASHO
Asphalt mat	1.0	1.0
Cement-treated stone base	1.0	0.52
Stone subbase	0.35	0.31
Select material in subbase	0.0	0.25
Cement-stabilized subgrade	0.4	–

In this investigation, the total thickness of the asphaltic concrete (AC) mat—i.e., the asphaltic concrete surface, binder, and base courses—is considered. The thickness equivalency of this material has been taken as 1.

In Virginia, the cement-treated stone base course (CTB), if provided, is usually below the asphaltic concrete mat and may vary in thickness from 4 in. to about 8 in. For the best correlation, the thickness equivalency of this material was found to be 1.4. Because there is limited experience with this material in Virginia, a thickness equivalency of 1.0 is recommended. At a later date this value may be increased. This value of 1.0 is recommended also because various investigators have found quite different values for this material. The AASHO Committee gives a value of 0.52, Chastain and Schwartz (6) give a value of 0.96, the Canadian Good Roads Association (7) recommends a value of 1.0, and Phang (8) gives a value of 2.0. Variations in the thickness equivalency of this material are probably caused by differences in factors such as environmental conditions, distance of the CTB layer from the top of the pavement, and mix design affecting the variation in the strength of the layer.

The use of cement-treated stone base is increasing in Virginia, and about 20 percent of the projects in the satellite study incorporate this material.

In Virginia the stone subbase (SSB) varies in thickness from 4 to 10 in. It is provided under the bituminous base. A thickness equivalency value of 0.35 has been recommended for this material from this investigation. The Asphalt Institute (9) and Phang recommended values of 0.37 and 0.31 to 0.33, respectively. Chastain and Schwartz recommend a value of 0.46 for Illinois. About 75 percent of the projects in the satellite study have a stone subbase under the bituminous base.

Select material is a low-cost material irrespective of its resilient properties and has a CBR of about 20. If used, it is laid over the subgrade and varies usually from 6 to 26 in. in thickness.

Multiple regression analysis showed that the thickness equivalency value of select material tends to be zero. Because select material does not appear to contribute appreciably to reducing deflections, its thickness equivalency value is taken to be zero. About 60 percent of the projects in the satellite study have select material.

In Virginia, cement-treated subgrades (CTS) were first provided over highly resilient soils because they do not compact properly. Cement-treated subgrade reduced the effect of soil resiliency, reduced deflection, and provided a good working platform. Its use has spread over the Piedmont area and some areas in the coastal plain and mountain regions. The thickness of the CTS layer varies from 6 to 12 in.

The best value of the thickness equivalency of CTS is found to be 0.4. The AASHO Road Test did not recommend any value. About 50 percent of the projects in the satellite study have CTS.

Evaluation of Soil Support Value

After using Eq. 3 to evaluate the thickness equivalencies of the materials in the pavement, it became apparent that Eqs. 3 and 6 required modification to the following form:

$$\log d = a_0 + a_1 (D + \text{subgrade factor}) \quad (7)$$

$$d = \left[\frac{1}{(1 + r^2 + H^2)^{0.5}} \right]_{H=0}^{H=a_1 h_1} + \ldots + \text{subgrade factor} \quad (8)$$

The values of the subgrade factor for the three soil areas are given in Table 2.

TABLE 2

SUBGRADE FACTORS

Soil Areas	Eq. 7	Eq. 8
Resilient soils in Piedmont (1, 2, and 3 in Fig. 1)	0	0
Non-resilient sandy soils in Coastal Plains (4 in Fig. 1)	3.0	0.008
Non-resilient clayey soils in Valley and Ridge (5 in Fig. 1)	2.0	0.005

TABLE 3

SOIL RESILIENCY VALUES

Soil	Classification	Resiliency Value
1	High-resilient soils	0.5
2	Medium-resilient soils	1.0
3	Low-resilient soil	1.5
4	Non-resilient soils, sands	3.0
5	Non-resilient soils, clayey	2.0

This increased soil support in clayey and sandy soil is obviously due to the inherent property of the soil and also the environmental factors. No other investigation to account for environmental conditions has been conducted.

It is, however, recommended that 50 percent deduction be made from the calculated thickness index until experience indicates the desirability of deducting the full value of the factor.

As a part of this investigation, a subgrade soil resiliency classification map for Virginia was prepared (Fig. 1). The approach and basis of this classification are discussed in Appendix B. The classification is based on the AASHO soil classification and the textural soil classification of about 200 projects throughout Virginia. In each project the number of samples varied from 2 to 30.

Thus, as explained in Appendix B and shown in Figure 1, the soils in Virginia have been divided into five classifications. Soils 1, 2, and 3 with high, medium, and low resiliency were arbitrarily given a value of 0.5, 1.0, and 1.5 respectively. The soil support values (SSV) of these three soils were then obtained by multiplying the Virginia CBR value of the soil by its resiliency value.

A correlation between SSV, traffic, and thickness index for the satellite pavements in the resilient soils of the Piedmont area was determined. In this correlation, the data for the satellite pavements in soils 4 and 5 (i.e., sandy and clayey) were incorporated, and the resiliency value of their soils determined. The resilient values of the sandy (Coastal Plains) and clayey (Valley and Ridge) soils were found to be 3.0 and 2.0 respectively. Thus, the resilient values of the soils given in Table 3, were partly assumed and partly derived.

Figure 1 shows these classifications by soil number. For the area marked 4 and 5, it is suggested that a resiliency factor equivalent to the mean of the two classifications, i.e., 2.5, be taken. For projects located on the border of the two classifications, mean values of the two classifications could be taken, although it would be better to

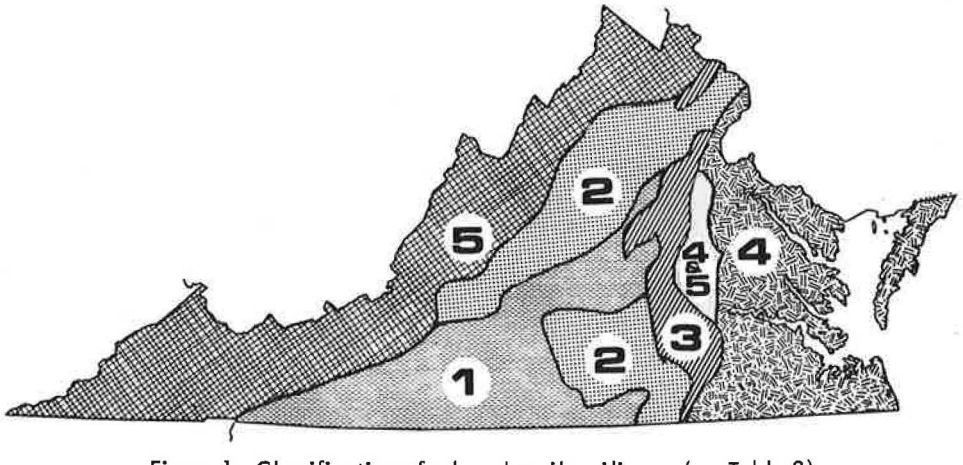

Figure 1. Classification of subgrade soil resiliency (see Table 2).

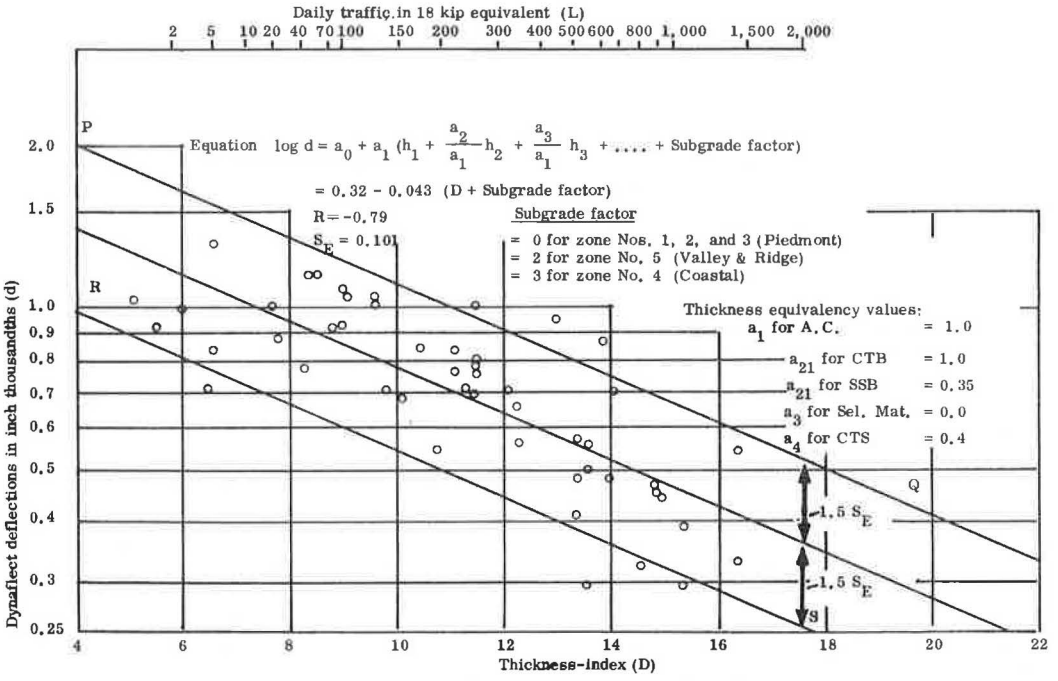

Figure 2. Thickness index correlated with deflections and traffic by AASHO equation.

study the soil and determine its AASHO and textural classifications and then determine its resiliency as discussed in Appendix B.

Choice of Equation for Design

With the thickness equivalency values in Table 1 and with the subgrade factors in Table 2, the pavement deflections obtained in the springs of 1967 and 1968 were correlated with the thickness index, D, in Eqs. 7 and 8. The correlation values varied from 0.75 to 0.79, which indicated a high rate of correlation. Equation 7 showed a better correlation than did Eq. 8. This shows that the AASHO equation (Eq. 7) gives a better correlation than the theoretical equation. It is, therefore, evident that the AASHO equation could be adopted for design. A plot of 1967 data with Eq. 7 is shown in Figure 2.

DESIGN METHODS FOR PAVEMENTS IN VIRGINIA

Design by Correlation Between Thickness Index and Deflection

Numerous investigations, including the AASHO Road Test, have shown that as the thickness and/or strength of the pavement layers increase, the pavement deflection decreases.

This investigation has shown that log of pavement deflection is a straight-line function of the sum of the thickness index and the subgrade factor. This was confirmed from both the 1967 and 1968 Dynaflect data taken on the 54 satellite projects. Based on this correlation, the following equation is recommended for use:

$$\log d = 0.32 - 0.043\, a_1 (h_1 + 0.35\, h_2 + 1.0\, h_{21} + 0.0\, h_3 + 0.4\, h_4 + \text{subgrade factor}) \quad (9)$$

TABLE 4

FLEXIBLE PAVEMENT DESIGN CHART OF THE VIRGINIA HIGHWAY DEPARTMENT

Traffic Category (1)	Daily Equivalent 18-kip Axle Loads (2)	Stabilized Subgrade[a] (in.) (3)	Subbase[a] (in.) (4)	Base (5)	Binder Course (6)	Surface Course (7)
I	0-7	6	none	4-6 in.[a]	none	P&DS[c]
IA	8-16	6	none	6-8 in.[b]	none	P&DS[d]
II	17-124	6	4-8	3 in. B-3 (345 lb)	none	165 lb S-4 or S-5 (1.5 in.)
IIA	125-224	6	4-8	4 in. B-3 (460 lb)	none	165 lb S-4 or S-5 (1.5 in.)
III	225-329	6	4-8	6 in. B-3 (690 lb)	none	165 lb S-5 (1.5 in.)
IV	330-429	6	6-10	6 in. B-3 (690 lb)	165 lb I-2 (1.5 in.)	100 lb S-5 (1.0 in.)
V	430-659	6-12	6-10	8 in. B-3 (920 lb)	none	165 lb S-5 (1.5 in.)
VI	660 and over	6-12	8-12	8 in. B-3 (920 lb)	165 lb I-2 (1.5 in.)	100 lb S-5 (1.0 in.)

[a] Minimum depth of subgrade stabilization and subbase will depend on soil conditions and design CBR value.
[b] Stone base.
[c] Prime and double seal on Contract I; 165-lb plant mix on Contract II when warranted.
[d] Prime and double seal on Contract I; up to 300-lb plant mix on Contract II.

The relationship based on this equation for 1967 data is shown in Figure 2. In this figure lines PQ and RS include 86 percent of the area under the normal curve. Thus, we may conclude that, according to the design standards in Virginia, the deflections would lie within lines PQ and RS.

This relationship is adaptable for pavement design in Virginia by superimposing over Figure 2 the traffic scale (columns 1 and 2 of Table 4) of the Virginia Department of Highways design method. Figure 2 could, therefore, be used to determine the thickness index needed for a given traffic category, based on the pavement design method in Virginia. The figure would also indicate the amount of likely Dynaflect deflection.

As an illustration of a design based on this method, assume a traffic category between 225 and 329 and a subgrade soil that does not need a cement-treated subgrade (Fig. 2 and Table 4). A design based on an average deflection of 0.80 to 0.96 x 10^{-3} in. would be appropriate. Further, the pavement should have a thickness index between 8.6 and 10.5, i.e., the pavement should be designed for an average thickness index of 9.5. Various choices in the structural cross section could be made as given in Table 5.

The flexible pavement design chart of the Virginia Highway Department (Table 4) recommends choice 2 only. With the help of this chart more choices in the selection of pavement cross sections could be available.

Seventy-four projects recently designed by the Virginia Department of Highways were evaluated by regression analysis to compare the thickness index by this method with the thickness index by the method presently used. The correlation coefficient was found to be 0.81, which indicated a high degree of correlation.

TABLE 5

PAVEMENT DESIGN CHOICES BASED ON THICKNESS INDEX AND DEFLECTION

Type of Layer	Choice 1	Choice 2	Choice 3
AC surface (S-5)	1.5 in.	1.5 in.	1.5 in.
AC base (B-3)	7.5 in.	6.0 in.	4.5 in.
Stone subbase	0	6.0 in.	4 in.
Cement-treated subgrade	0	0	6 in.
Thickness index	9.0	9.6	9.8

Design by Correlation Between Thickness Index and Daily Traffic

By using the strength equivalencies as determined in this investigation, the thickness index of the sections recommended by the Virginia Department of

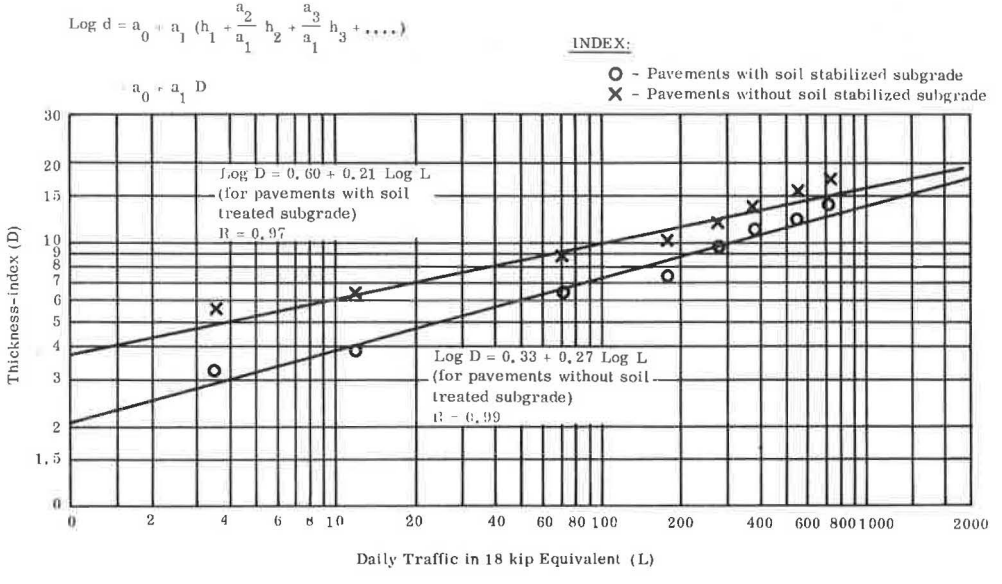

Figure 3. Thickness index correlated with traffic by AASHO equation (Eq. 7).

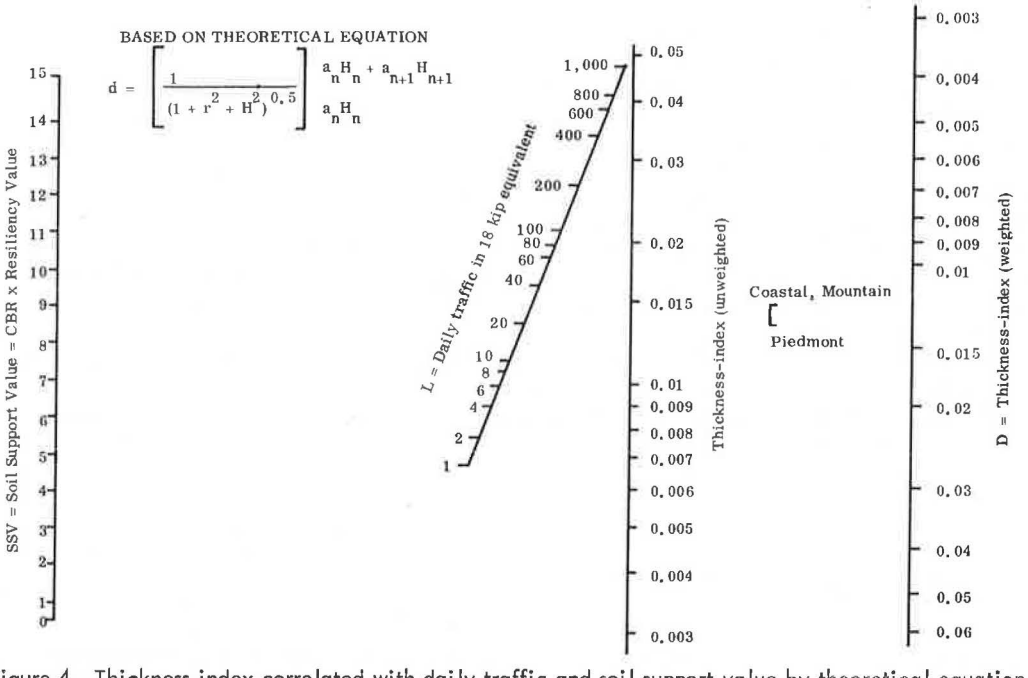

Figure 4. Thickness index correlated with daily traffic and soil support value by theoretical equation.

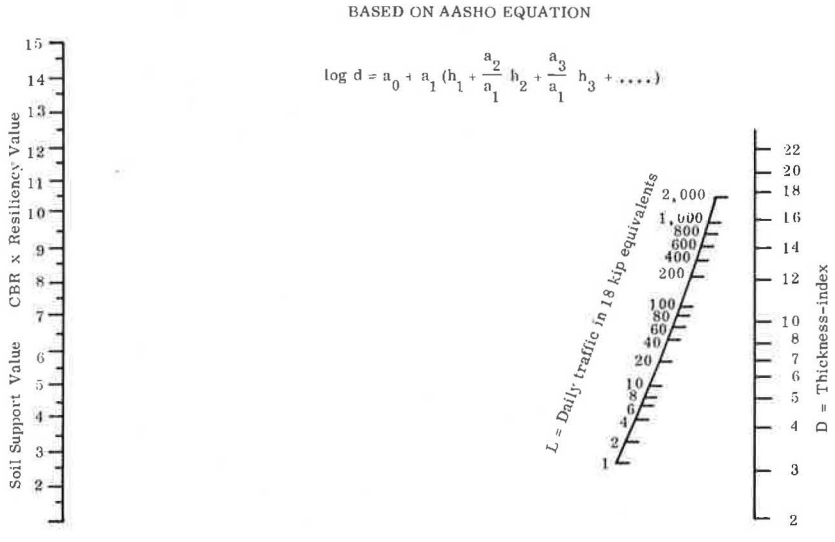

Figure 5. Thickness index correlated with daily traffic and soil support value by AASHO equation.

Highways were correlated with the daily traffic as given in Table 4 by means of Eqs. 7 and 8 separately. Both equations gave the same correlation. The values are as follows: (a) with cement-treated subgrade, R = 0.97 and (b) without cement-treated subgrade, R = 0.99. The use of the AASHO equation is more acceptable only because of its simplicity in application for design. This correlation, shown in Figure 3, could be used for design of flexible pavements in Virginia.

Design Based on SSV, Daily Traffic, and Thickness Index

A third variable, SSV based on CBR and resiliency, was introduced in the relationship between daily traffic and the thickness index discussed previously. Nomographs were drawn for Eqs. 7 and 8 separately and are shown in Figures 4 and 5.

The thickness index obtained from the nomograph based on the theoretical equation needed slight corrections for the subgrade factor. The corrections are also shown in Figure 4. The thickness index obtained from the nomograph based on the AASHO equation (Fig. 5) did not need a separate correction for the subgrade factor. The SSV scale was considered to have made the necessary corrections.

To verify and modify these nomographs, 74 new projects were studied for their soil support values, daily traffic, and thickness index. It was found that:

1. Soil support values above 15 do not effect changes in the thickness index of the pavement in these projects and hence the soil support scale was made to vary from 0.5 to 15; and

TABLE 6

PAVEMENT DESIGN CHOICES BASED ON THICKNESS INDEX, SSV, AND TRAFFIC

Type of Layer	Choice 1	Choice 2	Choice 3	Choice 4
AC surface course (S-5)	1.5 in.	1.5 in.	1.5 in.	1.5 in.
AC base course (B-3)	8.5 in.	7.5 in.	6.5 in.	5.5 in.
Cement-treated base	0	0	0	4 in.
Stone subbase	4 in.	6 in.	6 in.	0
Select material	0	0	0	0
Cement-treated subgrade	4 in.	6 in.	8 in.	4 in.
Thickness index	13.0	13.5	13.3	12.6

2. The present pavement design method provides the same design for daily traffic of 660 18-kip equivalents and any value higher than this.

The traffic scales in Figures 4 and 5 have, therefore been extended up to 1,000 and 2,000 18-kip equivalents respectively. The higher values are extrapolated.

The nomograph in Figure 5 can be utilized for determining the thickness index required for the design of new pavements based on subgrade soil properties and traffic in terms of daily 18-kip equivalents, or it can be used for maintenance by evaluating the modified thickness for the revised traffic in terms of daily 18-kip equivalents. As a design example, consider a project that has a design CBR value of 7.1 and design daily traffic of 329 18-kip equivalents and that lies in a medium-resilient soil area of silts and clays in the Piedmont region. The SSV is, therefore, equal to 7.1 x 1.0 = 7.1 and, from the nomograph based on the AASHO equation in Figure 5, the thickness index of the pavement is 13.2. Design choices for this value of thickness index are given in Table 6.

Any one of these three methods could be adopted in Virginia without any change in the field and laboratory method of evaluation. The methods provide more choices in selection of materials and their thicknesses, as shown in Tables 5 and 6, than does the present method of design. They have been made more sophisticated by the use of thickness equivalency values. Of these three methods, the one with SSV and traffic is recommended for use.

CONCLUSIONS

Several conclusions drawn from this investigation of satellite study projects are applicable to paving materials and designs used in Virginia.

1. The following thickness equivalency values could be considered for design in Virginia, with the layers placed in the order described (any layer could be omitted but not interchanged):

Type of Layer	Thickness Equivalency
Asphalt mat	1.0
Cement-treated stone base	1.0
Stone subbase	0.35
Select material	0.0
Cement-treated subgrade	0.4

2. The deflection of a pavement is a function of its thickness index; the higher the thickness index, the lower the deflection.

3. Comparison of a theoretical equation and the AASHO Road Test equation has shown that both give the same magnitude of evaluation and they are equally good for design purposes. Because application of the AASHO Road Test equation is much simpler, its use is recommended.

4. The recommended methods for design give more choices in the selection of materials and their thicknesses than does the present method of design in Virginia. Further, the recommended methods are more sophisticated through use of thickness equivalency values. One of the recommended design methods takes account of the soil support value, which includes the effect of environmental factors.

ACKNOWLEDGMENTS

It is a pleasure to acknowledge the help received from C. S. Hughes and the staff of the Pavement Section. Mr. Hughes was available at all times for free and open discussions and guided the study so that it would serve the best interests of the Virginia Department of Highways. He also offered helpful criticism of this paper. The author is also grateful for the encouragement and support given by the late Dr. Tilton E. Shelburne, State Highway Research Engineer.

REFERENCES

1. Interim Guide for Design of Flexible Pavement Structures. AASHO Committee on Design, Oct. 1962.
2. Vaswani, N. K. AASHO Road Test Findings Applied to Flexible Pavements in Virginia. Virginia Highway Research Council, Charlottesville.
3. The AASHO Road Test. HRB Spec. Rept. 61.
4. Burmister, D. M. Theory of Stresses and Displacements in a Layered System for Application to the Design of Airport Runways. HRB Proc., Vol. 23, pp. 126-154, 1943.
5. Vaswani, N. K. Design of Pavements Using Deflection Equations From AASHO Road Test Results. Highway Research Record 239, pp. 76-94, 1968.
6. Chastain, W. E., and Schwartz, D. R. AASHO Road Test Equations Applied to the Design of Bituminous Pavements in Illinois. Highway Research Record 90, pp. 3-25, 1965.
7. A Guide to the Structural Design of Flexible and Rigid Pavements in Canada. Canadian Good Roads Association, Sept. 1965.
8. Phang, P. A. Interim Report for Full Scale Road Experiments. D. H. D. Report No. RR 136, Dept. of Highways, Ontario, May 1968.
9. Thickness Design—Asphalt Pavement Structures for Highways and Streets. 7th Ed., The Asphalt Institute, Sept. 1963 and March 1964.

Appendix A

BASIS OF THE GENERAL FORM OF EQUATION 4

$$\text{Deflection } d = A\left[\frac{1}{(1 + cr^a + H^a)^b}\right]_{H_1}^{H_2}$$

if

a, b, and c = constants;
A = deflection modulus, a function of Poisson's ratio, elastic modulus, and a given system of loading;
d = pavement deflection;
E = modulus of elasticity of the material;
H = vertical distance of the point where the deflection is to be determined from the load point;
H_1 = vertical distance of the top of the layer from the top of pavement;
H_2 = vertical distance of the bottom of the same layer from the top of the pavement;
P = load applied;
r = horizontal distance of the point where the deflection is to be determined from the load points;
μ = Poisson's ratio of the material;
w = deflection at a point under consideration;
Δw = compression of a layer = difference between the deflection at top (i.e., at depth H_1) and bottom (i.e., at depth H_2) of the layer in inches;
w_1 = deflections at the top of a layer at a distance H_1 from the top of the pavement; and
w_2 = deflection of the bottom of the same layer at distance H_2 from the top of the pavement.

Compression of any layer in a homogeneous isotropic and semi-infinite elastic solid is given by the following equations:

Boussinesq's equation

$$w - w_1 - w_2 = A \left[\frac{2(1 - \mu)\, r^2 + (3 - 2\mu)\, H^2}{(r^2 + H^2)^{3/2}} \right]_{H_1}^{H_2} \qquad \text{(a)}$$

Westergaard's equation

$$w = w_1 - w_2 = A \left[\frac{H}{(2r^2 + H^2)^{3/2}} \right]_{H_1}^{H_2} \qquad \text{(b)}$$

The above two equations could be written in a general form as

$$w = A \left[\frac{1}{(cr^a + H^a)^b} \right] \qquad \text{(c)}$$

and

$$w = w_1 - w_2 = A \left[\frac{1}{(cr^a + H^a)^b} \right]_{H_1}^{H_2} \qquad \text{(d)}$$

To satisfy the following four boundaries

$H = 0$ and $r = 0$
$H = \infty$ and $r = 0$
$H = 0$ and $r = \infty$
$H = \infty$ and $r = \infty$

the equation has been slightly modified as follows:

$$w = A \left[\frac{1}{(1 + cr^a + H^a)^b} \right]_{H_1}^{H_2} \qquad \text{(e)}$$

$$d = \sum \Delta w = \sum A \left[\frac{1}{(1 + cr^a + H^a)^b} \right]_{H_1}^{H_2} \qquad \text{(f)}$$

Appendix B

CLASSIFICATION BASED ON RESILIENCY OF SOILS

The factors on which the degree of soil resiliency depends are as follows:

1. Amount and size of mica in the soil—The resiliency increases with an increase in size and quantity of mica.
2. Orientation of the mica flakes—Resiliency is greatest when the particle orientation is essentially perpendicular to the direction of the applied load.
3. Soils from the C-horizon are more resilient than soils from the B-horizon. Since subgrade cuts lie mostly in the C-horizon and the tops of fills consist of soils from this horizon, it is the one being considered for classification.

For the purpose of the design of pavements, Virginia soils have been divided as follows:

1. High-resilient soils—A-5 or A-4 (with G.I. of 5 and up). Both classifications should have a large percent passing No. 200 sieve and also high mica content.

2. Medium-resilient soils—(a) A-4 (with G.I. of 5 and up) having a large percent passing No. 200 sieve but with low mica content; (b) sandy silt with high mica content.
3. Low-resilient soils—A-7-5 or micaceous clay.
4. Non-resilient soils, sandy—A-1, A-2, A-3, or A-4 (with G.I. less than 5).
5. Non-resilient soils, heavy clay or organic—A-4-2, A-6, A-7-6, or A-8.

Generally, low-resilient soils do not contain mica and the resiliency is due to silt only.

Discussion

F. P. NICHOLS, JR., National Crushed Stone Association—It may be of some help to the reader of the foregoing paper and another paper by the same author (5) to recall some of the background data that contributed to the development of the author's proposed flexible pavement design methods. This assumes, of course, that a reader some years hence is faced with the task of reviewing the literature on pavement design in the never-ending quest for a truly reliable method based either on elastic theory or pure empiricism.

Vaswani has not seen fit to refer to two readily available papers (10, 11) that describe the development of much of the data he has used. Nor does he refer to any of a number of unpublished progress reports that further amplify the data; Figure 4 of his 1968 paper (5) was lifted directly from one such report. Perhaps his reason for omitting these references is that his conclusions, based on elaborate statistical and mathematical analysis of the same or similar data, are diametrically opposed to those drawn by the author of the earlier papers.

The first omission, from HRB Bulletin 269, published in 1960 (10), traced the development of "black base" designs in Virginia beginning with a local aggregate job in an area where commercial aggregates were unavailable. That report also described the first experimental project on US 58, which was designed to determine if possible what thickness of "black base" might solve performance problems being experienced on other projects along this corridor built with lighter bituminous mat thicknesses. To summarize, the problem definitely was not solved by more than doubling the thickness of the bituminous-bound upper layers. Had the "thickness equivalency" concept been applied to these findings alone, stone base would have had to be assigned a higher value than black base in this experiment.

The 1960 report also mentioned the start that had been made toward "getting to the bottom of the problem" through other experimental installations. The approach here was to ensure more reliable support at the foundation level in areas of scarcity of stone or other acceptable subbase aggregates by means of subgrade stabilization with cement or lime.

A 1962 paper (11) demonstrated the obvious superiority of increasing the foundation support over increasing the thickness of surface type materials. Several projects, with and without subgrade stabilization, of similar age, and in similar soil areas, were compared. Results show the marked reduction in deflection values accomplished through improved foundation support.

A paper presented in 1963 (12) was listed in Vaswani's 1968 paper. However, the one mention of it presented an erroneous interpretation of what was actually stated therein with regard to excessive rather than tolerable deflections. This paper's summary showed that, except in the Piedmont section of Virginia, "the magnitude of deflection apparently has little to do with the problems of pavement behavior," because none was excessively high. Further, it showed that, of 24 pavements in the Piedmont built without stabilized subgrades, deflections measured on the 14 with black bases were not significantly different on the average from those on the 10 without. (Both averages were considered excessively high.) Similarly, of 16 that did have stabilized subgrades, there were very minor differences between average deflection values on the 9 with black bases and on the 7 without (neither average was excessively high). The obviously significant differences were between the average deflections measured on the

pavements built on stabilized foundations and those on pavements not so well supported; stabilization at the bottom, rather than at the top, cut the deflections almost in half.

Vaswani's design procedure is based on "thickness equivalencies" that are "determined" once and for all from deflections measured by the Dynaflect (13), a machine that measures a pavement's response to relatively light, pulsating loads. The paper's introduction indicates that performance equivalencies are directly related to the ability of materials in question to reduce these minute deflections. The author's Table 1 shows unique equivalency values for broad classes of material such as asphaltic mixtures, cement-treated stone bases, untreated stone subbases, select materials (worthless), and cement-stabilized subgrade soils, regardless of the material's thickness, quality, or position in the structure. In effect, he says that a pavement consisting of 7 in. of any combination of hot bituminous mixtures laid on any soil is equivalent to one consisting of 4 in. of the highest quality bituminous mixtures laid on better than $8\frac{1}{2}$ in. of the best graded, highest quality crushed stone, slag, or gravel that can be obtained. Further, one infers that any increase in bituminous base thickness, per inch, is equivalent to an increase of 2.86 in. of crushed aggregate.

This is in direct conflict with statements made by Foster (14), who has shown that beneath a 3-in. hot-mixed bituminous surface at the AASHO Road Test, a 4-in. high-quality hot-mixed bituminous base performed about as well as slightly more than 3 times that thickness of the poorly compacted crushed limestone base used there, a thickness equivalency of about 3 to 1. However, Foster shows that an 8 in. thickness of the bituminous base was equivalent to 16 in. of the limestone, an average equivalency of only 2 to 1. Thus, if the first 4 in. had a 3 to 1 equivalency, the next 4 in. must have had an equivalency hardly more than 1 to 1 to produce the average value of 2 to 1.

Foster had stated earlier (15) that the Road Test subbases and bases were weaker than they would have been in a normally built highway—that they should have been better compacted. He stated further that "the thickness differential between bituminous-treated and standard base course would be less in sections with standard base courses compacted to higher densities."

It is not the purpose of this discussion to describe fully a design approach better than that developed by Dr. Vaswani. Its primary purpose is to point out again the fallacy of a constant "thickness equivalency" concept.

But in addition, a major objection must be voiced against the nomograph (Fig. 5) recommended for determining total design strength in terms of thickness index D; the trifling difference of 2 or 3 in. in asphalt concrete thickness requirements for equal traffic but for soil support values differing from 1 to 15 cannot be supported by pavement performance records in Virginia. It is also in considerable conflict with the latest revision of the Virginia CBR design chart, originally described in 1954 by Woodson (16).

References

10. Nichols, F. P., Jr. Flexible Pavement Research in Virginia. HRB Bull. 269, pp. 35-50, 1960.
11. Nichols, F. P., Jr. Effect of Compaction and Subgrade Stabilization on Deflections and Performance of Virginia Pavements. Proc., Internat. Conf. on Structural Design of Asphalt Pavements, Univ. of Michigan, pp. 12-13, 1962.
12. Nichols, F. P., Jr. Deflections as an Indicator of Flexible Pavement Performance. Highway Research Record 13, pp. 46-65, 1963.
13. Scrivner, F. H., Swift, G., and Moore, W. M. A New Research Tool for Measuring Pavement Deflection. Highway Research Record 129, pp. 1-11, 1966.
14. Foster, Charles R. Prepared Discussion. Proc., Second Internat. Conf. on Structural Design of Asphalt Pavements, Univ. of Michigan, p. 657, and author's closure, p. 988.
15. Foster, Charles R. Prepared Discussion. Proc., First Internat. Conf. on Structural Design of Asphalt Pavements, Univ. of Michigan, pp. 12-13, 1962.
16. Woodson, D. D. Designing Flexible Pavements (Virginia). HRB Research Report 16-B, pp. 56-58, 1954.

N. K. VASWANI, Closure—I very much appreciate Mr. Nichols' comments. The 1968 paper was based on data most of which were collected under his direction, except those for the last two years. For the most part, I agree with the conclusions made in his reports prior to 1966. As a result of my mathematical and statistical analysis I, in fact, seem to have described his thinking in numerical values with some additional conclusions such as the one from Figure 3 of my paper.

The 1968 paper and the present one give a high strength equivalency value to soil cement, which agrees with Nichols' remarks that a strong foundation is necessary for weak resilient soils. The first project on US 58, sponsored by Nichols, clearly demonstrated the necessity for a strong foundation layer such as soil-cement, soil-lime, or cement-treated stone.

I would like to mention that the principle of thickness equivalency indicates the total pavement strength needed. After the strength is determined, the success of the design depends on the designer's making a proper choice of the materials.

Regarding tolerable deflections, Figure 5 of my 1968 paper clearly shows that tolerable or permissible deflection is a function of the strength or thickness index of the pavement and is not a fixed value. The tolerable or permissible deflection depends on the sum of the strengths of the individual layers and not on the thickness and strength of one particular layer.

In his discussion, Nichols seems to indicate that the value of the thickness equivalency of any material is a function not only of the strength of the material but also of the depth at which it is laid below the top of the pavement. This certainly is true. For example, a cement-treated aggregate base placed directly under an asphalt concrete mat has a thickness equivalency of 1 for pavements in Virginia. The same material when placed in the subbase instead of the base will have lower strength equivalency values. Foster's interpretation of the AASHO Road Test results (14) was applied to the pavement design chart in Virginia. It showed that the thickness equivalency values reported in this paper give about the same thickness index values as given by Foster's curves.

Nichols states that the thickness equivalency value is a function of the quality of the material. This is also true. The thickness equivalency values determined in this investigation are for materials that satisfy the specifications of the Virginia Department of Highways.

Nichols states that the major objection in the design chart in Figure 5 is the difference of 2 to 3 in. in asphalt concrete thickness for soil support values differing from 1 to 15. This difference—if so—is the difference in the thickness index, which could be equivalent to 6 to 9 in. of stone aggregate base or 4 to 8 in. of soil cement.

Development of Traffic Parameter for Structural Design of Flexible Pavements in Minnesota

EUGENE L. SKOK, JR., Civil Engineering Department, University of Minnesota

•THE LOADING on a highway pavement is composed of applications of axle loads of various weights. The axle loads range from less than 2,000 lb on a single axle to more than 50,000 lb on a set of tandem axles. To determine the load effect on a pavement during its design life it is necessary to obtain the number of loads and the weight distribution operating over the pavement. For some design procedures this is done by assigning a specific load to the highway section. Another method is to relate the design to the amount of total traffic in average daily traffic (ADT) and the number of heavy trucks expected to use the highway (HCADT). The latter is the method used for the present Minnesota flexible pavement design procedure (1).

At the AASHO Road Test it was possible to determine the relative effect of the loadings used because a particular section of road was subjected to repetitions of one magnitude of load. The relative effect of the loads on the performance of pavement sections can be used to convert each load repetition to an equivalent number of repetitions of a base load. For a number of design procedures, including the AASHO Interim Guide, an 18,000-lb axle is used as the base load (2, 3, 4).

Even though a fairly precise determination can be made of the load equivalency factors, the calculation of the total equivalent 18,000-lb single axle loads is approximate because the distribution of axle loads on a pavement can only be estimated. When all loads on a road section are the same, such as at the Road Test, there is no problem involved with determining the summation of equivalent axle loads, but when actual highway loadings are being considered, approximations must be made to estimate the distribution of axle weights within a given truck type and the distribution of the various truck types over a particular section of road. During the last five years a comprehensive study has been made of flexible pavement design and performance in Minnesota. This study was based on measurements and observations on 50 test sections, all on existing state highways. As a part of this study it was necessary to have a determination of the traffic loads on each section. The distribution of the various truck types for the 50 test sections could not be determined accurately from the available statewide data.

Therefore, a traffic study was started in 1964 by the Planning Research Section of the Minnesota Department of Highways for these test sections. The traffic study has been used to obtain the distributions mentioned plus the total volume of traffic to use the roadway at each test section. The distribution and volumes are used to (a) calculate the total equivalent 18,000-lb axle loads that the section has been subjected to since it was last resurfaced, and (b) determine what traffic parameters best predict the total equivalent loads on a pavement section and how accurately these parameters predict the equivalent axle loads.

The first part of this paper is a presentation of the traffic study made on the Minnesota test sections and analysis of the data. The analysis has been programmed for the CDC 6600 computer. The statewide weight distribution and volume distribution data for the year can be put into the program to bring the traffic for each test section up to date. This is done in general by assuming that 1964, which is the year the traffic study was run, is the base year and that the distributions on each test section vary as the statewide distributions for subsequent years.

Paper sponsored by Committee on Flexible Pavement Design and presented at the 48th Annual Meeting.

It has been assumed that a comprehensive traffic study cannot be made when a pavement is to be designed. In the second part of this study correlations have, therefore, been made between the equivalent axle loads and (a) average daily traffic (ADT), (b) the heavy commercial average daily traffic (HCADT), and (c) the summation of Types 4 plus 5 trucks. It is shown that the equivalent loads can be predicted with increasing accuracy using the first three parameters in order as listed. The errors in these predictions are related to design thickness.

TOTAL LOAD IN TERMS OF EQUIVALENT 18,000-LB SINGLE AXLE LOADS

To analyze the performance of the Minnesota test sections based on the concepts of the AASHO Road Test and based on a good estimate of the load effect on the pavements, it is necessary to estimate the total equivalent number of 18,000-lb axle loads since the pavement section was built. Even though accurate determinations of the load equivalency factors based on the performance of the sections at the Roat Test have been made, the calculation of the total equivalent loads for a highway section is approximate because the distribution of the axle loads or the numbers of the various axle loads cannot be obtained exactly.

A traffic study on the Minnesota test sections was performed by the Planning Research Section of the Minnesota Department of Highways in 1964 to fill in an estimate of these distributions on the test sections.

The traffic study included the following operations on 41 of the 50 test sections:

1. Weigh all trucks passing a location during a 16-hour period on a weekday in each of three seasons.
2. Classify vehicles during 16-hour periods on a weekday, Saturday, and Sunday in each of the four seasons.
3. Count traffic for seven consecutive days in each of the four seasons to provide average daily traffic volumes (ADT).

Only 41 traffic stations were used because nine of the locations could represent distributions for two test sections.

The procedure to determine the total number of equivalent wheel loads over a section since it was constructed as summarized in the following has been performed on each test section through 1964, 1965, 1966, and 1967. It is assumed that it is desirable to update this information in future years. The method outlined has therefore been put into a computer program that, when statewide data for a given year have been added, adds on the traffic estimate for each test section using the 1964 traffic study as a base and modifies the weight and volume distributions based on ratios of the statewide data. The computer program is available on request from either the Civil Engineering Department of the University of Minnesota or the Minnesota Department of Highways Planning Research Section.

Truck Factors

Truck factors have been calculated for each of five types of trucks for each test section in 1964 using the weight data from the traffic study. A truck factor (TFS) is defined as the average number of equivalent 18,000-lb axle loads that the pavement section is subjected to with one passage of that truck type. If, for instance, a Type 5 truck factor is 1.5, then on the average every Type 5 truck that passes over the test section would have the effect of 1.5 18,000-lb axle loads when the effect of its five axles are summed together. For the traffic analysis, trucks are classified into the following six types:

Type	Description
0	Single unit, 4-tire
1	Single unit, 2-axle, 6-tire
2	Single unit, 3-axle
3	Tractor-truck or semitrailer, 3-axle
4	Tractor-truck or semitrailer, 4-axle
5	Tractor-truck or semitrailer, 5-axle

The weighing part of the 1964 traffic study was done at four times (cycles) during the year: (a) early spring, during load restrictions; (b) late spring, after load restrictions; (c) summer; and (d) fall. The weighing done for the early spring was actually done in the spring of 1965, but was assumed as part of the 1964 data.

A computer program called TRUFAC was set up to calculate truck factors for each cycle for each test section using the weight data. TRUFAC essentially accepts the number of axles in 2,000-lb weight classes for single axles and tandem axles, multiplies the number of axles in each weight class by the load equivalency factor for that weight class, sums the products, and divides by the number of trucks in that truck type classification giving the average number of equivalent 18,000-lb axle loads for that type truck. This final value is the truck factor. The equivalency factors have been obtained (5) to show the relative effect of the various axle loads on the performance of a pavement section as indicated by the AASHO Road Test equations.

Truck factors have been determined for Types 1 through 5 trucks using TRUFAC. The truck factors calculated for individual seasons at each test section were weighted assuming the following time distribution: 2 months for spring, 3 months for fall, and 7 months for the summer truck factor. The late spring value was averaged with the summer value to obtain a summer truck factor for weighting.

To study the variations in truck factors, the highways were broken down into three classes and the variations in truck factor with season for these groups were considered. The three classifications are the following:

Class A—Highways carrying interstate trucks and very few local trucks.
Class B—Medium-high traffic roads with some interstate trucks and some local trucks.
Class C—Low traffic loads with almost all local trucks.

There are 8 sections classified as Class A, 15 sections as Class B, and 18 sections as Class C.

Table 1 summarizes the truck factors obtained on these classes of roads for the three cycles of the year. Two things are of interest in this table. First, the spring restrictions have a slight effect on the truck factors for Classes A and B roads and have a greater effect on Class C roads, which are generally restricted in the spring. Second, in all cases the fall truck factors are significantly higher than the spring or summer values (primarily because of harvest time). These variations justify the use of seasonal truck factors and the weighting of them by time to determine a yearly truck factor. In a number of cases the yearly truck factor for Class C roads was quite different from the overall average for a given truck type. In cases where an extremely high or low value represented a very small number of trucks, designated maximum or minimum values of truck factor for the various truck types were used. It was reasoned that over the years a truck factor nearer the average would be appropriate. Table 2 gives the minimum and maximum limits on truck factors set up. These limitations primarily affected Class C roads.

TABLE 1

SUMMARY OF SEASONAL TRUCK FACTORS BY ROAD CLASSES

Road Class	Season	Truck Type				
		1	2	3	4	5
A	Spring	0.210	0.273	0.947	1.249	1.682
	Summer	0.277	0.492	0.745	1.362	1.640
	Fall	0.291	0.701	1.410	1.750	1.948
B	Spring	0.144	0.213	0.544	1.428	1.850
	Summer	0.215	0.273	0.811	1.408	1.893
	Fall	0.216	0.304	0.837	2.062	2.199
C	Spring	0.113	0.232	0.126	0.659	0.411
	Summer	0.184	0.311	0.186	1.097	1.827
	Fall	0.278	0.424	0.665	1.077	1.988
All	Spring	0.150	0.240	0.687	1.253	1.678
	Summer	0.219	0.352	0.619	1.329	1.737
	Fall	0.256	0.454	1.028	1.761	2.034

Weight Distributions

TABLE 2

MINIMUM AND MAXIMUM TRUCK FACTORS USED FOR 1964 YEARLY TRUCK FACTORS

Limit	Truck Type				
	1	2	3	4	5
Minimum	0.100	0.150	0.208	0.500	0.500
Maximum	0.500	0.800	None	2.250	2.300

The variation in weight of the five types of trucks back to 1952 has been estimated by using statewide weight distributions for each type of truck obtained from the annual traffic reports of the Minnesota Department of Highways Planning and Programming Division. Before 1963, the tables did not include a breakdown between tandem and single axle loads, which made it impossible to calculate directly the statewide truck factors (SWTF) for Types 2, 4, and 5 trucks from the traffic reports.

In the Bureau of Public Roads 1965 Truck Weight Study (5), a procedure was suggested for projecting tandem axle effect back for previous years when only the all-axle category was available. This method consists of calculating the ratio of single axles to all axles in each weight category for the earliest year this information is available (1963). This ratio is then used to estimate the number of single axles in each weight group for each type of truck. The remainder of all axles divided by two is assumed to be the number of tandem axles in that weight group. This procedure was used to estimate the statewide truck factors for each type truck for each year previous to 1963. The results from this method of estimating tandem axles have been incorporated in the computer program for estimating variation in truck factor.

A plot of the truck factors is shown in Figure 1. Of special interest is the increase in weight of the Type 4 and Type 5 trucks in the last three or four years. The ratio of the statewide truck factors for a given year to the 1964 statewide truck factors is used to modify the truck factors for each test section for the year of interest. This has been done for each test section back to the year when it was last overlaid. Provision for this calculation has also been made in the computer program so that statewide truck factors are used to modify the test section truck factors as the statewide traffic reports are made available in each future year.

Truck Type and Volume Distributions

The 1964 truck type distribution has been determined for each test section using the volume data from the 1964 traffic study. The distribution is set up as the percentage of heavy commercial traffic that includes Types 1, 2, 3, 4, and 5 trucks. The percentages obtained for each season have been weighted to calculate a 1964 percent distribution for each test section.

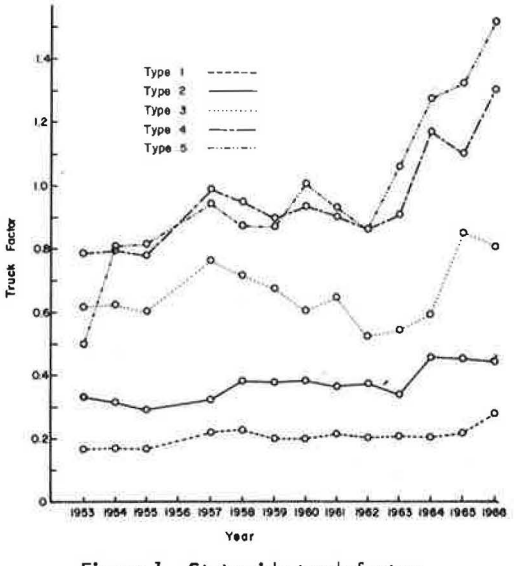

Figure 1. Statewide truck factors.

It is assumed that the volume distribution of heavy commercial trucks can vary from year to year. To estimate the variation from year to year the statewide volume data are used. These data were again obtained from the annual traffic reports. The "axles counted" data are used to determine this statewide yearly distribution. The variation of distribution from year to year is determined by taking the ratio of these percentages to the 1964 percentage and multiplying the 1964 test section distributions by these ratios. The sums of these calculated distributions are apportioned up or down to 100 percent so that the calculated percentages can be used along with the HCADT to determine the number of each type of truck for each test section and each year. A plot of the state-

wide yearly percentage distributions is shown in Figure 2. The general increase in the percentage of Type 5 trucks in the last four years is of interest. The use of statewide distribution data is recommended for updating the traffic volume data each year in the future. Provision has been made in the computer program for inclusion of these data from the annual statewide traffic reports.

The total HCADT for each test section in 1964 is obtained from the traffic study. The HCADT does not include 4-tired, 2-axle trucks (defined as Type 0 trucks).

The variation in HCADT is estimated by using traffic flow maps furnished by the Traffic and Planning Section of the Minnesota Department of Highways. Again, using 1964 as the common denominator, ratios of CADT from the traffic flow maps were obtained for each test section location and each year back to when the individual test was constructed. CADT, which includes Type 0 trucks, was used because this is the value along with total ADT that is shown on the maps. Ratios of CADT can be assumed to be the same as ratios of HCADT because the percentage of Type 0 trucks has remained essentially constant from 1952 through 1967.

From the preceding information, the number of heavy commercial trucks per day (HCADT) traveling in one direction (i.e., over the test section) can be determined for each test section and each year. This is referred to in the program as HCADT (J, K) where J refers to each test section 1 to 50 and K refers to the year from 1952 to the present year (PY). When HCADT (J, K) is multiplied by each of the percent distributions for each year, the number of each type of truck is obtained for each test section and each year. This set of values is referred to as ANOTKS (I, J, K).

With TFS (I, J, K) and ANOTKS (I, J, K) determined from the previous paragraphs, an estimate of the equivalent 18,000-lb axle loads contributed by each truck, each year, on each test section can be obtained by multiplying corresponding elements of these arrays. The resulting array is represented by DTEAL (I, J, K), the daily total equivalent axle loads for each type truck (I), each test section (J), and each year (K).

The summation

$$\sum_{I=1}^{5} \text{DTEAL (I, J, K)} = \text{DTEAL (J, K)} \qquad (1)$$

gives the daily equivalent axle loads for each test section and each year. To get the total equivalent 18,000-lb axle loads for a given year, the DTEAL (J, K) is multiplied by 365, giving the YTEAL (J, K).

To obtain the summation of equivalent axle loads for a test section, the summation

$$\sum_{K=YC}^{PY} \text{YTEAL (J, K)} = \text{SYTEAL} \qquad (2)$$

is made, where YC is the year constructed and PY is the present year. This is called the SYTEAL (summation of yearly total equivalent axle loads). The YTEAL for the year constructed is divided by two because it is assumed that traffic ran for half the year of construction. Table 3 is a list of the 1967 yearly 18,000-lb axle loads for each test section plus the estimated summation of the equivalent 18,000-lb axle loads for each test section through 1967. This table shows the wide variation in traffic found on the Minnesota test sections.

To carry this procedure through the next year (in this case, 1968), it is necessary to

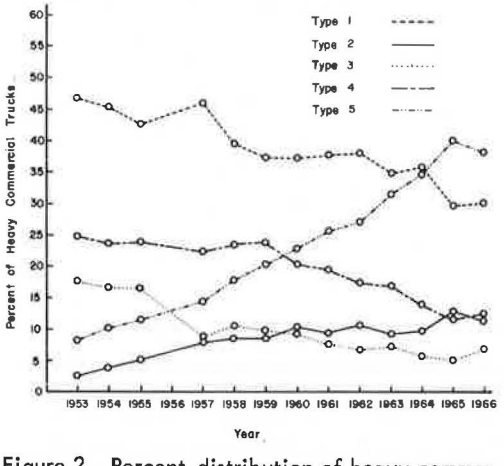

Figure 2. Percent distribution of heavy commercial traffic.

TABLE 3

1967 YEARLY EQUIVALENT 18,000-LB AXLE LOADS AND SUMMATION OF EQUIVALENT 18,000-LB AXLE LOADS THROUGH 1967

Test Section	Year Built	1967 Yearly N18	Σ N18 Through 1967	Test Section	Year Built	1967 Yearly N18	Σ N18 Through 1967
1	1958	113, 510	851, 724	28	1956	—	34, 647[b]
2	1954	—	69, 930[b]	78[a]	1965	7, 128	15, 788
52[a]	1965	24, 182	53, 016	29	1956	—	20, 898[b]
3	1961	25, 596	107, 049	30	1961	222, 115	995, 833
4	1958	16, 511	98, 957	31	1959	12, 367	84, 338
5	1958	6, 576	44, 215	32	1957	6, 194	50, 261
6	1960	162, 168	669, 927	33	1957	40, 906	272, 691
7	1961	14, 658	97, 143	34	1959	134, 589	737, 715
8, 9	1953	40, 112	388, 359	35	1958	15, 677	88, 628
10	1958	3, 867	25, 587	36	1961	42, 189	187, 263
11	1961	9, 536	61, 314	37	1961	32, 944	131, 606
12	1956	6, 966	60, 526	38	1956	48, 511	325, 947
13, 14	1962	31, 574	123, 679	39, 40	1953	19, 625	145, 253
15	1960	328, 581	1, 530, 470	41	1955	—	640, 540[b]
16	1957	65, 530	539, 128	91[a]	1964	218, 369	630, 200
17, 18	1959	76, 480	385, 125	42	1962	12, 565	45, 906
19	1957	99, 046	743, 533	43	1959	553	4, 036
20	1955	70, 612	371, 262	44	1963	7, 269	27, 841
21, 22	1961	25, 303	141, 060	45	1959	6, 674	25, 825
23	1961	131, 402	488, 325	46	1961	6, 773	26, 819
24	1956	4, 198	36, 830	47	1957	20, 501	166, 545
25	1956	2, 294	26, 054	49	1955	32, 856	260, 985
26, 27	1961	1, 457	7, 025	50	1954	7, 911	53, 047

[a]Sections overlaid since 1963 continued to be observed with a number of 50 plus the original number.
[b]Total equivalent 18,000-lb axle loads before being overlaid.

have (a) the annual statewide traffic report for that year, and (b) the traffic flow map or some estimate of the CADT for each test section. The annual traffic report is used to determine the truck factor ratios (changes in weight distribution) of the trucks by type and the volume distribution change of the various type trucks necessary to modify the results of the 1964 traffic study to make it applicable for the present year. The annual traffic reports are usually available in April of the following year. The traffic flow maps are only available for the even years. For an intervening year, such as 1965, the same CADT could be assumed without a great error. With the 1966 traffic flow map available, it is then possible to interpolate between 1964 and 1966 to get a better estimate for 1965. These data can be changed easily in the computer program.

The procedure developed in this section is valid for updating the traffic value on each test section as long as there is no abrupt change in the traffic pattern for the given section. For instance, if an Interstate highway opened parallel to a section, the heavy traffic would most likely be altered materially. The traffic flow map for that year would show the decrease (if any) in the total volume, but would not indicate the decreased number of Types 4 and 5 trucks nor possibly their general decrease in weight caused by the shifting of through traffic to the Interstate highway. If a change in traffic pattern such as this occurs, it is advisable to make another traffic study at the test section location. To ensure that no extraneous traffic conditions have developed on any of the test sections, it would be advisable to conduct another traffic study every 5 or 10 years. The frequency at which these traffic studies are made is dependent on the funds available for such a study. The field work represented here costs approximately $85,000. A future study would only have to be run three times per year rather than four, but more time would be required to obtain complete information on some of the low-traffic sections.

Based on the results of the study made in 1964, a future study could be modified in the following ways. As shown previously, there is a significant difference in truck factors between spring, summer, and fall. It would therefore be advisable to weigh and count trucks in each of these seasons. The spring cycle should be during the spring restriction period and the fall cycle preferably should start after September 1. It would be advisable to make weight distribution determinations only on test sections where more than ten of each type of truck can be weighed during a reasonable length of time. Volume distribution data should be gathered until at least one of each type of truck has

passed the given location. This is important in areas where very low traffic occurs, because it is known that sometime one of a given type of truck will pass by. When one Type 5 truck every three or four days is added up over the life of the pavement it may be the major contributor to total loads to which the pavement is subjected.

Based on the data obtained from the traffic study made in 1964 it has been recommended that the traffic for the Minnesota test sections and any other load determinations based on the equivalent axle load determinations be made at the site being considered and then projected to other years based on statewide variations from year to year. This recommendation is based on a comparison of truck factors in 1964 from a number of the test sections and on the statewide data. Some of the truck factors for 1964 are summarized in Table 4, which gives truck factors for four test sections, the average truck factors for the three classes of roads as defined previously for the overall flexible pavement investigation traffic study, and the statewide traffic from the annual traffic report. Test Sections 1, 15, and 19 are all on US 10 and TS 6 is on US 2 near Duluth. The interesting thing about the three test sections on US 10 is that TS 19 generally has low truck factors compared with TS 1 and TS 15, especially for Types 4 and 5 trucks. It is felt that this low truck factor is caused by the fact that TS 19 is located at a permanent weighing station. Overloaded trucks may be "permanently" avoiding the permanent weighing station. The overall data for the special traffic study also result in somewhat higher truck factors than calculated from the statewide traffic report for 1964. The increase of over 0.50 is significant for Type 5 trucks, as is the increase of about 0.25 for Type 4 trucks. This also may be caused by the use of permanent weighing stations for statewide data collection. These variations show the importance of making traffic surveys for test sections at the location of the sections rather than considering statewide data when the summations of equivalent axle loads are being determined. This is important when considering the loading a research study section has had imposed on it, but is of lesser importance when considering traffic for design purposes.

PREDICTION OF AXLE LOADS FOR PAVEMENT DESIGN

By means of the procedures just presented, the total traffic that has passed over a section of highway can be estimated. The procedure involves a rather comprehensive traffic survey (weight and volume) and the setting up of a computer program that brings the traffic up to date each year. To design a pavement based on equivalent axle loads, it is necessary to estimate the present magnitude of traffic and to be able to project this value into the future over the design period. To do this for design purposes, it is not always practical to run a load distribution study, but it is easier to estimate the ADT, HCADT, or make some estimate of the number of heavy trucks that will be using the road. Using the 1964 traffic study and the variation in statewide traffic, correlations have been developed to show how these traffic parameters correlate with the equivalent 18,000-lb axle loads. The errors in these approximations are converted to

TABLE 4

COMPARISON OF 1964 TRUCK FACTORS

Source	Truck Type				
	1	2	3	4	5
TS 1	0.312	0.151	1.409	1.445	1.789
TS 6	0.464	0.365	0.260	2.242	1.671
TS 15	0.379	0.616	0.161	1.784	1.958
TS 19	0.167	0.236	0.240	0.660	0.710
All Class A	0.267	0.508	0.945	1.440	1.724
All Class B	0.203	0.271	0.773	1.575	1.962
All Class C	0.196	0.326	0.296	1.019	1.631
All Traffic Study Data	0.217	0.359	0.733	1.424	1.801
Statewide from 1964 Traffic Report	0.205	0.452	0.596	1.171	1.276

thicknesses so that the correlations can be evaluated. In the first part of this section, the estimated yearly equivalent loads for the last 12 years are considered to try to estimate the probable future growth of traffic in terms of equivalent axle loads. This factor is necessary for future designs to help determine the load-life of the pavement. The variation in the correlation of HCADT with equivalent loads over the last 10 years is studied and a method is suggested for predicting future growth of equivalent 18,000-lb axle loads based on HCADT.

VARIATION OF RATE OF APPLICATION OF LOADS WITH TIME

To design a highway using the equivalent load concept it is necessary to predict the future growth of traffic in terms of equivalent loads for the design period into the future. As has been shown by the traffic volumes on Minnesota test sections, the number of equivalent loads is not only dependent on the volume of traffic, but also very much dependent on the weight characteristics and the percentage of the different types of trucks.

Two design methods that currently use a growth factor for design with the equivalent load concept are the Asphalt Institute method (4) and the California method (6). A growth factor of 3 percent per year is used, which is inherent in the determination of traffic for the Asphalt Institute design (4, Appendix A). For the California traffic determination, it is assumed that traffic in terms of equivalent wheel loads increases 50 percent in ten years. This is equivalent to a yearly growth factor of 4.14 percent.

To see how these factors compared with the results of the traffic analysis on the Minnesota test sections, the yearly equivalent axle loads for the preceding 12 years were taken as a percentage of the 1965 yearly equivalent axle loads and averaged for the Classes A, B, and C roads as defined previously. The percentages were averaged for each of the classes of sections. It was found that the values for Classes A and B roads were very similar. These two classifications were therefore combined and the averages for this "heavy" category and the Class C (light) category were determined separately. Even though the variation in each of these percentages is based on the same statewide data, there is on the average about a 10 percent higher value of percentage for the light traffic roads. This actually represents a slower growth rate. The lower growth rate for the lower traffic roads can be attributed to the lower percentage of Types 4 and 5 trucks on these roads. The Types 4 and 5 trucks have shown the greatest increase in weight over the last 10 to 12 years. It was found that the growth of the heavy roads can be best represented by a growth factor of greater than 10 percent per year and the lighter traffic roads can be represented by a growth factor of about 8 percent per year. These values of growth factor are considerably higher than those previously mentioned. It is felt that the last 12 years represent a period of abnormally high growth in truck weights and volume of truck traffic. For estimating future traffic growth, a value between 5 and 8 percent would be adequate. This is only an overall value, however, and when a specific estimate is being made, many local factors could materially affect the growth factor anticipated.

Correlation of Equivalent Loads With Other Traffic Parameters

The relationships obtained when 18,000-lb equivalent axle loads are correlated with three traffic parameters on a pavement section are presented in this section. The parameters used for correlation are (a) the two-way average daily traffic at the section location (ADT), (b) the one-way heavy commercial traffic (HCADT as previously defined) at the section, and (c) the daily summation of the number of Types 4 and 5 trucks at the section in one direction.

The initial correlations are made using the data from the 1964 traffic study on the Minnesota test sections. Initial plotting indicated that the data appeared to fall into two categories—one with traffic greater than 150 daily equivalent loads, and the other with less than 150 daily equivalent loads. Test Section 19 was left out of the correlations because the data from this section deviated greatly from the overall trends. Comparison of arithmetic and logarithmic plots and error terms showed that log-log correlations were the best.

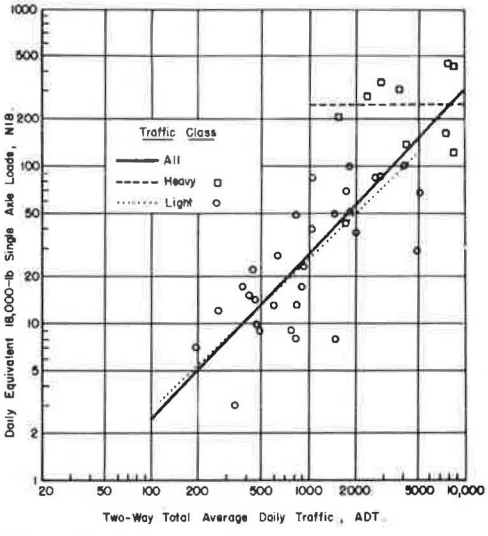

Figure 3. Percent of 1965 annual equivalent 18,000-lb single axle loads for heavy traffic test sections.

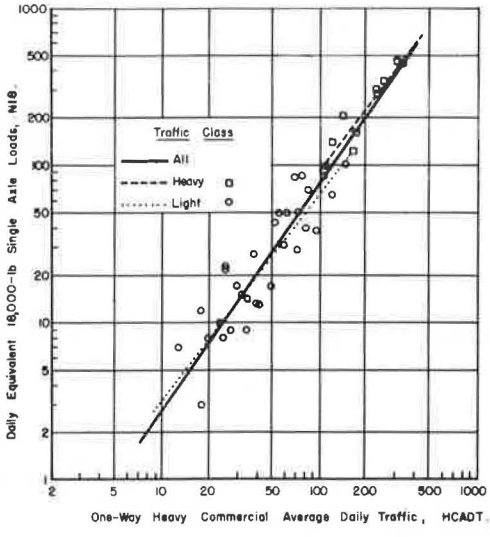

Figure 4. Percent of 1965 annual equivalent 18,000-lb axle loads for light traffic test sections.

Figures 3, 4, and 5 and Table 5 show the correlations of the three parameters and daily N18 using logarithmic axes. The data show that a better correlation is achieved by separating the light and heavy traffic.

Table 6 gives the error thickness of granular base, using Eq. 18 from an Asphalt Institute monograph (7). When log N18 is used, one unit of thickness represents a given standard error because thickness is related to the log N18 in the equation. An error factor is also listed in Table 6 for each traffic parameter and category. This factor represents the percent accuracy to which N18 can be estimated using the given parameter. For instance, the error factor is 1.240 for heavy traffic using HCADT. This means that N18 can be predicted to a percentage accuracy of ± 24 percent (actually x 1.24 or ÷ 1.24). This accuracy represents a thickness of granular base of about 0.6 in.

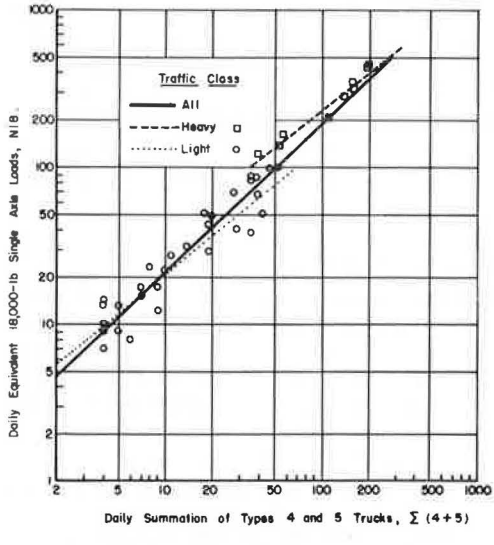

Figure 5. Logarithmic relationship between daily equivalent 18,000-lb axle loads and two-way total average daily traffic.

TABLE 5

CORRELATIONS FOR PREDICTING EQUIVALENT AXLE LOADS WITH LOG-LOG RELATIONSHIPS

Form of Equation: $\log N18 = a_0 + a_1 \log (X)$

X	Traffic Conditions	a_0	a_1	Standard Error
ADT	Light	-1.204	0.853	0.328
	Heavy	2.399	-0.002	0.228
	All	-1.725	1.052	0.367
HCADT	Light	-0.816	1.307	0.229
	Heavy	-0.671	1.317	0.093
	All	-1.006	1.433	0.217
Σ(4+5)	Light	0.506	0.824	0.169
	Heavy	0.819	0.776	0.051
	All	0.396	0.944	0.163

TABLE 6

ERROR IN THICKNESS OF GRANULAR BASE OWING TO STANDARD ERROR OF CORRELATIONS USED TO ESTIMATE N18

Traffic Parameter	Category	Error Factor	Gravel Equivalent Thickness Error (in.)
ADT	Light	2.126	1.8
	Heavy	1.691	1.3
	All	2.328	2.0
HCADT	Light	1.695	1.3
	Heavy	1.240	0.6
	All	1.649	1.2
Σ (4 + 5)	Light	1.475	0.9
	Heavy	1.124	0.3
	All	1.455	0.9

TABLE 7

MINNESOTA TRAFFIC CATEGORIES CONVERTED TO DAILY EQUIVALENT 18,000-LB AXLE LOADS USING THE 1964 CORRELATION

Two-Way HCADT Range	One-Way HCADT Range	Daily 18,000-lb Axle Loads
<150	<75	<43
150-300	75-150	43-107
300-600	150-300	157-392
600-1100	300-550	390-867
>1100	>550	>867

The errors in thickness obtained using the arithmetic relationships were greater than those in Table 6. It is slightly better to break the roads down into heavy and light traffic categories. The better correlation using Σ (4 + 5) as the independent variable is obtained because in most cases the Type 4 plus Type 5 trucks made up about 70 to 90 percent of the equivalent loads on the pavements for 1964.

From the accuracies shown in Table 6, it is apparent that an estimate of equivalent loads using HCADT should be adequate and that slightly better accuracy would result if a good estimate of the number of daily Type 4 plus Type 5 trucks could be obtained.

The following equations have been suggested to predict N18 from HCADT for design purposes.

$$\log N18 = -0.816 + 1.307 \log (HCADT) \quad \text{for HCADT} < 150 \tag{3}$$

$$\log N18 = -0.671 + 1.317 \log (HCADT) \quad \text{for HCADT} > 150 \tag{4}$$

For the present Minnesota Department of Highways design procedure, the two-way HCADT is used as a design parameter (1). The HCADT used in this presentation is a one-way HCADT. Table 7 gives the ranges of HCADT presently used converted to daily equivalent 18,000-lb axle loads using this 1964 correlation.

VARIATION IN CORRELATION BETWEEN TRAFFIC AND LOADS

It has been found by the Traffic and Planning Section of the Minnesota Department of Highways that the HCADT on most Minnesota highways is increasing at a rate of 3 percent per year. For the estimation of loading on a pavement using the HCADT, the correlation between HCADT and daily N18 is used. To design a pavement, consideration must be made of the increase in N18 projected into the future through the design period. When HCADT is used to predict N18 over a design period of 20 years, two factors can increase that cause an increase in N18 each year. These are (a) an increase in HCADT which is around 3 percent per year as indicated above (this may vary somewhat depending on local traffic conditions), and (b) an increase or decrease in daily N18 predicted for a given HCADT. A change in correlation could significantly affect the total design N18 over the design period. The correlations to show the effects discussed are considered in the remainder of this section.

The correlation between N18 and HCADT shown in Figure 4 is for the year of the traffic study (1964). To study the variation of this correlation with time, the daily N18 for each test section used in the traffic study was determined for each year from 1956 through 1966. Table 8 gives the results of these correlations for the 11 years. The equation is the same log-log model and results in equally good correlations for each year as shown by the squared correlation coefficients and the standard errors.

To see what these correlations represented in terms of daily N18, the predicted N18 were calculated for each year for one-way HCADT values of 75, 150, 300, and 550.

TABLE 8

RESULTS OF CORRELATIONS BETWEEN N18 AND HCADT FOR 1956 THROUGH 1966 USING NO BREAKDOWN OF TRAFFIC

$\log N18 = a_1 + a_2 \log (HCADT)$

Year	a_1	a_2	Squared Correlation Coefficient	Standard Error
1956	-0.9079	1.317	0.912	0.180
1957	-0.8445	1.293	0.910	0.183
1958	-0.8672	1.342	0.898	0.199
1959	-0.9884	1.385	0.922	0.177
1960	-0.9464	1.362	0.923	0.170
1961	-0.9196	1.352	0.925	0.164
1962	-0.9854	1.362	0.935	0.148
1963	-0.7153	1.259	0.787	0.272
1964	-0.8945	1.373	0.906	0.188
1965	-0.8004	1.355	0.912	0.180
1966	-0.7645	1.359	0.927	0.171

TABLE 9

PERCENT INCREASE IN DAILY EQUIVALENT 18,000-LB LOADS RELATIVE TO HCADT

Period Prior to 1965	HCADT			
	75	150	300	550
10 years	4.2	5.7	6.9	6.7
4 years	12.5	17.3	21.8	25.9
3 years	17.8	15.9	12.5	12.3

These values correspond to the present design limits of 150, 300, 600, and 1100 two-way HCADT. The daily N18 values were plotted on a log scale so that a constant slope represents a constant rate of increase assuming a compound percentage increase. There was not a constant rate of increase over the 11-year period. In fact, there is somewhat of a decrease in the correlations from 1958 through 1962. This can be explained by the fact that more Type 5 trucks relative to Types 3 and 4 trucks were coming into use during that period. The Type 5 trucks generally had a slightly lower truck factor because the loads on tandem axles have a lower load equivalency ratio. In the past four or five years, as trucks have been loaded more efficiently, these loads have gone up and the correlation is at a high level and increasing. To estimate the amount of increase in daily N18 per year relative to HCADT, three lines were drawn through the data from the last 11 years. The lines represent rates of increase for ten years, four years, and three years. The rates of increase represented by the lines are given in Table 9. For the last three years the rate of increase is lower than for the last four years for the two highest categories of HCADT. The increases for three and four years are about the same for the lower two HCADT categories. The rates for the ten-year period are about half or less the slopes of the later years.

To consider the increase in these correlations into the future, a number of factors should be considered. The sag in the relationships from 1958 and 1962 was most likely caused by the greater use of Type 5 trucks. The period from 1962 to the present exemplifies a time when the Types 4 and 5 trucks are being used more efficiently and thus, on the average, these trucks would be heavier. This trend will most likely not continue for more than two or three more years. The percentage increases over 12 percent are thus considered high and a value of 5 to 8 percent per year is recommended. This percent increase along with the 3 percent increase in HCADT per year yields an 8 to 11 percent increase in N18 per year. When the maximum allowable axle loads are considered it can be seen that these values would be exceeded after three or four years at a rate of increase of 15 percent and after about ten years at a rate of 10 to 12 percent per year. Using an overall rate of increase of 5 percent results in a factor of 2.5 in 20 years and using 12 percent results in an 8.6-fold increase. It is felt that the lower percent increase should be used so that gross overdesign will not occur. If it is found that there is more increase in loading and the pavement is failing because of it, an overlay can be added after any number of years of service.

SUMMARY AND CONCLUSIONS

At the AASHO Road Test it was possible to determine the relative effect of the loadings used because a particular pavement section was subjected to repetitions of only one magnitude of load. The relative effect of the loads on the performance of pavement sections can be used to convert each load repetition to an equivalent number of repetitions of a base load. These load equivalencies can be used to convert mixed traffic to a number of equivalent 18,000-lb axle loads. A procedure has been developed for de-

termining on a computer the total equivalent 18,000-lb axle loads on each test section. To do this it was necessary to determine the load and volume distribution of traffic on the individual test sections rather than using statewide data. Annual statewide data can be used to modify the distributions determined from the traffic study. Both the number and weight of the Type 5 trucks have increased as shown in Figures 1 and 2. The weights of Types 1, 2, and 3 trucks are about the same over the last 15 years.

The equivalent 18,000-lb axle loads can best be predicted from the daily sum of Type 4 plus Type 5 trucks on a section of road. However, the prediction using the HCADT is only slightly worse and is recommended for designing flexible pavements. The log-log relationships shown as Eqs. 3 and 4 can be used for the correlation and should be updated each year. It is recommended that the HCADT continue to be used for traffic determinations and that an increase of 5 percent in N18 relative to HCADT and an increase of 3 percent in HCADT be used for design purposes if no other particulars are known about the design traffic. It is thus recommended that an annual growth factor of 8 percent in N18 be used for design purposes. With subsequent correlations of the Minnesota test sections in future years, the growth factor can be verified or modified.

Further studies should be continued in an attempt to relate the truck factors to the type of road, location, etc. The additional studies should not be made at permanent weighing stations because these are apparently being avoided by some heavy trucks. With the traffic values being calculated each year, other correlations between type of road and the weight distributions should be considered. A study should also be considered for which every vehicle is counted and classified and every truck is weighed over a period of a week or even a month to see how accurate various samples of this total would be in predicting equivalent 18,000-lb axle loads.

ACKNOWLEDGMENTS

The study reported in this paper is part of a research project that is a cooperative venture between the Minnesota Department of Highways and the University of Minnesota. The Department's Planning Research Section performed the field work and the University has done most of the analysis work. The project is being conducted under the Highway Planning and Research Program financed jointly with federal-aid funds of the U.S. Department of Transportation, Bureau of Public Roads, and with state funds of the Minnesota Department of Highways. The opinions, findings, and conclusions expressed in this paper are the author's and not necessarily those of the Bureau of Public Roads.

REFERENCES

1. Flexible Pavement Design Standards. Minnesota Department of Highways Design Manual, St. Paul, July 1, 1964.
2. AASHO Interim Guide for the Design of Flexible Pavement Structures. American Association of State Highway Officials, Oct. 1961.
3. Shook, J. F. Development of Asphalt Institute Thickness Design Relationships. Proc. AAPT, Dallas, Texas, 1964.
4. Thickness Design—Asphalt Pavement Structures of Highways and Streets. The Asphalt Institute, Manual Series No. 1, March 1964.
5. 1965 Truck Weight Study (RCS 38-20-7). Bureau of Public Roads Instructional Memorandum 50-1-65, April 19, 1965.
6. Materials Manual of Testing and Control Procedures, Vol. 1. California Division of Highways, Sacramento.
7. Developments in Thickness Design of Asphalt Pavement Structures. The Asphalt Institute, Oct. 1963.
8. Kersten, M. S., and Skok, E. L., Jr. Application of AASHO Road Test Results to Design of Flexible Pavements in Minnesota. Paper presented at 48th Annual Meeting and included in this Record.

Temperature Distribution Within Asphalt Pavements and Its Relationship to Pavement Deflection

HERBERT F. SOUTHGATE and ROBERT C. DEEN, Kentucky Department of Highways, Lexington

A method has been developed to estimate the temperatures at depth in an asphaltic concrete pavement utilizing the measured pavement surface temperature and the 5-day average air temperature history. Temperature prediction nomographs were developed for each hour between 6 a.m. and 5 p.m. This temperature prediction method is independent of the season of the year. A method for adjusting Benkelman beam deflections for temperature effects has been developed and is presented. This enables the deflections taken at any temperature to be adjusted to a reference temperature, thus making possible direct comparisons of deflections.

An analysis of AASHO Road Test data was made using the Boussinesq and Burmister equations and charts. The results indicate that the temperature-modulus of elasticity relationship is curvilinear, has the same basic shape found by Kallas in the laboratory, and has the same basic shape as the temperature-deflection adjustment factor curve. There appears to be a linear relationship between deflection adjustment factors and modulus of elasticity. Therefore, there seems to be a temperature-deflection-modulus of elasticity correlation between field test data and theory.

•ASPHALTS "soften" as the temperature increases and "stiffen" as the temperature decreases, and measurements have shown that the deflection and rebound of asphalt pavements in response to loads are affected to a significant degree by temperature. Historically, pavements that deflect greatly under traversing loads are short-lived. Pavements that undergo minimal deflection at some maximum load are either inherently more rigid or are more firmly supported than those that undergo greater deflection. The rigidity or "stiffness" of asphaltic concrete is not a direct measure of strength, nor is deflection an inverse measure of the strength of a pavement structure. Strength is usually expressed as the load or stress that causes overt failure, whereas stiffness or rigidity is concerned only with load-deflection (or stress-strain) relationships. It seems reasonable that the deflection of a pavement decreases as the thickness of the asphaltic concrete is increased, and that the strength of the pavement structure is thereby increased. Therefore, in the case of a pavement that has a more or less uniform degree of support, deflection and thickness are empirical indicators of strength and structural adequacy. For lesser but uniform degrees of support, greater thicknesses of asphaltic concrete are compensating, effectively reducing deflection and strengthening the pavement system. Of course, the supporting capabilities of underlying soil or base courses may be improved and/or thickened to accomplish the same effect. Elastic and viscoelastic theories have been extended and perfected, fatigue theories of failure have been studied, and each of these has been related with some degree of confidence to load and deflection.

Paper sponsored by Committee on Flexible Pavement Design and presented at the 48th Annual Meeting.

Surface deflection (or rebound) remains the most measurable response of a pavement to an applied load. Adjustment of measured deflections to a common (or base) temperature offers further hope of reducing the temperature variate and improving the correlation between load-deflection and classical theory.

Pavement surface temperature alone does not suffice to account for the dependency of deflection on temperature; and, because temperatures at depths are known to influence deflections, subsurface temperatures must be either measured in situ or estimated from other correlations. The purpose of this research (1) is (a) to develop a method for estimating the temperature at any depth in a flexible pavement up to 12 in. thick, and (b) to analyze the temperature-deflection data generated in the AASHO Road Test (2) to show that temperature adjustment factors are generally applicable to Benkelman beam deflection measurements of bituminous pavements and to determine the magnitude of these adjustment factors.

METHOD AND ANALYSIS

Analysis of Temperature Records

The data used to develop the temperature distributions and the prediction criterion were those recorded in 1964 and 1965 at the Asphalt Institute's laboratory at College Park, Maryland (3).

In this analysis, data for 12 consecutive months were punched on cards to facilitate data processing and analysis. A study of the data revealed that in normal weather and at a given hour, the temperature at a given depth was approximately the same percentage value of the surface temperature, even though the surface temperatures fluctuated from day to day. For a given depth, temperature fluctuations followed an orderly pattern and were influenced primarily by the surface temperature.

The data showed that a short period of rain or extensive cloud cover reduced the surface temperature and influenced the temperatures at shallow depths. However, extended periods of inclement weather reduced the surface temperature to nearly the level of the air temperature and proportionately decreased the temperature throughout the 12-in. pavement thickness. Air temperatures generally dropped and recovered more slowly than the pavement surface temperature. Therefore, air-temperature history was an indication of previous long-term influences on the temperatures at various depths.

Mean daily air temperatures, a measure of the air-temperature history, were computed as the average of the highest and lowest air temperatures for each day. This particular method was chosen for the following reasons:

1. The U.S. Weather Bureau uses this system for each reporting weather station, and thus air temperature data would be readily available;
2. The U.S. Weather Bureau report does not contain air temperatures for each hour of the day;
3. This method has some precedence in engineering work.

Consideration of air-temperature history provided an interesting and valuable result, as shown in Figures 1 and 2. In Figure 1, a linear relationship between mean pavement temperatures (average of temperatures at the 0.125-, 4.0-, and 8.0-in. depths) and 0.125-in. depth temperatures is shown for each calendar month. The relationship of the months, their temperature ranges, and the seasonal changes in temperatures can be readily seen. The addition of mean monthly air temperature to each respective monthly line in Figure 1 produced Figure 2. The addition of air-temperature history to each respective month reduced the scatter of the data such that one straight line could replace all of the monthly lines. Similar analyses for 4- and 12-in. thick pavements indicated the same general relationships.

Regression Analysis of Temperatures With Respect to Depth

The only daily temperature data that were deleted prior to regression analysis were eliminated for one of two reasons: either the recorder was out of operation because of maintenance, or the first two days of recorded pavement temperatures after a missing

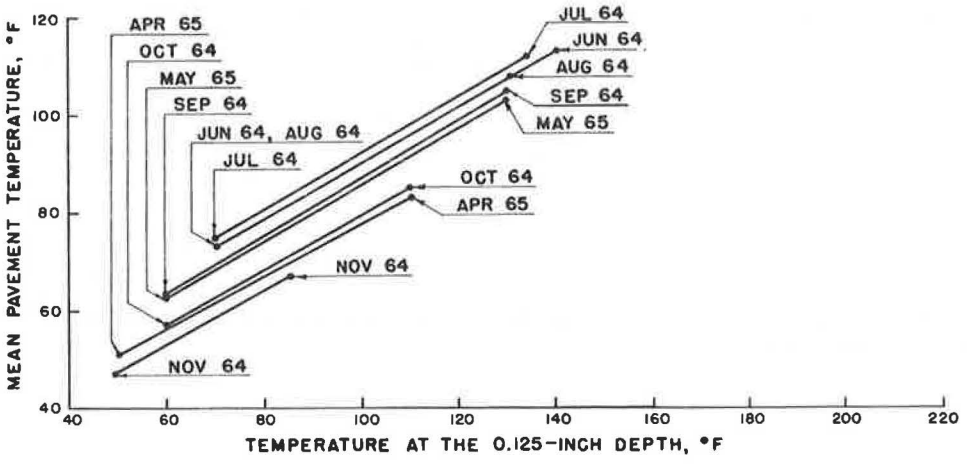

Figure 1. Mean pavement temperature by calendar month for an 8-in. thick pavement at 1:00 p.m. vs temperature at the 0.125-in. depth.

day of data were eliminated because the antecedent air temperatures were also missing from the source data. This resulted in the elimination of 47 days of data. Therefore, data for 318 days were used in the final analysis.

To develop relationships to be used in later analyses, a regression analysis was made of the temperature-depth data. Because the method of estimating temperatures would ultimately be used to adjust Benkelman beam deflections, data taken from 6 a.m. through 5 p.m. were analyzed because most deflection tests would be performed during these hours.

To approximate the temperature-depth relationships for a given hour, a review of the data suggested the need for a polynomial equation of the form

$$Y = C_1 + C_2X + C_3X^2 + \ldots + C_nX^{n-1} \quad (1)$$

where

Y = temperature in degrees F at depth X,
X = depth in inches from the pavement surface, and
$C_1, C_2, C_3, \ldots C_n$ = coefficients determined by the method of least squares.

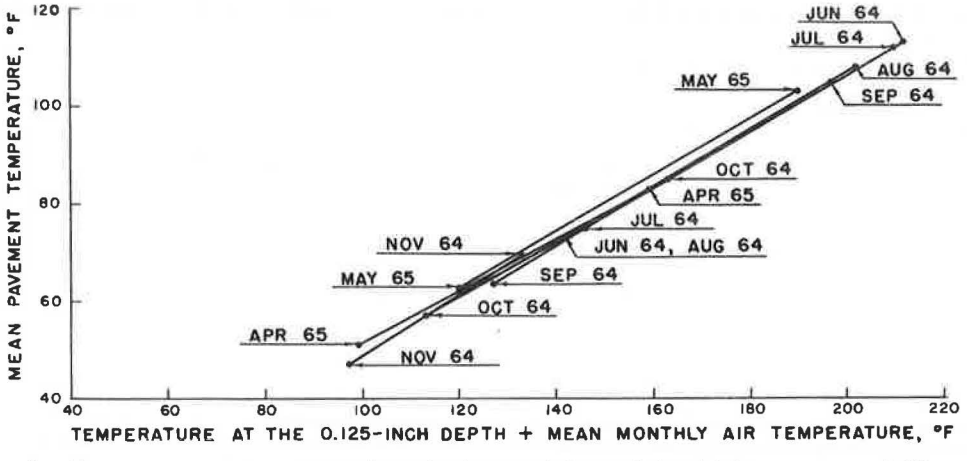

Figure 2. Mean pavement temperature by calendar month for an 8-in. thick pavement at 1:00 p.m. vs temperature at the 0.125-in. depth plus 30-day mean air-temperature history.

Results showed that at 6, 7, and 8 a.m., a third-order polynomial provided the best fit, and a fourth-order polynomial was very nearly as accurate. For the remaining hours, a fifth-order polynomial gave the best fit, and again the fourth-order was very nearly as accurate. Therefore, a fourth-order polynomial was chosen to approximate data for all hours.

Standard errors of estimate were calculated and the maximum difference between the observed temperature value and the value calculated from the polynomial was recorded. Analysis showed that the average standard error of estimate was approximately 0.50 F—the least being 0.09 F and the maximum being 2.20 F. The maximum difference between the observed and calculated temperatures ranged from 0.17 F to 4.54 F and an average of 318 values yielded 0.95 F. The large differences, such as the 4.54 F, were verified by inspection of the temperature-depth data and revealed that the real distribution was erratic. Days of data were picked at random, and further checks between observed and calculated values indicated that the curves were smooth and in close agreement with measured temperatures at the respective depths.

The temperatures at the surface and at each ½-in. increment of depth through 12 in. were calculated by means of the fourth-order polynomial equation determined for the respective day. Temperatures so calculated were plotted as ordinate values vs the measured surface temperature plus an average air-temperature history preceding the day of record (a separate graph for each depth was prepared). The plot for the 6-in. depth is shown in Figure 3. The average air-temperature history was computed for 5 days prior to the day of record. The optimum number of days for the air-temperature history was determined by further investigations described below.

The addition of an average air-temperature history to the surface temperatures was found to produce a favorable shift in the abscissa values in relation to the fixed ordinate values. Average air temperatures were computed for 1, 2, 3, 5, 7, and 10 days preceding each day of record. Each set of data was adjusted and evaluated in terms of standard error of estimate. The standard error of estimate decreased to a minimum when 2 days of air-temperature history were added and then increased as the number of antecedent days increased. The minimum standard error of estimate for the 6-in. depth and for the hours 6 a.m. through 9 a.m. and 6 p.m. and 7 p.m. occurred when a 10-day

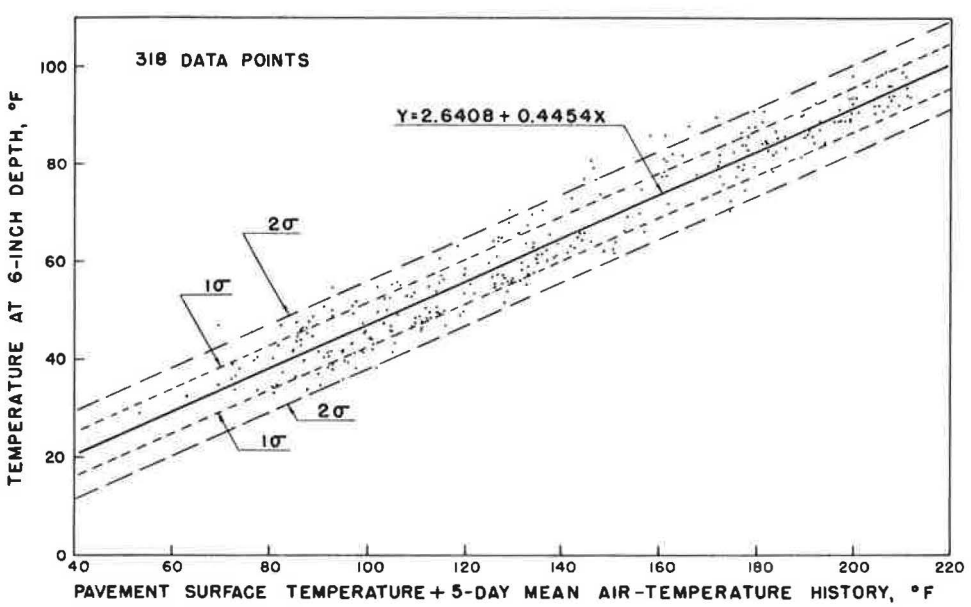

Figure 3. Temperature at the 6-in. depth vs measured pavement surface temperature at 1:00 p.m. plus 5-day mean air-temperature history.

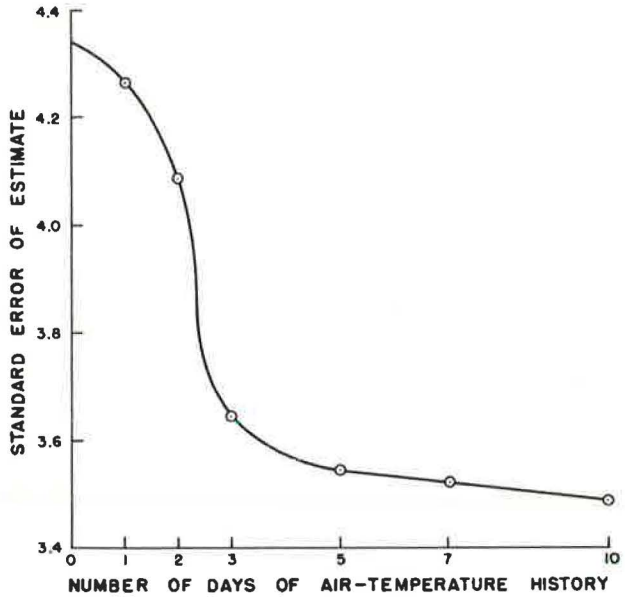

Figure 4. Standard error of estimate for all depths and all hours vs number of days of air-temperature history.

average air-temperature history was added, and for the hours of 10 a.m. through 5 p.m., a 2- to 5-day average air-temperature history was optimum.

Figure 4 was drawn to find the number of days of average air temperatures that gave the least standard error of estimate for all depths and all hours under consideration.

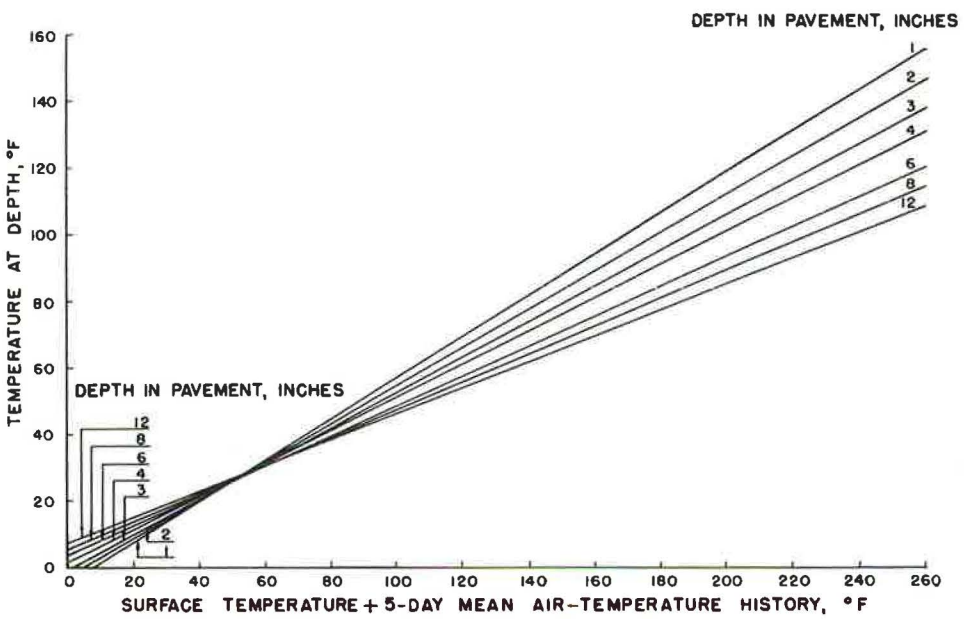

Figure 5. Temperature-depth prediction graph at 1:00 p.m. for pavements greater than 2 in. thick.

As can be seen, accuracy does not increase significantly beyond the 5-day point. Therefore, only the 5 previous days are considered to be significant. Further analysis of the standard errors of estimate showed that the 5-day average air-temperature history sufficed for all depths greater than 2 in. The least standard errors of estimate for the depths 0 in. through 2 in. indicated that the best estimate was obtained by the use of the surface temperature alone. Pavement temperatures in the top 2 in. of the pavement are more directly dependent on the hour of the day and the amount of heat absorption, whereas temperatures at depths greater than 2 in. are assumed to be a function of the surface temperature, amount of heat absorption, and the past 5 days of temperature history.

A complete set of curves giving the best estimate of temperature at the several depths and by hour of the day was developed. Because of space limitations, only the set of curves for 1 p.m. is shown in Figure 5 as a typical example.

Development of Deflection Adjustment Factors for Temperature Effects

Two types of adjustment factors were considered. The first was to assign an incremental deflection to each degree of temperature difference between the pavement temperature and the reference or standard temperature. This type of correction was employed by Kingham and Reseigh (4) and by Sebastyan (5); however, the magnitude of suggested corrections differed. The second method considered was the use of a dimensionless, multiplicative factor that could be applied to a measured deflection at some known surface temperature or a known mean temperature of the pavement. No known reference in the literature mentions the second method.

Inspection of the AASHO Road Test curves (2, Figs. 89a, 89b, 89c, and 90a) suggested that the dimensionless, multiplicative factor method might be more appropriate. Therefore, in this study, the above AASHO Road Test curves were transformed to semilogarithmic plots, temperature being the logarithmic scale. The data plotted as straight lines, and the slopes of the individual curves for each loop were very nearly parallel. However, the slopes for the several loops were not parallel. The equation for the straight lines was

$$M = \frac{Y_2 - Y_1}{\log T_2 - \log T_1} \tag{2}$$

where

M = slope of the straight line,
Y_1, Y_2 = deflection values, and
T_1, T_2 = mean pavement temperatures in degrees F corresponding to the Y_1 and Y_2 deflection values respectively.

After the slope had been determined, the deflections were computed for mean pavement temperatures of 30 through 150 F, at 10 F-intervals, by the equation

$$Y_3 = Y_1 + M(\log T_3 - \log T_1) \tag{3}$$

where

Y_3 = deflection at the temperature T_3,
Y_1 = same Y_1 used in Eq. 2,
M = slopes as determined in Eq. 2,
T_3 = temperature at which the deflection was computed, and
T_1 = same T_1 used in Eq. 2.

A mean temperature of 60 F was chosen as the reference temperature, T_{60}.

The adjustment factors were derived from the equation

$$AF = \frac{Y_{60}}{Y_3} \tag{4}$$

where

AF = the adjustment factor used to adjust measured deflections due to temperature effects,
Y_{60} = computed deflection in inches for the mean pavement temperature 60 F from Eq. 3, and
Y_3 = computed deflection in inches for a particular mean pavement temperature T_3 from Eq. 3.

Table 1 shows the results of calculations for the 4-in. pavement on Loop 5. Each of the 12 adjustment factor curves in Figure 6 are the results of computations according to Eqs. 2, 3, and 4, and the curves are plotted arithmetically with mean pavement temperature, T_3, on the ordinate axis and the adjustment factor, AF, on the abscissa axis. Deflections, Y_3, computed from the 12 individual curves at a given mean pavement temperature, T_3, were added and averaged to obtain the final adjustment factor curve shown in Figures 6 and 7.

Further analysis showed that there may be a relationship among average structures within a given loop—that is, except for the 8.6-in., asphalt-treated base curve, which for some unknown reason was an outlier. There was no consistent relationship between loops and substructures as evidenced by the 2-in. surfacing on Loop 3 and the 6-in. surfacing on Loop 6, where the total structural thicknesses were 9 and 24 in. respectively; yet each had the same adjustment factor curve. The same situation was present with regard to the 4-in. surfacing on Loop 3 and the 16.1-in., asphalt-treated base section that had total structural thicknesses of 11 and 24.1 in. respectively. These structural relationships may have been obscured by the AASHO approach of averaging deflections for a given surfacing thickness within a loop; however, the AASHO structural-equivalency equation showed that in some cases the structural indexes were vastly different. Further analyses might be made of the AASHO data (2, Figs. 89a, 89b, 89c, and 90a) with the raw data grouped according to surfacing thicknesses and structural indexes without regard to locations.

The adjustment factor curve for temperature effects is applicable only to creep-speed deflections because the source data used in the analysis were taken at creep speed. Further analysis would be required to establish applicability to deflections taken at other than creep speed. The adjustment factor curve is applicable to any loading as long as the deflection is to be adjusted to the reference temperature for that same loading.

Relationship Between Temperature-Adjustment Factors and Modulus of Elasticity of Asphaltic Concrete

Reflection on the Boussinesq equation for deflections at the center of a flexible plate

$$Y = \frac{1.5\ Pa}{E} \tag{5}$$

where Y = surface deflection in inches, P = unit load on circular plate, a = radius of plate, and E = modulus of elasticity of the material, discloses that the deflection is a

TABLE 1

RESULTS OF CALCULATIONS SHOWING DEVELOPMENT OF DEFLECTION ADJUSTMENT FACTORS FOR THE 4-INCH PAVEMENT ON LOOP 5 OF THE AASHO TEST ROAD

Temperature, T_3 (F)	Deflection, Y_3, at Temperature T_3 (in.)	Adjustment Factor	Temperature, T_3 (F)	Deflection, Y_3, at Temperature T_3 (in.)	Adjustment Factor
40	0.01562	1.7106	100	0.04071	0.6563
50	0.02173	1.2293	110	0.04333	0.6167
60	0.02672	1.0000	120	0.04571	0.5846
70	0.03094	0.8636	130	0.04790	0.5578
80	0.03460	0.7723	140	0.04993	0.5351
90	0.03783	0.7063	150	0.05182	0.5156

T_1 = 52 F = average pavement temperature, T_A
T_2 = 80 F = average pavement temperature, T_A
Y_1 = 0.0228 = deflection corresponding to T_1
Y_2 = 0.0346 = deflection corresponding to T_2

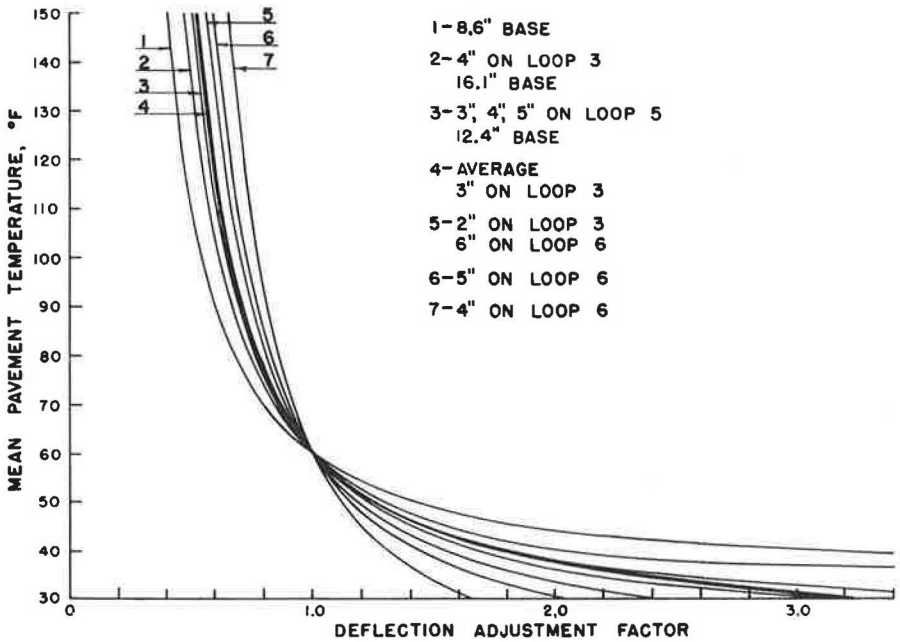

Figure 6. Mean pavement temperature vs deflection adjustment factors for various loops.

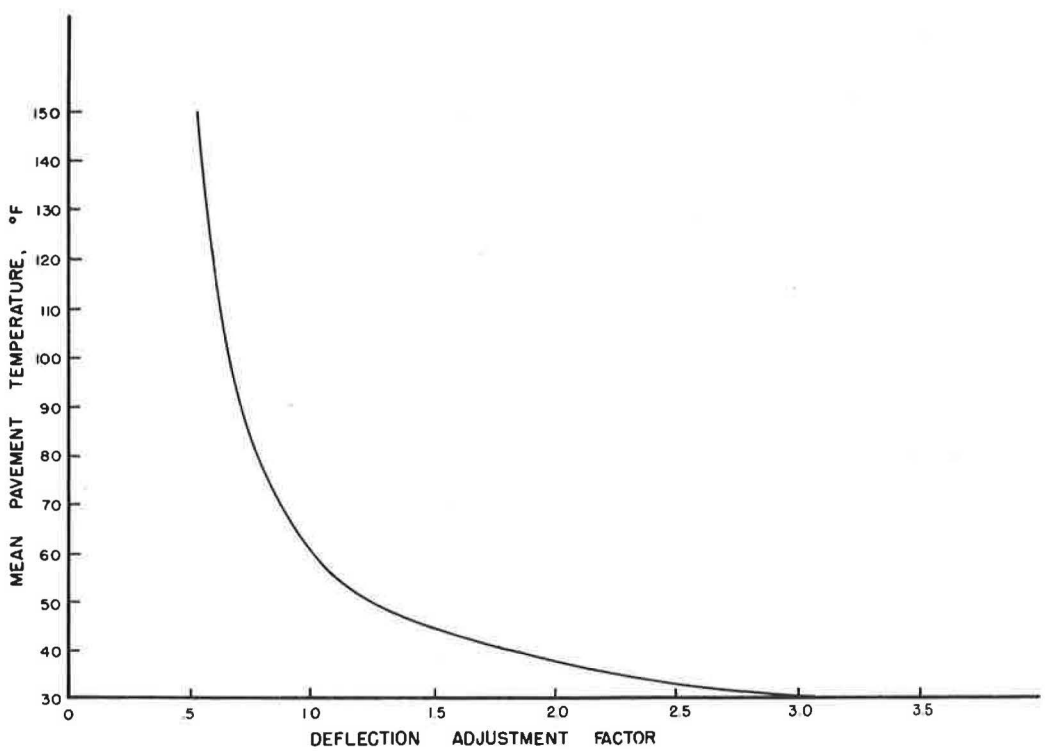

Figure 7. Mean pavement temperature vs average deflection adjustment factor.

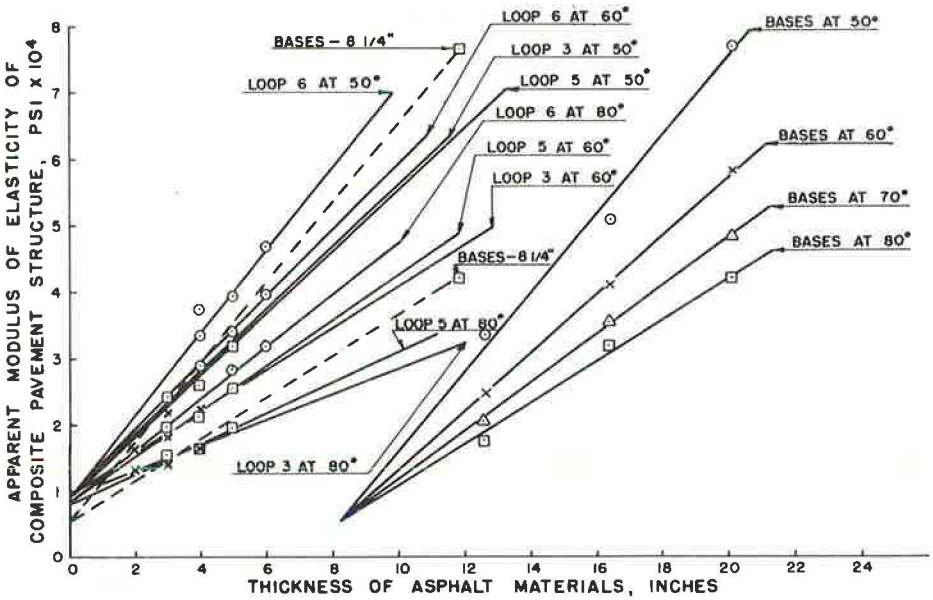

Figure 8. Apparent modulus of elasticity of composite pavement structure vs pavement thickness.

linear function of load as well as the modulus of elasticity of the material, which may be affected by temperature. In turn, Burmister's equation for deflections under a flexible plate, using a two-layered elastic system (6),

$$Y = \frac{1.5\ Pa}{E_2} F_2 \tag{6}$$

where E_2 = modulus of elasticity of lower layer, and F_2 = dimensionless factor depending on the ratio of moduli of elasticity of the subgrade and pavement as well as the depth-to-radius ratio, indicates that deflections are also a function of pavement thickness and the modulus of elasticity of the pavement layer and the underlying material. The load and the radius of contact area could be considered constant for a given axle load and tire pressure.

The surface deflections (2, Figs. 89a, 89b, 89c, and 90a) were used to calculate the modulus of elasticity by the Boussinesq equation (Eq. 5). This was an apparent modulus, E_c, of the composite structure of the pavement. When these values were plotted against respective thicknesses of asphaltic concrete (Fig. 8), a straight line could be passed through the data points for a given loop section at each temperature; and, upon extrapolation to zero thickness (or temperature-affected thickness, in the case of asphalt-treated bases), the respective lines converged at an approximate value of 8,400 psi. This was considered to be the subgrade modulus E_2 of Burmister's two-layered, elastic theory equation. The F_W factors were obtained by

$$F_W = \frac{E_2}{E_c} \tag{7}$$

where F_W = Burmister's settlement coefficient.

Burmister's influence curves (6) were used to obtain the ratio of E_1 to E_2. The modulus of elasticity of the asphaltic concrete was obtained from

$$E_1 = N \times E_2 \tag{8}$$

where

$$N = \frac{E_1}{E_2}$$

The foregoing calculations were made using the deflections at various temperatures and the E_1 values were avaraged for each temperature. Simultaneous solution of the equation

$$\log_{10} E_1 = \frac{A}{T_A} + B \tag{9}$$

where

T_A = absolute temperature (degrees R = degrees F + 460),
E_1 = average modulus of elasticity of asphaltic concrete at T_A, and
A, B = constants,

for two different temperatures determined the values A and B. Extrapolated values for E_1 at 30 F, 40 F, 100 F, 120 F, and 140 F were then calculated. Figure 9 shows that the resulting modulus of elasticity of the asphaltic concrete pavement has a curvilinear relationship with temperature. Note that the shape of the curve is very similar to the adjustment factor curve shown in Figure 7. The shape of the temperature-modulus curve derived by elastic theory clearly substantiates the adjustment factor curve derived by statistical procedures. A correlation graph is shown in Figure 10. It is seen that the adjustment factor and modulus of elasticity are related at any stated temperature by the equation given in Figure 10.

Comparison of Derived Temperature Distributions and Adjustment Factors With Data From Other Test Roads

Data are being gathered by the Asphalt Institute (7) from a test site at San Diego, California. The flexible pavement at this test site contains thermocouples embedded in

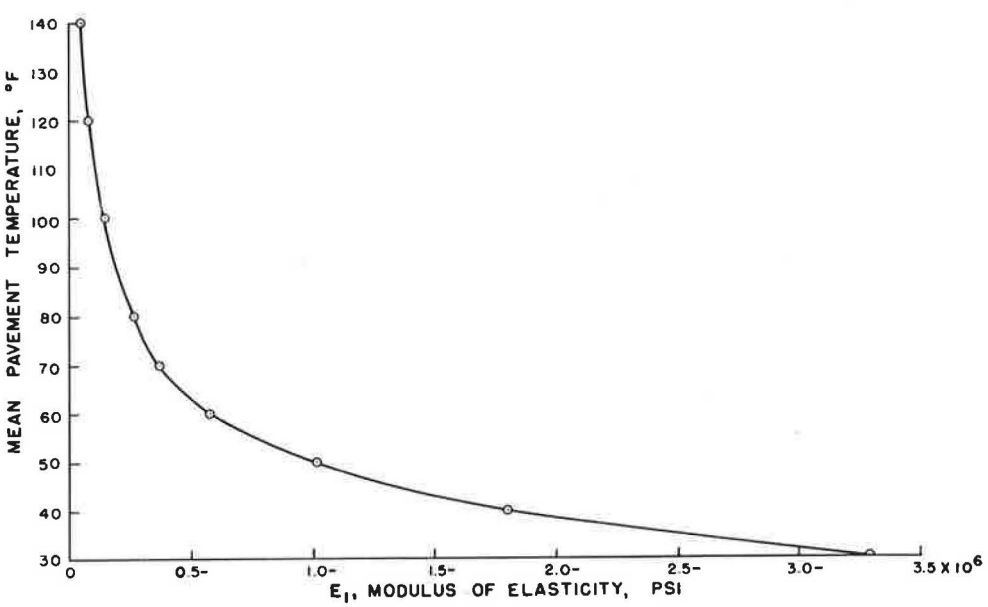

Figure 9. Mean pavement temperature vs modulus of elasticity for asphaltic concrete pavement.

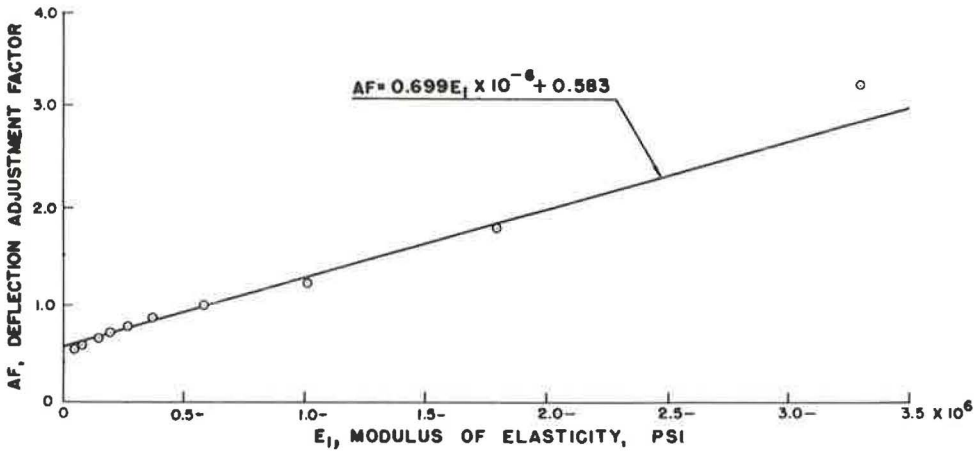

Figure 10. Correlation between deflection adjustment factor and modulus of elasticity for an asphaltic concrete pavement.

the pavement, and temperatures are being recorded. Two days of temperature distributions, October 6, 1966, and February 17, 1967, together with their respective 5 days of high and low air temperatures have been received from the Asphalt Institute and checked by the temperature prediction procedure described in this report. The predicted temperatures varied generally within ±6 F from the observed temperatures at the various levels. The Asphalt Institute also furnished temperature distribution data for the Colorado test pavement reported by Kingham and Reseigh (4). Table 2 contains the summary of the analyses for both California and Colorado data, each compared to the temperatures predicted by the method reported herein and developed from the College Park data. A few temperatures fell outside two standard errors of estimate; however, most of the data are well within these tolerances.

TABLE 2

COMPARISON OF MEASURED PAVEMENT TEMPERATURES AT SAN DIEGO AND COLORADO TEST SITES WITH ESTIMATION OF TEMPERATURES BY METHOD BASED ON COLLEGE PARK DATA

Location	Depth (in.)	Number of Observations	Average Difference Between Observed and Estimated Temperatures (F)	Standard Deviation (F)
Colorado	2.00	59	-2.68	5.03
	4.60	4	-4.75	6.61
	5.50	5	-1.40	3.55
	5.75	25	+1.72	5.51
	6.00	25	+1.96	5.94
	7.50	4	-0.25	3.71
	9.00	5	+1.60	4.24
	10.50	50	+2.82	7.09
San Diego	3.00	2	0.00	0.00
	3.10	2	-2.00	1.41
	3.40	2	-6.00	6.00
	3.50	11	-3.50	4.69
	6.50	2	-2.50	2.55
	9.40	11	+0.09	2.50
	9.50	2	-2.50	2.55
	10.80	2	-2.50	2.55
	11.50	2	-3.50	3.54

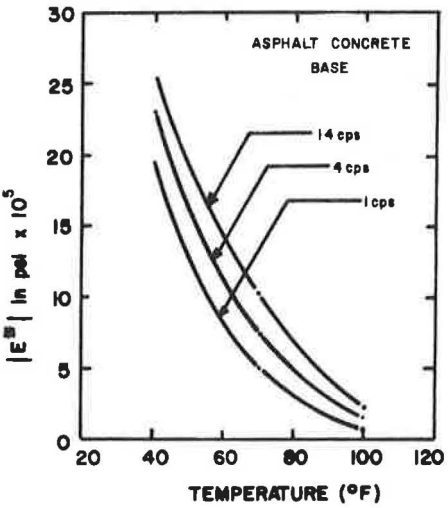

Figure 11. Relationship Between |E*| and temperature for various loading frequencies (8, p. 933).

An interesting comparison between modulus of elasticity of asphaltic concrete, E_1, derived from the AASHO data (Fig. 9) and laboratory measurements of the complex modulus, |E*|, is also provided by Kallas and Riley's tests (8) on asphaltic concretes used on the Colorado test pavement (4). In Figure 11 (from 8, Fig. 3b), showing |E*| plotted against temperature, |E*| was determined by sinusoidal tension and compression loading. The most favorable agreement is with respect to the 1-cps loading frequency. The similarity between this curve and the curve in Figure 7 seems extraordinary.

SUMMARY AND RECOMMENDATIONS

A practical and reasonably accurate method of estimating the temperature distributions within flexible pavements has been developed. This method can be used to analyze deflection data at any time if the hour of the day and the surface temperature are included in the recorded data.

The relationship between mean pavement temperature and deflection allows any deflection test value to be adjusted to a reference temperature if the mean temperature of the pavement at the time of testing is known or is estimated by the method outlined herein.

Further study is needed to test the assumption that the average air-temperature history allows this system of estimating pavement temperature distributions to be used in other areas of the world. Additional data are needed to determine whether the average air-temperature history adequately takes into account the effects of latitude and altitude on pavement temperatures.

Theoretical analysis of the AASHO Road Test pavement deflection data by the two-layered elastic theory shows a curvilinear relationship between modulus of elasticity of asphaltic concrete and temperature. The magnitude of the moduli are such that a straight-line relationship exists between moduli and the multiplicative, temperature-deflection adjustment factors.

ACKNOWLEDGMENTS

This report has been prepared as a part of Research Study KYHPR 64-20, "Flexible Pavement Study Using Viscoelastic Principles," sponsored cooperatively by the Kentucky Department of Highways and the U.S. Department of Transportation, Federal Highway Administration, Bureau of Public Roads. The opinions, findings, and conclusions in this report are not necessarily those of the Bureau of Public Roads.

REFERENCES

1. Southgate, H. F. An Evaluation of Temperature Distribution Within Asphalt Pavements and Its Relationship to Pavement Deflection. MSCE thesis, Univ. of Kentucky, 1968.
2. The AASHO Road Test: Report 5—Pavement Research. HRB Spec. Rept. 61E, pp. 86-111, 1962.
3. Kallas, B. F. Asphalt Pavement Temperatures. Highway Research Record 150, pp. 1-11, 1966.
4. Kingham, R. I., and Reseigh, T. C. A Field Experiment of Asphalt-Treated Bases in Colorado. Proc. Second Internat. Conf. on Structural Design of Asphalt Pavements, Univ. of Michigan, pp. 909-930, 1967.

5. Sebastyan, G. Y. The Effect of Temperature on Deflection and Rebound of Flexible Pavements Subjected to the Standard CGRA Benkelman Beam Tests. Proc. 42nd Convention, Canadian Good Roads Association, pp. 143-161, 1961.
6. Burmister, D. The Theory of Stresses and Displacements in Layered Systems and Applications to the Design of Airport Runways. HRB Proc., Vol. 23, pp. 126-148, 1943.
7. Laboratory Activity Report No. 67-2. The Asphalt Institute, Aug. 1967.
8. Kallas, B. F., and Riley, J. C. Mechanical Properties of Asphalt Pavement Materials. Second Internat. Conf. on the Structural Design of Asphalt Pavements, Univ. of Michigan, pp. 931-952, 1967.

Discussion

N. K. VASWANI, Virginia Highway Research Council—The authors are to be complimented on their attempt to account for the effect of temperature on pavement deflection. Clarification of two points may prove to be helpful.

Some of the most important data that led to the authors' conclusions are an analysis of the AASHO data given in Figures 89a, 89b, and 89c and Figure 90a of the AASHO Road Test Report 5. The authors do not seem to have taken the actual data points, but instead the generalized curve for which the correlation and standard deviation values are not known.

In Figure 6 of the paper, seven curves are shown, each based on the AASHO data mentioned. The degree of correlation (or amount of error) existing between the data obtained from the AASHO curves and the curves given in Figure 6 is also not known.

Figure 7 is the average of the seven curves in Figure 6. In Figure 6, the further the distance from the base point (i.e., 60 F of deflection adjustment factor = 1.0), the greater the error in averaging. It is therefore believed that, although this investigation shows the trend, the percentage error is unknown.

The AASHO Road Test and any number of field and laboratory investigations have shown that the pavement strength is the sum of the strengths of each layer, and that this strength can be generalized as

$$\text{deflection, y, is a function of } (E_1h_1 + E_2h_2 + \ldots)$$

where E_1 and E_2 are the strength coefficients of the materials in each layer of the pavement with thickness h_1 and h_2 respectively. According to the authors, the modulus of asphaltic concrete, E_1, is a function of the temperature. Thus it follows that, according to the above equation, the change in temperature resulting in the change in the value of E_1 should be an additive quantity for correlating with y, the deflection, as indicated by Kingham and Reseigh (4), rather than a quantity to multiply by $(E_1h_1 + E_2h_2 + \ldots)$, which in effect would change the contributing strength of other layers too. The reason that the authors used the multiplying quantity in their analysis may be the result of the adoption of Burmister's elastic theory.

R. IAN KINGHAM, The Asphalt Institute—Southgate and Deen are to be commended for reducing the enormous bulk of temperature data obtained by Kallas on thick asphalt pavements to a mathematical form that can be used to predict pavement temperatures at any depth in an asphalt pavement layer. With such predictions, a mean pavement temperature can be determined for use in correcting Benkelman beam deflections to a 60 F standard temperature. This discussion is limited to the derivation of the adjustment

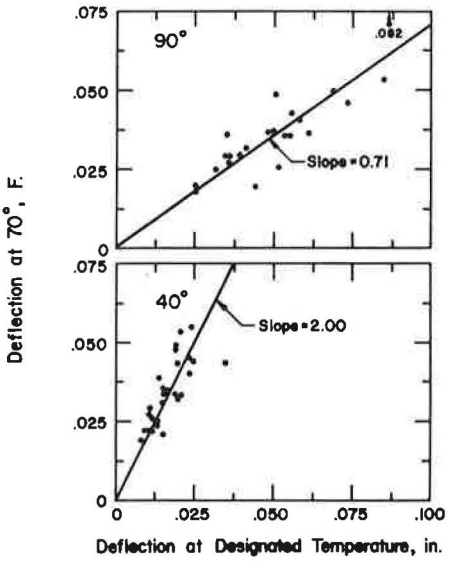

Figure 12. Colorado deflection-temperature data.

factors that the authors suggest can be used to correct beam deflections for temperature.

To derive adjustment factors for correcting beam deflections to 60 F, the authors were limited to data published from the AASHO Road Test. They assumed that the mean pavement temperature for the AASHO data was the average of the top, middle, and bottom of the pavements being tested. It is believed that the top, middle, and bottom temperatures of an asphalt concrete layer 4-in. thick were used. For this reason, temperatures reported for thicker asphalt layers may have been subject to bias.

This would explain in part why the effect of temperature on deflection seemed to decrease at higher temperature ranges. This trend influenced the authors' choice of a mathematical model to fit the data. In order to compute deflection adjustment factors for temperatures other than those measured at the AASHO Road Test, extrapolations from 90 to 140 F had to be made using the mathematical model, and thus the correction factors were highly dependent on the choice of mathematical model. Another limitation of the adjustment factors was the reference temperature of 60 F. It is believed that 70 F would have been a better choice because it represents more nearly the median for the temperatures normally experienced in deflection testing throughout the United States and Canada.

For several years this discussant has been concerned with developing technology for correcting Benkelman beam deflections to a standard temperature (10). Such corrections are very important when deflections are used to determine asphalt concrete overlay thicknesses (11). Data from two full-scale experimental base projects, which were in Colorado (4) and San Diego County, California (12), were collected to explore this problem. These data, plus some published by the Canadian Good Roads Association (5, 13) and the Road Research Laboratory (14), shed further light on the relationship between mean pavement temperature and the Benkelman beam deflection measurement.

All the data considered were obtained by measuring deflections at a point while pavement temperatures varied throughout the course of a day. Deflections plotted against the mean asphalt layer temperature showed a linear relationship for the temperature ranges that can be expected over a 24-hour period. This finding for full-depth asphalt pavements from the Colorado Experimental Base Project has been reported previously by this discussant (10). Also, more nearly linear relationships were found for the AASHO Road Test data when mean temperatures were determined without the known bias. A theoretical analysis also suggested that the relationship is approximately linear for a 30 to 40 F temperature span. For temperatures ranging from 30 to 140 F, however, the trend was curvilinear with greater temperature influence at higher temperatures.

As a result of the field measurements and theoretical studies, this discussant selected a linear mathematical model to fit measurement data for each pavement point. The resulting equations were used to compute deflections for certain designated temperatures. Extrapolations greater than 10 F were avoided. Deflections at these selected temperatures were then plotted against the 70 F deflection as shown in Figure 12. The excellence of fit of the data to a straight line through the origin shows that a multiplying factor, of the type proposed by Southgate and Deen, is a good method of adjusting beam deflections. The slope of the linear fit through the origin is, of course, the adjustment or multiplying factor for the temperature in question.

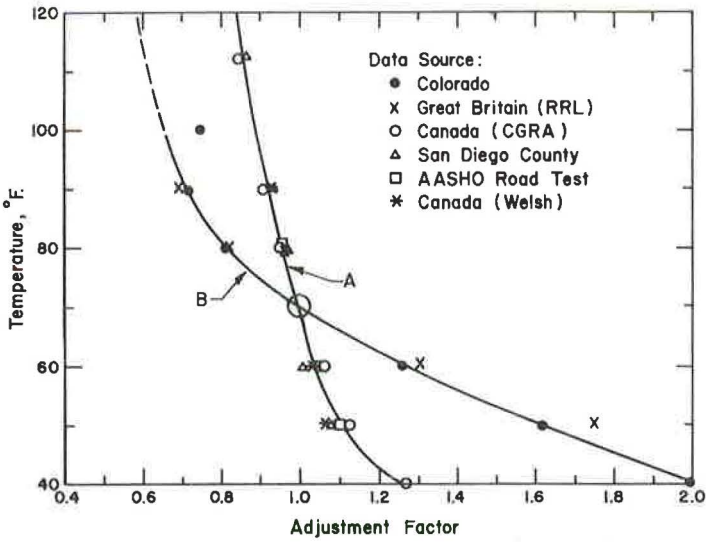

Figure 13. Derivation of adjustment factor curves.

Plots similar to Figure 12 were made for data from each source. The resulting slopes were plotted against their respective temperatures. These results are shown in Figure 13. Two relationships are evident. The Curve A included data primarily from granular base pavements and represents strong support to the thin asphalt layer (less than 4 in.). Curve B represents test data from thick asphalt pavements (4 in. or more) laid directly on weak subgrades.

Figure 13 provides two adjustment factor curves for use in correcting beam deflections to a standard temperature of 70 F. The choice of curves involves some judgment. Considering the data sources for each curve, it is recommended that Curve A, the curve representing the smaller correction factors, be used in the majority of instances. The second curve, Curve B, providing large correction factors, represents an extreme situation where the asphalt layer is thick and weakly supported.

References

9. Benkelman, A. C., Kingham, R. I., and Fang, H. Y. Special Deflection Studies on Flexible Pavement. HRB Spec. Rept. 73, pp. 102-125, 1962.
10. Kingham, R. I. A New Temperature Correction Procedure for Benkelman Beam Rebound Deflections. Asphalt Institute Research Report 69-1, 1969.
11. Asphalt Overlays and Pavement Rehabilitation. The Asphalt Institute, Manual Series No. 17, 1969.
12. Kingham, R. I. Full-Scale Experimental Base Construction in San Diego County. ASCE National Meeting on Transportation Engineering, San Diego, 1968.
13. Welch, D. A. Use of the Benkelman Beam in Municipal Street Design, Maintenance and Construction. Proc. 42nd Convention, Canadian Good Roads Association, 1961.
14. Road Research, 1965-1966. Report of the Director of Road Research. Road Research Laboratory, Ministry of Transport, United Kingdom, 1967.

H. F. SOUTHGATE and R. C. DEEN, Closure—The authors appreciate the interest shown in the paper by Vaswani and Kingham. The comments made by Vaswani are well taken and offer the opportunity to reemphasize points mentioned in the paper.

Because the study reported in the paper was of a feasibility and pilot nature, and because of certain pressing needs to analyze field deflection measurements, the actual data points represented by the curves in Figures 89a, 89b, and 89c and Figure 90a of the AASHO Road Test—Report 5 were not used. Instead, the generalized curves were analyzed and therefore the correlations and deviations are not known. The authors indicated that a more precise analysis might be made in the future by considering the actual data points instead of the generalized curves.

The authors did assume that the definition for surfacing temperature given on page 104 of Report 5 on the AASHO Road Test was correct. Because the term "surfacing temperature" was not redefined for Figures 89 and 90 of the report, it must be assumed that the surfacing temperature was the average of the top, middle, and bottom temperatures of the actual layer thickness rather than of a 4-in. layer.

By definition, the adjustment factor at 60 F was taken to be one and is so indicated in Figures 6 and 7. This does not necessarily suggest that the error in estimating the deflection adjustment factor is less at this temperature than at other temperatures. Much of the scatter indicated by the various curves in Figure 6 may be, in part, due to the averaging effect of the AASHO curves over pavements of various structural thicknesses and components. Selection of the reference temperature seems to be somewhat arbitrary and analyses of deflection measurements should not be altered by use of adjustment factor curves based on different reference temperatures. Figure 7 can be easily adjusted to any other temperature that one desires to use as a reference or base.

It is interesting to note that the adjustment factor curve shown in Figure 7 of the paper falls between Kingham's Curves A and B (Fig. 13), which may be considered extreme cases of pavement construction. Because the adjustment factor curve in the paper was based on Figures 89 and 90 of the AASHO Road Test report, and therefore included averaging effects, it is not surprising that the curve of Figure 7 falls between Curves A and B of Kingham's discussion.

Further analysis of field deflection measurements since the paper was submitted have been made using the deflection adjustment factor curve given in Figure 7 of the paper. Amazingly good agreement has been found between the deflections as adjusted for temperature and the theoretical deflections computed by an n-layered computer program for the analysis of elastic-layered pavement systems. This comparison increased the authors' confidence in the adjustment factor curve and, more importantly, in the shape of the temperature adjustment factor curve.

To repeat what was indicated by the authors in the paper and by Vaswani in his discussion, further analysis of the AASHO Road Test data is needed to determine the actual magnitude of the adjustment factors and to develop the proper and precise relationship between temperature and adjustment factor with respect to the structural makeup of the pavement system. Until this more detailed analysis of actual field data points can be made, it is felt that the adjustment factor curve in Figure 7 provides an adequate first approximation of the temperature effects on pavement deflections.

Detecting Seasonal Changes in Load-Carrying Capabilities of Flexible Pavements

WILLIAM M. MOORE, FRANK H. SCRIVNER, RUDELL POEHL, and
M. B. PHILLIPS, Texas Transportation Institute, Texas A&M University

ABRIDGMENT

•THE MAIN EFFORT of this research was directed toward finding an instrument capable of measuring—with speed, accuracy, and economy—seasonal changes in the strength of flexible pavements and showing how it could be used in a program to protect pavements from overloading during critical periods. The instrument selected was the Dynaflect, a trailer-mounted device that loads the pavement dynamically and indicates the corresponding deflection at several points on the surface. Operated by one man and towed by a passenger car, the Dynaflect appears to meet the requirements for the job. Tests were made with the Dynaflect on pavements at locations ranging from Springfield, Ill., northward to Duluth, Minn. The tests revealed that the annual strength history of pavements in northern climates is divisible into four distinct periods: (a) a period of deep frost and high strength, (b) a period of rapid strength loss, (c) a period of rapid strength recovery, and (d) a period of slow strength recovery. The second and third periods together constitute the critical period for flexible pavements.

A series of correlation studies indicated that Dynaflect measurements could be used with reasonable accuracy to predict the results of plate bearing tests and Benkelman beam deflection tests as well as the curvature of the pavement in the vicinity of a heavy wheel load. Thus, the Dynaflect apparently could be substituted for other instruments being used to detect seasonal changes in strength. In addition, the Dynaflect, although not the most economical to operate, proved to be more sensitive than the other instruments to changes in strength. The research resulted in suggested warrants for deciding when, where, and how long to impose reduced load limits, and what those load limits should be. It appears that if these warrants were used to control the placement and removal of load restrictions, some reduction in the duration of the restricted period might result.

Paper sponsored by Committee on Flexible Pavement Design and presented at the 48th Annual Meeting.

Equivalent Axle Loads for Pavement Design

JOHN A. DEACON, Assistant Professor of Civil Engineering, University of Kentucky;
and
ROBERT C. DEEN, Assistant Director of Research, Kentucky Department of Highways

One significant means for evaluating the relative destructive effects of repetitive vehicular loading on highway pavements is the equivalent axle load concept. To apply this concept to design situations, proper methods must be available for making valid predictions of equivalent axle loads for design that are based on data gleaned from traffic volume counts, vehicle classification studies, and loadometer surveys. This paper reports on the development and testing of such a predictive method for rural highways in Kentucky. The problem was treated as three separate but interrelated parts: (a) development of a proper methodology and identification of pertinent traffic parameters, (b) identification of relevant local conditions that serve as indicators of the composition and weights of the traffic stream, and (c) development of significant relationships between the traffic parameters and the local conditions. Percentages of the various vehicle types and the average equivalent axle loads per vehicle were selected as the most significant traffic parameters. These were empirically related by multiple regression and other techniques to the set of local conditions, which included road type, direction, availability and quality of alternate routes, type of service provided, traffic volume, maximum allowable gross weight, geographical area, and season. The resultant methodology was judged to be sufficiently accurate, simple, reasonable, and usable to satisfy the problem requirements. It is recommended for use, however, only when valid, long-term vehicle classification and weight data are unavailable for the route under investigation.

•PROPER structural design of highway pavements requires an evaluation of the destructive effects of the anticipated vehicular loading. The concept of load equivalency provides a means for expressing these destructive effects in terms of a single measure, the equivalent axle load (EAL). The design EAL's represent the equivalent number of applications of a standard or base axle load anticipated during the design life.

Kentucky has been estimating design EAL's since adopting the load equivalency concept in the mid-1940's (1). Average estimates obtained at several locations have been found to agree remarkably well with the actual average EAL's that were accumulated. However, when EAL estimates at specific locations were compared with actual accumulations, an unacceptably large variation was often found, illustrating the need for a more careful determination of the effects of local conditions on significant traffic parameters.

The objectives of this study are (a) to establish a methodology for obtaining accurate estimates of design EAL's, (b) to identify those characteristics of a particular route or

Paper sponsored by Committee on Theory of Pavement Design and presented at the 48th Annual Meeting.

locale that affect the composition and weight of traffic, and (c) to provide a means for relating significant traffic parameters to the local conditions. The study is limited to analyses of data obtained in predominantly rural areas and assumes that accurate estimates of average daily traffic (ADT) are available.

CURRENT METHODS FOR PREDICTING DESIGN EAL'S

The procedure used in Kentucky for estimating design EAL's is based on analyses of four traffic parameters: ADT, average percent trucks, average number of axles per truck, and average load distribution of truck axles (composite axle-load distribution) (2). Initial estimates of these parameters are based on data from traffic volume counts, vehicle classification counts, and weight studies at loadometer stations. A series of additive and multiplicative adjustments are applied to convert these initial estimates to averages for the design period (3). Proper manipulation of these averages yields predictions of the number of applications of truck axle loads that fall within designated axle load intervals. Application of load equivalency factors and subsequent summation produce the design estimate.

The prime deficiency in this technique is the manner of relating initial estimates of the four parameters to local conditions. This is currently accomplished through the judgment of the designer, who normally considers one of the following as the basis for the estimates: (a) data from a nearby loadometer station, (b) data from a loadometer station having similar characteristics, or (c) statewide averages for all loadometer stations in the designated traffic-volume group. This method has been relatively unsuccessful in the past. It ignores a wealth of available classification data, and it affords no basis for predictions if unusual or changing traffic conditions are anticipated.

In California, the composition of the traffic stream (percentages of the various vehicle types) is estimated separately from the axle load distributions (4, 5). This is advantageous because much more data are commonly available for composition (classification counts) than for weights (loadometer surveys). Furthermore, the computations are simplified by expressing the axle load distributions in terms of unit EAL's, defined as the average EAL's per vehicle. Local conditions enter the analysis primarily in the estimation of vehicle-type percentages based on classification counts at similar locations. Some consistency is assumed in the average unit EAL's among the many types of highways within the state, although modifications can be made at the discretion of the designer.

Two investigations conducted in Texas shed additional light on both methodology and the effects of local conditions. The first of these (6) was concerned primarily with methodology. Pertinent parameters of the traffic stream include ADT, percentage of trucks, number of single and tandem axles per 100 vehicles, and composite axle load distributions for both single and tandem axles. Estimates of the percentage of trucks are based on an analysis of historical data that relates percentage of trucks to ADT. The number of both single and tandem axles per 100 vehicles is obtained from a cross-classification tabulation based on volume group, percentage of trucks, and highway classification. Finally, the composite axle load distributions are related to percentage of trucks on the basis of historical data. The local conditions that enter the analysis are traffic volume and highway classification.

The second investigation (7) employed a slightly different methodology but focused attention on estimation of axle load distributions at one location on the basis of measurements at other locations. It was concluded that design axle load distributions should be obtained from measurements at a nearby loadometer station if such measurements are available and if design and traffic conditions are nearly identical. If not, the statewide average distributions should be used, except for highways approaching Interstate design standards.

Recently, Ulbricht (8) reported a method for estimating design EAL's based on two parameters of the traffic stream: ADT and an equivalency coefficient. The equivalency coefficient is the average EAL per vehicle and reflects the proportions and weights of all vehicle types in the traffic stream. To estimate design EAL's, it is recommended that vehicle weight and classification data be used directly. Only if such data are unavailable should an estimate be made by taking the combined product of average ADT,

the equivalency coefficient, the number of years, and 365. Local conditions are considered through a relationship between the equivalency coefficient and a three-celled classification of highway type by truck usage.

This brief review indicates that there has been very little in-depth study of the effects of local conditions on the pertinent traffic parameters and that there has been little agreement on the proper traffic parameters and methodology to accomplish the desired objectives.

PROPOSED PROCEDURES

Review of the Kentucky procedure suggested that deficiencies existed not only in the method for relating the traffic parameters to local conditions but also in the method for specifying the relevant traffic parameters. Search for a more acceptable procedure led to the adoption of an empirical approach that relied on correlations of significant traffic parameters with local conditions of potential importance.

Parameters and Methodology

Because it was desirable to maximize use of all available data, two types of parameters were considered, one dependent on vehicle classification counts and the other dependent on loadometer surveys. Percentages of the various vehicle types were chosen as parameters to represent the classification data. These seemed to offer significant advantages over the percentage of trucks and the number of axles per truck because they allowed consideration of vehicle types such as buses that heretofore had been excluded, they maximized the amount of information available for other than pavement-design purposes, they lent more insight into the basic characteristics of the traffic stream, and they were thought to be more sensitive to changing local conditions. The vehicle types selected for investigation included cars; buses; single-unit, two-axle, four-tired (SU-2A-4T) trucks; single-unit, two-axle, six-tired (SU-2A-6T) trucks; single-unit, three-axle (SU-3A) trucks; combination, three-axle (C-3A) trucks; combination, four-axle (C-4A) trucks; and combination, five-axle (C-5A) trucks. These represented all major vehicle types for which data had been accumulated in Kentucky during the 17-year study period of 1950-1966.

The parameters selected to represent the vehicle weight data were the unit EAL's or the average EAL's per vehicle. This selection was based primarily on the criterion of simplicity, since alternate parameters such as axle load distributions are much more difficult to treat statistically and handle computationally. Unfortunately, some information is lost by collapsing the axle load distributions into a single measure, and some flexibility is sacrificed by the necessity to preselect the set of equivalency factors.

These traffic parameters and the ADT were used to compute the design EAL's as follows:

$$\text{Design EAL's} = 365(N)(ADT_{eff}) \sum_i (P_i)(UEAL_i)$$

where

N = design period in years,
ADT_{eff} = average or effective ADT during the design period,
P_i = predicted fraction of the total traffic stream made up of vehicle type i, and
$UEAL_i$ = corresponding average unit EAL's.

If desired, this equation can be appropriately modified to consider directional and lane distributions.

Local Conditions

Once the proposed methodology was established and the traffic parameters of interest identified, it was then necessary to identify those local conditions thought to be significantly related to the composition of the traffic stream and the weights of the vehicles included in it. These local conditions were to serve as the basic independent variables from which estimates of the dependent variables could be made.

TABLE 1

IDENTIFICATION OF LOCAL CONDITIONS

Local Condition	Code	Description
Road Type	1	Interstate-numbered
	2	US-numbered
	3	KY-numbered
	4	Other
Direction	1	North-south
	2	East-west
Alternate route	1	Alternate route is inferior
	2	No alternate or alternate of same quality
	3	Alternate route is superior
Service provided	1	Primary service to major recreation
	2	Significant service to major recreation
	3	Some service to recreation
	4	Ordinary
	5	Some service to mining
	6	Significant service to major mining
	7	Primary service to major mining
	8	Some service to industry
	9	Primary service to industry
Volume (ADT)	1	0- 499
	2	500- 999
	3	1,000-1,999
	4	2,000-2,999
	5	3,000-3,999
	6	4,000-5,999
	7	6,000-7,999
	8	8,000- 9,999
	9	10,000-13,999
	10	14,000-or more
Maximum allowable gross weight	1	30,000
	2	42,000
	3	59,640
	4	73,280
Geographical area	1	Western Kentucky
	2	South Central Kentucky
	3	North Central Kentucky
	4	Eastern Kentucky
Year	1	1950-1951
	2	1952-1953
	3	1954-1955
	4	1956-1957
	5	1958-1959
	6	1960-1961
	7	1962-1963
	8	1964-1965
	9	1966
Season	1	Winter (Jan.-Mar.)
	2.	Spring (Apr.-June)
	3	Summer (July-Sept.)
	4	Fall (Oct.-Dec.)

Several general guidelines were available to aid this selection. Any apparently relevant local condition had to be amenable to analysis for purposes of making forecasts and analyzing historical data. Some rationale had to be formulated to tentatively substantiate the relationships between the traffic parameters and the local conditions. Finally, it was desirable to exclude from the set of local conditions any predictive characteristics of the traffic stream except ADT. Extensive review of available data in light of these guidelines led to establishment of the set of local conditions identified in Table 1.

The road-type category was established to provide an indication of the percentage of through trucks in the traffic stream. Categorization by route number simplified the process of analysis. The direction category reflects a geographical situation in which the bulk of Interstate truck traffic in Kentucky travels primarily on north-south routes. Accordingly, a two-celled classification was used to represent direction, the importance of which was thought to diminish as the local-service use of the route increased. The significance of the availability and quality of alternate routes became apparent when traffic parameters on certain routes were studied during time periods in which alternate routes having superior geometric design features were opened to traffic.

A large number of routes in Kentucky provide access to areas in which rather unusual types of traffic are generated. Most notable are those coal mining areas in which most of the coal is carried over some segment of the highway system. To make possible proper estimates of EAL's in these areas, the service-provided category was established. Traffic volume has long been associated with other significant parameters of the traffic stream and, because it must be independently projected, was included in the set of local conditions. Equally as significant is the legal maximum allowable gross weight. Kentucky had four different maximum gross weights during the study period, and increases in this legal limit have invariably led to an increase in the percentages of the large combination vehicles. So significant is the effect that much of the variability in the traffic parameters, which in the past has been attributed to the time factor, is in reality a reflection of changing legal weight limitations.

Traffic characteristics, particularly for primarily local-service routes, were felt to reflect in part the social and economic characteristics of the residents in an area. Consideration of this factor in the analysis was ensured by dividing the state into four major geo-

graphical areas, each of which is relatively homogeneous with respect to socioeconomic environment. The year has been considered in past procedures as a major independent variable and was retained in this analysis primarily for this reason. Season is known to have a significant effect on the composition of the traffic stream (for example, the percentage of trucks) and was to be included in the set of local conditions to provide correlations with historical data.

CORRELATION OF TRAFFIC PARAMETERS WITH LOCAL CONDITIONS

These nine local conditions served as the independent variables with which the traffic parameters were correlated. Extensive analysis verified the significance of these local conditions, although the relative importance of each varied according to the particular parameter under evaluation. Criteria for assessing the suitability of various meaningful relationships included accuracy, simplicity, reasonableness, and predictability. In addition, the relationships had to be amenable to predicting traffic parameters for combinations of local conditions for which little or no data had been obtained in the past.

Data Sources

Vehicle weight data were available from the operation of loadometer stations throughout the state. Two types of loadometer surveys included routine coverage at the permanent loadometer stations and two special weight surveys. Approximately 10 permanent loadometer stations have been operated each year since 1942 (3). These provided the bulk of weight data for the high-volume and important routes. The two special weight surveys were conducted during the spring and summer months of 1957 and 1964. These provided much of the weight data for low-volume facilities. During the study period, approximately 69,000 vehicles were weighed at 51 different rural locations.

Vehicle classification data were available from the loadometer surveys, from automatic traffic-recording stations, from special classification surveys, and from origin-and-destination studies. A total of 1,871 counts were taken at 730 different rural locations, and approximately 6,100,000 vehicles were counted.

Methods

The dependent variables in the analysis (vehicle-type percentages and unit EAL's) were treated as continuous variables. The independent variables (the local conditions) were treated as classification sets. Because of this method for data representation and because of the plausibility of strong interactions among many of the local conditions, a combinatorial analysis or cross-classification tabulation was thought to be relevant to the problem. With this method the available data are grouped into categories representing each feasible combination of the independent variables, and the averages of the dependent variables within each combination serve as the best estimates of future traffic characteristics. Because the number of possible combinations of the local conditions was excessive, however, the combinatorial analysis was judged to be unsuitable.

The most convenient method for estimating the traffic parameters is to compute statewide gross means without regard to local conditions. However, because the effects of local conditions can be considered only by modifying the gross means based on intuition and judgment, this approach was likewise judged to be inappropriate.

The first method seriously considered was an evaluation of the effects of the local conditions through a series of correction or adjustment factors applied to the gross means. There is one correction factor for each local condition, and its value is determined by the local-condition code. To apply this procedure, the gross means are first computed. The average residuals between the actual parameter values and the gross means are then computed for each value of one preselected local condition. The process is repeated for the second and all subsequent local conditions by computing average residuals between observed values and those predicted for previously analyzed local conditions. The entire process is iterated to eliminate possible effects of the chosen sequence of local conditions.

TABLE 2

SUMMARY DESCRIPTION OF METHODS FOR CORRELATING TRAFFIC PARAMETERS WITH LOCAL CONDITIONS

Description	Nomenclature
Combinatorial means, full interaction	None
Gross means, no consideration of local conditions	None
Correction factor based on gross means, no interaction, iterative	FACT1
Correction factor based on classified means, limited interaction, iterative	FACT2
Multiple regression, averages, no interaction	MULTRA
Multiple regression, dummy variables, no interaction	MULTRD

Interactions among a limited number of local conditions can be considered by a slight modification of this procedure. Classified means computed for various combinations of the interacting local conditions are substituted for the gross means and the process continued as enumerated above.

Of somewhat more appeal than the intuitive correction-factor techniques are multiple regression techniques, which are supported by sound mathematical and statistical theory. The first multiple regression technique is basically one of obtaining weighted averages. Thus average estimates of each parameter are obtained for each different local condition. Multiple regression techniques are used to assign weights to each local condition for the purpose of obtaining weighted averages for final predictions.

The second multiple regression technique makes use of dummy variables and is designed specifically for independent variables which are treated as classification sets (9). The number of dummy variables, which assume values of either zero or one, required to represent each local condition is the number of classification sets for that condition less one. Thus, 40 dummy variables are required to represent the nine local conditions of Table 1. Theoretically, the procedures can be generalized to include interactions among two or more of the local conditions by redefining the dummy variables so that each variable corresponds to one combination of the interacting local conditions. Practically, this greatly increases the number of dummy variables and was not attempted because computer program limitations restricted the number of dummy variables to 50 (10).

The foregoing methods for correlating the traffic parameters with local conditions are summarized in Table 2. For all practical purposes, FACT1, MULTRA, and MULTRD were found to yield results of comparable accuracy. MULTRD offers certain advantages of simplicity, however, and a more appealing basis for development. Where a limited number of interactions are important, FACT2 was adjudged to be the most feasible approach.

Vehicle-Type Percentages

Extensive analyses showed that FACT2 is the superior technique for relating the vehicle-type percentages to the local conditions. Multiplicative correction factors were chosen because their use precludes estimation of negative percentages. The number of possible combinations of the various local conditions and the number of available data sets were the bases for limiting the interacting local conditions to three. Eight of the most promising combinations of three local conditions were selected intuitively and analyzed jointly on the basis of relative accuracy and predictability. As a result of this analysis, road type, maximum allowable gross weight, and traffic volume were judged to exhibit the most significant interactions among those investigated.

Problems were soon apparent in treatment of the year variable. Prior work indicated that no trend relationship existed between additive correction factors for C-4A truck predictions and year. The same disturbing tendencies were observed for other vehicle types and for multiplicative correction factors as well. Accordingly, year was excluded from the set of local conditions with an average reduction in accuracy as measured by the correlation coefficient of about 5 percent.

The criterion of reasonableness dictates that the sum of the predicted percentages must equal 100 percent. Because the percentage of each vehicle type is predicted independently, the initial estimates will rarely total 100 percent. A simple adjustment procedure, whereby each initial estimate is multiplied by 100 and divided by the sum of the initial predictions, was adopted.

TABLE 3

ACCURACY OF VEHICLE-TYPE PERCENTAGE ESTIMATES

Vehicle Type	Mean Percent	Standard Deviation	Standard Error		Correlation Coefficient	
			Uncorrected	Corrected[a]	Uncorrected	Corrected[a]
Cars	71.67	7.13	5.71	5.65	0.60	0.61
Buses	0.86	0.62	0.48	0.48	0.62	0.62
SU-2A-4T	9.09	3.87	2.62	2.57	0.74	0.75
SU-2A-6T	8.51	3.90	3.23	3.23	0.56	0.56
SU-3A	1.00	2.38	2.13	2.12	0.45	0.45
C-3A	3.94	4.15	2.69	2.68	0.76	0.76
C-4A	4.10	4.37	2.68	2.68	0.79	0.79
C-5A	0.82	2.16	1.56	1.54	0.69	0.70

[a]Estimates of vehicle-type percentages were corrected to a total of 100 percent.

The procedures described were used to estimate vehicle-type percentages for comparison with actual percentages obtained from past vehicle classification counts. The results of this accuracy comparison are summarized in Table 3. Despite the relative inaccuracy of the technique, it was found superior to others investigated on the basis of the criteria of accuracy, simplicity, reasonableness, and predictability.

Unit EAL's

One of the major disadvantages of the unit-EAL parameter is that the load equivalency factors must be preselected. This shortcoming was partially alleviated by considering three types of unit EAL's—Kentucky, AASHO, and modified AASHO. The modified AASHO EAL's were computed using only AASHO load equivalency factors for single axles.

Because of the limited amount of vehicle weight data, consideration of interactions among even a limited number of local conditions was felt to be unwarranted. In spite of this, preliminary analyses indicated that an approach such as gross means would be inappropriate because the local conditions did measurably affect the average unit EAL's. Consideration was limited to multiple regression techniques because the residual techniques offered no known additional advantages.

The method finally selected for relating unit EAL's with local conditions made use of additive factors derived using multiple regression with dummy variables. Three of the

TABLE 4

ACCURACY OF UNIT EAL ESTIMATES[a]

Vehicle Type	EAL Type	Mean Unit EAL	Standard Deviation	Standard Error		Correlation Coefficient		Number of Vehicles Weighed
				Uncorrected	Corrected[b]	Uncorrected	Corrected[b]	
SU-2A-4T	KY	0.0415	0.644	0.632	0.630	0.19	0.21	12,389
	AASHO	0.0061	0.030	0.030	0.030	0.19	0.20	
	MAASHO[c]	0.0061	0.030	0.030	0.030	0.19	0.20	
SU-2A-6T	KY	3.1945	4.121	3.758	3.752	0.41	0.41	23,389
	AASHO	0.1787	0.088	0.081	0.081	0.38	0.38	
	MAASHO	0.1787	0.088	0.081	0.081	0.38	0.38	
SU-3A	KY	10.0445	16.129	12.973	12.867	0.59	0.60	2,180
	AASHO	0.3391	0.289	0.235	0.234	0.58	0.58	
	MAASHO	0.5290	0.440	0.363	0.362	0.56	0.57	
C-3A	KY	8.8944	6.560	6.109	6.973	0.36	0.37	12,143
	AASHO	0.6071	0.270	0.253	0.253	0.35	0.35	
	MAASHO	0.6071	0.270	0.253	0.253	0.35	0.35	
C-4A	KY	15.2519	9.848	7.766	7.759	0.61	0.61	14,321
	AASHO	0.8076	0.328	0.227	0.226	0.72	0.72	
	MAASHO	0.9872	0.435	0.302	0.301	0.72	0.72	
C-5A	KY	18.3338	15.225	11.478	11.471	0.66	0.66	4,302
	AASHO	0.7865	0.452	0.347	0.347	0.64	0.64	
	MAASHO	1.2088	0.705	0.530	0.530	0.66	0.66	

[a]No weight data were available for cars or buses.
[b]Negative estimates were transformed to zero.
[c]Modified AASHO procedures were used.

local conditions had to be excluded from the analysis. Season was omitted because all available weight data had been limited to the late spring or summer months. Service provided was eliminated because of the relative scarcity of weight data representative of each of the service-provided categories. Unfortunately this caused a significant reduction in accuracy (a reduction in the correlation coefficients of about 15 percent) and suggests that more accurate future estimates may be partially dependent on the weighing of vehicles on roads representing each of the service-provided categories. The year variable also had to be eliminated from the analysis. Data again indicated that it would be extremely difficult, if not impossible, to estimate the correction factors for future years. Furthermore, because of the interrelationships between year and maximum allowable gross weight, the correction factors for maximum allowable gross weight appeared incongruous when year was included as an independent variable.

The procedures described were used to estimate unit EAL's for comparison with actual unit EAL's obtained from past weight data. The results of this accuracy comparison are summarized in Table 4. The correlation coefficients reveal that the accuracy of the estimates leaves much to be desired. However, no other technique yielded superior accuracies as long as it was stipulated that the technique had to represent a valid, predictive procedure. It is apparent from Table 4 that this method of accounting for the effects of local conditions is superior to the gross means approach. The best accuracy was generally achieved for those vehicle types that contribute most significantly to the EAL accumulations.

ACCURACY VERIFICATION

Several empirical methods were investigated for predicting the pertinent traffic parameters. These included optimal methods that could meet the criteria of accuracy, simplicity, reasonableness, and predictability. The true validity of the proposed model could not be assessed solely on the basis of estimates of the individual traffic parameters. Of considerably more significance is the accuracy of estimates of design EAL's or of estimates of pavement thickness resulting therefrom.

To make such a determination, EAL's were estimated and compared to actual EAL's for all stations at which both vehicle classification and weight data had been obtained. There were 51 such stations representing a total of 225 counts. Of these, 9 were stations for which 11 or more years of data were available, and 18 were stations for which 7 or more years were available. Thirty-one of the stations were represented by only 1 or 2 years of data.

The first comparisons were made on the basis of EAL's per 1,000 vehicles for the 225 individual counts; these are summarized in Table 5. The correlation coefficients are relatively small, which indicates that a large portion of variability in EAL's per 1,000 vehicles for individual counts remains unexplained. This was thought to result in large part from the extreme variability in the actual EAL's that are accumulated at individual stations from year to year. Such variability is depicted in Figure 1a for station 8, for which 14 years of data were available. This figure suggests that if the daily EAL's were accumulated over a period of years, the actual and predicted accumulations might tend to converge. Figure 1b shows that, following a 6-year period of initial instability,

TABLE 5

ACCURACY OF ESTIMATES OF EAL'S PER 1,000 VEHICLES FOR 225 INDIVIDUAL COUNTS

Type	Actual Mean	Standard Deviation	Standard Error	Correlation Coefficient
Kentucky (EWL's/1,000 vehicles)	1,535.4	1,405.3	1,173.1	0.55
AASHO (EAL's/1,000 vehicles)	82.4	54.5	42.4	0.63
Modified AASHO (EAL's/1,000 vehicles)	96.9	70.8	52.2	0.68

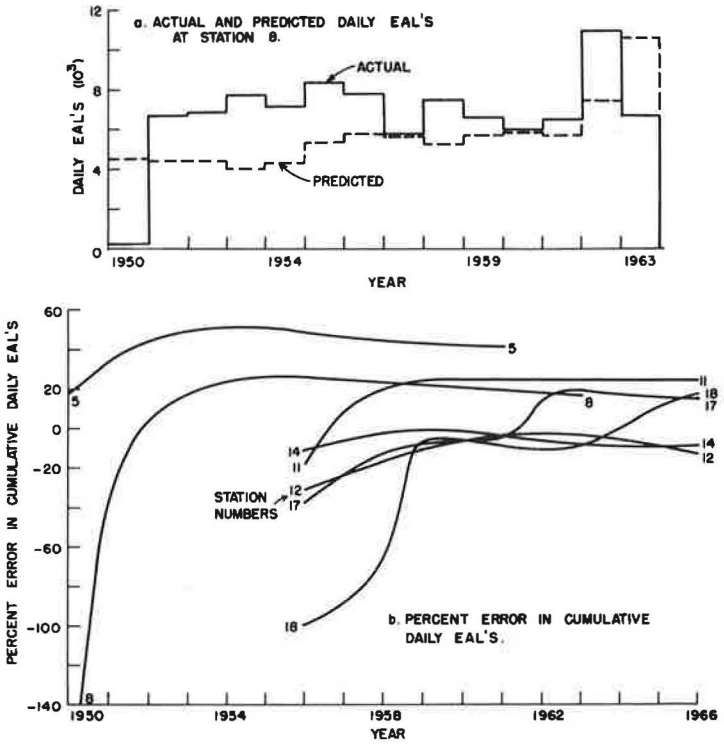

Figure 1. Variability in Kentucky daily EAL's.

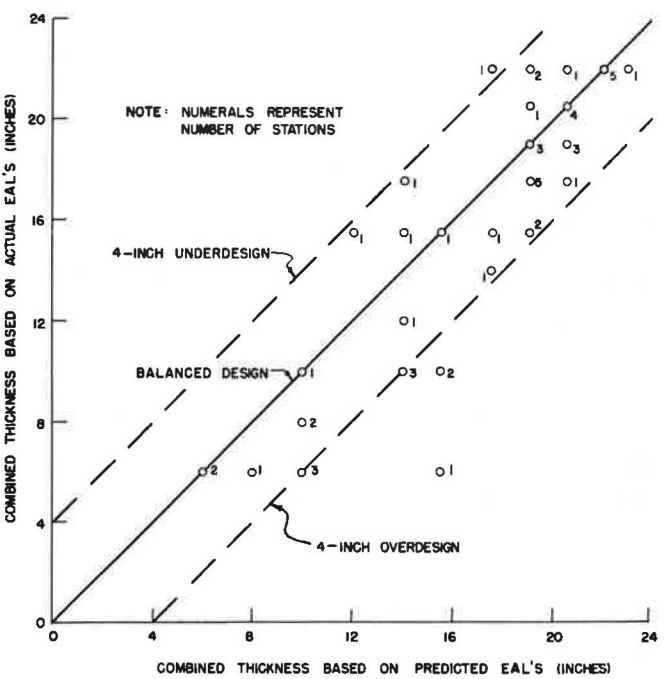

Figure 2. Flexible pavement thickness based on actual and predicted 20-year EAL accumulations.

the percentage of error between actual and predicted EAL's at station 8 did tend to become reduced as the number of years increased. By extrapolation, the percentage of error at the end of a 20-year design period would be about 6 percent, certainly a tolerable error.

Similar curves for 6 of the remaining 8 stations for which 11 or more years of data had been accumulated are also shown in Figure 1b. These curves verify that the percentage of errors tends to become reduced and stabilized as time increases. This is of extreme significance because flexible pavement designs in Kentucky are usually based on a 20-year period.

As a further means for validating the proposed methodology, the influence of the accuracy of the EAL estimates on the accuracy of the design pavement thicknesses was also investigated. First the actual and estimated EAL's for each of the 51 locations were extrapolated to 20-year accumulations. Then the combined flexible pavement thicknesses including base and pavement were determined for a design CBR of 5 (2). Figure 2 summarizes the results of these determinations. Differences in the thicknesses based on estimated actual and predicted EAL's seem rather large at first glance. However, it should be recalled that actual data were available for periods of only 1 or 2 years for 31 of the 51 stations represented in Figure 2. This would, of course, decrease the reliability of the estimates of 20-year accumulations of EAL's. Figure 2 shows 27 overdesigns, 16 balanced designs, and 8 underdesigns.

CONCLUSIONS

This search for a responsive technique to estimate EAL accumulations for pavement-design purposes required extensive data compilations and the development of many relevant summaries. Only limited data are presented, however, because of space limitations and because most of the data are valid only for Kentucky conditions. The interested reader will find the complete data tabulations elsewhere (11). The significant conclusions of this study are as follows:

1. The best basis for predicting EAL's for pavement-design purposes remains data taken from a nearby reference station if that station has characteristics similar to the location in question, at least 3 or 4 years of data are available, and due consideration is given to possible future effects of changing local conditions.
2. The recommended predictive methodology, when no suitable reference data are available, contains a set of traffic parameters that enter the design computations directly, a set of local conditions that can be considered as determinants of the traffic parameters, a set of relationships that define the manner in which the local conditions (independent variables) affect the traffic parameters (dependent variables), and a predictive equation.
3. The optimal traffic parameters for EAL estimates have been identified as ADT, percentages of the various vehicle types, and their unit EAL's.
4. The recommended method for predicting vehicle-type percentages consists of a set of basic percentages determined jointly by road type, volume, and maximum allowable gross weight and a series of multiplicative correction factors determined and applied independently by direction, season, alternate routes, service provided, and geographical area.
5. The recommended method for predicting unit EAL's is based on a multiple regression model that considers the effects of road type, direction, alternate routes, volume, maximum allowable gross weight, and geographical area in an additive fashion.
6. The proposed method for predicting design EAL's is sufficiently accurate for use in designing flexible pavements.

ACKNOWLEDGMENTS

The material presented in this paper is based on Research Study KYHPR-64-21, Determination of Traffic Parameters for the Prediction, Projection, and Computation of EWL's, conducted by the Kentucky Department of Highways in cooperation with the U.S. Bureau of Public Roads. The opinions, findings, and conclusions in this report are not

necessarily those of the Bureau of Public Roads or the Highway Department. The authors wish to acknowledge the assistance of W. Stutzenberger and D. Shyrock of the Division of Planning, Kentucky Department of Highways, and F. Cook, G. Hamby, C. Hays, R. Lynch, and R. Sumner of the Division of Research. Use of the University of Kentucky Computer Center is also acknowledged.

REFERENCES

1. Baker, R. F., and Drake, W. B. Investigation of Field and Laboratory Methods for Evaluating Subgrade Support in the Design of Highway Flexible Pavements. Bull. 13, Univ. of Kentucky Engineering Experiment Station, Sept. 1949.
2. Drake, W. B., and Havens, J. H. Kentucky Flexible Pavement Design Studies. Bull. 52, Univ. of Kentucky Engineering Experiment Station, June 1959.
3. Faulkner, P. A. Determination of Flexible Pavement Cost Indices for Use in the Analysis of Highway-User Tax Responsibilities by the Incremental Method. MSCE thesis, Univ. of Kentucky, 1956.
4. Hveem, F. N., and Sherman, G. B. Thickness of Flexible Pavements by the California Formula Compared to AASHO Road Test Data. Highway Research Record 13, pp. 142-166, 1963.
5. Planning Manual of Instructions, Part 7: Design. California Division of Highways, April 1959.
6. Derdeyn, C. J. A New Method of Traffic Evaluation for Pavement Design. Highway Research Record 46, pp. 1-10, 1964.
7. Heathington, K. W., and Tutt, P. R. Estimating the Distribution of Axle Weights for Selected Parameters. Report 1, Departmental Research, Texas Highway Department, 1966.
8. Ulbricht, E. P. A Method for Comparing Alternate Pavement Designs. Report 28, Joint Highway Research Project, Purdue University, Nov. 1967.
9. Guidelines for Trip Generation Analysis. U.S. Bureau of Public Roads, June 1967.
10. Statistical Library for the S/360 Programs and Subroutines. Computer Center, Univ. of Kentucky, July 1967.
11. Deacon, J. A., and Lynch, R. L. Determination of Traffic Parameters for the Prediction, Projection, and Computation of EWL's. Division of Research, Kentucky Department of Highways, Aug. 1968.

Computation of Equivalent Single-Wheel Loads Using Layered Theory

Y. H. HUANG, Assistant Professor of Civil Engineering, University of Kentucky

A method based on elastic layered theory and programmed for a high-speed computer was developed for determining equivalent single-wheel loads for dual wheels. It was found that equivalent single-wheel loads based on equal vertical deflection at the pavement-subgrade interface were generally greater than those based on equal vertical stress or equal surface deflection.

The effect of various factors on equivalent single-wheel loads was investigated, using equal-interface deflection criterion. It was found that the ratio between the total load on dual wheels and the equivalent single-wheel load depends on three factors: pavement thickness, wheel spacing, and modulus ratio, which is the ratio of the moduli of elasticity of pavement and subgrade. Charts that give the interface deflection under a circular load for various pavement thicknesses, offset distances, and modulus ratios are presented so that the equivalent single-wheel load for any given loading and pavement condition can be determined.

An important fact revealed by this study is that the equivalent single-wheel load increases appreciably with the increase in modulus ratio. The current method of assuming that pavements are homogeneous media with a modulus ratio of unity always gives an equivalent single-wheel load that is too small and is not in line with the findings of the WASHO Road Test.

•THE CONCEPT of equivalent single-wheel load has long been used in the structural design of flexible pavements. Separate criteria for multiple-wheel loading need not be developed if the multiple-wheel loads are converted to an equivalent single-wheel load so that the design criteria based on single-wheel loads can still be applied. This procedure is particularly suited for the design of airport pavements, because the wheel configuration of airplanes is quite variable, and it is not convenient to have separate design criteria for each plane. Although the axle and wheel configuration of trucks has been fairly standardized, the concept can be used to determine the effect of special vehicles on highway pavements, or to find axle spacings and loads that will produce no greater detrimental effect than that produced by a given load on a single axle.

Various theoretical methods (1, 2), mostly based on elastic theory, have been devised to determine the equivalent single-wheel load for dual or multiple wheels. The applicability of the elastic theory is based on the fact that, after a few load applications, the deflections of a flexible pavement under each load application are essentially elastic in the sense that they are almost completely recoverable (3). It has further been found that the performance of flexible pavements can be related to these elastic deflections, and that a high degree of correlation exists between deflection and rutting (4). Consequently, a comparison of theoretical stresses or deflections in pavements, based on

Paper sponsored by Committee on Theory of Pavement Design and presented at the 48th Annual Meeting.

elastic theory, will give a general indication of the equivalency between single- and multiple-wheel loads as related to pavement performance.

REVIEW OF PAST WORK

The study of equivalent single-wheel loads was first initiated by the U. S. Corps of Engineers during World War II, when the B-29 bombers were introduced with dual-wheel assemblies. A theoretical consideration of the vertical and shear stresses in an elastic half space and an experimental measurement of the vertical deflections at the interface between pavement and subgrade were used by Boyd and Foster (5) in presenting a semirational method of determining equivalent single-wheel loads, which had been used by the Corps of Engineers to produce dual-wheel design criteria from single-wheel criteria. The method assumes that the equivalent single-wheel load varies with the pavement thickness. For thicknesses smaller than half the clearance between dual wheels, the equivalent single-wheel load is equal to half of the total load. However, for thicknesses greater than twice the center-to-center spacing of wheels, it is equal to the total load. By assuming a straight-line relationship between pavement thickness and wheel load on logarithmic scales, one can readily obtain the equivalent single-wheel load for any intermediate thickness. The same method has been used by the Federal Aviation Administration for the design of flexible airport pavements (1).

The application of the method and the subsequent completion of accelerated traffic tests revealed that design criteria based on the foregoing method were not very safe, and an improved method was developed by Foster and Ahlvin (2). In this method, the pavement is considered as a homogeneous, elastic, and semi-infinite half space, so that the vertical deflections at a depth equal to the thickness of pavement can be obtained from available solutions (6). A single-wheel load that has the same contact radius as one of the dual wheels and results in a maximum deflection equal to that caused by the dual wheels is designated as the equivalent single-wheel load (ESWL).

In a previous paper (7), the author extended the work of Foster and Ahlvin by considering the pavement as a two-layer elastic system, thus taking the ratio of the moduli of elasticity of the pavement and subgrade into account. A chart was developed by which the ESWL for any combinations of pavement thickness, modulus ratio, wheel spacing, and contact radius could be obtained by a simple calculation and interpolation. It was shown that the ESWL increased appreciably with the increase in modulus ratio and that the use of layered theory would give a larger equivalent wheel load that was more in line with traffic data. However, the chart is limited because it is applicable only to dual wheels, or to multiple wheels that can be approximated by a set of duals. Furthermore, the computation was based on equal contact radius instead of equal contact pressure (i.e., the single wheel and each of the dual wheels have the same contact radius instead of the same contact pressure), although it is illustrated that the ESWL's based on equal contact radius are not too much different from those based on equal contact pressure.

The purposes in this study are (a) to develop a method for computing ESWL's based on equal contact pressure and Burmister's two-layer elastic theory (8); (b) to compare the ESWL's computed on the basis of the criteria of equal interface stress, equal surface deflection, and equal interface deflection; (c) to find the effect of various factors on ESWL's by using one of the criteria considered to have the most potential; (d) to compare the theoretical findings with traffic data to ascertain the limitations of the theory; and (e) to present a set of stress or deflection charts by which ESWL's for any given pavement thickness, modulus ratio, and axle and wheel configuration can be determined.

DESCRIPTION OF METHOD

The computation of ESWL can be based on either equal-stress or equal-deflection criteria. Assume, for example, that the maximum stress or deflection that occurs under a set of dual wheels is known. A single wheel that has the same contact pressure and results in a stress or deflection of the same amount is said to be equivalent to these duals.

In this study, only the vertical stress at the pavement-subgrade interface and the vertical deflections, both on the surface and at the interface, were considered. Boyd and Foster (5) showed that the computed ESWL's based on equal shear stress were not too much different from those based on equal vertical stress.

Assumptions

The pavement is assumed to be a two-layer elastic system. Layer 1, which includes the surface, base, and subbase courses, has a thickness, h, and an average modulus of elasticity, E_1; layer 2, which represents the subgrade, is of infinite thickness with a modulus of elasticity, E_2. Both layers are infinite in extent and consist of incompressible materials with a Poisson's ratio of 0.5.

The single-wheel load and each of the dual-wheel loads are applied over a circular area, the radius of which is such that a given contact pressure, q, will be obtained, i.e.,

$$a = \sqrt{\frac{P}{\pi q}} \tag{1}$$

where

a = contact radius under each wheel load,
P = load applied to each wheel, and
q = contact pressure.

The boundary and continuity conditions employed by Burmister (8) are assumed to be valid. The layers are in continuous contact as indicated by the continuity in vertical stresses, shear stresses, vertical deflections, and radial deflections. The surface is free of normal stresses outside the loaded area and free of shear stresses throughout.

Stresses and Deflections Under a Single-Wheel Load

The interface stress, σ, surface deflection, w_0, and interface deflection, w_1, due to a circular load can be computed by the following formulas (7, 9, 10):

$$\sigma = q\,\theta \tag{2a}$$

$$w_0 = \frac{qa}{E_2} \cdot F_0 \tag{2b}$$

$$w_1 = \frac{qa}{E_2} \cdot F_1 \tag{2c}$$

where θ = stress factor. It may be expressed in the form

$$\theta = -(1 - N)\frac{a}{h}\int_0^\infty J_0\left(m\frac{r}{h}\right) J_1\left(m\frac{a}{h}\right)\left[\frac{(1+m)e^{-m} - N(1-m)e^{-3m}}{1 - 2N(1+2m^2)e^{-2m} + N^2e^{-4m}}\right]dm \tag{3a}$$

Surface deflection factor, F_0, may be expressed as

$$F_0 = \frac{1.5}{(E_1/E_2)}\int_0^\infty J_0\left(m\frac{r}{h}\right) J_1\left(m\frac{a}{h}\right)\left[\frac{1 + 4Nme^{-2m} - N^2e^{-4m}}{1 - 2N(1+2m^2)e^{-2m} + N^2e^{-4m}}\right]dm \tag{3b}$$

Interface deflection factor, F_1, is

$$F_1 = 1.5\,(1 - N)\int_0^{\infty} J_0\left(m\frac{r}{h}\right) J_1\left(m\frac{a}{h}\right)\left[\frac{(1 + m)e^{-m} - N(1 - m)e^{-3m}}{1 - 2N(1 + 2m^2)e^{-2m} + N^2e^{-4m}}\right]\frac{dm}{m} \quad (3c)$$

where

$$N = \frac{E_1 - E_2}{E_1 + E_2} = \frac{(E_1/E_2) - 1}{(E_1/E_2) + 1},$$

E_1/E_2 = modulus ratio,
J_0 and J_1 = Bessel function of the first kind, order 0 and 1 respectively,
r = radial distance from the center of loaded area to the point where the stress or deflection is to be sought,
a = contact radius,
h = thickness of layer 1, and
m = a parameter.

The infinite integrals in Eq. 3 were evaluated by a numerical method programmed for an IBM 360 computer at the University of Kentucky. Because the maximum stress or deflection due to a single-wheel load always occurs under the center of the wheel, the maximum stress or deflection can be obtained by letting $r = 0$ in the evaluation.

In the case of dual-wheel loads, the maximum stress or deflection can be obtained by superposition. The stress or deflection due to each wheel load was computed independently and then superposed to obtain that due to all wheels. For instance, the stress or deflection factor under a set of dual wheels at a point having a distance r_l from the left wheel and r_r from the right is the sum of two factors, each obtained by substituting $r = r_l$ and $r = r_r$ respectively into Eq. 3. Because the maximum stress or deflection occurs at some point between one wheel and the centerline of the dual, the stress or deflection at several points must be computed and the maximum value obtained. The ESWL can then be determined by a graphical method (1).

COMPARISON OF CRITERIA

To compare the ESWL's computed on the basis of different criteria, a conventional 32,000-lb tandem-axle load was chosen. This type of loading was used in both the WASHO and the AASHO Road Tests, so the resulting information obtained from these tests can be used to compare the theoretical findings presented here.

Figure 1 shows the proposed wheel loads applied to a two-layer system. The load on each axle is 16,000 lb and that on each wheel is 8,000 lb. Although the actual wheel loads are applied over dual tires, assume that they are applied on a single tire over a circular area. It can be shown that this assumption has very little effect on the ESWL, as long as the single-wheel load is also assumed to be applied on a single tire. Since the contact pressure is 70 psi, the contact radius can be determined from Eq. 1,

$$a_d = \sqrt{\frac{8{,}000}{\pi \times 70}} = 6 \text{ in.}$$

Under the given loads, it was found that on the surface the maximum deflection occurred under one wheel; at the interface, however, the maximum stress or deflection occurred anywhere between one wheel and the centerline of the two wheels. A computer program was developed to compute the vertical stresses and deflections at the six points shown in Figure 1 and obtain the maximum values.

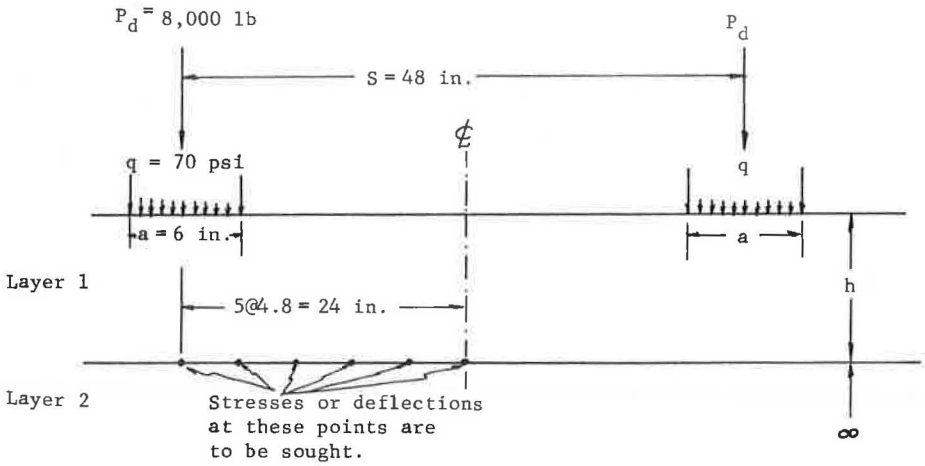

Figure 1. Proposed wheel loads.

To indicate the relationship between the total load on dual wheels and the ESWL, a parameter called load factor, L, which is a ratio between the total load and the ESWL, was employed:

$$L = \frac{2P_d}{ESWL}$$

Table 1 gives the load factors computed by three different criteria for various pavement thicknesses and modulus ratios. It can be seen that all three criteria have the same trend, i.e., the load factor decreases with the increase in thickness and modulus ratio. The interface deflection criterion generally gives the smallest load factor or the largest ESWL. Because the use of interface deflection was on the safe side, it was adopted for more detailed analyses.

EFFECT OF VARIOUS PARAMETERS ON LOAD FACTOR

Theoretically, in addition to modulus ratio, the magnitude of load factor depends on the following four parameters: (a) total load, $2P_d$, (b) contact pressure, q, (c) wheel spacing, S, and (d) pavement thickness, h. The effect of each of these parameters on load factor was investigated using the equal-interface deflection criterion.

TABLE 1

COMPARISON OF LOAD FACTORS COMPUTED BY DIFFERENT CRITERIA

Pavement Thickness (in.)	Criterion	E_1/E_2						
		1.0	2.5	5.0	10.0	25.0	50.0	100.0
6	Interface stress	2.00	2.00	2.00	2.00	2.00	1.98	1.95
	Surface deflection	1.77	1.77	1.77	1.73	1.66	1.60	1.52
	Interface deflection	1.79	1.78	1.76	1.73	1.66	1.60	1.51
16	Interface stress	1.99	1.97	1.93	1.86	1.73	1.62	1.49
	Surface deflection	1.77	1.66	1.57	1.47	1.32	1.23	1.16
	Interface deflection	1.67	1.60	1.52	1.43	1.30	1.22	1.15
24	Interface stress	1.96	1.89	1.81	1.72	1.57	1.45	1.36
	Surface deflection	1.77	1.61	1.48	1.36	1.24	1.17	1.12
	Interface deflection	1.55	1.45	1.36	1.28	1.18	1.13	1.08

TABLE 2

EFFECT OF TOTAL LOAD ON LOAD FACTOR

Total Load (kip)	E_1/E_2						
	1.0	2.5	5.0	10.0	25.0	50.0	100.0
4	1.67	1.63	1.54	1.45	1.33	1.22	1.16
8	1.67	1.62	1.54	1.45	1.32	1.22	1.15
16	1.67	1.60	1.52	1.43	1.30	1.22	1.15
32	1.63	1.57	1.50	1.40	1.28	1.20	1.14

TABLE 3

EFFECT OF CONTACT PRESSURE ON LOAD FACTOR

Contact Pressure (psi)	E_1/E_2						
	1.0	2.5	5.0	10.0	25.0	50.0	100.0
40	1.64	1.57	1.51	1.41	1.29	1.21	1.14
70	1.67	1.60	1.52	1.43	1.30	1.22	1.15
110	1.67	1.61	1.54	1.44	1.31	1.22	1.15
180	1.70	1.63	1.56	1.45	1.33	1.23	1.17

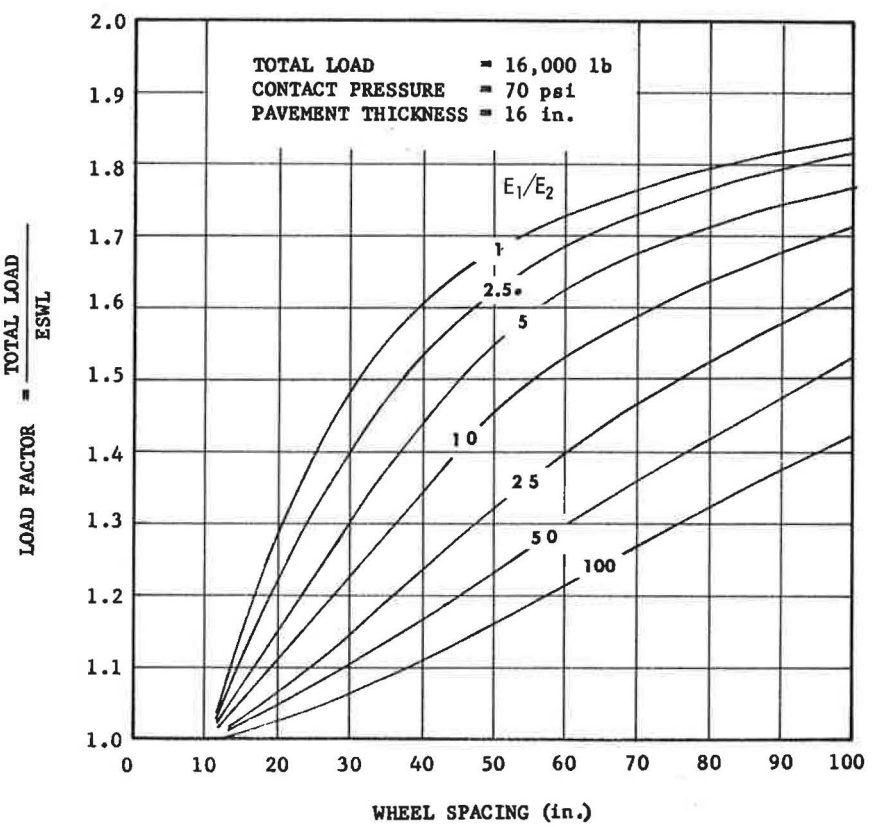

Figure 2. Effect of wheel spacing on load factor.

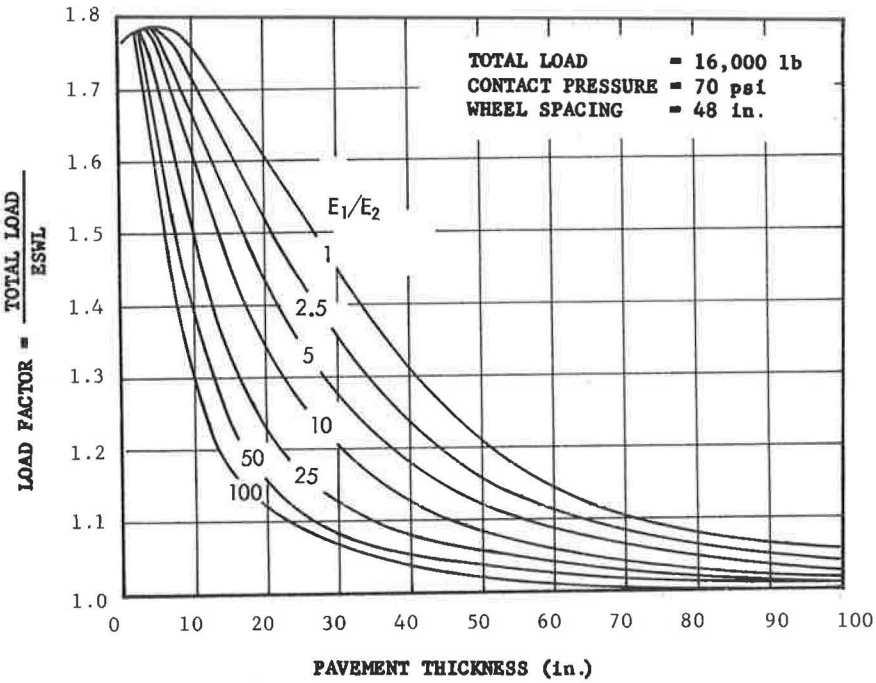

Figure 3. Effect of pavement thickness on load factor.

Effect of Total Load

Table 2 gives the effect of total load on load factor. The computation was based on average conditions with q = 70 psi, S = 48 in., and h = 16 in. The load factor decreases slightly with the increase in total load. An eight-fold increase in total load only causes a decrease in load factor by not more than 0.06. This is the reason the load factor, instead of the ESWL, was used because the load factor is practically independent of the total load, whereas the ESWL changes with the total load.

Effect of Contact Pressure

Table 3 gives the effect of contact pressure on load factor. The computation was based on P_d = 8,000 lb, S = 48 in., and h = 16 in. The load factor increases slightly with the increase in contact pressure. However, under the given pavement and loading conditions, the effect of contact pressure is not significant.

Effect of Wheel Spacing

Figure 2 shows that wheel spacing has a tremendous effect on load factor. The larger the wheel spacing, the greater the load factor. For smaller modulus ratios, the effect of wheel spacing is more conspicuous at smaller spacings as indicated by a rapid change in the slope of the curves. For larger modulus ratios, the effect is more conspicuous at larger spacings because of the superior load-distributing characteristics of the pavement.

Effect of Pavement Thickness

Figure 3 shows the effect of pavement thickness on load factor based on the proposed wheel loads shown in Figure 1. The load factor generally decreases with an increase in pavement thickness. However, at very small thicknesses, say, less than 6 in., the load factor may increase with the increase in thickness.

COMPARISON WITH ROAD TESTS

One of the main objectives of the WASHO Road Test (11) was to determine the effect of various axle loads, both single and tandem, on flexible pavements. In this test, the combined thickness of surfacing and base courses was 6 in., one with 4 in. of asphaltic concrete surfacing on 2 in. of crushed gravel base course, and the other with 2 in. of surfacing on 4 in. of base. The thicknesses of gravel subbase were 0, 4, 8, 12, and 16 in. Thus, the total thickness of pavement structure over the basement soil varied from 6 to 22 in. with an average of 14 in. The following is an excerpt of the findings published by the Highway Research Board (11):

> Based on distress that occurred in the section with 4-in. surfacing, a tandem-axle load of 28 kip would have been equivalent in this test to a single-axle load of 18 kip. Similarly, a tandem-axle load of 33.6 kip would have been equivalent to the 22.4 kip single-axle load. Comparisons for sections with 2-in. surfacing, based on a graphic analysis which discounted the relatively erratic behavior of two of the ten sections, showed that a tandem-axle load of 28.3 kip in this test could have been equivalent to the single-axle load of 18 kip. Similarly, a tandem-axle load of 36.4 kip could have been equivalent to the 22.4 kip single-axle load. In general, the distress caused by tandem axles was equivalent to that caused by single axles of the order of two thirds of their weight.

Two points are quite significant in the above statement. First, the replacement of 2 in. of asphaltic concrete by 2 in. of crushed gravel would increase the load factor, which is the ratio between tandem- and single-axle loads, in one case from 1.55 to 1.57 and in another case from 1.50 to 1.62. This is in conformity with the layered theory that the larger the modulus ratio, the smaller the load factor, or the greater the ESWL. Second, the last statement indicates that the load factor for the test road was 1.5. This may illustrate that considering the pavement as a homogeneous medium (i.e., $E_1/E_2 = 1$) may not give a good prediction of ESWL's. As Figure 3 shows, the load factor for h = 14 in. and $E_1/E_2 = 1$ is 1.70, which is much greater than the 1.5 determined experimentally in the WASHO Road Test. Only when E_1/E_2 is increased to 10, which is typical for asphalt pavements, can a load factor of 1.5 be obtained. This indicates that the use of layered theory, by assuming that the pavement has a larger modulus than the subgrade, may give a better prediction of the effect of various wheel loads on pavement distress.

The theoretical findings presented here agree with the results of WASHO Road Test. However, the author does not claim that the use of layered theory and the equal-interface deflection criterion is valid under all circumstances. In fact, the experimental determination of ESWL's is affected by the magnitude of load as compared to the load-carrying capacity of the pavement, the latter being affected by many other environmental factors. For example, in the WASHO test road the 6-in. sections with 2-in. surfacing were completely destroyed by all of the four different axle loads. Based on the area damaged in 6-in. sections, it can then be said that there is no difference in the destructive effect of any of the vehicles involved. The same is true for the 22-in. sections with 4-in. surfacing where no damage was done by any of the four axle loads. However, under average conditions, with some portions of the pavement damaged and others intact, the theory developed may give a fairly good prediction of ESWL's.

It should be noted that the computation of ESWL's presented here is based on the elastic deformation only, which is more related to structural failures such as cracking. It does not include the plastic or consolidation type of deformation, which is more related to functional failures such as rutting. This distinction can be used to explain why contradictory conclusions regarding equivalent axle loads were obtained between the WASHO (11) and AASHO (4) Road Tests. In the WASHO Road Test, it was found that a 32,000-lb tandem-axle load was much more destructive than an 18,000-lb single-axle load whereas, in the AASHO Road Test, the 18,000-lb single-axle load was found slightly more destructive than the 32,000-lb tandem axle load. The difference is believed

to be caused by the use of pavement serviceability index in the AASHO Road Test for the determination of equivalent wheel loads. In addition to cracking and patching, this index is based on slope variance and rut depth, which were not considered in the WASHO Road Test. Because the ESWL based on layered theory is greater than that obtained from the AASHO Road Test, the use of layered theory is on the safe side.

The suggestion of using layered theory to compute ESWL's should not imply that the equivalencies obtained from the AASHO Road Test are no longer valid. In fact, if a pavement is overdesigned and its serviceability is of major concern, the equivalent loads as determined from the AASHO Road Test are quite adequate and should be used. On the other hand, if the pavement is underdesigned and the prevention of failures is a major factor, as is in the case of military or airport construction, the use of Burmister's two-layer theory, instead of Boussinesq's single-layer theory, is suggested.

CONCLUSIONS

In this study, a method was developed for computing equivalent single-wheel loads for dual wheels. The method is based on Burmister's two-layer elastic theory and assumes that both single and dual wheels have the same contact pressure. Three criteria—equal interface stress, equal surface deflection, and equal interface deflection—were investigated. It was found that, for a conventional 32,000-lb tandem-axle load, the equivalent single-axle loads determined by the equal-interface deflection criterion were generally the largest, whereas those determined by the equal-interface stress were the smallest. Because the use of the equal-interface deflection criterion was on the safe side, it was adopted for more detailed analyses.

To indicate the relationship between the total load on dual wheels and the ESWL, a parameter called load factor, which is a ratio of the total load and the ESWL, was employed. It was found that total load and contact pressure had a relatively small effect on load factor. However, the load factor decreases, or the ESWL increases appreciably, with an increase in pavement thickness and modulus ratio, or with a decrease in wheel spacing.

An important fact revealed by this study is that the ESWL increases appreciably with an increase in modulus ratio, E_1/E_2. The current method of considering pavements as homogeneous media (i.e., $E_1/E_2 = 1$) always gives an ESWL that is too small and is not in line with the findings of the WASHO Road Test.

ACKNOWLEDGMENTS

The study reported herein was part of a faculty research program sponsored by the Department of Civil Engineering, University of Kentucky. The support given by the University of Kentucky Computing Center through the use of the IBM 360 computer and related technical service is appreciated.

REFERENCES

1. Yoder, E. J. Principles of Pavement Design. John Wiley and Sons, pp. 41-48, 358, and 341, 1959.
2. Foster, C. R., and Ahlvin, R. G. Development of Multiple-Wheel CBR Design Criteria. Jour. Soil Mech. and Found. Div., ASCE, pp. 1647-12, May 1958.
3. Whiffin, A. C., and Lister, N. W. The Application of Elastic Theory to Flexible Pavements. Proc. Internat. Conf. on Structural Design of Asphalt Pavements, Univ. of Michigan, pp. 499-521, 1962.
4. The AASHO Road Test: Report 5—Pavement Research. Highway Research Board Spec. Rept. 61E, p. 137, 1962.
5. Boyd, W. K., and Foster, C. R. Design Curves for Very Heavy Multiple-Wheel Assemblies. In Development of CBR Flexible Pavement Design Method for Airfields—A Symposium. Trans. ASCE, Vol. 115, pp. 534-546, 1950.
6. Foster, C. R., and Ahlvin, R. G. Stresses and Deflections Induced by a Uniform Circular Load. HRB Proc., Vol. 33, pp. 467-470, 1954.

7. Huang, Y. H. Chart for Determining Equivalent Single-Wheel Loads. Jour. Highway Div., ASCE, pp. 115-128, Nov. 1968.
8. Burmister, D. M. The Theory of Stresses and Displacements in Layered Systems and Applications to the Design of Airports Runways. HRB Proc., Vol. 23, pp. 126-144, 1943.
9. Fox, L. Computation of Traffic Stresses in a Simple Road Structure. Road Research Tech. Paper No. 9, HMSO, London, 1948.
10. Huang, Y. H. Stresses and Displacements in Viscoelastic Layered Systems Under Circular Loaded Areas. PhD dissertation, Univ. of Virginia, 1966.
11. The WASHO Road Test: Part 2—Test Data, Analyses, Findings. HRB Spec. Rept. 22, 1955.

Appendix

DEFLECTION CHARTS

The data in this paper were based on a set of dual wheels, and the solutions were obtained by using a high-speed computer. In order to determine equivalent single-wheel loads when multiple wheels are encountered, or when a computer is not available, a set of charts based on Eq. 3c was developed (Figs. 4, 5, 6, and 7). These charts give the vertical deflections at the interface under a circular load for various pavement thicknesses and offset distances. Seven different modulus ratios, 1, 2.5, 5, 10, 25, 50, and 100, were employed so that the deflection for any intermediate modulus ratio can be obtained by interpolation.

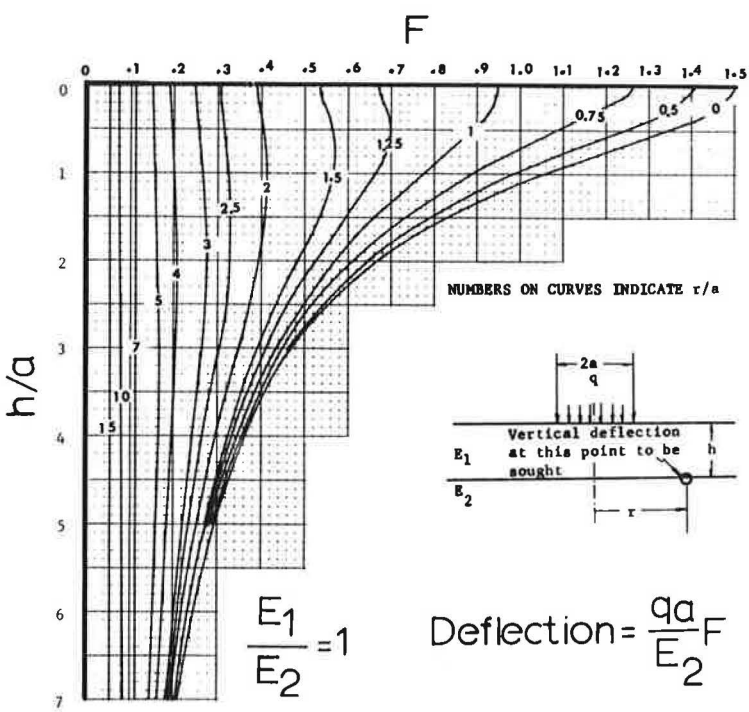

Figure 4.

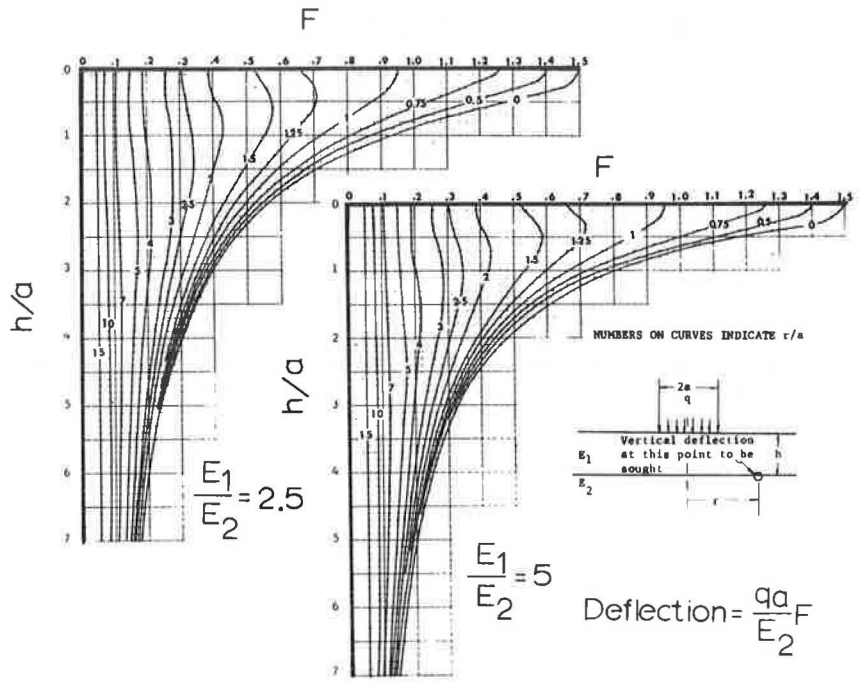

Figure 5.

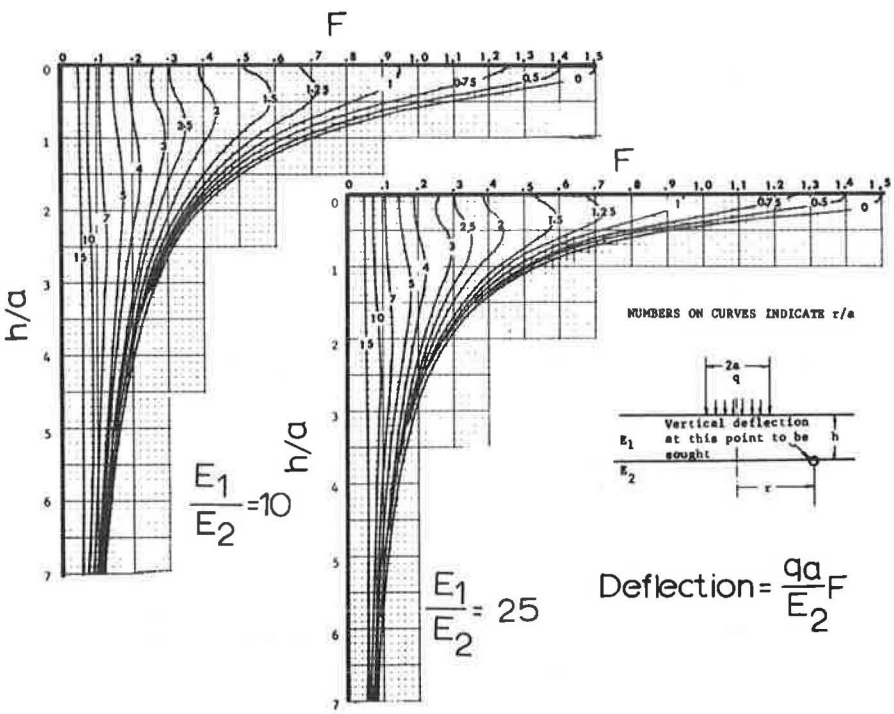

Figure 6.

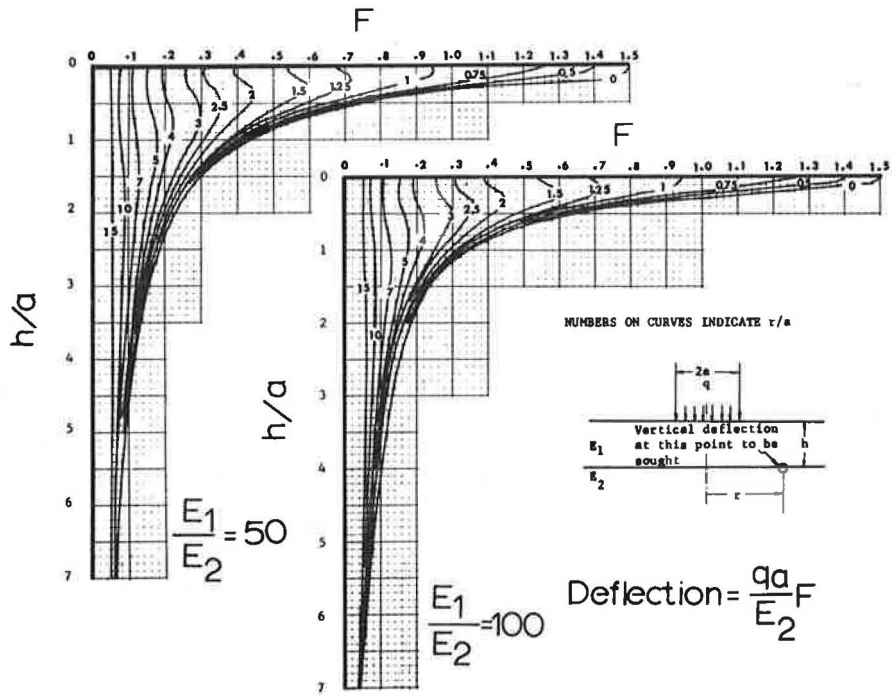

Figure 7.

For $E_1/E_2 = 1$, which is the case of a homogeneous medium, the chart checks quite closely with that presented by Foster and Ahlvin, indicating the correctness of the computer program. Because charts of this type for E_1/E_2 other than 1 are not available elsewhere, and because the deflection at the interface has been considered as a factor of pavement design, these charts may be of some practical use for those interested in the theoretical aspects of pavement design.

Analysis of Structural Behavior of Road Test Rigid Pavements

ALEKSANDAR S. VESIĆ and SURENDRA K. SAXENA, Duke University

ABRIDGMENT

•THE FIRST PART of this report is devoted to a critical review of existing theories of structural behavior of rigid pavements. These theories differ principally in the model selected to represent the subgrade supporting the pavement slab. Two principal models are being used: the elastic-isotropic solid, characterized by a modulus of deformation E_S and a Poisson's ratio ν_S; and the Winkler subgrade, characterized by a coefficient of subgrade reaction k.

It is shown that, with a suitable selection of coefficient k, theories based on the Winkler model for the subgrade can also furnish adequate answers for slabs resting on a subgrade behaving as an elastic-solid. However, there is no single value of k that can give perfect agreement of all static influences in a particular case, unless the subgrade thickness is limited to a maximum of 2.5 stiffness radii of the slab. The following analytical expressions are presented for evaluation of k for a slab of thickness h with deformation characteristics E, ν, resting on a subgrade of depth H with deformation characteristics E_S, ν_S:

Subgrade of infinite depth ($H \to \infty$)

$$k_o = 0.91 \sqrt[3]{\frac{E_S(1 - \nu^2)}{E(1 - \nu_S^2)}} \frac{E_S}{(1 - \nu_S^2)h} \tag{1}$$

or in simplified form,

$$k_o = \sqrt[3]{\frac{E_S}{E}} \frac{E_S}{(1 - \nu_S^2)h} \tag{2}$$

Subgrade of finite depth $\left(H \leq 1.38 \sqrt[3]{\frac{E}{E_S}}\, h\right)$

$$k_o' = 1.38 \frac{E_S}{(1 - \nu_S^2)H} \tag{3}$$

The second part of the report is devoted to study of structural behavior of rigid pavements of the AASHO Road Test. It is shown that the overall response of the AASHO subgrade to loads is comparable to response of an ideal isotropic-elastic solid. How-

Paper sponsored by Committee on Theory of Pavement Design and presented at the 48th Annual Meeting.

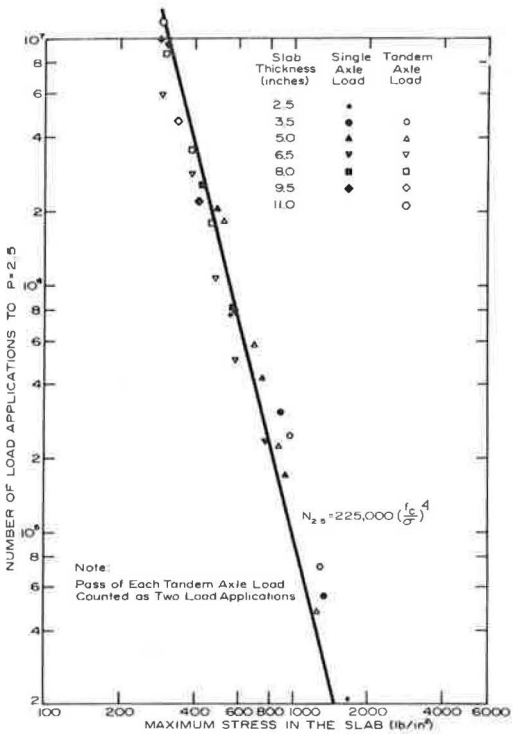

Figure 1. Relationship of performance to maximum combined tensile stress.

ever, with proper selection of the coefficients of subgrade reaction k, the Winkler subgrade model (used in the well-known Westergaard theory of rigid pavements) can also lead to good predictions of pavement stresses and deflections. As suggested by Eqs. 1 and 2, the coefficient k for the AASHO pavement/subgrade systems is a variable quantity that is inversely proportional to the pavement slab thickness.

It is also demonstrated that the combined tensile stress in pavement slabs represents the best indicator of pavement performance. If the critical stresses for each loading case and slab are plotted vs the number of load repetitions $N_{2.5}$ needed to reduce the serviceability index to 2.5, a unique relationship results for all slabs regardless of type of loading (Fig. 1).

This most significant finding confirms the soundness of a rational, mechanistic approach to design of rigid pavements. It demonstrates beyond doubt that failure in pavement performance is not a phemonenon of chance, as some statistical approaches tend to suggest, but a phenomenon that has a definite mechanical cause.

It can be shown that the data in Figure 1 can be fitted by the expression

$$N_{2.5} = 225{,}000 \left(\frac{f_c}{\sigma}\right)^4 \qquad (4)$$

in which f_c represents, as before, tensile strength of the pavement slab material in bending (for AASHO slabs f_c = 790 psi), and σ represents the maximum combined tensile stress in the pavement slab caused by traffic load Q moving in the anticipated average wheelpath position. (In existing design procedures, σ is computed as the absolute maximum stress caused by loads placed in some extreme positions such as slab edge or slab corner.)

Using Eq. 4 and considering the fact that the pavement stress σ for AASHO Road Test conditions is found to be proportional to wheel load Q and inversely proportional to approximately the 1.25 power of the slab thickness h, the following general relationship between principal variables in the AASHO Road Test can be established:

$$N_{2.5} = C\, f_c^4\, h^5\, Q^{-4} \qquad (5)$$

where C is a constant.

Equation 5 suggests that slab thickness should be increased as the fifth root of the anticipated number of load applications. This means that, under otherwise equal circumstances, the pavement life may be increased 1.8 times by adopting a 9-in. instead of an 8-in. slab thickness, and 3 times by adopting a 10-in. instead of an 8-in. slab thickness. At the same time the pavement life can be reduced to half by adopting a 7-in. instead of an 8-in. slab thickness.

It also follows from Eq. 5 that the pavement life varies as the fourth power of the concrete strength. This points out the importance of the quality of materials in pavement construction: a 10 percent increase in strength may mean a 50 percent increase in pavement life; a 20 percent increase in strength may mean doubling the pavement

life. At the same time, a 10 percent reduction in concrete strength may mean reducing the pavement life to 65 percent of the normal expectation; a 20 percent reduction in strength may mean reducing the life to 40 percent of the normal expectation.

Equation 5 may give us a rational basis for evaluation of effects of overload and mixed traffic on pavement life. A consistent 10 percent overload may reduce the pavement life to half the normally expected time. One application of double load is equivalent to 16 applications of normal load. At the same time 16 applications of the half-load in a mixed traffic should be equivalent to one application of normal load; 6,500 applications of a 2-kip axle load should be equivalent to one application of an 18-kip load.

The analyses leading to Eq. 5 furnish a rational basis for evaluation of equivalency of single and tandem loads under much more general conditions than possible in the past. With such an expression it becomes possible to predict in a rational way what would be the effect of using, on a certain pavement, tandem axle loads with different axle spacing or with a different distance between extreme wheels. Moreover, it becomes possible to predict with somewhat greater certainty the potential life of a rigid pavement subjected to traffic by a new vehicle that may be of entirely different characteristics than any other vehicle used in the past on similar pavements.

Asphalt Concrete Pavement Design—A Subsystem to Consider the Fatigue Mode of Distress

D. A. KASIANCHUK, Associate Professor of Engineering, Carleton University, Ottawa;
C. L. MONISMITH, Professor of Civil Engineering, Institute of Transportation and Traffic Engineering, University of California, Berkeley; and
W. A. GARRISON, Materials Testing Engineer, Contra Costa County Public Works Department, Martinez, California

In this paper a working model is presented for a subsystem to consider the fatigue mode of distress for asphalt concrete pavements. The design subsystem is divided into three general sections—(a) preliminary data acquisition, (b) materials characterization, and (c) analysis and evaluation. In developing a particular design with this subsystem, use is made of traffic and wheel load distributions, environmental conditions based on available weather records for the vicinity of the proposed design, multilayer elastic theory, resilient response of untreated granular materials and fine-grained soils, stiffness and fatigue characteristics of the asphalt concrete, and a cumulative damage hypothesis based on the simple linear summation of cycle ratios. To expedite the design process, the majority of the design computations have been programmed for use with a high-speed digital computer.

An example shows the use of the design procedure for a structural pavement section consisting of asphalt concrete resting directly on the subgrade soil. The design developed is shown for conventional materials and traffic to result in a thickness that is quite reasonable based on comparisons with other design methods. This particular subsystem would appear to have some advantages, however, in that it can be extended to consider loading conditions and material characteristics for which experience is not available.

•PROPER DESIGN of asphalt concrete pavements requires consideration of a number of complex and interrelated factors. Recent efforts have been made to formulate, in a systematic manner, pavement design systems that attempt to bring these factors together as the first step in the development of a more rational method of design (1, 2). Such a system is shown in Figure 1. Although the design of an asphalt concrete pavement in the manner suggested by this system is not presently possible, each of the considerations shown within it is real and should be included in some way in the design of every modern pavement.

One of the distress mechanisms included as a part of the rupture mode of distress shown in the limiting response block of Figure 1 is that of fatigue of asphalt concrete. It is the purpose of this paper to define considerations that are required to develop a subsystem to consider this mode of distress within the framework suggested in Figure 1. From these considerations, a working model is presented and illustrated by the design of a pavement structure to show the applicability and reasonableness of the method in current pavement design technology.

Paper sponsored by Committee on Theory of Pavement Design and presented at the 48th Annual Meeting.

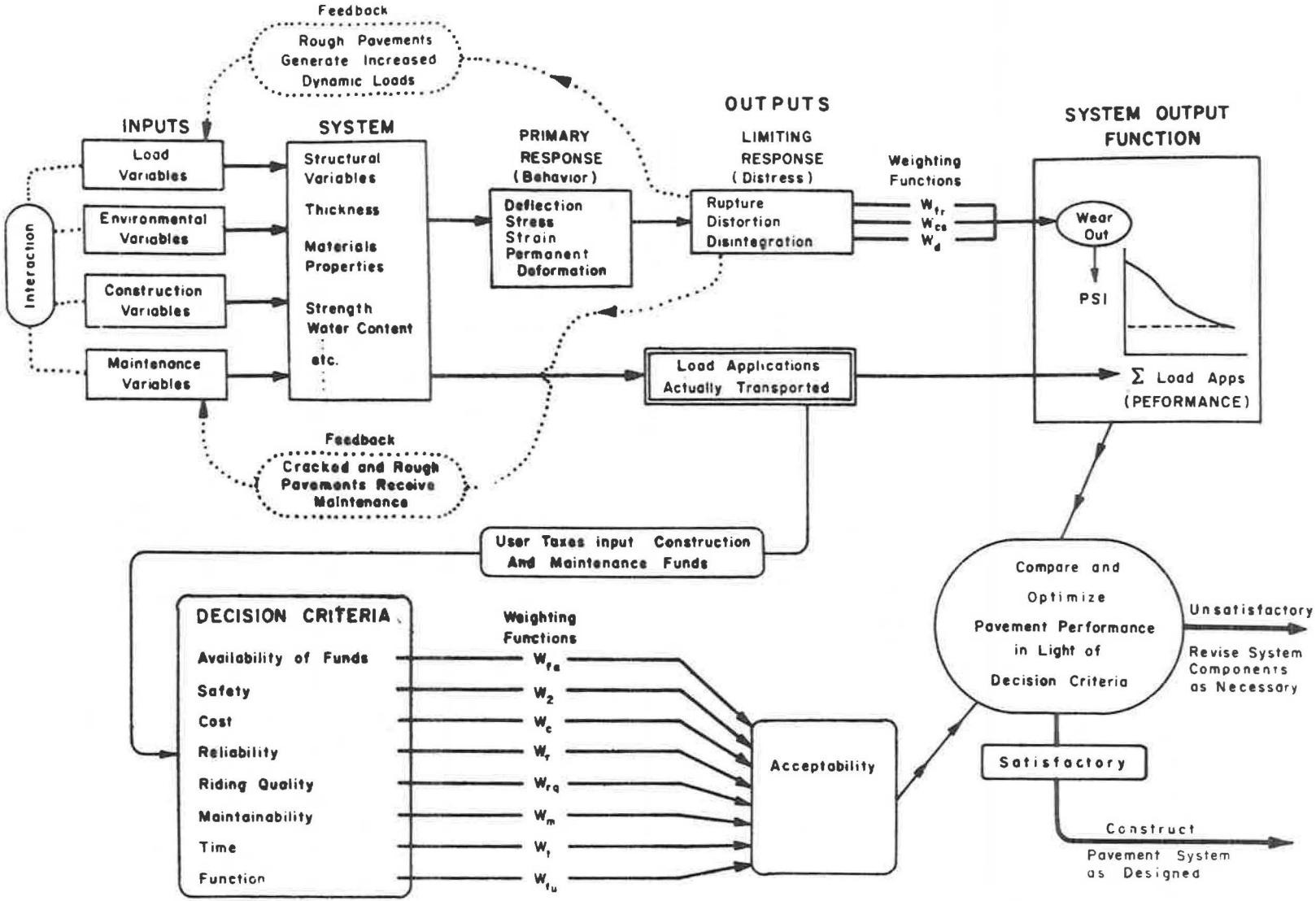

Figure 1. Block diagram of the pavement system (after Finn et al, 1).

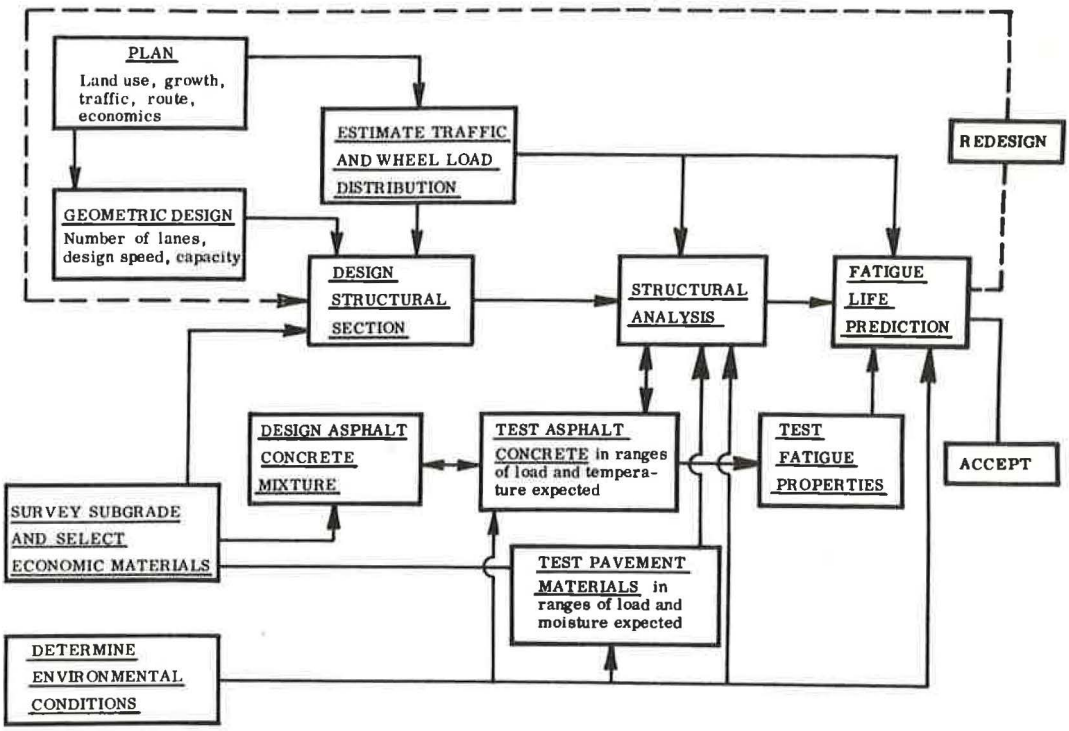

Figure 2. Block diagram of the fatigue subsystem.

THE FATIGUE SUBSYSTEM

A form that a design subsystem can take to consider fatigue is shown in Figure 2 in block diagram form. It should be noted that this fatigue subsystem constitutes only a small part of the whole system (Fig. 1).

The fatigue subsystem shown in Figure 2 can be seen to parallel the classical structural engineering approach, in which a structure is designed, its behavior under its anticipated service conditions analyzed, and its adequacy with respect to some distress criterion determined. This approach is employed because it is realized that the fatigue of asphalt concrete is only one mechanism of a number that can lead to distress within an asphalt concrete pavement structure. Other causes of distress can be analyzed using a similar line of reasoning and their study would form other subsystems to consider—for example, such distress modes as distortion, distintegration or low temperature fracture.

Considering the design subsystems shown in Figure 2, it will be noted that it divides itself naturally into three sections:

1. Preliminary data acquisition—(a) Estimate traffic and wheel load distribution to be served by the proposed facility on the basis of the type of highway, the nature of the area served, and the expected growth of the area; (b) survey subgrade soils traversed by the proposed route and perform routine identification tests; (c) select the most economic materials to be used in the construction of the highway; (d) determine the environmental conditions from available weather records for the vicinity of the proposed highway; and (e) design the asphalt concrete mixture to be used.
2. Materials characterization—(a) Test the asphalt concrete, subgrade soil, and any granular materials to be included in the section to determine their "elastic" properties in the range of service conditions expected in the life of the highway; and (b) test the fatigue properties of the asphalt concrete mixture.

3. Analysis and evaluation—(a) Define the seasonal variation in the stiffness of the asphalt concrete and the moisture content of the subgrade soil; (b) determine the expected response of the asphalt concrete layer in the trial design section to the action of the range of wheel loads and climatic environment; (c) predict the fatigue life of the trial design under the action of the expected traffic volumes; and (d) evaluate the trial design with respect to the adequacy of the section in providing an adequate design life for fatigue. If necessary, select another trial section and reanalyze.

It should be reemphasized that the design procedure is meant to consider only distress that might be caused by fatigue. Protection against other modes of distress must at present be embodied in the selection of the trial structural design.

APPLICATION OF PAVEMENT DESIGN PROCEDURE

The example to be presented is concerned with the design of the structural section for the widened portion of the Ygnacio Valley Road between Walnut Avenue and Oak Grove Road in the city of Walnut Creek and the unincorporated area of Contra Costa County, California. The proposed reconstruction includes the overlay of the existing two-lane pavement plus the widening of the facility to four lanes by the addition of new 12-ft wide traffic lanes on each side of the present roadway.

A full-depth asphalt concrete section was considered for the new construction involved in the widening primarily to alleviate the problems that would be encountered if excavation were required for a thicker structural section. Because the surface grade elevation is fixed by the existing roadway, a conventional structural section could be accommodated only by excavating into the silty clay subgrade soil whose water content increased with depth. It was the previous experience of the Materials Division of the Public Works Department of Contra Costa County that both excavation and compaction difficulties would be met in this situation. A thinner all-asphalt concrete section would not require this excavation, and the anticipated construction problems could be avoided.

A second factor, not considered during the selection of the design section, but nevertheless important to the design deliberations, is the possibility of the occurrence of saturated base conditions if a conventional section were constructed. The reconstruction involves consideration of the use of a landscaped median strip that would be irrigated. Because of the flat topography of the area and the characteristics of the subgrade soil, it is possible that any water reaching the base from the irrigation operation would remain in the section unless expensive positive drainage facilities were provided. A full-depth asphalt concrete section may thus be useful in such a situation.

The steps followed in the design and analysis of the structural section for this project will be briefly presented and ordered insofar as possible to conform to the fatigue subsystem presented here.

Traffic and Wheel Load Distribution

Initially, the only traffic information available for the project was a traffic index of 9.5 (3) that had been estimated by the Engineering Department of the city of Walnut Creek to represent the traffic that could be anticipated for a 10-year period following construction. Using this traffic index, a conventional structural section consisting of 0.50 ft of asphalt concrete, 0.85 ft of untreated aggregate base, and 1.05 ft of untreated aggregate subbase was selected. This thickness of structural section would have required considerable excavation into the silty clay subgrade, as noted earlier. Accordingly, it was deemed appropriate to consider a full-depth asphalt concrete section as an alternative.

Although the design subsystem utilized herein can accommodate detailed traffic data, it was necessary initially to use the estimate provided by Walnut Creek to make a preliminary selection for a full-depth asphalt concrete section to determine whether or not it would be worthwhile to pursue further the design of this type of pavement for the particular circumstances. The traffic index of 9.5 corresponds to 18,000,000 repetitions of a 5-kip wheel load, according to California pavement design procedure (3).

TABLE 1

MONTHLY WHEEL LOAD FACTORS BASED ON W-4 LOADOMETER STUDIES, CALIFORNIA, 1961 to 1966

Axle Load (kips)	2-Axle	3-Axle	4-Axle	5-Axle	6 or More Axles
under 3	2.354	0.224	1.230	0.422	2.104
3 to 7	18.871	16.438	22.275	20.873	23.805
7 to 8	2.127	6.126	7.200	7.062	7.687
8 to 12	4.135	12.700	15.480	16.029	28.362
12 to 16	1.752	6.830	9.210	15.899	21.024
16 to 18	0.569	2.228	3.570	12.402	5.957
18 to 20	0.168	0.397	0.930	2.165	0.973
20 to 22	0.015	0.046	0.075	0.084	0.192
22 to 24	0.008	0.007	0.015	0.029	0.087
24 to 26	0.001	0.004	—	0.008	0.148
26 to 30	—	—	—	0.006	0.198
30 to 35	—	—	—	0.001	—

This value was converted to an equivalent number of passages of an 18-kip axle load (9-kip wheel load) using the equivalent wheel load (EWL) concept of the State of California (3), and resulted in a traffic prediction of 1,600,000 applications of an 18-kip axle load in the 10-year design period. As will be seen, the preliminary full-depth asphalt concrete section selected utilizing these data (approximately 1 ft in thickness) suggested that it would be worthwhile to pursue this approach further. Accordingly, additional traffic data were obtained as planning for the project progressed.

Data obtained for the detailed analysis of the pavement section showed a present ADT of 16,500 vehicles per day, including 185 2-axle trucks, 107 3-axle trucks, 2 4-axle trucks, 126 5-axle trucks, and none with 6-axles or more. The figures represent the results of a traffic count taken on the existing facility. Using these daily figures of truck traffic and monthly wheel load factors determined from the statewide loadometer surveys from 1961 to 1966 (Table 1), the number of applications per month of each of the axle load groups was estimated. These values are given in Table 2.

Several other features of the traffic on the new facility were also estimated on the basis of available information. Because it was known that the major source of truck traffic on this road would be two quarries providing aggregate for construction in the surrounding areas, some consideration was given to the operations in these quarries to obtain the daily and seasonal variations in the traffic. This led to the assumption that the daily variation shown on the California Interstate general purpose route (Fig. 3) would adequately represent the anticipated pattern. The seasonal variation expected was one in which higher traffic volumes would be handled during the summer months, and to include this expectation the monthly traffic numbers given in Table 2 were proportioned accordingly. The values were increased to 1.2 times those shown in May to September inclusive and reduced to 0.8 times those shown in November to March inclusive. At the same time it was concluded that the assumption of a 5 percent annual growth rate in the truck traffic would be consistent with the expected development of the area.

This more detailed breakdown of the anticipated traffic was also analyzed to determine its degree of correspondence with the original estimate. Applying the EWL concept of the California pavement design procedure to the new data results in an actual traffic index for a 10-year design period of about 9.2. In the standard practice this value would be "rounded-up" to T.I. = 9.5, and thus the new data are shown to be consistent with the estimate used in the preliminary design.

TABLE 2

ESTIMATED AXLE LOAD DISTRIBUTION, YGNACIO VALLEY ROAD

Axle Load Group (kips)	Axle Load (kips)	Number per Month	Axle Load Group (kips)	Axle Load (kips)	Number per Month
under 3	3	515.1	18 to 20	19	348.2
3 to 7	5	7924.6	20 to 22	21	18.4
7 to 8	7.5	1955.7	22 to 24	23	5.9
8 to 12	10	4174.5	24 to 26	25	1.6
12 to 16	14	1816.6	26 to 30	28	0.8
16 to 18	17	1913.4	30 to 35	32.5	0.1

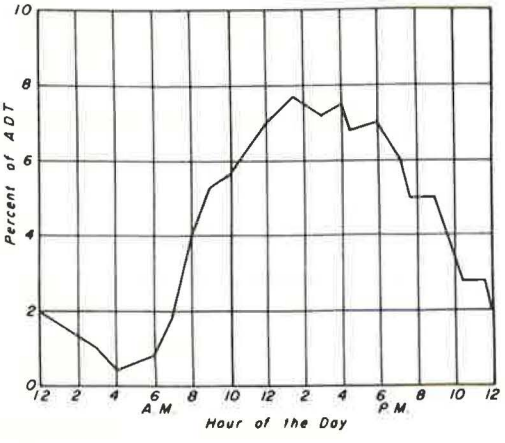

Figure 3. Hourly traffic variation, California general purpose Interstate route.

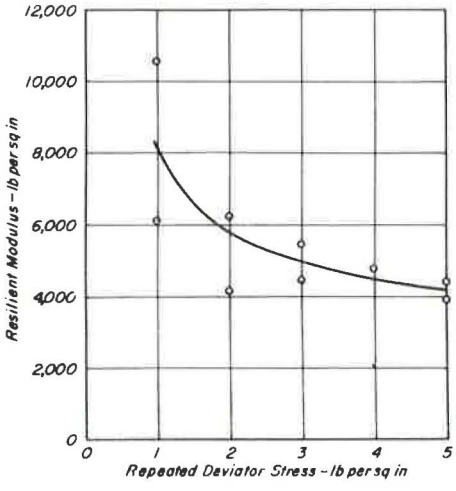

Figure 4. Results of repeated load tests, Ygnacio Valley Road subgrade soil.

Subgrade Soil Survey

The subgrade soil survey was conducted by the Materials Division of the Contra Costa County Public Works Department. Density, water content, and undisturbed samples were obtained at seven locations within the length of the project, including one location beneath the existing pavement. These tests indicated that a uniform subgrade soil—a silty clay—existed throughout the entire length.

Environmental Conditions

A composite weather record for the location was determined from several sources. The average air temperatures and daily ranges were taken from records kept at Buchanan Air Field, which is within 5 miles of the project location. The average wind velocity, solar insolation, and sky cover were obtained from the monthly records at San Francisco Airport and at Concord. The data used in the pavement temperature simulation are given in Table 3

Test Pavement Materials

The selection of a full-depth asphalt concrete section simplified this phase of the procedure to the determination of the properties of the subgrade soil. Resilient modulus

TABLE 3

WEATHER DATA USED IN THE SIMULATION OF PAVEMENT TEMPERATURES, YGNACIO VALLEY ROAD

Month	Average Air Temperature (F)	Daily Range (F)	Average Wind Velocity (mph)	Solar Insolation (Langleys per day)	Sky Cover (sunrise to sunset)
Jan.	46	18	6.2	182	7.0
Feb.	48	21	7.0	287	6.0
Mar.	52	23	8.8	426	5.5
April	59.5	26	9.3	547	4.8
May	61.5	28	9.9	642	3.8
June	66	31	9.8	701	2.0
July	69	33	9.1	685	0.9
Aug.	72	33	8.9	621	1.1
Sept.	66.5	31	7.7	506	1.4
Oct.	62.5	27	6.6	374	3.3
Nov.	54	21	5.8	248	5.3
Dec.	44.5	13.5	5.8	157	7.2

TABLE 4

COMPUTED STRAINS IN PAVEMENT SECTIONS IN AUGUST

Thickness (in.)	Subgrade Vertical Compressive Strain, ϵ_v (in. per in. x 10^{-4})	Asphalt Concrete Tensile Strain, ϵ_T (in. per in. x 10^{-6})
8	5.72	350
12	2.94	167
16	1.90	99

determinations were made over a range in deviator stresses on undisturbed samples recovered from beneath the existing pavement. The resilient modulus is determined from the expression

$$M_R = \frac{\sigma_d}{\epsilon_r}$$

where

M_R = modulus of resilient deformation, psi;
σ_d = repeatedly applied deviator stress, psi; and
ϵ_r = resilient (recoverable) axial strain, in. per in.

Each of the samples was subjected to approximately 40,000 repetitions of each of five repeated deviator stress levels (duration, 0.1 sec; frequency, 20 repetitions per min), and the resilient modulus determined using the resilient deflection corresponding to 25,000 repetitions. The data obtained are shown in Figure 4.

It was assumed that the conditions of density and moisture content at which these samples existed in the field would be those conditions that could be expected to exist under the proposed pavement, and that these conditions would be relatively stable. The results were thus used to characterize the subgrade throughout the entire year.

Poisson's ratio, ν, for the silty clay was not determined in the laboratory; however, for the analyses to be presented subsequently, ν was assumed equal to 0.5. This value would appear reasonable for the expected conditions of the soil in situ.

Design Structural Section

Temperature simulation for this pavement using the data in Table 3 and the method developed by Barber (4) indicated that the highest monthly averages would be experienced in August. Using typical properties of the materials under these conditions, strains were calculated for 8-, 12-, and 16-in. thick layers of asphalt concrete under a 9-kip wheel load with dual tires using layered system elastic theory (5). An iterative procedure was used to ensure compatibility of the vertical compressive stresses at the subgrade and the modulus of the subgrade (Fig. 4). Table 4 indicates the levels of strains obtained in these calculations.

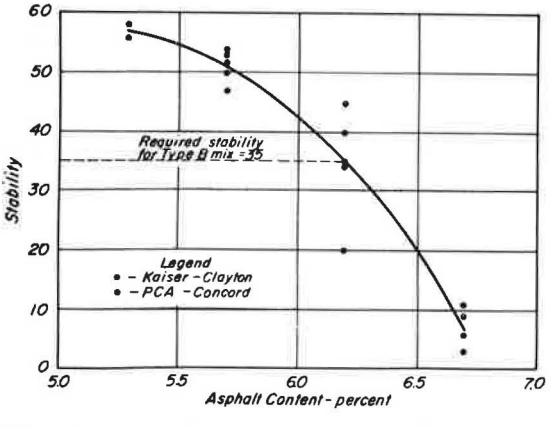

Figure 5. Results of stabilometer tests, Ygnacio Valley Road.

The vertical compressive strain at the subgrade level should be kept below about 6.5 x 10^{-4} in. per in., according to the Shell analysis of pavements designed according to the CBR procedure (6). From Table 4 it can be seen that each of the trial thick-

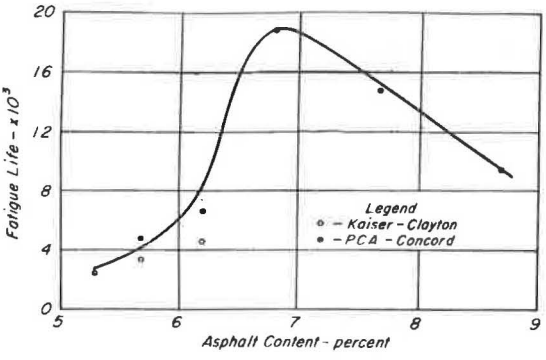

Figure 6. Results of controlled stress fatigue tests at 150-psi tensile stress showing effect of asphalt content, Ygnacio Valley Road.

nesses provides sufficient thickness to achieve this level during the month when the mixture stiffness is at a minimum.

The fatigue behavior of the asphalt concrete is assumed to be controlled by the horizontal tensile strain on the underside of the asphalt bound layer. A strain level of about 150×10^{-6} in. per in. was considered to be a reasonable maximum value based on previous experience because fatigue lives of at least 10^6 repetitions are obtained at this strain level (7). (As noted earlier, the estimated design traffic index of 9.5 corresponds approximately to 1.6×10^6 repetitions of the 9-kip wheel load.) The value of strain for the 12-in. thickness (Table 4) is sufficiently close to this value. Accordingly, this thickness was selected for more detailed analysis.

Design Asphalt Concrete Mixture

Special consideration was given to the design of the asphalt concrete mixture to be used in this pavement to provide a compromise between the stability requirements and requirements for best fatigue resistance.

A mixture was first designed using the standard California stabilometer procedure by the Materials Division of Contra Costa County. The results of the tests are shown in Figure 5. Although tests were performed on mixes fabricated using aggregates from each of the two major sources in the area, the results were treated as one set of data, these aggregates being almost identical in terms of petrography, surface texture, and shape throughout the range of sizes. A 60-70 penetration grade asphalt cement supplied by the Chevron Asphalt Company was incorporated in the design mixture to take advantage of the higher stiffness and consequent longer fatigue life that it would afford in this situation (7). Figure 5 shows that the asphalt content satisfying the stability requirement for Type B mixes (i.e., stability 35 at 140 F) is 6.2 percent. In line with standard California practice, this value is reduced by 0.3 percent to allow for expected field variation, and the design asphalt content is quoted as 5.9 percent.

At the same time, fatigue test specimens were prepared in the laboratory, containing the same aggregates and with asphalt contents ranging from 5.3 to 8.7 percent. Controlled-stress fatigue tests were performed on these specimens. Figure 6 shows the mean fatigue lives determined in these tests at a stress level of 150 psi and indicates that the best fatigue performance would be provided by a mixture containing an asphalt content of 6.7 percent.

The elements of the necessary compromise can be seen by comparing the two mixture designs, i.e., 5.9 percent vs 6.7 percent. The selection of the optimum design, however, takes some other facts into consideration. The stability requirement is based on the necessity of providing adequate resistance to deformation at the highest temperatures to be experienced by the pavement. This criterion, in general, places a maximum on the amount of asphalt that can be incorporated into the mixture. Consideration of the pavement temperature simulation, however, indicates that the lower portion of a full-depth asphalt concrete section will not attain the high maximum temperatures experienced at the surface. Higher asphalt contents can then be tolerated in the lower portion without sacrificing the stability of the layer.

Increase in the asphalt content of a mixture will also provide additional benefits in terms of increased ease of compaction and increased resistance to weathering. Thus, the decision to suggest a higher asphalt content for the mixture to be used in the lower portion of the layer is based on some other criteria in addition to the provision of the

TABLE 5

TRAFFIC WEIGHTED-MEAN STIFFNESS VARIATION, YGNACIO VALLEY ROAD, 10^3 PSI

Month	0 to 4 in.	4 to 8 in.	8 to 12 in.	Month	0 to 4 in.	4 to 8 in.	8 to 12 in.
Jan.	1,720	1,840	1,890	July	175	230	270
Feb.	1,410	1,570	1,640	Aug.	162	210	244
Mar.	1,030	1,250	1,280	Sept.	267	342	389
April	580	700	770	Oct.	480	580	636
May	430	535	600	Nov.	1,030	1,170	1,225
June	245	316	365	Dec.	1,880	1,980	2,020

best resistance to fatigue. On these grounds it was recommended that the uppermost 3 in. of the section be produced of an asphalt concrete containing 5.9 percent asphalt with the lower portion of the layer containing 6.2 percent.

Structural Analysis

The asphalt concrete layer was represented for the purposes of the layered elastic system calculations as three 4-in. layers. The traffic weighted-mean stiffness of each of these layers was obtained by a procedure outlined in the Appendix. The monthly variation of these stiffness values is given in Table 5.

The complete structural analysis of this pavement is greatly simplified by the fact that the tensile strain in the asphalt concrete can be represented as a linear function of wheel load magnitude for any given condition of asphalt concrete stiffness. In this pavement the only layer whose modulus is a function of stress level, and hence wheel load, is the subgrade soil. The variation in stress level in this material is greatly attenuated by the action of the 12-in. asphalt concrete layer. This leads to only small variation in the subgrade modulus with changes in the wheel load, especially when compared with the constant values of stiffness of the asphalt concrete layers in any given month. The number of individual representations of the pavement for the purposes of calculation of the tensile strain in the asphalt concrete need not be compounded by the number of wheel load magnitudes being considered.

The results of the calculation of the tensile strain in the asphalt concrete for the August traffic weighted-mean stiffness values are shown in Figure 7. These calculations were performed taking into account the variation of the subgrade modulus with stress level using an iterative method for solving the stresses in a multilayered elastic system (13). It can be seen from this figure that the results may be represented in terms of the slope of the line relating the tensile strain in the asphalt concrete to the axle load magnitude. This slope has been termed the normalized strain, B, such that

$$\epsilon = BW \qquad (1)$$

where

- ϵ = the tensile strain in the asphalt concrete;
- W = the axle load magnitude; and
- B = the normalized strain, which is a function of the stiffness of the asphalt concrete in the month under consideration.

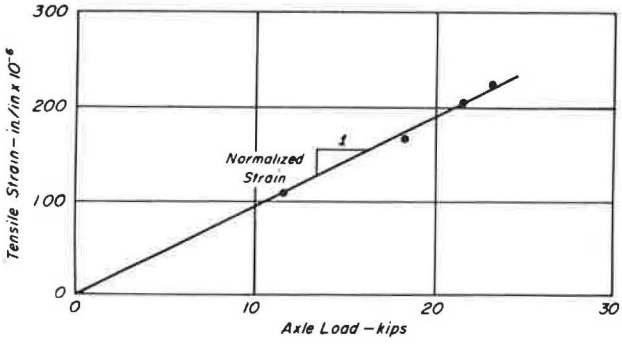

Figure 7. Tensile strain against axle load, Ygnacio Valley Road, August.

Figure 8 shows the results of the structural analysis calculations for the Ygnacio Valley Road pavement presented in terms of normalized strain.

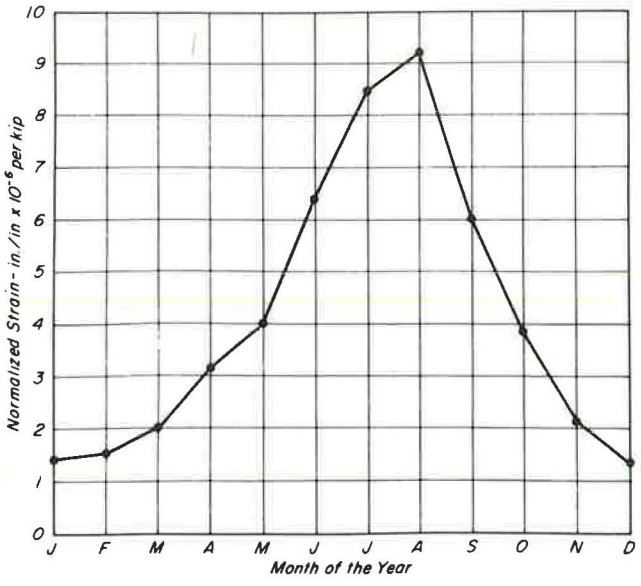

Figure 8. Seasonal variation in normalized strain, Ygnacio Valley Road.

It should be noted that this simplification is not generally applicable, especially where untreated granular materials are included in the structural section. The variation in modulus of base and subbase materials with stress level requires that the iterative procedure be applied for each wheel load magnitude (8).

Test Fatigue Properties

Controlled-stress fatigue tests were performed on laboratory-prepared specimens of the asphalt concrete mixture containing 6.2 percent asphalt. This is the mixture suggested for the lower portion of the asphalt concrete layer where the maximum tensile strains will occur in the field. These tests, performed at a time of loading of 0.1 sec and a frequency of stress applications of 100 per minute (9), yielded the following fatigue equation:

$$N_f = 1.33 \times 10^{-7} \frac{1}{\epsilon_{mix}}^{3.222} \quad (2)$$

where

N_f = number of applications to failure at strain level, ϵ_{mix}; and
ϵ_{mix} = mixture strain, in. per in.

with a standard error of estimate of 0.212.

Fatigue Life Prediction

Prediction of the fatigue life was made using a form of the linear summation of cycle ratios. This compound-loading hypothesis suggests that fatigue failure occurs when

$$\sum \frac{n_i}{N_i} = 1 \quad (3)$$

where

n_i = number of applications at strain level i, and
N_i = number of applications to cause failure in simple loading at strain level i.

Fatigue life prediction simply becomes determination of the time at which this sum reaches unity. A computer solution developed to facilitate computation is summarized as follows:

1. The tensile strain vs stiffness relationship for each axle load was stored (in this case the normalized strain data shown in Figure 7 simplified this step).
2. The tensile strain under each wheel load magnitude was obtained from the appropriate relationship by a numerical interpolation procedure at the stiffness value representing the month under consideration.
3. The fatigue life that would be expected under simple loading at that strain level was determined from the fatigue curve developed for the asphalt concrete. At the same time, the fatigue life corresponding to a 90 percent confidence level was obtained, assuming a logarithmic normal distribution of fatigue life at any strain level (13).
4. The cycle ratio for each of the strain levels (axle load groups) was formed using the number of applications per month of each axle load group (n_i) shown in Table 2 and the fatigue life at each strain level determined from Eq. 3.
5. The sum of the cycle ratios per month was taken and the process repeated for consecutive months until, first, the sum at the 90 percent confidence level reached unity, and then, the sum at the mean level reached unity. This process included the seasonal variation in monthly traffic and the annual rate of increase noted earlier.
6. The fatigue life predictions at the two levels of confidence were taken as the times at which these values were obtained.

The following predictions resulted:

1. The mean fatigue life will be 11.7 years.
2. At a 90 percent confidence level, the shortest probable fatigue life will be 6.6 years.

These predictions indicate that the 12-in. section considered should have adequate resistance to fatigue distress to provide for the 10-year design life required in this highway.

DISCUSSION OF FINDINGS

The reasonableness of the recommended 12-in. asphalt concrete layer can be seen by comparing it with thicknesses indicated by use of other design methods:

Method	Reference	Thickness (in.)
State of California, A	(3)	19.3
State of California, B	(16)	13.5
Asphalt Institute	(10)	13
Shell Group Method	(11)	11
AASHO Interim Guide	(12)	9.5

The State of California design B shown was provided by the Materials and Research Department of the Division of Highways (16) and was based, in part, on deflection predictions based on Dynaflect measurements taken on the subgrade soil at this location.

These comparisons indicate that the design section selected through the use of the fatigue subsystem corresponds reasonably with thicknesses obtained using a number of existing design methods. Because these existing procedures probably embody resistance to other modes of distress as well as fatigue, some confidence that the proposed design is adequate with respect to these other modes is also obtained.

At this point it should be emphasized, however, that an advantage of this design subsystem, as compared to existing procedures, is that it permits detailed consideration of the particular set of conditions under which the pavement is expected to perform because fatigue life is predicted as a function of anticipated traffic, subgrade and asphalt concrete material properties, and environmental variables, and their expected interaction at a specific location.

SUMMARY

In this paper a working model has been presented for a subsystem to consider the fatigue mode of distress. This proposed method permits incorporation of realistic material properties into the design process within the framework of elastic layer theory to define the potential for cracking of the pavement structure under repetitive traffic loading. The subsystem has been shown for conventional materials and traffic to result in thicknesses that are quite reasonable, based on comparisons with other existing design methods. This particular subsystem would appear to have some advantages, however, when compared to existing procedures in that it can be extended to consider loading conditions and material characteristics for which experience is not now available. Moreover, as other subsystems considering additional distress modes become available, this subsystem can be incorporated within the general systems framework shown in Figure 1 because a specific mode of failure has been delineated.

ACKNOWLEDGMENTS

Some of the concepts presented herein resulted from an investigation supported by the Materials and Research Department of the California Division of Highways and the U.S. Bureau of Public Roads. Neither agency has reviewed the research findings.

The fatigue test data were obtained by Dr. J. A. Epps, a former research assistant at the Soil Mechanics and Bituminous Materials Laboratory of the University of California.

Mr. George Dierking of the Institute of Transportation and Traffic Engineering staff prepared the figures.

REFERENCES

1. Finn, F. N., Hudson, W. R., McCullough, B. F., and Nair, K. An Evaluation of Basic Material Properties Affecting Behavior and Performance of Pavement Systems. Paper presented at 47th Annual Meeting of the Highway Research Board, January 1968.
2. Hutchinson, B. G., and Haas, R. C. G. A Systems Analysis of the Highway Pavement Design Process. Highway Research Record 239, pp. 1-24, 1968.
3. Test Method No. California 301-F. Materials Manual, California Division of Highways.
4. Barber, E. S. Calculation of Maximum Pavement Temperatures From Weather Reports. HRB Bull. 168, pp. 1-8, 1957.
5. Warren, H., and Dieckmann, W. L. Numerical Computation of Stresses and Strains in a Multiple-Layer Asphalt Pavement System. Internal Report, Chevron Research Corporation, Sept. 1963 (unpublished).
6. Dormon, G. M., and Metcalf, C. T. Design Curves for Flexible Pavements Based on Layered System Theory. Highway Research Record 71, 1964.
7. Monismith, C. L. Asphalt Mixture Behavior in Repeated Flexure. Report No. TE 66-6, Univ. of California, Berkeley, Dec. 1966.
8. Monismith, C. L., Kasianchuk, D. A., and Epps, J. A. Asphalt Mixture Behavior in Repeated Flexure: A Study of an In-Service Pavement Near Morro Bay, California. Report No. TE 67-4, Univ. of California, Berkeley, Dec. 1967.
9. Deacon, J. A. Fatigue of Asphalt Concrete. DEng thesis, Univ. of California, Berkeley, Dec. 1967.
10. Thickness Design. Manual Series No. 1, The Asphalt Institute, College Park, Maryland, 1963.
11. Izatt, J. O., Lettier, J. A., and Taylor, C. A. The Shell Group Methods for Thickness Design of Asphalt Pavements. Paper presented at Annual Meeting of the National Asphalt Paving Association, Jan. 1967.
12. AASHO Interim Guide for the Design of Flexible Pavement Structures. American Association of State Highway Officials, Oct. 1961.
13. Kasianchuk, D. A. Fatigue Considerations in the Design of Asphalt Concrete Pavements. PhD disseration, Univ. of California, Berkeley, Aug. 1968.

14. Heukelom, W., and Klomp A. J. G. Road Design and Dynamic Loading. Proc., AAPT, Vol. 33, 1964.
15. Van Dratt, W. E. F., and Sommer, P. Ein Gerät Zur Bestimmung der Dynamischen Elastizitätsmoduln von Asphalt. Strasse und Autobahn, Vol. 35, 1966.
16. Letter from Materials and Research Department, California Division of Highways, to Public Works Director, Contra Costa County, Oct. 25, 1967.

Appendix

TRAFFIC WEIGHTED STIFFNESS

Both temperature and traffic vary with hour of the day. Some account of this may be taken through the use of the concept of traffic weighted-mean stiffness (13). The calculation of this weighted mean has been programmed for the computer and a brief outline of the flow of the program will indicate the operations performed.

1. The weather data for the locality, the variation of the traffic with hour of the day, and the mixture properties are stored. Mixture properties include properties of recovered asphalt (penetration and ring and ball softening point), asphalt content, aggregate specific gravity, percent air voids, and volume concentration of aggregate.
2. The temperature at 12 midnight is calculated using Barber's procedure (4).
3. Mixture stiffness using the procedure developed by the Shell investigations (14, 15) is computed corresponding to this temperature and a specified time of loading.
4. The procedure is repeated for each hour of the succeeding 24 hours.
5. The arithmetic mean value of the two hourly values for the stiffness of the asphalt concrete is taken as the hourly mean stiffness, S_i.
6. The traffic weighted-mean stiffness, S_{tr}, is calculated from

$$S_{tr} = \frac{\sum_{i=1}^{i=24} S_i \cdot tr_i}{100}$$

where tr_i = traffic, in percent ADTT, in the hour i.

Stiffnesses calculated in this way have already been given in Table 5 for each month of the year and for the depth considered. The variation of mixture stiffness with depth (at a time of loading of 0.015 sec) is shown in Figure 9. Figure 10 shows the range of stiffnesses that can be expected throughout the year.

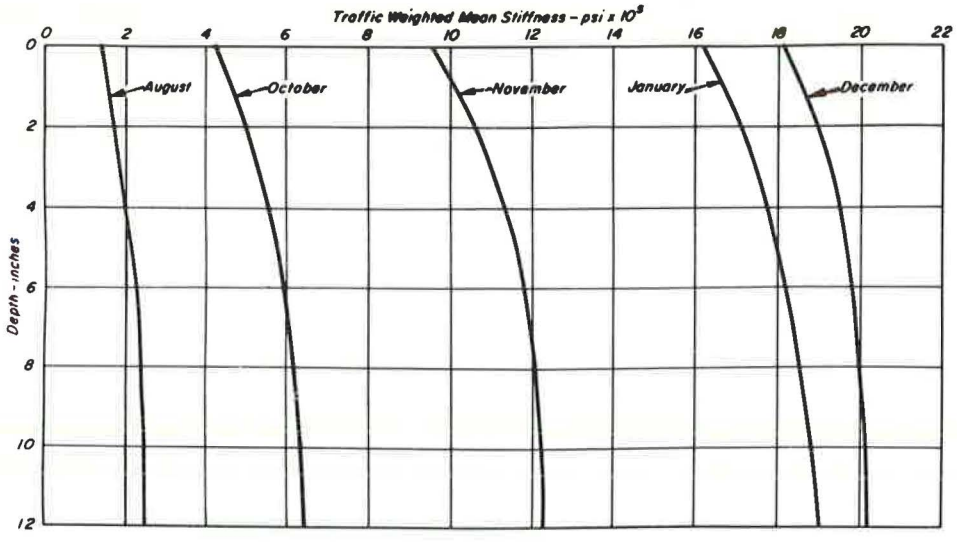

Figure 9. Traffic weighted-mean stiffness of asphalt concrete vs depth for various months during the year.

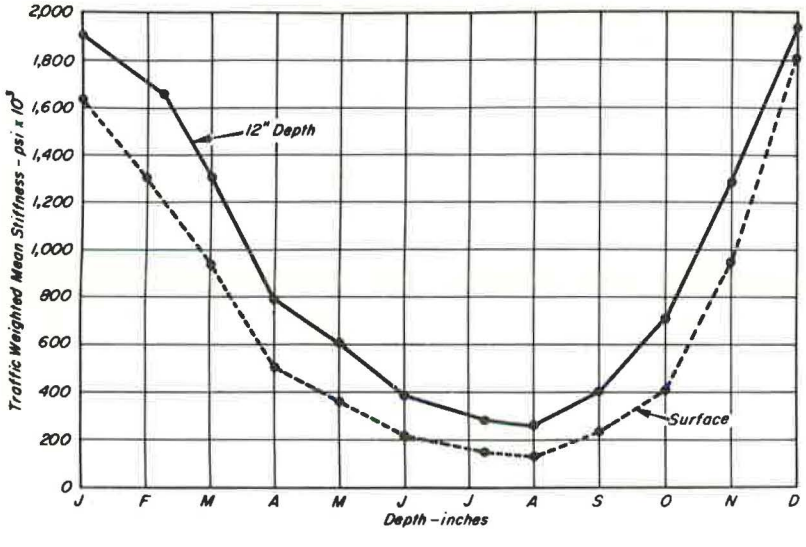

Figure 10. Variation of traffic weighted-mean stiffness of asphalt concrete throughout the year, both at surface and 12-in. depth.

An Integrated Approach to Analysis and Design of Pavement Structure

A. C. LEMER and FRED MOAVENZADEH, Department of Civil Engineering, Massachusetts Institute of Technology

The nature of general engineering decision-making is discussed in terms of three phases: goal formulation, search, and selection. Pavement design is discussed within this logical framework. It is argued that only by using an orderly and well-documented approach to design and analysis will the pavement field be able to keep pace with rapidly expanding engineering technology. Some explicit search and selection techniques are suggested for both their immediate usefulness and as examples of the many new tools becoming available through the use of the computer. A hypothetical example is described to demonstrate the application of the ideas in the paper.

•PAVEMENT design is a specialization of engineering design and has problems that are specialized examples of more general design procedures. By beginning with the general problem-solving and decision process, one may gain insight into what the requirements are for a rational and logical design procedure, and how these requirements may best be met in pavement design. The desirability of such a rational and logical basis for design is threefold:

1. To make the valid personal experience of the individual designer available in a useful form to all members of the field;
2. To keep pace with rapidly changing materials technology, and take full advantage of the opportunities offered by modern sciences; and
3. To allow optimal use of the potential benefits of the computer and the possibilities for man-machine interaction.

With these thoughts in mind, a general model of problem solving is first defined. This model is then used as a skeleton on which the body of the pavement design process is built.

One may identify three principal phases in the problem-solving process: goal formulation, search, and selection (11).

Goal formulation includes identifying the problem and establishing in some explicit form the objectives of solution. The nature of the results to be achieved are specified with the desired level of achievement. For pavements, specification might include safety or dependability. The formulation of the goal statement is difficult because there is often no easy way to measure the level of goal fulfillment, and attempts to define and evaluate goals are often subjective, changing with time and personality.

In describing the performance of a proposed solution to a problem, a set of value-effected variables is used. These are variables over which the designer exercises some control and by which he arrives at an estimate of how well the solution satisfies the goal statements. In the simplest case, goal statements may be constraints on these value-effected variables, exemplified in the case of highways by serviceability or traffic capacity. Specific design requirements are stated as levels of value-effected variables that must be achieved by a satisfactory solution.

Paper sponsored by Committee on Theory of Pavement Design and presented at the 48th Annual Meeting.

Search is a process by which solutions to these specific requirements are generated. The solutions are specified by values of decision variables, such as pavement thickness or modulus of elasticity of the materials that the designer chooses. Search procedures are as simple as the standard design of steel tension members or as esoteric as nonlinear optimization programming.

Selection follows after a series of possible actions is accumulated. The consequences of actions are predicted, evaluated in terms of the value-effected variables, and compared with the goal statement. A rank ordering of the actions is established by this evaluation. Rationality then dictates the selection of the first-ranked alternative.

A final phase of the model is the goal and search revision that becomes necessary as new information becomes available through observation of the results of selection and implementation of the action. Success or failure of a new technique or material prompts a change in the designer's perception of what is possible, or leads to a revision of the search-selection methods to provide a better prediction of the consequences of actions. For example, research may reveal that asphaltic pavements are best characterized by viscoelastic rather than elastic models. Implementation of this finding requires no change in the overall framework of the process. This phase makes the problem-solving process a dynamic process—each part changes with time, personality, and changing perception.

THE HIGHWAY PAVEMENT SYSTEM

This problem-solving process may be used to organize pavement design decisions. While the following discussion is a general approach to the problem, specific suggestions are made to assure immediate usefulness of this framework. Wherever possible, these suggestions will be concrete and developed; where this is not possible, those areas in which research will be most helpful are indicated.

Goal Development

Highways are basically a public commodity, used by society as a whole. It seems most logical that one should derive the specific goals of the highway pavement from those more general goals of society. Assuming that the society desires to make the optimal use of its resources to achieve the greatest overall benefit, a specific statement of the purposes of the designer aware of this goal might be as follows: The designer should provide a surface that will accommodate transportation at the desired level (speed and volume), with a high degree of economy and reliability, and for an optimum time as governed by current resources and future expectations. More specifically, the primary concern of the pavement designer is to provide a structure possessing adequate serviceability qualities throughout its design life (8). Such adequate qualities will produce a pavement that is ridable, safe in terms of comfort and frictional characteristics, and that will maintain its structural integrity. These qualities should be provided at low cost to society.

These statements begin to define the goal space; to place these statements in a convenient form, a tree diagram may be used (Fig. 1). Such a diagram is a plan of the goal space and is helpful in that it indicates not only the particular items to be considered, but also a structural relationship among the items. It must be realized that the tree is something of an oversimplification; that is, unconnected items will often have important effects on one another. Further, as indicated before, the problem at hand is but a small portion of a larger one, and parts of this larger problem will have some influence on operations and decisions in pavement design.

The pavement designer, then, is concerned with the description and selection of the action that will fulfill the requirements represented in these goals. The goal space, as shown in Figure 1, is a framework for evaluation and selection. This procedure will be discussed later.

Search

The object of a search technique is to generate possible solutions to a problem. While there are currently a number of pavement search techniques in the form of

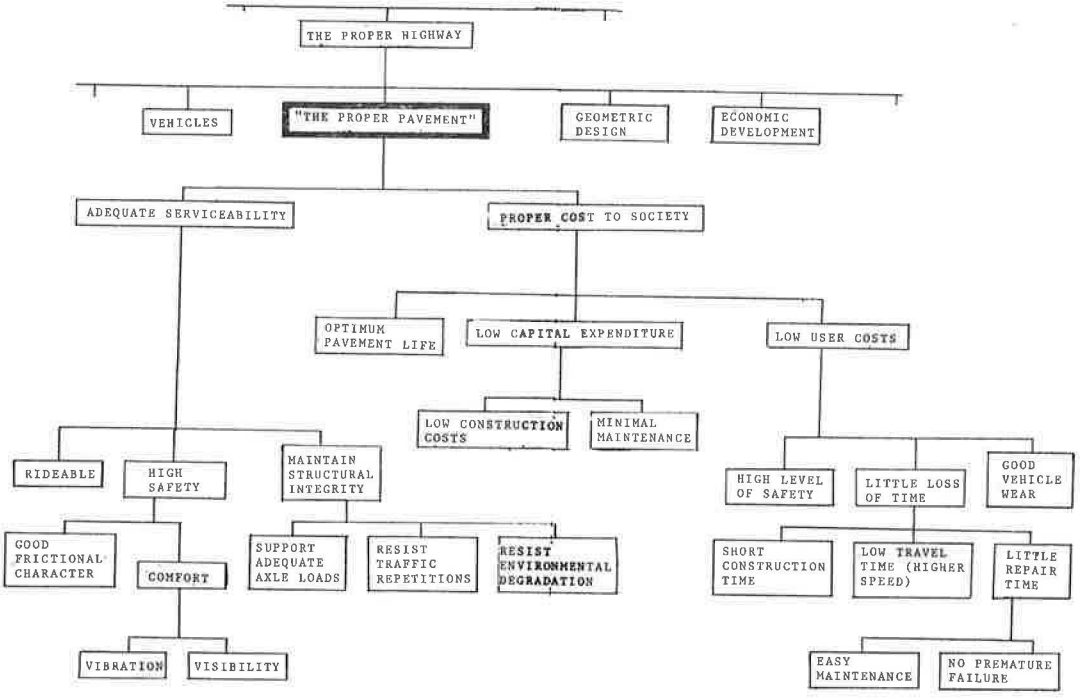

Figure 1. The highway pavement goal space.

standard design procedures, it is desirable to have a technique that will accommodate new technology as it becomes available and that will act as a prod to the development of new ideas.

One such technique is that of hierarchical decomposition (2). This technique is essentially a categorizer of the areas of concern within a specifically stated program of requirements. Briefly, a problem is represented as a linear graph composed of nodes, representing the requirements, and paired links between nodes, representing connections and relationships among requirements. Decomposition of this graph—the problem—presents the designer with a series of smaller and, it is hoped, more tractable subproblems. Solutions to the smaller problems are combined and adapted to build an overall solution to the problem. Concentration on any one of these subproblems will produce a solution that is well suited for that subproblem and that, through systematic consideration of the remaining concerns, is expanded to become a complete solution.

As specific application, a list was prepared of 47 causes for unsatisfactory performance of a pavement. This list was accumulated by examination of texts (3, 15) and discussion with people in the field of pavement design. This list was evaluated for the relationships among requirements, as subjectively viewed by the authors, and submitted for computer decomposition.

The computer decomposition is shown in Figure 2. The actual list of items (at the lowest level of the tree) is the only direct output, and it has been convenient to put some descriptive labels on the upper portions of the branches. These labels are intended to be helpful guides and not perfectly accurate descriptions of the groups they cover.

The first point made by this decomposition is that the designer should consider on an equal basis theory (design and planning) and practice (construction and maintenance). The divergence between the assumptions of design and analysis and the actual field condition is often forgotten or ignored. The engineer forgets the plan when it leaves the office. At best, this divergence is rationalized by large factors of safety.

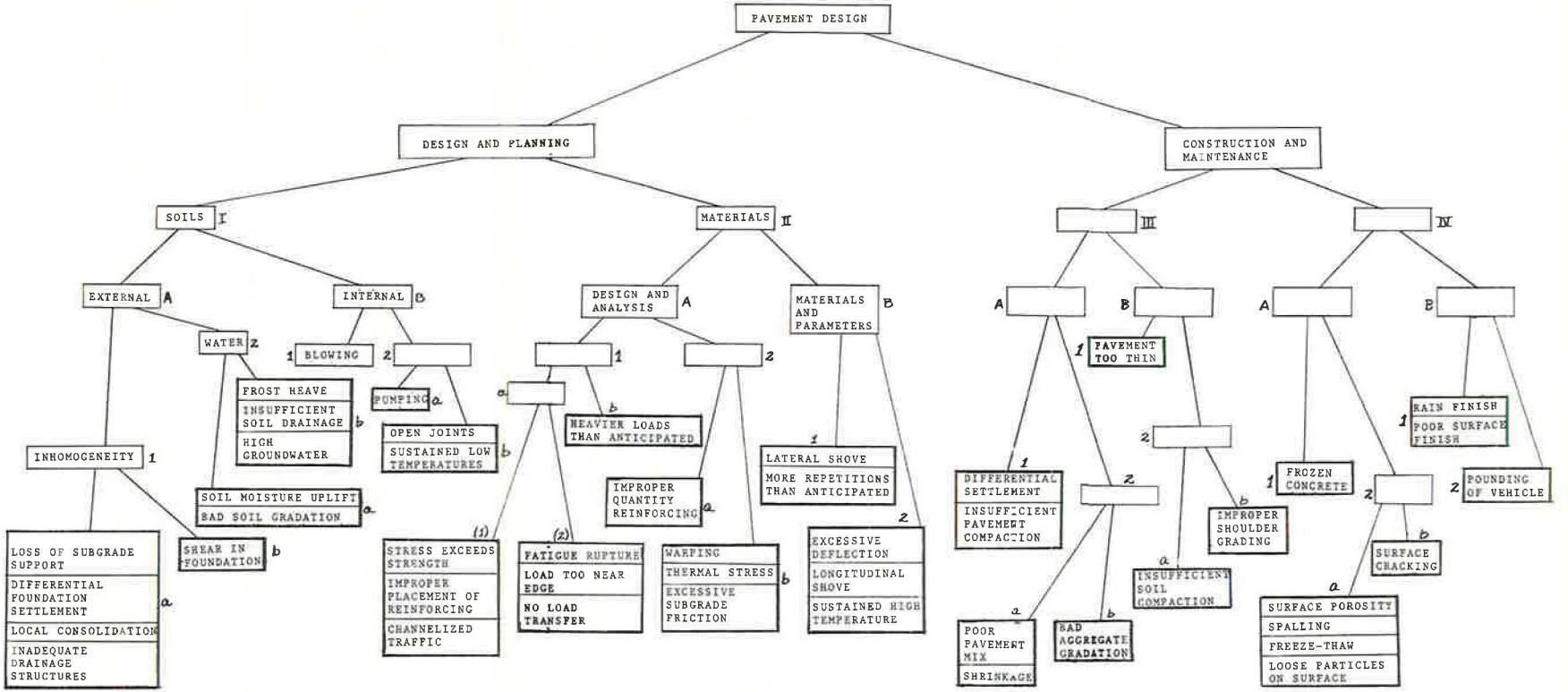

Figure 2. Pavement search guide.

The entire chart will not be discussed in this paper; the items in it are straightforward statements of what a pavement should not do in order to be satisfactory. The designer will have certain preferences as to which of the lowest level requirements are of greatest importance. These preferences are established by the problem at hand, as it is perceived by the designer. For example, in an area of unfavorable geological conditions, the designer may feel that the group IA1a in Figure 2 is the principal concern because the local soils are quite varied and poor in quality.

Having identified his principal area of concern, the designer will generate an action—propose a rough design—that emphasizes a solution to the special problem. He then will expand his concern to include related requirements, check for compliance, and modify where necessary. Finally, he will have a complete design that reflects his feelings on the relative importance of the various requirements.

This process may be repeated, using new ideas at the same starting point or starting at another point, to generate a series of possible alternative actions. Each action will be adequate to satisfy the overall requirements of the problem while emphasizing one portion. One of this series of actions is chosen for final implementation.

Selection

Two questions must be answered in the selection process: (a) How is an action described in order to make it operationally comparable with other alternatives? and (b) How are these actions measured and compared with respect to goal fulfillment? These questions call for measures of performance; the quality of performance determines the degree of goal fulfillment for the pavement.

In Figure 1, the goal space, one sees a diversity of concerns. These concerns may be separated into four broad categories: (a) the physical state of the pavement—its riding quality; (b) the passage of time and its effects on the pavement and its economics, i.e., rising costs and physical deterioration; (c) the elements of chance that enter the real-world problem, as with materials variability; and (d) the capital expenditure required. Associated with each of these broad categories are a number of lower-level parameters that directly describe the pavement system for design and construction.

The primary task is to go from these description parameters, the decision variables, to the goal variables. The following paragraphs suggest methods for considering the four goal categories that are, in fact, interrelated and perhaps inseparable.

Performance and Time: Serviceability—The purpose of a pavement design method is to provide a specific selection of materials, combined and structured in a specific configuration, to satisfy a specific set of environmental and service requirements. Of the various methods currently used, only those based on the serviceability concept offer any promise of usefulness for a rational selection of design alternatives. Other methods generally consider only one type of load.

The concept of serviceability and a present serviceability index were proposed and developed by AASHO in 1958. The idea was to develop a description, a single-number serviceability index, for a pavement in terms of its ridability as experienced by the user, and then to be able to design for a desired level of serviceability over a specified period of time.

A new pavement is said to have an initial level of serviceability, represented by a present serviceability index, PSI_0. As time and traffic pass, the quality of the pavement deteriorates until it reaches some value considered and defined to be the minimum acceptable. At this level, PSI*, the pavement is said to have failed and is in need of extensive repair. The length of time required for this to occur is the failure age, A*.

Serviceability is defined in terms of human response; it is judged by the discomfort imposed upon the user. Several methods, of varying degrees of objectivity, have been suggested and used to evaluate this discomfort (1, 9). Research is still needed to perfect a technique.

Once a definition and measurement are developed, the next step is to determine those physical properties that affect serviceability for a pavement. Various investi-

gators have presented a variety of analyses using qualities such as longitudinal profile and degree of cracking and patching (4, 5, 7).

Finally, experimental data must be gathered to develop predictors of serviceability history as a function of design decision variables, such as material parameters and layer thickness. From data thus gathered (AASHO Road Test, Canadian Good Roads Association), design methods are developed (10, 11).

The general area of serviceability and the factors describing it require much research. If clear identification can be made of those factors of a pavement that define and influence serviceability, then theoretical models may be developed to predict the behavior of these factors as a function of materials, design configuration, and environment. The primary shortcoming of the design procedures developed from the road tests is their lack of general applicability. New materials and methods may not be used, and the methods have limited usefulness in new climatic situations.

Research should thus be directed toward finding general ways to describe the factors influencing pavement performance and to developing valid measures of these factors. Then, more accurate models must be formulated and put into useful form to allow the prediction of performance for any material and design-construction-environment combination.

The Role of Chance: Reliability—In dealing with the real world one is faced with the variability of nature. To a very large extent, the parameters of serviceability and failure age may be considered as random variables. The elements of chance and uncertainty must be considered in the rational design process.

These elements of chance may best be handled with the technique of realiability analysis, and the consideration of reliability as a design parameter. Reliability may be understood as the ability of a system to provide satisfactory and trustworthy service—the measure of reliability is a probability. Reliability is the probability that the system will perform in a satisfactory manner, for at least a given length of time, under a prescribed set of conditions (6). The framework for such an analysis is the mathematical description of the system, as used for design, into which the input data are entered as probabilistic functions derived from experimental and empirical observation. An accurate description of each requirement placed on the system and of the capabilities of the system to meet these requirements is needed.

In general, five specific elements are necessary for a reliability study: (a) a complete specification of the system in terms of its functional components, (b) a list of the objectives that the design is to fulfill, (c) a set of failure criteria, (d) a list of possible failure modes and the manner of their occurrence, (e) probabilistically stated data on the expected service conditions.

The first four of these elements may be seen to be essentially identical to those discussed previously in constructing the problem-solving process. Components are the description of a specific action. Objectives are the value-effected variables of goal specification. Failure modes are particular ways in which a loss of serviceability—the criterion—can occur.

Data on service conditions are gathered in the laboratory and in the field and fall roughly into categories of materials behavior and environmental variation. Concrete strength and subgrade support are representative of the first group; weather and traffic fit the latter.

Economic Analysis: Cost—It is not within the scope of this paper to review current methods in engineering economic analysis or to attempt to develop some new concept of economic analysis for pavement systems. It should be pointed out that this analysis, difficult for standard pavement types, is made more so by the introduction of new design possibilities. If consistency is maintained with the other goals of the highway pavement, consideration must be given to the ultimate economic value of developing new technology.

The implementation of a pavement action is in fact an experiment whose outcome will affect future decisions. The cost of implementing an action must be ultimately justified by the returns it brings. These two ideas must be jointly considered in the economic analysis. It is felt that some guidance in this area may be found in the use of Bayesian decision theory.

The Selection Process

The preceding discussion is directed at prediction and evaluation, the preliminaries of selection. In the actual process of selection, the decision-maker is faced with the problem of comparing the diverse measures of cost, serviceability, and reliability, along with any number of other minor criteria in the form of other scales of measurement and biases as to the relative importance of each measure.

An explicit selection process is now required. This process should be able to accommodate the multidimensional evaluation of actions and to work with a recognition of the complex nature of the goal variables. The procedure should require as little quantification of opinions and feelings from the decision-maker as possible and should at each point indicate clearly the considerations of a choice. One such procedure is the goal fabric formulation (12). The goal fabric analysis proceeds as follows:

1. Goals are listed and their interrelation and structure are determined. This step yields the goal fabric (Fig. 1).
2. The pairs of alternative actions are mapped by their consequences onto the goal fabric.
3. Following the structure of the goal fabric, dominance checks are made to determine at each level which of the two alternatives is preferred. Dominance is determined by greater value, either objectively as with dollars or subjectively as with aesthetic quality.
4. Comparison of the paired preferences yields a rank ordering of the set of alternatives. Rationality implies selection of the first-ranked action for implementation.

Review

The completion of the goal fabric analysis marks the end of the first stage of the decision process. At this point, a review is warranted to state concisely the results of the foregoing discussion.

1. A general statement of goals for the highway pavement is formulated, and goal variables are identified. An expanded structural presentation of goals is made.
2. A search technique is suggested as a means for structuring the design process and suggesting innovation in design alternatives.
3. While not specifically discussed, pertinent decision variables are suggested by the search presentation and the subsequent development of prediction tools. Decision variables include such quantities as material parameters and layer thickness.
4. Prediction-evaluation techniques are presented to allow the forecasting of consequences of an action and the description of these consequences by value-effected variables of cost, reliability, and serviceability.
5. A selection technique is suggested that makes possible the comparison of multidimensional evaluations and places the objective and subjective criteria of preference within an orderly framework.

New Directions: Goal Revision and the Computer

Before finishing this discussion some mention of the aspects of goal revision and the conduct of problem-solving within the computer environment is desirable.

Goal revision occurs as new technology becomes available (in the form of new materials or new understanding of system behavior), as each decision implemented in the real world generates data on performance, and as each cycle of the process gives the decision-maker greater insight into what is reasonable to be expected and possible to achieve. In this aspect the problem-solving is a sequential chain, as mentioned previously, and includes, as possible actions, data collection and further research to be considered with their costs and possible benefits. As suggested, the techniques of Bayesian decision theory offer promise in this area and have been given preliminary investigation by some researchers (8). The computer is invaluable in handling data.

EXAMPLE

The presentation of an example for highway pavements is a difficult task. On the one hand, an example may help to clarify and illustrate the discussion; on the other hand, a great deal of the data and techniques needed for the sucessful construction of a good example are not yet developed. Hence, the following is suggested as illustrative but by no means rigorous.

Assume that it is desirable to build a highway in a developing subtropical country. The estimate of traffic, for a 40-year period, is assumed to be absolutely certain, and is taken from the PCA thickness design manual examples (13). In a real situation, traffic would be estimated with growth rate and statistical prediction and might be specified in probabilistic terms. The 40-year design period has been specified by economic growth considerations, as most desirable for the country as a whole.

The goal structure previously described will be used. In general, the designer may find it desirable to develop his own specification of goals. Note that the difficulties of maintaining the pavement in sparsely populated regions imply the desirability of a low level of maintenance throughout the 40-year life, and that political expediency places a premium on fast construction.

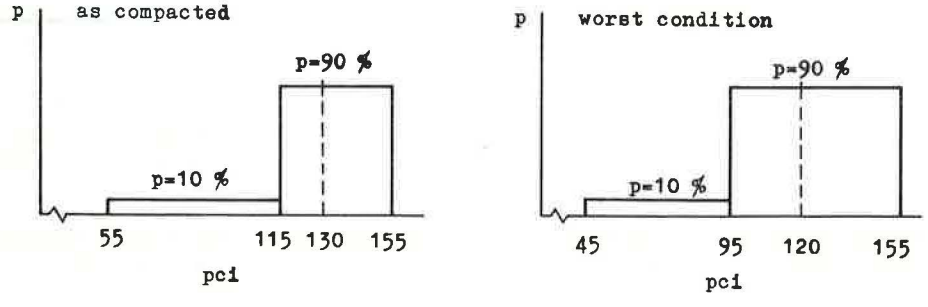

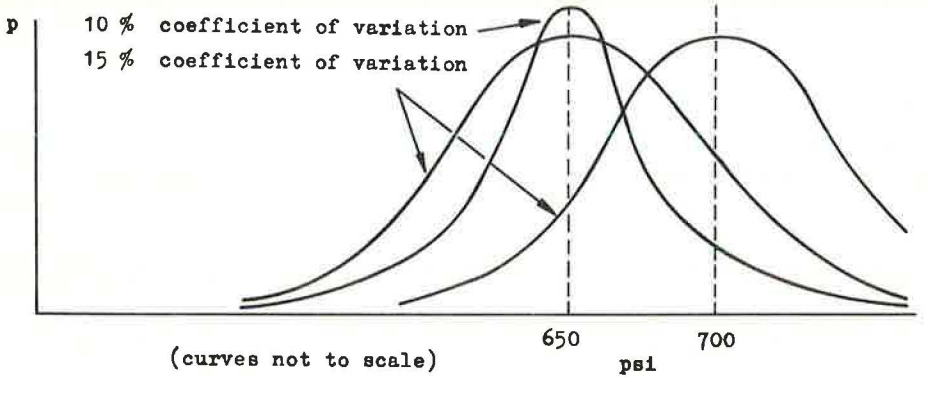

Figure 3. Probability distributions.

Phase one of the search most logically begins with the more standard types of pavement action, in this example, portland cement concrete. Standard design procedures are readily available, and these actions require little innovative thought. The first actions will be designed using the PCA method, which is based on the Westergaard stress analysis. This basis makes the method well suited to the requirements discussed previously for the rational scheme and the reliability analysis. It has been observed that a pavement of this sort, properly designed and constructed, will resist deterioration due to loads and will be most susceptible to failure caused by environmental effects, in this case, marked by rain and high temperatures.

Data are gathered in the form of distributions of probability of occurrence. One may design on the basis of mean value and use the distributions in the reliability computations. Necessary parameters are as follows (Fig. 3):

1. Combined k—The subgrade is susceptible to climatic and seasonal variations, and hence two distributions for k, subgrade modulus, are assumed. The first of these indicates the condition of subgrade and subbase as compacted and normally maintained. The second indicates the worst conditions, brought about by a critical combination of spring temperature and precipitation conditions. From climatic analysis it is found that there is a 30 percent probability that this latter condition will occur during the 40-year design life. The low k value "tail" on each of these two distributions accounts for the possibility of soft spots due to soil inhomogeneity and construction error.
2. Concrete modulus of rupture—This is the normal probability curve typically used in quality control. It is assumed that the use of the modulus of rupture, as determined from three-point bending tests, is valid for predicting the behavior of the concrete in service. In the first design, a coefficient of variation of 15 percent of the mean strength is used to reflect normally available quality control.
3. Trial depth—The possible variations of slab thickness due to construction practices should be taken into account, for these variations would have some effect on the stresses. For the sake of simplicity, however, these variations are ignored in this analysis.

By following the example in the PCA manual, one can eliminate the actual design computations, and the reader is referred to this publication. The first three pavement actions are satisfactory according to the design method. The first design is a 9-in. thick slab. Reliability computations are given in Table 1. Induced stresses are found from charted results of the Westergaard analysis. Allowable stress ratios for the given numbers of repetitions are experimental results. Probabilities are the normal probabilities that the specified concrete will have a strength less than or equal to the

TABLE 1

RELIABILITY FOR DESIGN 1

Axle Load (kips)	Induced Stresses (psi)				Expected Repetitions	Max. Allow. Stress Ratio	Probability Strength				Failure Expectation
	k = 50	k = 95	k = 115	k = 155			50	95	115	155	
30	362	312	300	282	3,100	0.68	0.095	0.024	0.016	0.008	0.023
28	342	296	285	267	3,100	0.68	0.066	0.013	0.009	0.004	0.016
26	325	276	260	244	6,200	0.66	0.053	0.009	0.004	0.002	0.009
24	300	255	246	232	163,000	0.55	0.140	0.022	0.019	0.009	0.014
22	275	243	234	221	639,740	0.50	0.152	0.047	0.024	0.019	0.023
54	405	346	330	315	3,100	0.68	0.288	0.075	0.047	0.027	0.069
52	395	335	320	305	3,100	0.68	0.236	0.055	0.034	0.019	0.044
50	375	323	310	294	30,360	0.61	0.359	0.109	0.072	0.042	0.077
48	368	313	303	289	30,360	0.61	0.352	0.079	0.059	0.036	0.071
46	350	300	294	281	48,140	0.59	0.281	0.076	0.061	0.038	0.069
44	340	287	276	264	150,470	0.55	0.367	0.095	0.064	0.041	0.078
42	325	278	261	249	171,360	0.55	0.271	0.068	0.037	0.021	0.074
40	315	261	249	237	248,060	0.53	0.288	0.054	0.032	0.019	0.044
										Total	0.611

Reliability = 39 percent

failure stress, equal to induced stress divided by allowable ratio. Failure expectation is the probability of failure. That is,

$$\text{expectation} = P(\text{strength} \leq \text{cumulative applied stress}) \times P(\text{stress} \geq \text{computed value})$$

At the 30-kip axle load

$$\text{expectation} = 0.70 \left[\frac{1}{2}(0.095 + 0.016)(0.10) + \frac{1}{2}(0.016 + 0.008)(0.90)\right] + 0.30 \left[\frac{1}{2}(0.095 + 0.024)(0.10) + \frac{1}{2}(0.024 + 0.008)(0.90)\right] = 0.023$$

Because deterioration is a primary concern, one possible action is to try closer quality control. Furthermore, there is strong indication that closer control will yield some net savings in materials. The second design is a repeat of the first, using a 10 percent coefficient of variation for concrete strength. Reliability computations are similar to those shown previously.

In an effort to realize some possible savings, the third action is an $8\frac{1}{2}$-in. slab of higher strength concrete, and again normal quality control is used. Computations are again similar.

No meaningful statement of costs is possible at this level of abstraction. The design assumptions imply that no maintenance will be necessary during the 40-year life, although practical experience indicates that this is not so. Savings might occur through reduction of waste in the second design (tighter quality control). The third design includes a $5\frac{1}{2}$ percent reduction in materials volume, but an increase in concrete strength requires an increase in cost for extra cement.

The next standard strategy is asphalt paving, following Asphalt Institute methods (3). A 20-year life is assumed and consideration of a resurfacing will be included, although the implicit assumption of no other extra maintenance is again made.

The traffic data are converted to a design traffic number of 248 for use in the design charts. Using published correlations of the subgrade support modulus k and the CBR value, one finds that the mean values for average and worst conditions are, respectively, 4.8 and 4.2. For the 20-year period, it is assumed that the probability of the worst condition is 0.15, half that for the 40-year period.

The initial design is full-depth asphalt concrete. It is found from the design chart that 10 in. are required for normal conditions, 11 in. for the worst condition. The 10-in. design is chosen, even though some reliability is sacrificed for economy.

The design method used is highly empirical, is based on the AASHO Road Test data, and represents a mean value curve-fitting of points. Some interpretation is required to get reliability. It has been observed (4) that for heavily traveled asphalt pavement deflection should be kept below a maximum of 0.050 in., as measured in the Benkelman beam test, if deterioration due to wheel loads is to be avoided. If this requirement is met, environmental factors will be the chief contributors to failure. These factors are supposedly accounted for in the design method. The CGRA data (4) are used to estimate the load resistance, and mean deflections and standard deviations are evaluated. Then the probability of load failure, assuming the normal distribution, is easily computed.

Reliability may then be computed in a manner similar to that shown for concrete pavements. Quality control of the pavement mix has been implicitly included in the variance of the deflection measurements.

In this hypothetical example, any of the foregoing alternative actions might require the development of a complete set of skills and supply capacities within the country,

because no large-scale asphalt or portland cement concrete production facilities or heavy construction equipment are immediately available. Hence, search for an innovative action appears very desirable. Figure 2 may be used, although in general the designer would apply the decomposition technique to his specific problem. One may simply overlook entries such as "frozen concrete," which are not particularly applicable in this problem. In the concern for low maintenance level, one notes that the foregoing standard actions are most susceptible to surface deterioration; one enters the chart at block IVA2a. The elimination of surface porosity, spalling, and related problems would be most beneficial. It is beyond the scope of this discussion to try to develop a rational means for designing an impermeable surface. The properly designed topcoat will provide a tough and impervious surface of good riding characteristics. Reliability would be computed on the basis of loads and surface wear.

Another approach to search might be through the desire for rapid construction. Perhaps precast concrete slabs would be a solution; they have an additional advantage of closer quality control and lead to possibilities of greater durability. Looking over the search tree, one sees that most of the problems are handled through materials control in the plant. Soils problems and subgrade support must be dealt with. One might try supporting the slabs on sills, which will act as strip foundations for a simply supported beam. If it is prestressed, a 4-in. thickness (assuming 5,000-psi mean compressive strength concrete is used) is found to be adequate. Reliability is here based on stress exceeding strength in the slab.

Table 2 summarizes the actions suggested and the scales by which these actions may be evaluated and compared. The level of design confidence indicates the designer's confidence in the design method and thus in the design. The reliability measure is as computed for failure modes assumed in design. The cost parameter would normally be some dollar value of total or annual cost. Special features indicate the entry to search, i.e., the special features on which the design is based. Fear of failure indicates the items not included in the reliability measure that are likely to cause trouble.

Rank ordering by preference is accomplished by comparing pairs of actions on the goal fabric. For example, action 2 is clearly preferred to action 1; all measures of goal achievement for the former are greater than those for the latter. Comparison of actions 2 and 4 is more difficult; whereas design confidence and reliability are lower, the design is more inclusive of possible failure factors, and costs might prove lower.

TABLE 2

PAVEMENT ACTIONS

Action		Level of Design Confidence	Reliability		Cost Parameter	Special Features	Fear of Failure
No.	Description		Measure (percent)	Basis			
1	PC concrete, 9-in. slab, 15 percent strength variation	A	39	Loads	x	Standard	Environmental
2	PC concrete, 9-in. slab, 10 percent strength variation	A	78	Loads	0.95x	Standard	Environmental
3	PC concrete, 8½-in. slab, high strength, 15 percent variation	A	39	Loads	0.98x	Standard	Environmental
4	Asphalt	C	67	Loads, environmental		Standard	Design statistics
5	PC concrete, epoxy topcoat, 10 percent strength variation			Loads, environmental		Environmental	
6	PC concrete, precast, 10 percent variation	B	85	Loads		Environmental, construction speed	Foundation losses

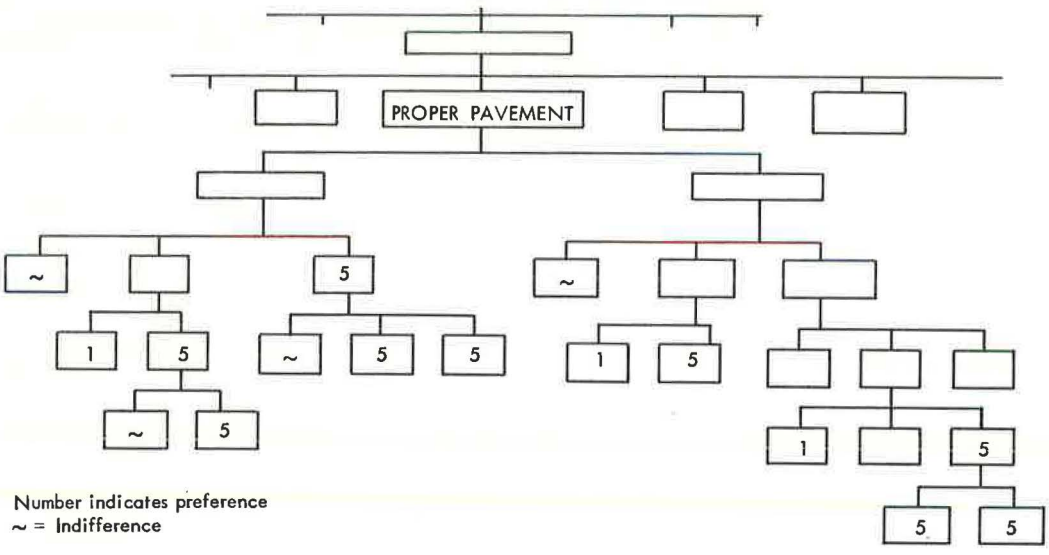

Figure 4. Goal fabric action.

One uses the goal fabric to structure the comparisons. Take, for example, actions 1 and 5. Figure 4 shows the goal fabric, and how one might begin mapping actions onto it. In some requirements one will have no preference, as with optimum pavement life. By mapping the lowest level preferences and comparing, one moves up the tree, expressing his feelings about the relative importance of requirements. For instance, the comparison of construction cost (1 preferred to 5) and maintenance cost (5 preferred to 1) will yield some total or annual cost to determine preference. Comparison of frictional characteristics (1 preferred to 5, epoxy may slicken) and comfort (5 preferred to 1, add color to epoxy with no additional cost) is more difficult.

In view of the gross assumptions made to arrive at Table 2, it would be meaningless to pursue ranking to completion. Even if all the analyses made were perfectly adequate and correct, two decision-makers might still be expected to arrive at different rankings. The purpose of this example, to illustrate an orderly, rational process for pavement design decisions, has been served. What is now required is further work and research to fill in this framework with the tools necessary to make this approach fully operational.

REFERENCES

1. The AASHO Road Test: Report 5—Pavement Research. HRB Spec. Rept. 61E, 1962.
2. Alexander, C., and Manheim, M. HIDECS 2: A Computer Program for Hierarchical Decomposition of a Set With an Associated Linear Graph. Research Rept. R62-2, MIT, Department of Civil Engineering, 1962.
3. Thickness Design, 7th Ed. The Asphalt Institute, 1963.
4. Pavement Evaluation Studies in Canada. Proc. Internat. Conf. on Structural Design of Asphalt Pavements, Univ. of Michigan, 1962.
5. Carey, W. N., Jr., and Irick, P. E. Performance of Flexible Pavements in the AASHO Road Test. Proc. Internat. Conf. on Structural Design of Asphalt Pavements, Univ. of Michigan, 1962.
6. Herrmann, C. R., and Ingram, G. E. The Analytical Approach and Physics-of-Failure Technique for Large Solid Rocket Reliability. Tempo Report, General Electric Company, Santa Barbara, 1961.

7. Housel, W. S. The Michigan Pavement Performance Study for Design Control and Serviceability Rating. Proc. Internat. Conf. on Structural Design of Asphalt Pavements, Univ. of Michigan, 1962.
8. Hutchinson, B. G. The Rationalization of Pavement Evaluation Decisions. Proc. Third Conf. of the Australian Road Research Board, 1966.
9. Hutchinson, B. G. The Measurement of Highway Pavement Performance. Proc. Second Internat. Conf. on Structural Design of Asphalt Pavements, Univ. of Michigan, 1967.
10. Liddle, W. J. Application of AASHO Road Test Results to the Design of Flexible Pavement Structures. Proc. Internat. Conf. on Structural Design of Asphalt Pavements, Univ. of Michigan, 1962.
11. Manheim, M. L. Problem-Solving Processes in Planning and Design. Prof. Paper P67-3, MIT, Department of Civil Engineering, 1967; also abridged version in Design Quarterly, No. 66/67.
12. Manheim, M. L., and Hall, F. L. Abstract Representation of Goals, a Method for Making Decisions in Complex Problems. Prof. Paper P67-24, MIT, Department of Civil Engineering, 1968.
13. Thickness Design for Concrete Pavements. Portland Cement Association, 1966.
14. Tons, E., Chambers, R. E., and Kamin, M. A. Layered Pavement Design Method for Massachusetts. Prof. Paper P64-31, MIT, Department of Civil Engineering, 1965.
15. Yoder, E. J. Principles of Pavement Design. John Wiley and Sons, 1959.

The Effect of Degree of Continuity Across a Void or Crack on Performance of Concrete Pavements

H. P. NIU, Assistant Professor of Civil Engineering, South Dakota School of Mines and Technology; and
GERALD PICKETT (deceased), Professor of Engineering Mechanics, University of Wisconsin

When a reinforced concrete pavement cracks, there is some reduction in rigidity. The reduction may result from imperfect transfer of moment across the crack or from imperfect transfer of both moment and shear, depending on the width of the crack and how well the pavement is reinforced. Analyses are made for deflections and moments in pavement loaded near a long, straight crack for various combinations of moment and shear transfer across the crack. Fourier integrals are used to solve the problem. Solution is first made for a concentrated load at a given point, and then Maxwell's reciprocal theorem is used to obtain deflections at that point due to distributed loads at any point. A program has been written for computing deflections and moments for any assumed efficiency of transfer. Representative results are given in the form of tables. Analyses are based on the assumptions that (a) except for the crack, the pavement bends in accordance with the Lagrangian equation for thin plates, and (b) the subgrade reaction is directly proportional to the local deflection. Present study shows that increasing efficiency of moment and shear transfer across a crack reduces the maximum deflections and moments in the pavement due to loads on the pavement.

•CONCRETE pavements usually crack, resulting in reduced load-carrying capacity and other undesirable features. Various remedies have been tried. These include spaced joints with load transfer devices, prestressing, and continuous reinforcement. The idea of continuously reinforced pavement is to control the width of the cracks rather than prevent them. With sufficient reinforcement the cracks may be kept so small that moment and shear are transmitted across them. The purpose of this investigation is to determine the stresses and displacement in a pavement under load as a function of the efficiency of transfer of moment and shear across a crack in the pavement.

In the analysis we shall assume that, except for one long, straight crack, the pavement bends in accord with the Lagrangian equation for thin plates and that the reactive pressure of the subgrade is proportional to the local deflection. Our interest will be in maximum moments and deflections caused by loads in the vicinity of the crack. The necessity for a general solution is avoided by considering first a concentrated load for which solutions of the homogeneous differential equation are adequate. Then, by using Maxwell's reciprocal theorem and an integration, we can find the deflection at a given point for a distributed load. Curvatures are found by appropriate differentiation and then moments and stresses are computed by the usual formulas for plates.

Paper sponsored by Committee on Theory of Pavement Design and presented at the 48th Annual Meeting.

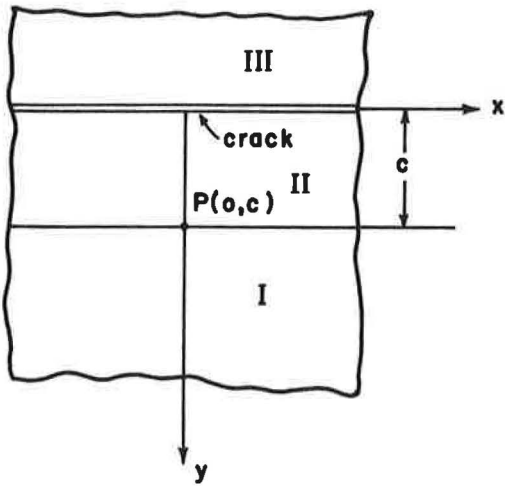

Figure 1. Pavement with a straight crack.

THEORETICAL DERIVATIONS

Pavement Equations

As shown in Figure 1, the x axis is placed at the crack and the y axis goes through the point of application of the concentrated load. This is the point (o, c) where c is the distance of the load from the crack. For purposes of the analysis, three regions are considered, depending on the y coordinate, as follows: Region I, $c \leq y$; Region II, $o \leq y \leq c$; and Region III, $y \leq o$.

With only the one concentrated load the homogeneous differential equation

$$D\nabla^2\nabla^2 w + kw = 0 \tag{1}$$

is applicable for each region. Symbols in this and other equations in this paper are defined as follows:

a, b, c = linear distances;
D = flexural rigidity of the slab;
k = subgrade modulus or weight density of equivalent liquid subgrade;
ℓ = $(D/k)^{1/4}$ for liquid subgrade;
M_x = bending moment per unit of length of the edges parallel to the x axis;
M_y = bending moment per unit of length of the edges parallel to the y axis;
P = total load on slab;
q = intensity of load on slab per unit of area;
w = deflection of slab;
x, y = rectangular coordinates;
α, β = variables of integration in Fourier integrals;
$\gamma = \alpha^2 + \beta^2$;
μ = Poisson's ratio;
ϕ, ρ = proportional constants;
∇^2 = Laplace operator;

Consider the following solutions of Eq. 1 for the three respective regions:

$$w_1 = \frac{P\ell^3}{\pi D}\int_0^\infty \cos \alpha x(A_1 \cos \beta y + B_1 \sin \beta y)e^{-\gamma y}\, d\alpha \tag{2}$$

$$w_2 = \frac{P\ell^3}{\pi D}\int_0^\infty \cos \alpha x(A_2 \cos \beta y \cosh \gamma y + B_2 \sin \beta y \cosh \gamma y + C_2 \cos \beta y \sinh \gamma y + D_2 \sin \beta y \sinh \gamma y)\, d\alpha \tag{3}$$

$$w_3 = \frac{P\ell^3}{\pi D}\int_0^\infty \cos \alpha x(A_3 \cos \beta y + B_3 \sin \beta y)e^{\gamma y}\, d\alpha \tag{4}$$

where

$$\gamma^2 = \frac{\alpha^2}{2} + \frac{\sqrt{1 + \alpha^4 \ell^4}}{2\ell^2}, \quad \beta^2 = -\frac{\alpha^2}{2} + \frac{\sqrt{1 + \alpha^4 \ell^4}}{2\ell^2} \tag{5}$$

$$\ell^4 = D/k \tag{6}$$

A_1, B_1, A_2, B_2, C_2, D_2, A_3, B_3 are arbitrary functions of the variable of integration α and are introduced for the purpose of satisfying four conditions at the boundary between Regions I and II and four conditions at the boundary between Regions II and III.

Each solution satisfies Eq. 1 and is capable of meeting all boundary requirements for the region to which it applies.

Boundary Conditions

For the analysis, each region is considered to extend to infinity in both plus and minus x directions and the solutions for each region are Fourier integrals in the x direction; therefore, no further consideration need be given to the boundaries at $x = \pm\infty$. The requirement that the deflection approach zero as y approaches $\pm\infty$ is met by using only positive values of γ from Eq. 5. There remain eight conditions to be satisfied as follows. At $y = c$,

$$w_1 = w_2 \tag{7}$$

$$\frac{\partial w_1}{\partial y} = \frac{\partial w_2}{\partial y} \tag{8}$$

$$D\left(\frac{\partial^2}{\partial y^2} + \frac{\mu \partial^2}{\partial x^2}\right)(w_1 - w_2) = 0 \tag{9}$$

$$\int_{-\epsilon}^{\epsilon} D \frac{\partial}{\partial y} \nabla^2 (w_1 - w_2) dx = P \tag{10}$$

For all positive values of ϵ, however small, P is the concentrated load. At $y = 0$,

$$D\left(\frac{\partial^2}{\partial y^2} + \frac{\mu \partial^2}{\partial x^2}\right)(w_2 - w_3) = 0 \tag{11}$$

$$D\left[\frac{\partial^3}{\partial y^3} + (2 - \mu)\frac{\partial^3}{\partial x^2 \partial y}\right](w_2 - w_3) = 0 \tag{12}$$

$$D\left(\frac{\partial^2 w_2}{\partial y^2} + \frac{\mu \partial^2 w_2}{\partial x^2}\right) = \rho\left(\frac{\partial w_2}{\partial y} - \frac{\partial w_3}{\partial y}\right) \tag{13}$$

$$D\left[\frac{\partial^3 w_2}{\partial y^3} + (2 - \mu)\frac{\partial^3 w_2}{\partial x^2 \partial y}\right] = -\phi(w_2 - w_3) \tag{14}$$

Equations 7, 8, and 9 express continuity of deflection, slope and moment between Regions I and II. Equation 10 expresses continuity of shear except at the point of the concentrated load where the proper discontinuity is provided, since

$$\int_{-\epsilon}^{\epsilon} \frac{P}{\pi} \int_0^{\infty} \cos \alpha x \, d\alpha \, dx = P \tag{15}$$

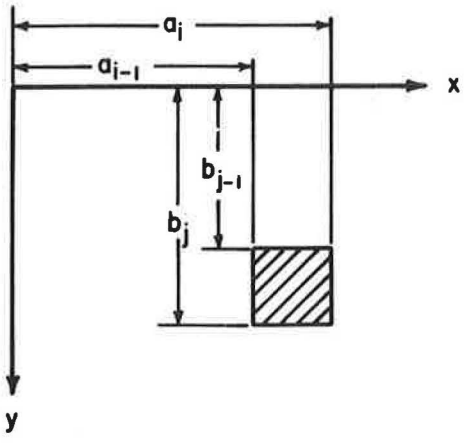

Figure 2. Area to be loaded divided into rectangles for deriving deflections.

and $\int_0^\infty \cos \alpha x \, d\alpha$ is the well-known Dirac delta function. Continuity of twist M_{yx} is satisfied when the other continuity conditions are met.

At the crack between Regions II and III there may be discontinuity in deflection and/or slope. Continuity of moment is expressed by Eq. 11. Continuity of twist and shear is replaced by continuity of reaction, Eq. 12, in accord with thin plate theory. Equation 13 states that the moment transmitted across the crack is proportional to the discontinuity in slope, and Eq. 14 states that the reaction transmitted is proportional to the discontinuity in deflection. If the proportionality constants ρ and ϕ are both infinite, there is perfect continuity; if they are both zero, there is no continuity. If there is moderate reinforcement, one might expect poor transmission of moment and good transmission of reaction.

Substitution of Eqs. 2, 3, and 4 into the eight boundary conditions, Eqs. 7 to 14, results in a matrix of equations. A FORTRAN program was written that computes the elements of the matrix and makes the solution for the eight conditions arbitrary functions of α for any given values of the nondimensional parameters $\alpha\ell$ and c/ℓ.

Deflections and Moments

If the deflection at any point (x, y) due to a concentrated load at point (o, c) were desired, it could be found by numerical integration of the applicable integral, Eqs. 2, 3, or 4. For this purpose the matrix of equations would be solved for the arbitrary functions for a sufficient number of properly spaced values of $\alpha\ell$. In like manner the moment at any point (x, y) due to the concentrated load could be found by numerical integration of the corresponding integral for moment. However, our interest is in deflections and moments due to distributed loads. Because the deflection at (o, c) due to a load at (x, y) is equal to the deflection at (x, y) due to a load at (o, c), the deflection at (o, c) due to a distribution load could be found by replacing P in the appropriate expression for w by q dx dy and integrating over the loaded area.

To avoid the tedious integrations suggested for a given loading distribution, influence charts for deflections are prepared. The area that may be loaded is divided into rectangular blocks, of which one is represented in Figure 2. The deflection, W(i, j) at point (o, c) due to a uniform load of q intensity over the i, j block shown, is given by

$$W(i, j) = w[a_i, b_j] - w[a_{i-1}, b_j] - w[a_i, b_{j-1}] + w[a_{i-1}, b_{j-1}] \qquad (16)$$

where the general term w[a, b] is found by integrating the appropriate expression for w with respect to x from zero to a and with respect to y from zero to b. For example, this gives for Region I

$$w(a, b) = \frac{q\ell^5}{\pi D} \int_0^\infty \frac{\sin \alpha a}{\alpha\ell[(\gamma\ell)^2 + (\beta\ell)^2]} [A_1 (-\gamma\ell \cos \beta b + \beta\ell \sin \beta b)$$

$$- B_1 (\beta\ell \cos \beta b + \gamma\ell \sin \beta b)] e^{-\gamma b} \, d\alpha \qquad (17)$$

Reciprocal relations do not in general apply between derivatives of deflections. That is, the curvature in the y direction at point (o, c) due to unit load at point (x, y) is not

equal to the curvature in the y direction at point (x, y) due to unit load at point (o, c). However, because c is the coordinate in the y direction for deflection at point (o, c), the curvature in the y direction at this point is $\partial^2 w/\partial c^2$ where w is the deflection. From these considerations the moments at point (d, c) due to a load at point (x+d, y) are given by

$$M_y = - D\left(\frac{\partial^2 w}{\partial c^2} + \mu \frac{\partial^2 w}{\partial d^2}\right) \tag{18}$$

$$M_x = - D\left(\frac{\partial^2 w}{\partial d^2} + \mu \frac{\partial^2 w}{\partial c^2}\right) \tag{19}$$

$$M_{xy} = (1 - \mu) D \frac{\partial^2 w}{\partial d \partial c} \tag{20}$$

where (x + d) has been substituted for x in the appropriate expression for w. After differentiation, d may be set equal to zero to obtain moments at (o, c).

Expressions for curvature in the x direction are readily obtained; thus for Region I the curvature $\partial^2 w_1/\partial d^2$ at (o, c) due to a uniform load over the region bounded by x – a, x = 0, y = 0, y = b is given by

$$\frac{\partial^2 w_1}{\partial d^2} = \frac{q\ell^3}{\pi D} \int_0^\infty \frac{\alpha\ell \sin \alpha a}{(\gamma\ell)^2 + (\beta\ell)^2} [A_1 (\gamma\ell \cos \beta b - \beta\ell \sin \beta b) + B_1 (\beta\ell \cos \beta b + \gamma\ell \sin \beta b)] e^{-\gamma b} \, d\alpha \tag{21}$$

In view of the lengthy analytical expressions, the curvature in the y direction is expressed by the central difference formula,

$$\frac{\partial^2 w}{\partial c^2} = \frac{w(o, c + \Delta c) - 2w(o, c) + w(o, c - \Delta c)}{(\Delta c)^2} \tag{22}$$

Finally, the moment M(i, j) under consideration at the point (o, c) due to a uniform load over the i, j block is given by

$$M(i, j) = m(a_i, b_j) - m(a_{i-1}, b_j) - m(a_i, b_{j-1}) + m(a_{i-1}, b_{j-1}) \tag{23}$$

where m is the value of the moment in question due to a uniform load over the whole area bounded by x = 0, x = a, y = 0, y = b.

NUMERICAL CALCULATIONS AND RESULTS

Representative results of the computations are given in Tables 1, 2, and 3. Table 1 gives C_w in the expression

$$w = C_w \, q\ell^4/2{,}000 \, D \tag{24}$$

where w is the deflection at the point (o, c) due to a uniform load of q intensity over a square area 0.1ℓ by 0.1ℓ with center at the designated x and y coordinates. In like manner, Table 2 gives C_m in the expression

$$M_x = C_m \, q\ell^2/10{,}000 \tag{25}$$

These two tables are for the special case of c = 0, i.e., at the edge of the crack, $\rho = 0.0$, i.e., no moment transfer across the crack, and $\phi = \infty$, i.e., perfect transfer of shear

TABLE 1

DEFLECTION COEFFICIENTS C_w
(See Eq. 24)

$C = 0.0,\ \rho = 0.0,\ \phi = \infty,\ \mu = 0.15$

y/ℓ \ x/ℓ	0.05	0.15	0.25	0.35	0.45	0.55	0.65	0.75	0.85	0.95
1.45	.9235	.9178	.9064	.8897	.8680	.8418	.8115	.7778	.7412	.7024
1.35	1.059	1.052	1.039	1.020	.9956	.9656	.9311	.8927	.8512	.8071
1.25	1.207	1.199	1.184	1.162	1.134	1.100	1.060	1.017	.9702	.9204
1.15	1.368	1.359	1.342	1.317	1.284	1.245	1.201	1.151	1.098	1.042
1.05	1.542	1.532	1.513	1.484	1.447	1.402	1.352	1.296	1.236	1.173
0.95	1.731	1.720	1.697	1.664	1.622	1.571	1.514	1.450	1.383	1.312
0.85	1.934	1.921	1.895	1.857	1.809	1.751	1.686	1.615	1.539	1.460
0.75	2.153	2.137	2.107	2.064	2.009	1.943	1.869	1.789	1.704	1.615
0.65	2.387	2.369	2.334	2.284	2.221	2.146	2.063	1.972	1.877	1.779
0.55	2.636	2.615	2.575	2.517	2.445	2.360	2.266	2.165	2.059	1.949
0.45	2.902	2.877	2.830	2.763	2.680	2.583	2.478	2.365	2.247	2.126
0.35	3.184	3.155	3.099	3.021	2.925	2.816	2.697	2.571	2.441	2.308
0.25	3.482	3.447	3.380	3.289	3.179	3.056	2.923	2.783	2.640	2.495
0.15	3.797	3.752	3.672	3.565	3.440	3.301	3.153	3.000	2.842	2.684
0.05	4.128	4.069	3.972	3.848	3.706	3.551	3.387	3.218	3.047	2.875

TABLE 2

MOMENT COEFFICIENTS C_m
(See Eq. 25)

$C = 0.0,\ \rho = 0.0,\ \phi = \infty,\ \mu = 0.15$

y/ℓ \ x/ℓ	0.05	0.15	0.25	0.35	0.45	0.55	0.65	0.75	0.85	0.95
1.45	2.808	2.744	2.620	2.443	2.222	1.968	1.692	1.405	1.116	.8348
1.35	3.225	3.147	2.997	2.783	2.518	2.216	1.890	1.555	1.222	.8992
1.25	3.703	3.608	3.424	3.164	2.845	2.485	2.100	1.710	1.325	.9567
1.15	4.253	4.135	3.908	3.591	3.205	2.774	2.321	1.865	1.422	1.003
1.05	4.888	4.740	4.459	4.068	3.598	3.081	2.546	2.016	1.508	1.034
0.95	5.627	5.439	5.084	4.598	4.023	3.402	2.771	2.156	1.576	1.044
0.85	6.491	6.248	5.795	5.184	4.477	3.729	2.985	2.275	1.619	1.026
0.75	7.513	7.192	6.602	5.826	4.951	4.050	3.177	2.363	1.627	.9737
0.65	8.736	8.300	7.516	6.516	5.428	4.347	3.330	2.407	1.590	.8800
0.55	10.22	9.611	8.541	7.236	5.882	4.593	3.424	2.394	1.502	.7398
0.45	12.08	11.17	9.663	7.945	6.271	4.757	3.438	2.310	1.354	.5501
0.35	14.48	13.02	10.82	8.568	6.537	4.805	3.356	2.150	1.147	.3110
0.25	17.74	15.15	11.89	8.991	6.621	4.712	3.171	1.912	.8925	.0227
0.15	22.48	17.28	12.56	9.098	6.494	4.471	2.914	1.568	.6552	-.3532
0.05	29.80	18.47	12.61	8.832	6.169	4.059	2.851	1.171	.4265	-.4148

TABLE 3

DEFLECTION AND MOMENT COEFFICIENTS
(See Eqs. 24 and 25)

c/ℓ	x/ℓ	y/ℓ	ρ/D	ϕ/D	C_w	C_m
0.5	0.05	0.45	0.0	0	4.667[a]	29.06[a]
0.5	0.05	0.45	0.0	1	3.483	26.99
0.5	0.05	0.45	0.0	100	2.770	23.58
0.5	0.05	0.45	0.0	1000	2.753	23.31
0.5	0.05	0.45	0.0	∞	2.753	25.51[a]
0.5	0.05	0.45	0.001	0.001	4.649	28.85
0.5	0.05	0.45	0.01	0.01	4.612	28.82
0.5	0.05	0.45	0.1	0.1	4.305	28.56
0.0	0.05	0.05	0.0	0.0	8.203[b]	56.42[b]
0.0	0.05	0.05	0.0	∞	4.128	29.80
0.3	0.05	0.05	0.0	∞	3.291	16.67
0.3	0.05	0.25	0.0	∞	3.123	25.53
0.3	0.05	0.45	0.0	∞	2.859	20.46
0.3	0.15	0.05	0.0	∞	3.257	14.08
0.3	0.15	0.25	0.0	∞	3.077	15.44

[a]Taken from Tables 2 and 3 of Influence Charts for Concrete Pavements, G. Pickett and G. K. Ray, ASCE Transactions, Vol. 116, 1951.
[b]The value seems to be too large.

across the crack. Table 3 gives selected results for various values of c, ρ, and ϕ. These three tables were prepared from a much larger body of computed data, including results for both C_w and C_m for the following cases and ranges of x/ℓ and y/ℓ:

c/ℓ	ρ/D	ϕ/D	x/ℓ	y/ℓ
0.	0.	∞	0-2.0	0-3.0
0.3	0.	∞	0-2.0	0-3.0
0.5	0.	∞	0-2.0	0-3.0
0.5	0.	1	0-1.0	0-1.
0.5	0.	100	0-1.0	0-1.
0.5	0.	1000	0-1.0	0-1.
0.5	0.001	0.001	0-1.0	0-1.
0.5	0.01	0.01	0-1.0	0-1.
0.5	0.1	0.1	0-1.0	0-1.

Because the solutions in every case were for areas 0.1ℓ by 0.1ℓ, a total of 2,400 of each of C_w and C_m were obtained. For each C_w a minimum of one infinite integral was evaluated, and for each C_m a minimum of three infinite integrals was evaluated. Simpson's rule was used in the numerical integration of the infinite integrals. The spacing of the intervals and the maximum value of $\alpha\ell$ used were varied until no further changes were detected in the first four significant digits of the integrated values. In like manner Δc was varied to obtain what was believed to be optimum accuracy in determining $\partial^2 w/\partial c^2$. As Δc is decreased accuracy is increased until round-off error dominates.

For each $\alpha\ell$ used, an eighth-order matrix of equations based on the eight boundary conditions was solved; 22 of the 64 elements of the matrix were zero, 14 were easily obtained, 8 involved two to three functions, 14 involved four to six functions, and 6 involved nine to ten functions. For example, in the four to six category was element (2, 5) given by

$$\beta\ell \sin \beta c \sinh \gamma c - \gamma\ell \cos \beta c \cosh \gamma c$$

where β and γ are given by Eq. 5. Therefore, considerable computational effort was involved. The computations were done on a CDC 1604 computer at the University of Wisconsin.

Space limitations do not permit further description of how the computations were made nor inclusion of more computed results. However, if one has an adequate computer available and the FORTRAN program used, he may obtain as many results similar to those shown in Tables 1 to 3 as desired. The program can be obtained on request from the author.

If Tables 1 and 2 are plotted to scale they become influence charts and as such can be used to obtain deflections and moments for any distribution of loading.

Examination of Table 3 shows the decrease in deflection and moment with increase in either or both moment and shear transfer across the crack. Comparison of perfect shear transfer with that of no shear shows that the deflection at the crack ($c = 0$) for loads near the crack ($y/\ell = 0.05$) is reduced to about half (8.203 to 4.128), and the moment at the crack is reduced to nearly half (56.42 to 29.80) by the shear transfer. This reduction is much less for points farther from the crack.

SUMMARY

This paper considers a cracked Westergaard pavement supported on a Winkler foundation and subjected to a normal load applied near the crack. After formulating integral equations to the problem we have determined numerical values of interest.

The present study shows that increasing efficiency of moment and shear transfer across a crack reduces the maximum deflections and moments in the pavement. If the results shown in the tables are plotted to scale and become influence charts, one can obtain deflections and moments for any distribution of loading. An available computer program will give deflections and moments for any assumed efficiency of transfer.

For the continuously reinforced pavement, where transverse cracks usually occur at close intervals, a similar approach can be extended to the problem by dividing the slab into more regions. The present analytical study is confined to an isolated crack, with continuous uncracked slabs on both sides.

ACKNOWLEDGMENTS

We wish to thank the Concrete Reinforcing Steel Institute Committee on Continuously Reinforced Concrete Pavement for suggesting the problem and providing some financial support, and the Wisconsin Research Committee for providing funds for the use of the CDC 1604 computer.

Analysis of Concrete Slabs on Ground Subjected to Warping and Moving Loads

K. H. LEWIS, Assistant Professor of Civil Engineering, University of Pittsburgh; and M. E. HARR, Professor of Soil Mechanics, Purdue University

A theory has been developed whereby stresses and deflections could be calculated for a series of rectangular slabs lying on a viscoelastic foundation and subjected to a moving load. The stresses and deflections are caused by the weight of the slab, the moving concentrated load, and the linear temperature (or moisture) variations that cause sufficient warping so that the slab is only partially supported by its foundation.

The support conditions were simulated by a Kelvin viscoelastic model, and zones (which depended on the value of subgrade reaction) were set up so that the solutions to the governing differential equations could be reduced to a set of simultaneous algebraic equations. The equations were solved with the aid of an IBM 7090 digital computer using a FORTRAN source program.

It was found that when partial support caused by warping exists, the tensile stress in the slab can increase with increasing velocity of load. Moreover, the maximum deflection (downward) need not occur when the velocity of the load is equal to zero. The reduction in subgrade support over a narrow region (8 ft or less) leads to deflections and stresses that are higher than those calculated using the initial value of subgrade reaction. This is particularly evident when the load is over the region of reduced subgrade reaction.

•IMPROVEMENTS in the performance of concrete pavements for highways and airports have been for many years the concern of civil engineers interested in these problems. This concern has been due not only to the ever-increasing cost of construction and maintenance but also to the preponderance of cracks that exist in pavements.

The development of these cracks depends on several factors, such as type of subgrade, deterioration of the concrete, temperature effects, and load (52), and, although they may or may not represent a failed condition, they do indicate deficiencies in the analysis, design, or construction of highway pavements. Cracks not only detract from the general appearance of a highway but also often lead to driving discomfort and pavement deterioration, especially when load transfer and subgrade support are lost.

Regarding the construction of concrete pavements, advancement in the development of the principles of soil mechanics has limited the use of poor subgrades and has virtually eliminated the use of soils susceptible to frost action and pumping. In addition, specifications that are geared to promote the use of sound concrete and the practice of good construction methods have become widespread (1, 47).

Refinements in construction procedures have been accompanied by development of methods of monitoring the factors influencing concrete pavements (15, 16), and strains as well as deflections of pavements can be determined for both static and dynamic loadings (11, 18). Temperature differences between the upper and lower faces of the slab can

Paper sponsored by Committee on Theory of Pavement Design and presented at the 48th Annual Meeting.

be measured with the use of thermocouples (51), and variations in moisture content can be established from the dielectric properties of concrete (3).

Today, the problem of material weakness has been reduced, if not solved, and significant progress has been made in the ability to build pavements and to measure their important properties. However, little has been done to upgrade the methods of analysis. Current procedures for designing and evaluating pavements (52) are still based on static loads and, except for introducing equivalent static loadings (2), they do not account for the dynamic response of the pavement to moving loads. Moreover, the pavement is usually assumed to be fully supported at all times even though this is often not the case (11, 21, 22).

The present trend in transportation is toward heavier loads and higher speeds and consequently there is an increasing need to be able to predict performance. This can be done only when more is known about the input and causal factors of traffic loads, curling, and loss of subgrade support. It is to help satisfy this need that this research was undertaken.

BACKGROUND

In the early stages of development, pavement design and road construction consisted of a collection of rule-of-thumb procedures based on empirical knowledge. As early as 1901, test roads were being used to determine the best type of pavement for the prevailing traffic (38). Between 1920 and 1940, much work was done on the classification of soils (5) and highway engineers were able to correlate pavement performance with subgrade types.

During World War II engineers were faced with the problem of designing pavements for greater wheel loads than previously thought necessary. Because they could not afford the long period of time that was required to develop design procedures based on past experiences, they sought a more rational basis of design. This search ultimately led to procedures that form the core of pavement design today.

Static Load Solutions

In 1884, Hertz (13) first published a solution to the problem of elastic plate on a Winkler-type foundation (50). However, it was not until the advent of Westergaard's solution in 1926 that a highway pavement was treated in this manner and the problem was approached from a purely theoretical point of view. Today, Westergaard's work still forms the basis of the analytical bent in pavement design.

Westergaard (48) solved the problem arising when a slab is fully supported on a Winkler foundation and subjected to static loads applied at the interior, free edges, and corners of the slab. Later, Kelley (23), Spangler (43), Pickett (34), and Westergaard (49) himself extended these original solutions to account for linear temperature variations. In 1957, Freudenthal and Lorsch (10) used the three fundamental models (Maxwell, Kelvin, and Standard Solid) to study the problem of an infinite beam on a viscoelastic foundation. Then in 1958, Hoskin and Lee (19) solved the problem of an infinite plate on a viscoelastic foundation.

All of these solutions neglect the shearing forces generated at the pavement-base interface. Several mechanisms have been offered to account for this effect. Filonenko-Borodich (9) considered a set of springs held together by a membrane, whereas Schiel (42) took a fluid that exhibited surface tension as his soil model. Pasternak (32) and Kerr (25), on the other hand, considered a beam of unit depth resting on a bed of interrelated springs as a foundation, and Pister and Williams (33) used the shear interactions suggested by Reissner (40). Perhaps the most realistic approach offered to account for shear in an elastic base is that given by Klubin (26), who expressed the pavement reaction by an infinite series of Tschebyscheff polynomials, which also accounts for the two elastic constants (modulus of elasticity and Poisson's ratio).

It should be noted that Klubin's solution is in fact an elastic solution and the others, which impose Winkler assumptions, are not. In spite of this, because the Winkler foundation affords a much simpler analysis and generally gives good agreement with field data, it will no doubt remain popular.

All of these analyses are based on the assumption that the slab maintains contact with its support at all points and at all times. Experimental and field studies (16, 21, 22) have shown this assumption to be seriously in error, and a few investigators have accounted for the effects of only partial support. In 1959, Leonards and Harr (28) solved the problem relating to a partially supported slab on a Winkler foundation subjected to linear temperature and/or moisture variations. Later, Reddy, Leonards, and Harr (39) extended this analysis by introducing nonlinear temperature variations as well as a viscoelastic foundation. In all of these analytical procedures, only symmetrical, statically applied loads were considered.

Dynamic Load Solutions

For many years, the problem of determining the stresses and deflections in a vibrating plate has been of interest primarily to mathematicians. Raleigh (37) and Lamb (27), using the classical beam theory developed by Euler (7) and Bernoulli (4), studied several problems dealing with the vibration of bars, membranes, and plates. Later, Ritz (41) elaborated on this work and made significant contributions toward the study of vibrating rectangular plates.

Recently, engineers have felt the need to account for the dynamic response of pavements, and several solutions have evolved. Pioneering these solutions was the work of Timoshenko (45), Hovey (20), and Ludwig (30) in their studies of the dynamics of rails subjected to moving loads. In 1943, Dorr (6), using Fourier integrals, extended the idea to a beam, but in all of these solutions the foundation was represented by a Winkler model that exhibited no viscous effects.

In 1953, Kenney (24) added the effects of linear damping and, by means of the method of undetermined coefficients, was able to examine the relationship between deflections and critical velocity. In a more recent work, Thompson (44) elaborated on Kenney's solution and showed that the solutions for the deflections fall into three distinct regimes. Specifically, Thompson showed that these regimes were defined by the value of the discriminant of the fourth-order characteristic equation. If the value of the discriminant as defined by

$$\Delta = 16\,[4\,(1 - \epsilon^2)\,\theta^8 - (8 - 36\epsilon^2 + 27\epsilon^4)\,\theta^4 + 4] \qquad (1)$$

where ϵ = the damping ratio, and θ = the velocity ratio, is greater than zero, the characteristic equation has no real roots. If Δ is equal to zero, there is one real, double root; and if Δ is less than zero, there are two real, unequal roots.

The solutions presented by Thompson demonstrate that at static conditions the deflection curve is symmetrical (with maximum deflection occurring under the load); but as velocity increases, the point of maximum deflection falls farther and farther behind the load. Upward deflections occur behind the moving load when Δ is greater than zero; however, when Δ is less than zero, there are no upward deflections (i.e., the deflected surface does not intersect the axis of zero deflection, but simply approaches it at some great distance behind the load).

Several investigators have also considered the road loading system as an interaction between two major components that are interdependent, namely vehicles and roads. Fabian, Clark, and Hutchinson (8) examined the elements of each component and developed some basic mathematical models. Analysis of their vehicle subsystem showed that the magnitude of the dynamic load is a function of vehicle dynamic properties and apparent road profile and may, in fact, be significantly greater than the static load. Quinn and De Vries (35) used an experimental procedure to determine the highway and vehicle characteristics and showed that, if these quantities are known, the reaction of a vehicle on a highway can be predicted.

In general, most of the analytical studies reported in the literature on moving loads on pavements (52) do not account for the interaction between vehicle and road. For the most part these reports show that, for fully supported pavements, the lower the velocity the greater the deflections and stresses in the slab. Measurements of displacement (15, 17, 18) generally support this finding; however, some data (11) do exist to suggest

the possibility that displacements may increase at velocities greater than 30 to 40 mph. Also to be noted is the fact that tests on tire forces on pavements (36) indicate that the "average" force produced on the pavement by a moving load increases with velocity.

Obviously, there are several interdependent factors, such as the vehicle's suspension system, tire pressures, and road profile, that should be included in the analysis of pavements. However, at the present time, the interaction between vehicle and pavement is not well understood. In spite of this, further insight into the highway problem can be gained by examining some of the simplifying assumptions that appear in current analyses of highway pavements. Thus, it is the object of this paper to obtain by analytical means the stresses and deflections in a partially supported concrete slab when subjected to a moving load. Such partial support may be caused by temperature and moisture gradients or by the weakening and partial or complete loss of subgrade.

FORMULATION OF PROBLEMS

Considered first is the problem of a slab lying on a foundation while subjected to moving loads as well as to temperature (and/or moisture) gradients that would cause upward curling. (Upward curling is understood to exist when temperature gradients cause the ends of the slab to rise vertically.) Second, an investigation will be made of weaknesses in the subgrade caused by conditions where (a) water has infiltrated under the pavement from the side of the roadway, or (b) a joint has opened or a crack has occurred in a warped pavement to such an extent as to enable it to regain complete contact with the foundation. When such an opening exists, water may infiltrate through the surface of the pavement. Under both conditions, the infiltration may weaken the subgrade and may eventually lead to pumping. The following assumptions are made for both problems in order to render them tractable:

1. A highway pavement can be represented by an array of rectangular plates.
2. The usual assumptions of plate theory hold; that is, the plate is homogeneous, is isotropic, and obeys Hooke's law; deflections are small in comparison to thickness; plane cross sections normal to the middle plane in the unstressed condition remain normal to this surface after bending; and the effects of rotatory inertia and shear deformation can be neglected.
3. The highway base material acts like a set of linear viscoelastic elements. The inertia of the material is neglected.
4. External forces acting on the plate are those caused by a constant-velocity line load and gravity.
5. The plates are subjected to changes in temperature (and/or moisture) that vary linearly with depth. The variation in temperature is constant on all planes parallel to the upper and lower plate surfaces and is independent of time.

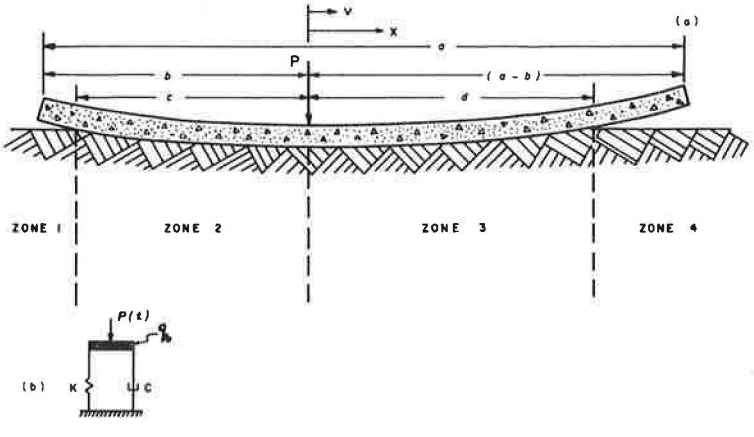

Figure 1. Section of warped slab.

PROBLEM OF PARTIAL SUPPORT CAUSED BY WARPING

In addition to the foregoing assumptions, further assumptions regarding the interaction between slabs are required. For the case studied here, it is assumed that no bending moment exists between slabs (this will be discussed later). However, some load transfer can be accounted for by specifying a shearing force between slabs equivalent to that existing in an infinite slab.

In general, the governing differential equation describing the pavement section illustrated in Figure 1 can be expressed as follows (31):

$$D\left(\frac{\partial^4 w}{\partial x_1^4} + 2\,\frac{\partial^4 w}{\partial x_1^2 \partial y_1^2} + \frac{\partial^4 w}{\partial y_1^4}\right) + \rho H\,\frac{\partial^2 w}{\partial t^2} = q(x_1, y_1, t) - p(x_1, y_1, t) \qquad (2)$$

where

D = flexural rigidity of the slab,
w = midplane deflection of the slab (positive downward),
x_1, y_1 = fixed coordinates,
ρ = density of the slab,
H = slab thickness,
q = surface loading,
p = foundation reaction, and
t = time.

Using assumption 3, the foundation reaction, p, may be expressed (Fig. 1b)

$$p(x_1, y_1, t) = C\,\frac{\partial w}{\partial t} + Kw$$

where C is the damping coefficient and K is the modulus of subgrade reaction. Applying the loading conditions implied by assumption 4, and assuming that the deflection does not vary in the y_1 direction, Eq. 2, for a constant cross section of pavement, becomes

$$D\,\frac{\partial^4 w}{\partial x_1^4} + \rho H\,\frac{\partial^2 w}{\partial t^2} + C\,\frac{\partial w}{\partial t} + Kw = q_0 + P(x_1, t) \qquad (3)$$

in which q_0 = unit weight of slab and P = the moving line load.

Employing the transformation, $x = (x_1 - vt)$, the equation reduces to a function of only the one variable, x. If in addition the moving load, P, is introduced with the boundary conditions, the following differential equations are obtained:

For zones 1 and 4,
$$D\,\frac{d^4 w}{dx^4} + \rho H v^2\,\frac{d^2 w}{dx^2} = q_0 \qquad (4a)$$

For zones 2 and 3,
$$D\,\frac{d^4 w}{dx^4} + \rho H v^2\,\frac{d^2 w}{dx^2} - Cv\,\frac{dw}{dx} + Kw = q_0 \qquad (4b)$$

The boundary conditions for the indicated zones may be summarized as follows:

$$M_1(-b) = 0 \qquad (5a)$$

$$V_1(-b) = \overline{V}(-b) \qquad (5b)$$

$$w_1(-c) = 0 \qquad (5c)$$

$$w_2(-c) = 0 \qquad (5d)$$

$$w_1'(-c) = w_2'(-c) \tag{5e}$$

$$w_1''(-c) = w_2''(-c) \tag{5f}$$

$$w_1'''(-c) = w_2'''(-c) \tag{5g}$$

$$w_2(0) = w_3(0) \tag{5h}$$

$$w_2'(0) = w_3'(0) \tag{5i}$$

$$w_2''(0) = w_3''(0) \tag{5j}$$

$$w_3'''(0) - w_2'''(0) = P/D \tag{5k}$$

$$w_3(d) = 0 \tag{5l}$$

$$w_4(d) = 0 \tag{5m}$$

$$w_3'(d) = w_4'(d) \tag{5n}$$

$$w_3''(d) = w_4''(d) \tag{5o}$$

$$w_3'''(d) = w_4'''(d) \tag{5p}$$

$$M_4(a-b) = 0 \tag{5q}$$

$$V_4(a-b) = \bar{V}(a-b) \tag{5r}$$

Solution of Problem

To obtain the solution for the case where the warped slab is as representd by Figure 1, the value of Δ (Eq. 1) is determined and Eqs. 4a and 4b are solved to obtain expressions for the deflections and stresses in the slab (29). The constants in the resulting set of nonlinear equations are then evaluated using the conditions listed in Eq. 5. In solving the set of nonlinear equations, an initial estimate of the solution was made using the fully supported slab. Then a method of functional iteration equivalent to an N-dimensional Newton's method was used with an IBM 7090 computer. With the constants determined, the stresses and displacements were then obtained. Using this same procedure, the other deflection patterns resulting from the moving load were analyzed (Fig. 2).

Results

Because of the large number of variables involved, it is impractical to present the results for all cases considered. Instead, numerical results are given for a few typical cases to illustrate general trends and for purposes of comparison with results previously obtained by others.

Using the left edge of the slab as origin, the moving load was considered at intervals of 4 ft and stresses and deflections were determined for combinations of the following data:

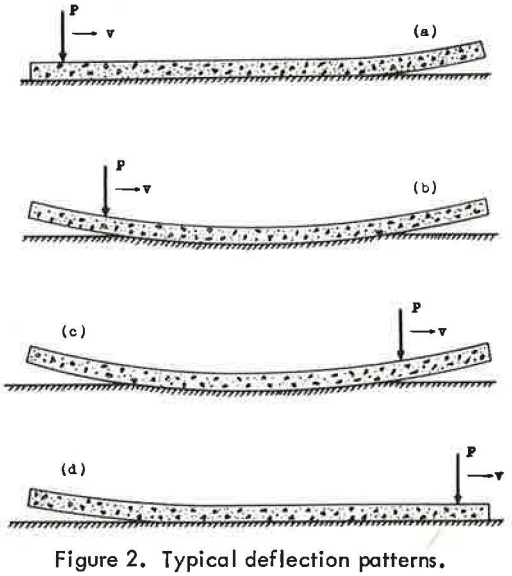

Figure 2. Typical deflection patterns.

μ = 0.15
E = 4×10^6 psi
a = 480 in.
H = 8, 10, 12 in.
K = 100, 200 pci
C_r = 1.5, 2.0
v = 0, 20, 40, 60, 80 mph
P = 125 lb/in. (the value of P was determined using an axle load of 18,000 lb over a pavement 12 ft wide)
q_0 = 150.9 pcf
ΔT = 20, 30, 40 F
β = 6×10^{-6} in. per in. per deg F

Typical curves for deflections and stresses are shown in Figure 3; Figures 4 and 5 show how maximum deflection and maximum stress vary with velocity when the difference between slab surfaces is 20 and 40 F. A record of the movement experienced by the ends of the slab is shown in Figures 6 and 7 as a function of the load position.

Discussion of Results

In developing the theory for this part of the analysis, it was assumed that a pavement could be represented by an array of rectangular slabs. Furthermore, it was assumed

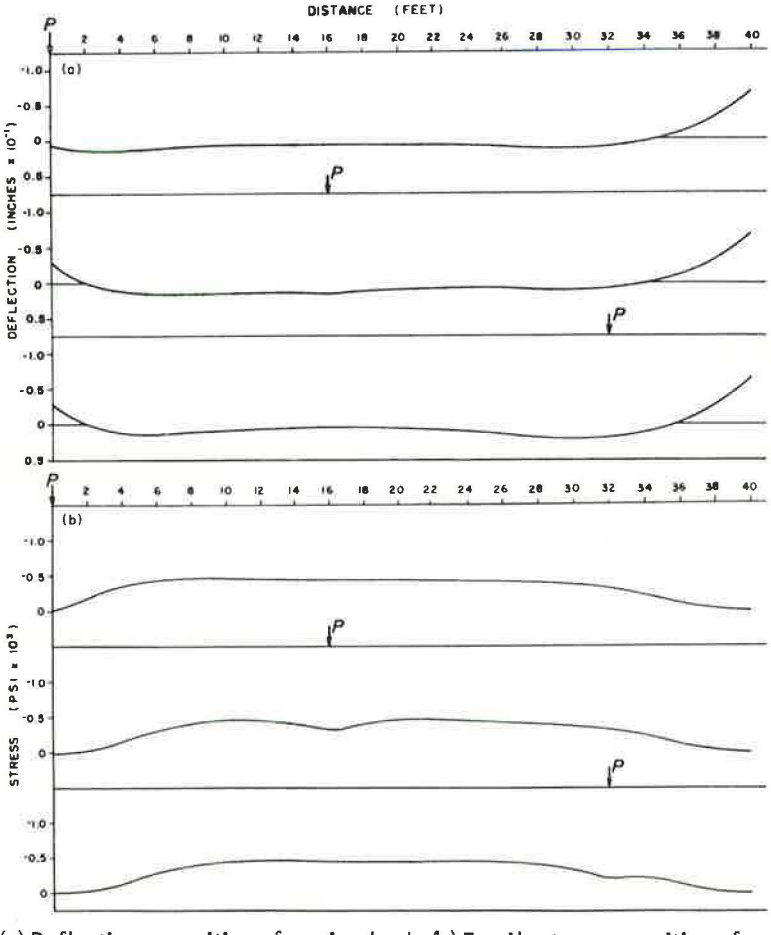

Figure 3. (a) Deflection vs position of moving load; (b) Tensile stress vs position of moving load; K_0 = 100 pci, H = 8 in., C_r = 1.5, ΔT = 30 F, v = 40 mph.

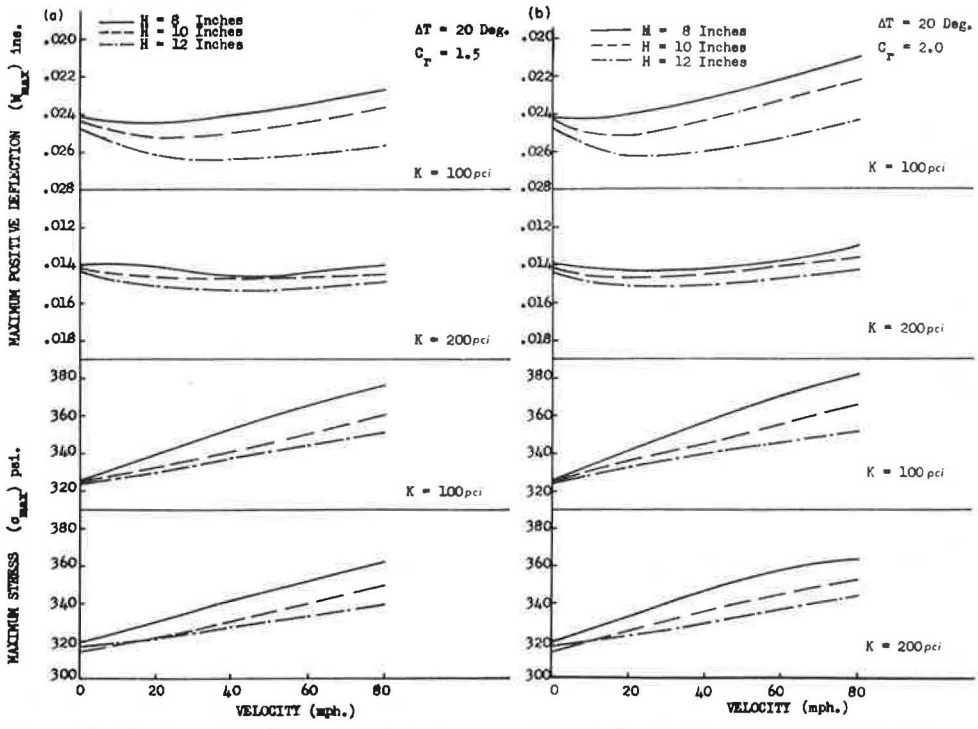

Figure 4. Maximum tensile stress and maximum positive deflection vs velocity of moving load: (a) $C_r = 1.5$, $\Delta T = 20$ F; (b) $C_r = 2.0$, $\Delta T = 20$ F.

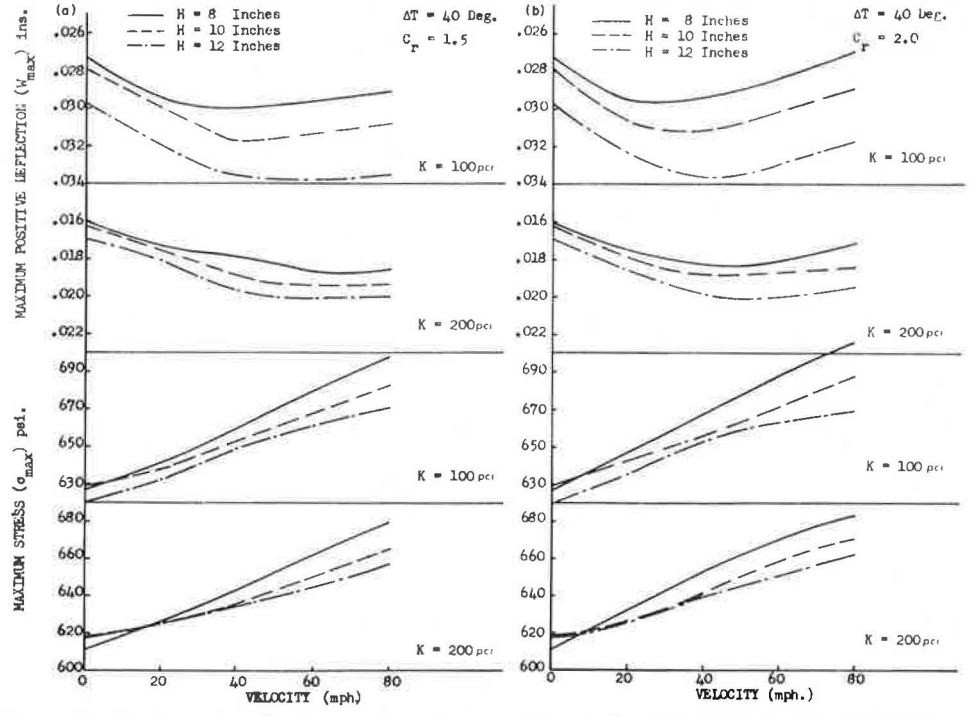

Figure 5. Maximum tensile stress and maximum positive deflection vs velocity of moving load: (a) $C_r = 1.5$, $\Delta T = 40$ F; (b) $C_r = 2.0$, $\Delta T = 40$ F.

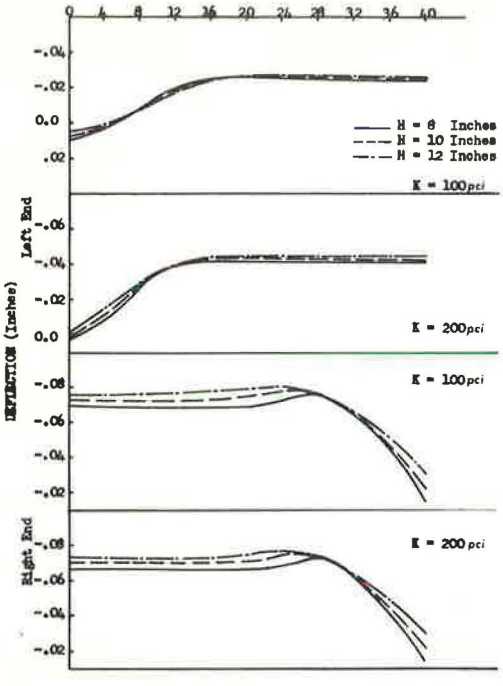

Figure 6. Deflection at ends of slab vs position of moving load (C_r = 1.5, ΔT = 30 F, v = 40 mph).

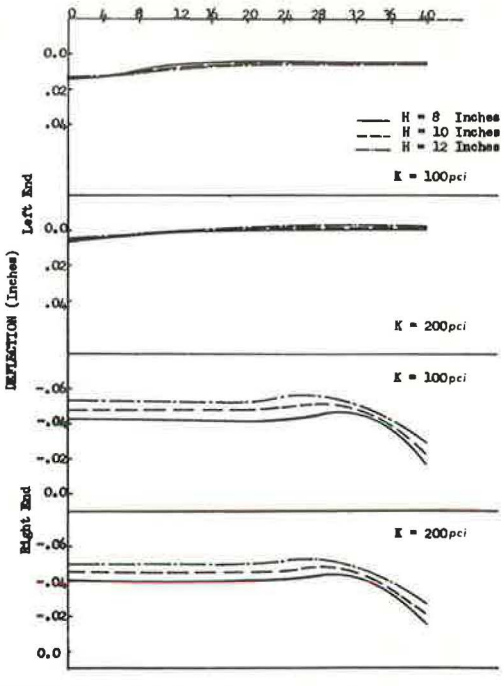

Figure 7. Deflection at ends of slab vs position of moving load (C_r = 1.5, ΔT = 30 F, v = 80 mph).

that the bending movement between slabs could be neglected while a shearing force equivalent to that in an infinite slab could be used to provide shear transfer. This seemed justifiable because of the relatively short depth of dowel embedment, and because the general nature of expansion and contraction joints is such as to permit the transfer of only very limited bending. For most highway work, dowel bars are only approximately 2 ft long, whereas the length of a slab averages about 40 ft; moreover, they are generally smooth and lubricated at one end to maintain freedom of horizontal movement between slabs. Under repetitive loading, these joints become looser and conceivably act more like a hinge, thus offering little or no moment transfer. On the other hand, substantial shear transfer could be experienced if the joint opening is small and the deflections are large enough to cause the development of a bearing pressure between dowel and concrete.

In any case, it should be noted that the magnitude of the moment and shear is really only significant in the near vicinity of the load itself. As a result, the solution is seen to be influenced by the values used for moment and shear transfer only when the load approaches the edges of the slab.

Figures 3, 4, and 5 demonstrate that for the case studied here, the damping ratio, C_r, does not greatly influence the values obtained for deflection and stress at low to moderate velocities; however, the higher value of C_r does result in a wider and less deflected trough (i.e., the depression under the load is wider but of smaller amplitude). In general, these figures tend to indicate that the pattern of the deflection and stress curves is mainly determined by temperature difference between slab surfaces and by the position of the moving load.

In the case considered here, temperature differences cause the ends of the slab to curl upward and become unsupported, while points midway between the midpoint and the ends of the slab experience an increase in positive deflection. For the positions of load shown in Figure 3, there is an increase in positive deflection and a decrease in tensile stress in the near vicinity of the load. However, as Figures 6 and 7 indicate, the radius of influence (wavelength of deflected surface) is not only a function of load

position but also of velocity. At low velocities, the radius of influence is small, but as velocity increases, this radius increases significantly behind the moving load. This characteristic, which was also observed by Thompson (44), plays an important role in the explanation of Figures 4 and 5.

For the case of an overdamped pavement ($C_r > 1.0$), it was initially anticipated that both the maximum deflection and stress would decrease with increasing velocity. However, Figures 4 and 5 indicate that, if curling is in evidence, this may not be the case. As was stated earlier, the maximum positive deflection in an unloaded slab subjected to moisture and/or temperature gradients that cause upward curling at the ends occurs somewhere near the one-quarter and three-quarter points of the slab. When a moving load is introduced, a wave train is set up and the deflected trough that lags the load becomes wider as velocity increases. In other words, the influence of the deflected trough behind the moving load increases with increasing velocity.

Therefore, if a slab that is initially curled upward at the ends is subjected to a moving load, there will be a tendency for the portion of the slab behind the load to become flatter and more fully supported as velocity increases (Figs. 6 and 7). As this flattening occurs, the maximum positive (downward) deflection behind the load increases until the velocity reaches a value that produces a reasonably flat, fully supported slab. Then a decrease in maximum positive deflection is experienced with further increases in velocity. Thus, in a slab that is curled upward at the ends, the maximum positive deflection does not occur at zero velocity, as is the case for fully supported slabs not subjected to moisture and/or temperature gradients, but at some velocity greater than zero.

As far as stresses are concerned, a line of reasoning similar to that used previously to explain the deflection pattern may be employed to account for the increase in maximum stress with increasing velocity shown in Figures 4 and 5. Increased velocities result in a greater tendency to flatten the slab and this in turn causes an increase in the tensile stress at the top of the slab.

As may be expected, the pattern as well as the magnitude of deflections and stresses obtained depends on the stiffness of the slab, the firmness of the subgrade material, and the temperature difference between slab surfaces. For the range of velocity studied, maximum positive deflection decreased as the value of subgrade reaction increased, and increases were experienced as pavement thickness and temperature gradients became greater. However, as Figures 4 and 5 show, the greater the resistance to flattening, the higher the velocity at which the curled surface becomes flat enough to result in a decrease in maximum positive deflection. In the case of stresses, the increase in temperature gradient from 20 to 40 F produced almost a 50 percent increase in stress, whereas the variation in pavement thickness and subgrade reaction did not appear to have much influence. The influence of the higher value of C_r on deflection and stress is also small. However, the fact that it produces a wider and less deflected trough is quite evident.

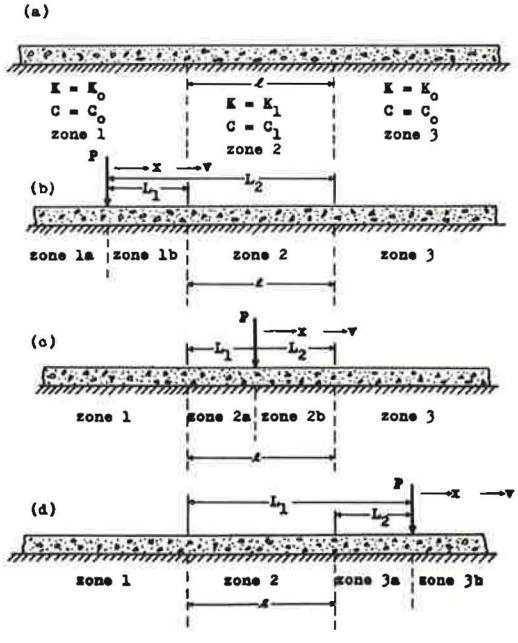

Figure 8. Infinite slab over region of reduced subgrade reaction.

EFFECT OF REDUCTION IN SUBGRADE SUPPORT

In this part of the paper, the main objective is to determine what effect a

reduction of the subgrade reaction would have on the stresses and deflections in a pavement subject to imposed vehicular loadings. For this case there is little loss in generality by assuming a particular value of shear and moment transfer between slabs. The procedure to be followed can be adapted to any degree of transfer. Therefore, for the present purpose where there is primary concern only for the region evidencing subgrade reduction, it is expedient to consider primarily the case of an infinite slab. As a special case, the condition that 50 percent shear and no moment transfer exist between two semi-infinite slabs is also examined.

The pavement section for the case of the infinite slab is shown in Figure 8. Here, the subgrade in its original form is represented by zones 1 and 3, whereas the area over which the reduction of subgrade reaction occurs is represented by zone 2. The differential equation describing the surface of the pavement is given by Eq. 4b.

To introduce the equivalence of a moving load, another zone must be added to the pavement. For example, in Figure 8 zone 1 is seen to be divided into two zones, 1a and 1b, and the force P is accounted for in the boundary conditions.

Solution of Problem

For the case when the moving load is over zone 1 and approaching zone 2, Eq. 4b is applied to each of zones 1a, 1b, 2 and 3, and solutions are obtained using the appropriate subgrade properties. The boundary conditions used in evaluating the constants are as follows:

$$w_{1a}(-\infty) = q_0/K_0 \tag{6a}$$

$$w'_{1a}(-\infty) = 0 \tag{6b}$$

$$w_{1a}(0) = w_{1b}(0) \tag{6c}$$

$$w'_{1a}(0) = w'_{1b}(0) \tag{6d}$$

$$w''_{1a}(0) = w''_{1b}(0) \tag{6e}$$

$$w''_{1b}{}'(0) - w''_{1a}{}'(0) = P/D \tag{6f}$$

$$w_{1b}(0) = w_2(L_1) \tag{6g}$$

$$w'_{1b}(L_1) = w'_2(L_1) \tag{6h}$$

$$w''_{1b}(L_1) = w''_2(L_1) \tag{6i}$$

$$w''_{1b}{}'(L_1) = w''_2{}'(L_1) \tag{6j}$$

$$w_2(L_2) = w_3(L_2) \tag{6k}$$

$$w'_2(L_2) = w'_3(L_2) \tag{6l}$$

$$w''_2(L_2) = w''_3(L_2) \tag{6m}$$

$$w'_2{}''(L_2) = w'_3{}''(L_2) \tag{6n}$$

$$w_3(\infty) = q_0/K_0 \tag{6o}$$

$$w'_3(\infty) = 0 \tag{6p}$$

After evaluating the constants in the resulting set of linear equations (29) using Crout's method of reduction with an IBM 7090 computer, the deflections and stresses were determined. The complete solution to the problem was obtained by applying this same procedure with suitable modifications to the schemes shown in Figure 8.

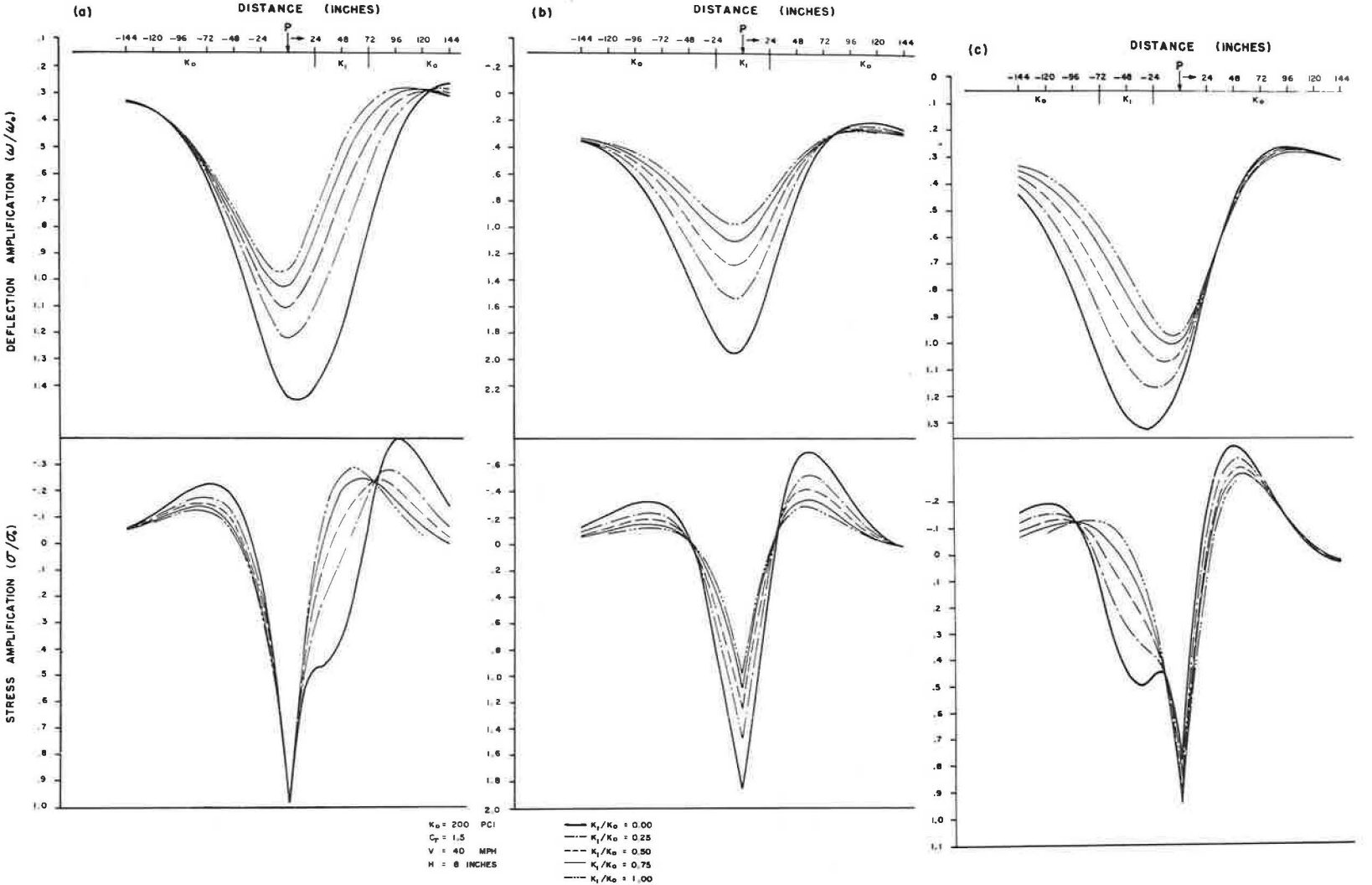

Figure 9. Deflection and stress amplification for load: (a) 2 ft behind region of reduced subgrade reaction; (b) at midpoint of region of reduced subgrade reaction; (c) 2 ft ahead of region of reduced subgrade reaction.

TABLE 1

DEFLECTION AND STRESS UNDER A STATIC LOAD (125 lb/in.)

H, in.	K_0 = 100 pci		K_0 = 200 pci	
	w_0, in.	σ_0, psi	w_0, in.	σ_0, in.
8	0.019144	150.607	0.010722	126.645
10	0.019017	113.948	0.010481	95.819
12	0.019449	90.726	0.010573	76.291

Results

To investigate the effect of a reduction in subgrade reaction, numerical results were obtained for combinations of the following data:

μ = 0.15
E = 4×10^6 psi
ℓ = 24, 48, 96 in.
H = 8, 10, 12 in.
K_0 = 100, 200 pci
K_1 = 0, 25, 50, 75, 100, 150, 200 pci
C_r = 1.5, 2.0
v = 0, 20, 40, 60, 80 mph
P = 125 lb/in.
q_0 = 150.9 pcf

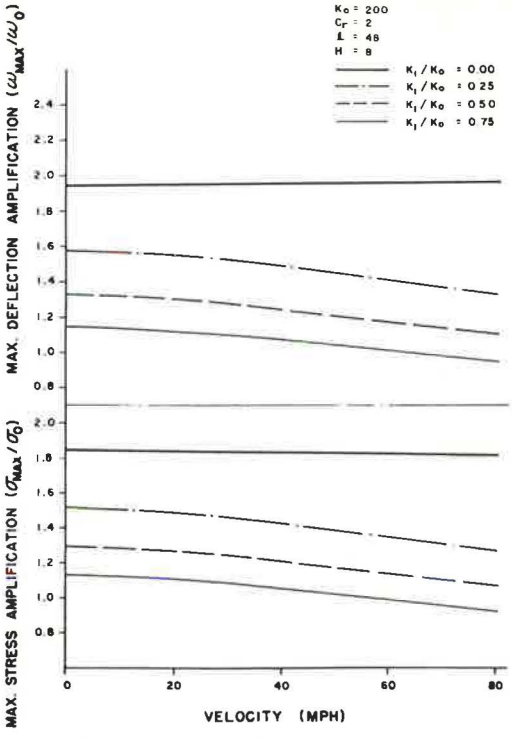

Figure 10. Maximum deflection and stress amplification vs velocity (K_0 = 200 pci, C_r = 2.0).

Some typical curves (in nondimensional form) for displacements and stresses for three positions of the load are shown in Figure 9. Values for the deflection and stress under a static load, P, are given in Table 1. These values may be used in Figure 9, with appropriate amplification ratios, to obtain the magnitudes of deflection and stress at a point.

Figure 10 shows the variation of maximum stress and deflection with velocity, whereas Figures 11 and 12 show the influence of the parameters ℓ and H. Curves similar to those in Figure 9 are shown in Figure 13 for the special case where there is only 50 percent load transfer and no moment transfer across a discontinuity in the pavement surface.

Discussion of Results

As shown in Figure 9, there is an increase in positive deflection amplification as the value of K_1/K_0 decreases. For the load positions shown, the increase is greatest when the load is over the zone of reduced subgrade reaction and least when the load is past this zone. As may be expected, when the load is moving over a homogeneous subgrade material, the point of maximum positive deflection lags the position of the load. However, if there is a zone of reduced subgrade reaction and the load is approaching this zone (as shown in Fig. 9a), the maximum deflection can lead the position of the load at low values of K_1/K_0. For the cases when the load is over the weakened region or has passed it, maximum positive deflection lags the load. This characteristic tends to increase as the load moves out of the weakened area.

With regard to stresses, a reduction in the value of K does not appear to influence the maximum stress very much unless the load is within the area of reduced K. However, as Figure 9 shows, it can affect significantly the shape of the curve at very low values of K_1/K_0.

For the three positions of load considered, the maximum stress, which always occurred under the moving load, reached its greatest value when the load was over the

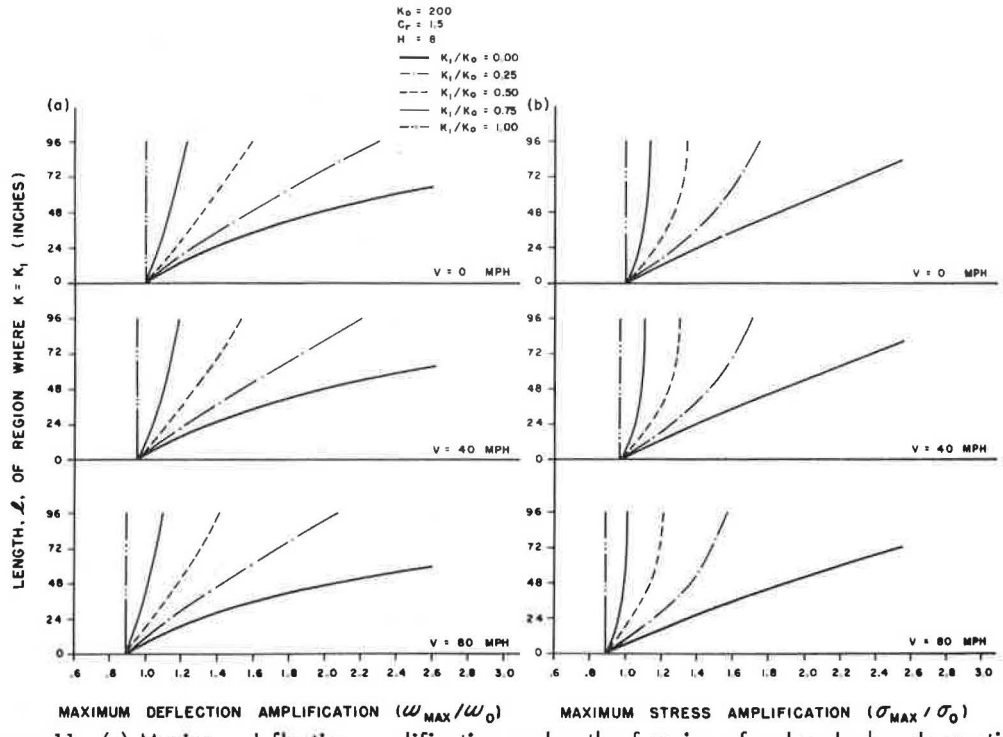

Figure 11. (a) Maximum deflection amplification vs length of region of reduced subgrade reaction; (b) Maximum stress amplification vs length of region of reduced subgrade reaction; K_0 = 200 pci, C_r = 1.5.

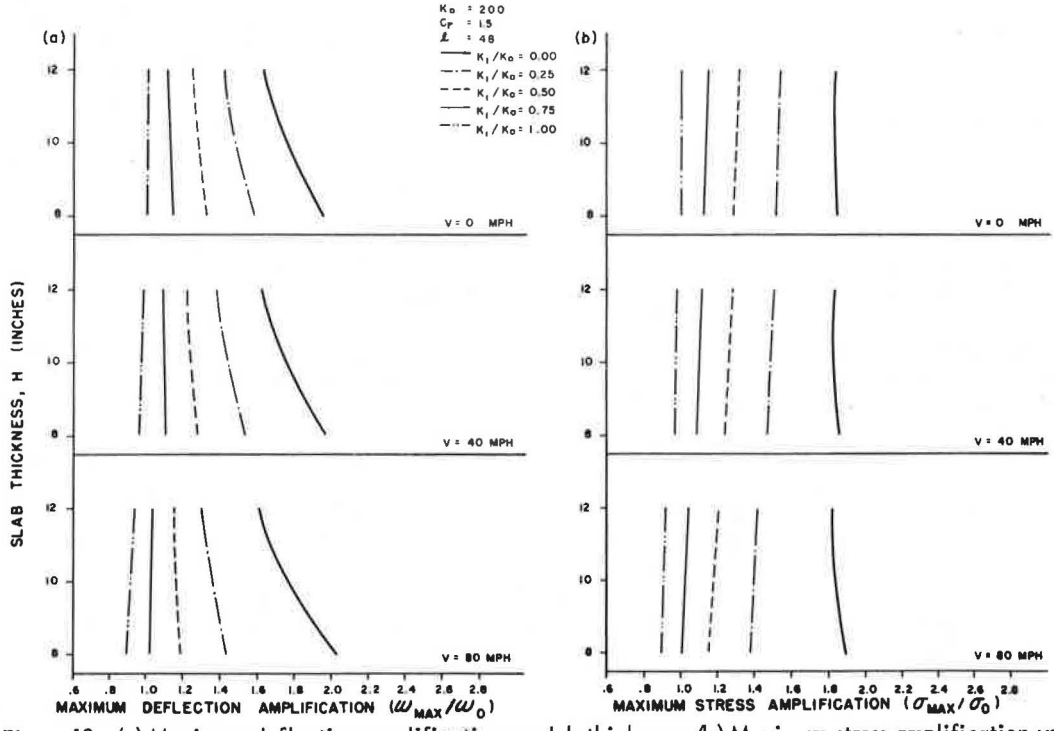

Figure 12. (a) Maximum deflection amplification vs slab thickness; (b) Maximum stress amplification vs slab thickness; K_0 = 200 pci, C_r = 1.5.

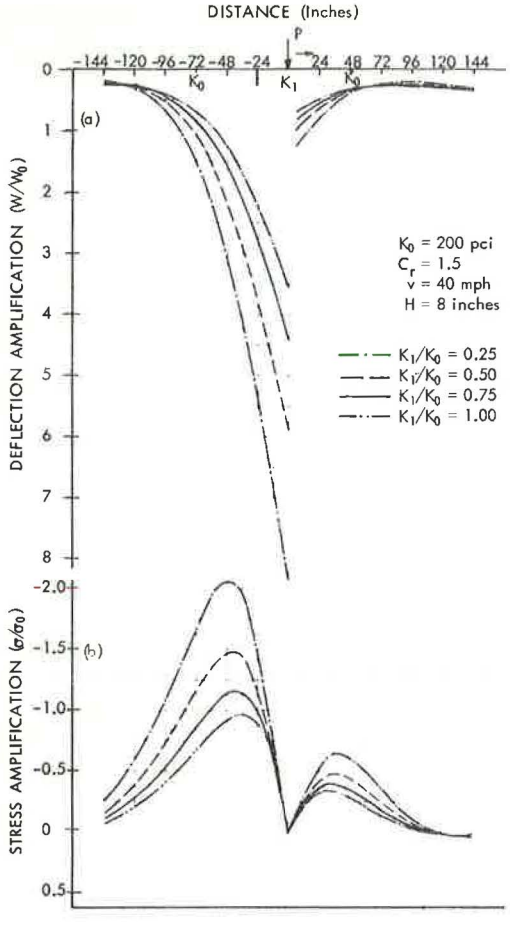

Figure 13. Deflection and stress amplification for load at midpoint of region of reduced subgrade reaction (no moment transfer across midpoint of region).

weakened zone; here, stress increased as K_1/K_0 decreased. In the case when the load is approaching the weakened zone, stress is again seen to increase with decreasing K_1/K_0. But after the load has passed this zone, the trend is reversed and the lower the value of K_1/K_0, the lower the stress under the load. This means that if a slab is lying on a subgrade exhibiting a soft spot, the stress experienced in the slab is greater when the load is moving toward the center of this weakened zone than when the load is moving away. Consequently, if failure caused by overstressing does occur, the signs of distress should appear somewhere between the center and the "back" edge of the soft zone.

Figure 10 shows that, except for very low values of K_1/K_0, deflection and stress amplification decrease with increasing velocity; however, the decrease appears to be more pronounced for the smaller value of initial subgrade reaction, K_0. Here also the higher value of C_r yields the lower value of maximum deflection and stress.

The influence of the length of the weakened region is shown in Figures 11a and 11b. In these figures, both the maximum stress and deflection are seen to increase, for all values of K_1/K_0 less than 1, as the region of reduced subgrade reaction becomes larger. The stiffer the subgrade material is initially, the greater the increase in deflection and stress. However, in the case of stress, this is only discernible at low values of K_1/K_0.

In general, the influence of the thickness of the pavement on stress and deflection amplification was only significant at low ratios of K_1/K_0. As shown in Figures 12a and 12b, deflection amplification decreases as thickness increases when the value of K_1/K_0 is approximately equal to 0.7 or less, whereas stress amplification remains relatively insensitive to variation in thickness. Again, these plots show that for constant K_1/K_0 ratios less than 1, the initially stiffer subgrade leads to the greater increase in stress and deflection. This suggests that, if the possibility of development of soft spots in the subgrade material exists, it may be better to avoid the use of stiff subgrades.

In Figure 13, there is a clear indication of what may happen when, in addition to the reduction in subgrade reaction, 50 percent of load transfer is lost. Deflections are substantially increased near the point of discontinuity, especially when the load is over the weakened region. For example, for $K_1/K_0 = 0.5$ in Figure 13, the deflection amplification for a point under the moving load is 5.85, compared to 1.26 in Figure 9b. Another important aspect to note is the large relative movement that occurs between the edges of the slab (i.e., edges situated at the midpoint of the weakened region). This movement not only causes bumpy driving, but may also lead to further pavement distress.

As for stresses, Figure 13 shows that for the special case considered the maximum stress need not occur under the moving load. In fact, the maximum stress experienced in this case is not only behind the load, but is also correspondingly higher than that

obtained in Figure 9b. For the other two positions of the load, the use of no-moment-transfer and 50 percent shear transfer did not greatly influence the values previously obtained in Figure 9 for maximum stress as long as the ratio of K_1/K_0 was high (approximately = 0.8). However, when the ratio of K_1/K_0 was lowered to 0.25, significant reduction in stress was experienced. Obviously, at high values of K_1/K_0, the load in this case has to be fairly close to the weakened region before conditions existing at the midpoint of the region become important.

SUMMARY AND CONCLUSIONS

In the first part of this study it is shown that, when a pavement is subjected to upward curling, it is possible to experience an increase in maximum positive deflection as velocity is increased, and then a decrease in maximum positive deflection with further increases of velocity. The velocity at which the decrease in maximum positive deflection sets in seems to depend on several factors, including the thickness of the slab, the temperature difference between its surfaces, the stiffness of the foundation, and the degree of damping. In general, it appears that higher velocities are needed to effect a decrease in maximum positive deflection as slab thickness, stiffness of foundation, and temperature increase, and as the degree of damping decreases.

In the case of stresses, maximum stress increased with increasing velocity. The thinner the pavement and the lower the value of subgrade reaction and damping coefficient, the higher the stress. However, there was not a great difference in the values of stress obtained. What seemed to matter most was the difference in temperature between the surfaces of the slab. Increases in the temperature difference resulted in large increases in stress and maximum positive deflection for all values of velocity studied. This observation tends to indicate that temperature difference between slab surfaces is the overriding factor governing the magnitude of stress and deflection that may be obtained, whereas factors such as velocity, thickness of pavement, modulus of subgrade reaction, and degree of damping act more or less to exaggerate or minimize the pavement distress caused by temperature and/or moisture gradients.

In the second part of the study, where the influence of a reduction in subgrade reaction was studied, it was clearly shown that both maximum deflection and maximum stress increased as the region became weaker. The increase experienced was quite pronounced when the load was within the weakened region and moving toward its center. Thus, if a pavement is designed with a particular value of subgrade reaction and a weakened zone develops because of the softening of the ground (as may be the case during spring thaw), the stresses produced in the slab in the near vicinity of the weakened zone will very likely be higher than anticipated.

If there is a significant reduction of subgrade support (even to within 75 percent of the original value of K_0), maximum deflection and stress should still follow the well-known trend and decrease with increasing velocity. However, when there is complete loss of subgrade support, both the maximum stress and deflection can increase with increasing velocity. For the hypothetical case where pavements of equal thickness are built on different subgrade material, it appears that for a constant percentage loss of subgrade support, the pavement built on the stiffer subgrade material should experience a greater increase in stress and deflection. In the case where there is also a loss of load transfer, deflections as well as stresses may be substantially increased and large relative movement may be experienced near the points of discontinuity in the surface of the slab.

In conclusion, we find that on the basis of the assumptions stated herein, this study indicates that (a) contrary to common opinion, an increase in velocity can produce an increase in deflection and stress; (b) of all the variables considered herein (temperature differences, velocities, thickness of pavement, moduli of subgrade reaction, and degrees of damping), the temperature difference between slab surfaces was shown to be the overriding factor governing the magnitude of maximum stress and deflection; (c) there is reason to believe that any meaningful interpretation of the performance of pavements as determined by measured strains and/or deflections of the slab must give due regard to the effects of warping; and (d) stresses and deflections within a slab can be sensitive to localized reductions in subgrade support.

ACKNOWLEDGMENT

This study was made possible by the financial assistance of the Joint Highway Research Project between the Indiana State Highway Commission and Purdue University.

REFERENCES

1. Standard Specifications for Highway Materials and Methods of Sampling and Testing. 8th. Ed. American Association of State Highway Officials, 1961.
2. Proposed Recommended Practice for Design of Concrete Pavements. Jour. ACI, Vol. 28, No. 8, Feb. 1957.
3. Bell, J. R. A Study of the Dielectric Properties of Hardened Concrete With Respect to Their Utility as Moisture Indicators. PhD thesis, Purdue University, 1963.
4. Bernoulli, D. Comenentarii Academiae Scientiarum Imperialis Petropolitanie. Vol. 13, 1751.
5. Contributions to Soil Mechanics 1925-1940. Boston Society of Civil Engineers, Boston, 1940.
6. Dorr, J. Der unendliche, federnd gebettete Balken unter dem Einfluss einer gleichformig bewegten Last. Ing.-Arch., Vol. 14, 1943.
7. Euler, L. Methodus inveniendi lineas curvas maximi minimive proprietate gandentes. Additamentum, De curvis elasticis, 1744.
8. Fabian, G. J., Clark, D. C., and Hutchinson, C. H. Preliminary Analysis of Road Loading Mechanics. HRB Bull. 250, pp. 1-19, 1960.
9. Filonenko-Borodich, M. M. Some Approximate Theories of the Elastic Foundation (in Russian). Llchenyie Zapiski Moskovskogo Gosudarstvennogo Universiteta, Mekbanica No. 46, 1940.
10. Freudenthal, A. M., and Lorsch, H. G. The Infinite Elastic Beam on a Linear Visoelastic Foundation. Jour. Eng. Mech. Div., Proc. ASCE, Jan. 1957.
11. Geldmacher, R. R., Anderson, R. L., Dunkin, J. W., Partridge, G. R., Harr, M. E., and Wood, L. E. Subgrade Support Characteristics as Indicated by Measurements of Deflection and Strain. HRB Proc., Vol. 36, pp. 479-496, 1957.
12. Harr, M. E., and Leonards, G. A. Warping Stresses and Deflections in Concrete Pavements. HRB Proc., Vol. 38, pp. 286-320, 1959.
13. Hertz, H. R. Ueber das gleichgewicht schwimmender elastischer Platten. Annalen der Physik und Chemie, Vol. 22, 1884.
14. Hetenyi, M. Beams on Elastic Foundation. Univ. of Michigan Press, Ann Arbor, 1946.
15. Road Test One—MD. HRB Spec. Rept. 4, 1952.
16. The WASHO Road Test, Part 1: Design, Construction, and Testing Procedures. HRB Spec. Rept. 18, 1954.
17. The WASHO Road Test, Part 2: Test Data, Analyses, Findings. HRB Spec. Rept. 22, 1955.
18. The AASHO Road Test: Report 5—Pavement Research. HRB Spec. Rept. 61E, 1962.
19. Hoskin, B. C., and Lee, E. H. The Analysis of Loaded Flexible Surfaces Over Subgrades With Viscoelastic Material. Tech. Rept. No. 5 (Final), Div. of Applied Mechanics, Brown Univ., Providence, Rhode Island, July 1958.
20. Hovey, B. K. Beitrag zur Dynamik des geraden Eisenbahngleises. Dissertation, Göttingen, Germany, 1933.
21. Hveem, F. N. Slab Warping Affects Pavement Joint Performance. Jour. ACI, Vol. 47, 1951.
22. Hveem, F. N. Types and Causes of Failure in Highway Pavements. HRB Bull. 187, pp. 1-52, 1958.
23. Kelley, E. F. Applications of the Results of Research to the Structural Design of Concrete Pavements. Public Roads, Vol. 20, Nos. 5-6, pp. 83-126, 1939.
24. Kenney, J. T., Jr. Steady State Vibrations of Beam on Elastic Foundation for Moving Load. Jour. Appl. Mech., Vol. 21, Dec. 1954.

25. Kerr, A. D. Viscoelastic Winkler Foundation With Shear Interactions. Jour. Eng. Mech. Div., Proc. ASCE, June 1961.
26. Klubin, P. I. Computations of Beams and Circular Plates on Elastic Foundations (in Russian). Inzhenernii Sbornik, Vol. 12, 1952.
27. Lamb, H. On Waves in an Elastic Plate. Proc. Royal Society (London), 93A, 1916.
28. Leonards, G. A., and Harr, M. E. Analysis of Concrete Slabs on Ground. Jour. Soil Mech. and Found. Div., Proc. ASCE, June 1959.
29. Lewis, K. H. Analysis of Concrete Slabs on Ground and Subjected to Warping and Moving Loads. Joint Highway Research Project, No. 16, Purdue Univ., Lafayette, Indiana, June 1967.
30. Ludwig, K. Die Verformung eines beiderseits unbegrenzten elastisch gebetteten Geleises durchlasten mit konstanter Horizontalgeschwindigkeit. Proc., Fifth Internat. Cong. Appl. Mech., Cambridge, Massachusetts, 1938.
31. Nowacki, W. Dynamics of Elastic Systems. John Wiley and Sons, 1963.
32. Pasternak, P. L. On a New Method of Analysis of an Elastic Foundation by Means of Two Foundation Constants (in Russian). Gosudarstvennoe Izdatelstro Literaturi po Stroitelstvu i Arkhitekture, Moscow, 1954.
33. Pister, K. S., and Williams, M. L. Bending of Plates on a Viscoelastic Foundation. Jour. Eng. Mech. Div., Proc. ASCE, Oct. 1960.
34. Concrete Pavement Design, 2nd Ed. Portland Cement Association, Chicago.
35. Quinn, Bayard E., and De Vries, Thomas W. Highway Characteristics as Related to Vehicle Performance. HRB Bull. 250, pp. 20-39, 1960.
36. Quinn, B. E., and Wilson, C. C. Can Dynamic Tire Forces Be Used as a Criterion of Pavement Condition. Report No. 32, Joint Highway Research Project, Purdue Univ., 1963.
37. Raleigh, Lord. On the Free Vibrations of an Infinite Plate of Homogeneous Isotropic Elastic Matter. Proc. London Mathematical Society, Vol. 20, 1889.
38. Ray, G. K. History and Development of Concrete Pavement Design. Jour. Highway Div., Proc. ASCE, Jan. 1964.
39. Reddy, A. S., Leonards, G. A., and Harr, M. E. Warping Stresses and Deflections in Concrete Pavements: Part III. Highway Research Record 44, pp. 1-24, 1963.
40. Reissner, E. A Note on Deflection of Plates on a Viscoelastic Foundation. Jour. Appl. Mech. Vol. 25, No. 1, March 1958.
41. Ritz, W. Uber eine neue Methode zur Lösung gewisser variations Probleme der mathematischen Physik. Crelle's Journal, Vol. 135, 1909.
42. Schiel, F. Der Schwimmende Balken. Zeitschrift für angewandte Mathematik und Mechanik, Vol. 22, 1942.
43. Spangler, M. G. Stresses in the Corner Region of Concrete Pavements. Iowa Engineering Experiment Station, Bull. 157, 1942.
44. Thompson, William E. Analysis of Dynamic Behavior of Roads Subject to Longitudinally Moving Loads. Highway Research Record 39, pp. 1-24, 1963.
45. Timoshenko, S. P. Collected Papers. McGraw-Hill, New York, 1953.
46. Timoskenko, S. P. Theory of Plates and Shells. McGraw-Hill, New York, 1959.
47. Standard Specifications for Construction of Roads and Bridges on Federal Highway Projects. U.S. Bureau of Public Roads, FP-57, Jan. 1957.
48. Westergaard, H. M. Stresses in Concrete Pavements Computed by Theoretic Analysis. Public Roads, April 1926.
49. Westergaard, H. M. Analysis of Stress in Concrete Roads Caused by Variations of Temperature. Public Roads, May 1927.
50. Winkler, E. Die Lehre von der Elastizität und Festigkeit. Praga Dominicus, 1867.
51. Wiseman, Joseph F., Harr, Milton E., and Leonards, Gerald A. Warping Stresses and Deflections in Concrete Pavements: Part II. HRB Proc., Vol. 39, pp. 157-172, 1960.
52. Yoder, E. J. Principles of Pavement Design. John Wiley and Sons, New York, 1959.

Prediction of Subjective Response to Road Roughness by Use of the Rapid Travel Profilometer

L. F. HOLBROOK, Testing and Research Division, Michigan Department of State Highways

•A PRIMARY PURPOSE in measuring road profiles (either elevation, slope, acceleration, or jerk) is to predict their effect on driver response. Studies of human response to motion have often been confined to purely laboratory investigations directly relating known physical inputs (acceleration) to their physiological or psychological consequences. Experiments such as those conducted in the AASHO Road Test (1) have sought to empirically establish the relationships between physical road properties and subjective driver response. These experiments differ in two important ways from traditional research:

1. The physical input (road profile) is not experienced by the subject (driver) directly, but through the complex modifying machinery of the automobile. Thus, even if the road input were originally known, it would be substantially transformed by the interposition of a vehicle between road and driver. Depending on vehicle speed and resonance, the longer, gently rolling profile elevation differences (long wavelengths) would cause the driver to experience very low frequencies (in cycles per second), whereas the short, choppy differences would result in relatively high frequencies, most of which would be attenuated by the vehicle and human body itself.
2. The human response to this band of frequencies is both physiological and psychological. Although some research has been devoted to the physiological aspects (2), the AASHO-type studies and the present investigation seek to measure the psychological. The reason for this emphasis is that, regardless of the motions to which drivers are subjected, it is their subjective opinion or response that counts. As this report and others (3) show, measurement of subjective response has both limitations and pitfalls. Nevertheless, it is a goal of sufficient importance to warrant continued effort.

In this study, the interposition of vehicle between subject and road will be acknowledged only to the extent that different vehicles are used. No vehicle characteristics are examined, because our purpose is to examine possible relationships between road profile per se and subjective response. The Michigan Rapid Travel Profilometer (RTP) is ideally suited to the measurement of road profiles for the reasons discussed by Darlington and Milliman (4). Some of the pertinent advantages are reviewed here.

A serious problem with moving-straightedge profilometers is that they introduce distortions into the measured profile. Put another way, these instruments do not have "flat" frequency (cycles per foot) response characteristics. The RTP frequency response is flat for a much larger range than required by roughness research.

Many of the problems discussed in the roughness literature center around the question of which profile frequencies are relevant to road roughness (5, 6). Clearly, those low frequencies induced by the long, "hill-valley" profile wavelengths, while passed by the vehicle and experienced by the driver, are not responsible for what we call "roughness". Similarly the very short, "choppy" wavelengths induce such high frequencies that they are largely damped or filtered out by the vehicle-human body system. There is, then, a middle range of profile wavelength, whose amplitude best relates to roughness. Attempts to filter profiles have usually been aimed at eliminating the long waves (detrending) and have required arbitrary decisions on method and degree. Moreover, these methods

Paper sponsored by Committee on Surface Properties—Vehicle Interaction.

often color the resulting profile, thereby compromising its value. The RTP can be preset to recover from the total profile only those frequencies thought relevant to roughness.

The resulting filtered profile is then analyzed by examining elevation deviations from an average elevation base line. It is mathematically convenient to square these deviations, sum them, and divide by the profile length. The resulting quantity (parameter) is called mean square deviation or variance. However, the total variance is composed of contributions from each wavelength found in the filtered profile. By a suitable technique called power spectral density (PSD) analysis the contributions to total variance made by the various wavelength regions can be estimated. The value of PSD analysis is that these variance contributions can be independently examined for their relevance to subjective response. Once the desired range of frequencies is determined, RTP equipment can be adjusted accordingly, thereby producing a profile specifically of interest to ride research.

Even if roughness can be satisfactorily obtained from profiles, there remains the question of how to measure subjective response. Highway and automotive researchers have generally used category scales. These scales require the subject to pick a category in a manner consistent with the degree of subjectively experienced roughness (some studies ask for judgments on "serviceability"). A special case of the category scale, the graphic rating scale, has achieved considerable popularity in road serviceability and automobile ride studies, following the lead of the AASHO Road Test (7, 8, 9, 10). Briefly, the subject is required to mark on a line his response to highway roughness or serviceability.

An entirely different approach to the problem of psychological measurement—often used in psychophysics—is found in the magnitude estimation methods. These require the subject to compare several objects or experiences and report their subjective ratio. Often one experience is held constant and called the standard, although this is not necessary. Unfortunately, the category and magnitude methods do not always produce the same scales. If only a ranking of psychological responses is desired, choice of scaling techniques makes little difference; i.e., both methods should generate the same relative subjective order. If, however, we wish to manipulate the scale mathematically, we must be able to measure psychological ratios or at least differences. Under these conditions, choice of scaling methods could affect the mathematical relationship between subjective response and road roughness, whether measured by roughometer or profilometer. If, in turn, we expect to relate subjective response in terms of either roughness or serviceability, which are closely related (9) to design and construction variables, as in the AASHO Road Test, these relationships could also be affected. The implication is that for this type of experiment, the relative importance of the various design factors may depend on the scaling method used in measuring human judgments.

In order to explore these problems, two field experiments were conducted (Fig. 1). The first consisted of 96 observers rating 16 roads and was designed to (a) examine differences among types of category rating scales, (b) examine the difference between subjective responses under normal driving conditions and under conditions of restricted sight and sound (blindfolds and earphones), and (c) examine the effects on subjective response of different passenger car sizes. The category scales selected (Fig. 2) were (a) a graphic rating scale used with 32 observers rating each of 16 roads, (b) a series of photometrically evenly spaced gray papers arranged as sectors of a circle representing nine categories of ride roughness from "excellent" to "unbearable", and (c) a sequence of eleven words pre-ranked by a rating panel to represent the ride continuum, again from "excellent" to "unbearable". In addition the three scales were cross-classified with eight different passenger cars (spanning the range of automobile weight found on American roads today). As a check on visual and aural "halo" effects—contamination of subjective response caused by stimuli other than those under measure (3, 11)—half of the 96 subjects were blindfolded and half were provided with sound-insulating earphones. The 96 subjects were able to use the three category scales with equal effectiveness; the agreement among subjects, as measured by the coefficient of concordance, was about the same ($W = 0.85$) for all scales. Also, the three category scales agreed very closely on the ranking of the 16 roads. Consequently, no evidence was found to suggest that the type of category scale selected has any bearing on either

Test Series I

Test Car	Linear Scale				Gray Scale (Category)				Word Scale (Category)			
	E/B*	E/NB	NE/B	NE/NB	E/B	E/NB	NE/B	NE/NB	E/B	E/NB	NE/B	NE/NB
1	1-subject 16-roads	1-subject 16-roads	1-subject 16-roads	1-subject 16-roads	1-subject 16-roads	1-subject 16-roads	1-subject 16-roads	1-subject 16-roads	1-subject 16-roads	1-subject 16-roads	1-subject 16-roads	1-subject 16-roads
2	"	"	"	"	"	"	"	"	"	"	"	"
3	"	"	"	"	"	"	"	"	"	"	"	"
4	"	"	"	"	"	"	"	"	"	"	"	"
5	"	"	"	"	"	"	"	"	"	"	"	"
6	"	"	"	"	"	"	"	"	"	"	"	"
7	"	"	"	"	"	"	"	"	"	"	"	"
9	"	"	"	"	"	"	"	"	"	"	"	"

*E : Subject wearing ear insulators.
NE : Subject not wearing ear insulators.
B : Subject wearing blindfolds.
NB : Subject not wearing blindfolds.

Test Series II

Road	Ratio Scale	
	Smoothness	Roughness
1	20-Subjects	20-Subjects
2	"	"
3	"	"
4	"	"
5	"	"
6	"	"
7	"	"
37	"	"

Figure 1. Experiment design for Test Series I and II.

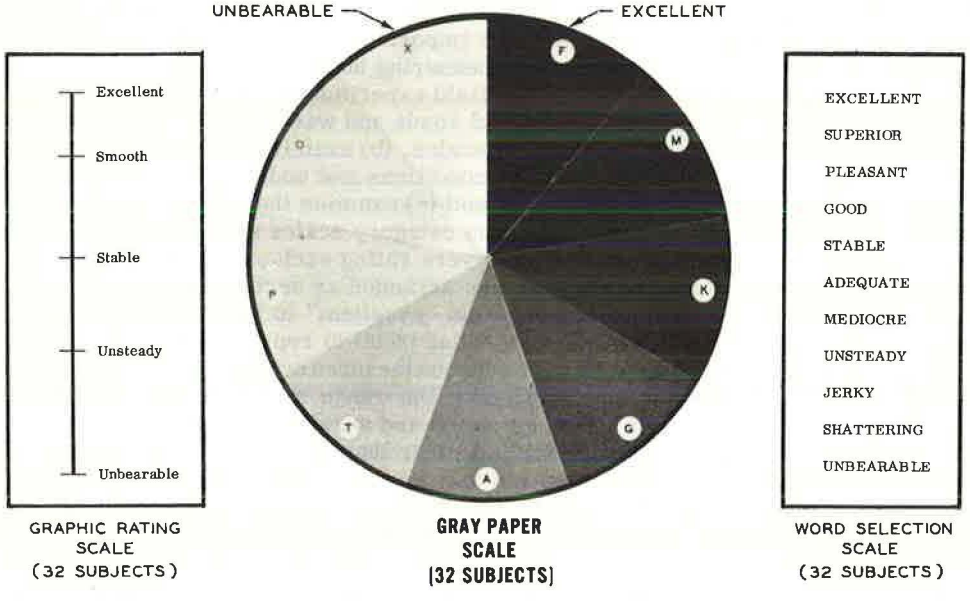

Figure 2. Types of category scales used in Test Series I.

subjective road rating agreement or position. Differences on the same scale caused by blindfolds and earphones were not measurable. Differences caused by cars were measurable but not of sufficient magnitude to significantly affect the main issue of this report.

In the light of these findings, it seemed reasonable to combine the data from the three category scales into a common scale based on 96 subjects. The three scales cannot be combined directly into an overall scale because category sizes and meanings are not comparable. However, there is a technique whereby information from each of the three scales can be merged into a common scale. The method, first developed by Thurstone (11, 12, 13), is generally known as "pair comparison" scaling and is developed from the following formula of basic statistics:

$$S_i - S_j = z_{ij} \sqrt{\sigma_i^2 + \sigma_j^2 - 2\sigma_i \sigma_j r_{ij}} \qquad (1)$$

where

S_i = subjective response to stimulus (road) I,
S_j = subjective response to stimulus (road) J,
σ_i^2 = variance of subjective response S_i to stimulus (road) I,
σ_j^2 = variance of subjective response S_j to stimulus (road) J,
r_{ij} = correlation between subjective response S_i and subjective response S_j, and
z_{ij} = standardized normal deviate representing with a normal curve of unit variance the proportion of times S_i is greater than S_j.

Thus, by knowing only the proportion of subjects stating that S_i is greater (rougher) than S_j we can generate the distance on the subjective scale between S_i and S_j.[1] This is true only if the other variables in Eq. 1 are known, or if they can be assumed constant or zero. The correlation term in Eq. 1 is generally assumed to be zero or constant. To test this assumption, the linear scale responses for 32 subjects were intercorrelated for all 120 road combination pairs in Test Series I. It is recognized that these intercorrelations are produced by means of a scaling procedure at issue in this report. However, comparison of scaling procedures using and excluding the correlation term in Eq. 1 indicates that it is of minor importance. Consequently, the approximate correlation values obtained by virtue of the linear scale should be adequate.

The existence of road intercorrelation can be explained by the well-known fact that subjects tend to impress personality and experience on the response scale. For example, if some subjects generally rate roads rough, and others tend to rate roads smooth, this will show up as positive correlation among the road ratings. Figure 3 shows the relationship between all possible S intercorrelations and the ratio of the corresponding roughness values, R greater/R lesser. Apparently, for roads comparable in roughness, subjective responses tend to correlate positively, whereas roads having great roughness differences are not subject to intercorrelation at all. For this study, the correlation coefficient in Eq. 1 is computed from the following equation determined by least squares from the data shown in Figure 3:

$$r = -0.56 \log (R_G/R_L) + 0.59 \qquad (2)$$

---

[1]The scale developed from Eq. 1 does not follow the conventional procedure expounded by Thurstone. The matrix of all possible proportions P was converted to the z matrix as usual. This matrix was then multiplied by the $\sqrt{\sigma_i^2 + \sigma_j^2 - 2\sigma_i \sigma_j r_{ij}}$ matrix. This provided 16 road scales each based on relationships to a given road. The 16 scales were then regressed on each other providing revised estimates of road separations. This process was iterated several times until the correlation matrix converged to an average value of 1.0.

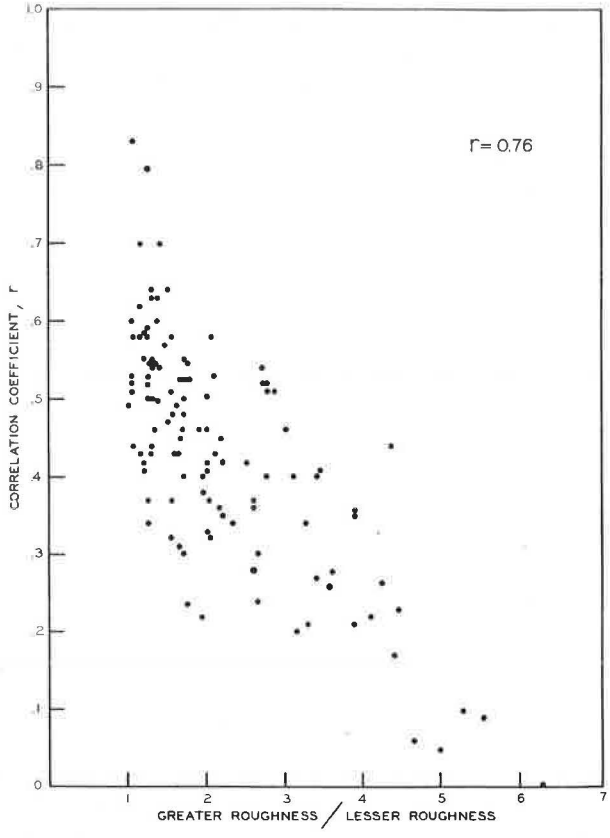

Figure 3. Relationship between subjective response intercorrelations and roughness.

Figure 4 shows that the conventional linear scale (Fig. 2), as used in the AASHO study, can be reproduced by Eq. 1 when the variance terms σ_i^2, σ_j^2 are held constant and equal. Equation 1 then becomes

$$S_i - S_j = z_{ij} \sqrt{2C} \sqrt{1 - r_{ij}}$$

Because $\sqrt{2C}$ is a factor in all scale separations $(S_i - S_j)$, it is omitted and Eq. 1 becomes

$$S_i - S_j = z_{ij} \sqrt{1 - r_{ij}} \qquad (3)$$

The units in Figure 4 are unimportant because these are interval subjective scales, and have no meaningful zero point. Consequently, the slope and intercept are irrelevant. What is important, however, is the degree of fit exhibited by the two scaling methods. Figure 4 shows excellent agreement (correlation of 0.99) between these two methods. Therefore, it is evident that the linear scale is a special case of the pair comparison scale when the variances of subjective response are assumed constant throughout the full roughness range.

We are now in a position to examine the effects of roughness level on response variance, and consequently, the subjective scale itself. Attempts by others to assess response

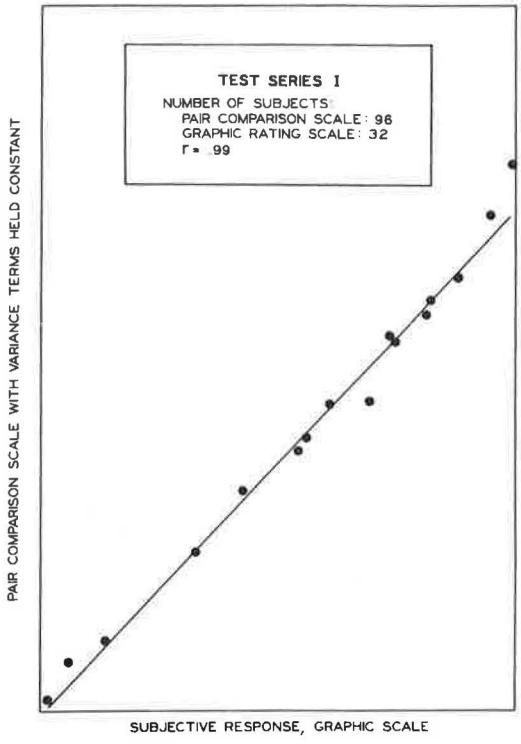

Figure 4. Relationship between graphic rating scale and pair comparison scale of Eq. 3.

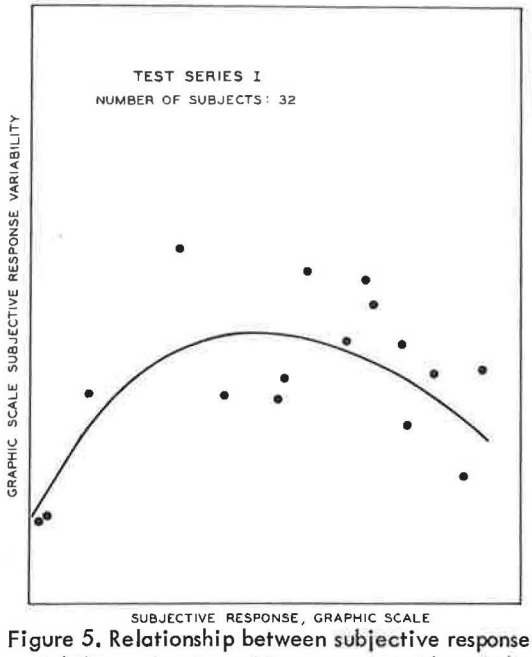

Figure 5. Relationship between subjective response variability and scale position as measured by graphic rating scale.

variability have been made by directly taking the individual linear scale responses for a given road and directly forming their variance. Plots of σ^2 vs mean panel rating tend to show that σ^2 is greatest in the midrange of roughness. Yoder and Milhous (9) suggest that panel rating variation is a minimum for very rough and very smooth pavements. For the data of Test Series I the linear scale responses were first standardized to eliminate individual idiosyncracies, and a common measure of variability (the inner-quartile range) was plotted against median responses (Fig. 5). This procedure shows the same contraction of dispersion at the scale end points as suggested by Yoder and Milhous (9). The question arises as to whether these results are inherently characteristic of human response to road roughness, or are merely due to the distortion introduced by an inadequate scaling procedure.

Intuitively, it would seem that subjective response dispersion should not increase, reach a maximum, and then decrease as indicated by Figure 5. Rather, judgment difficulty, and hence response dispersion, should increase with roughness, the maximum occurring at the rough end of the scale. ("Dispersion" and "variability" are general terms referring to the spread of data; variance and inner-quartile range are each mathematical measures of it.) Moreover, there is a wealth of psychophysical experience that conflicts with the curve of Figure 5. (Weber's law states that the "just noticeable difference" between two stimuli increases in proportion to the stimulus magnitude; i.e., $\Delta M = KM$. Weber's law and its variations are reputed to be applicable over a very large range of psychophysical phenomena.) Thus, we have good reason to doubt the uniform variance assumption of Eq. 3, and hence the validity of the linear scale itself. These comments notwithstanding, the scale produced by Eq. 3 is plotted against the roughness level in Figure 6. Notice that the relationship is of the form

$$S = A \log R \qquad (4)$$

Equation 4 is predictable (14) and is generally found when category scaling is plotted against physical input (15). For example, the log of slope variance was selected as the best predictor of "serviceability" in the AASHO Road Test (1).

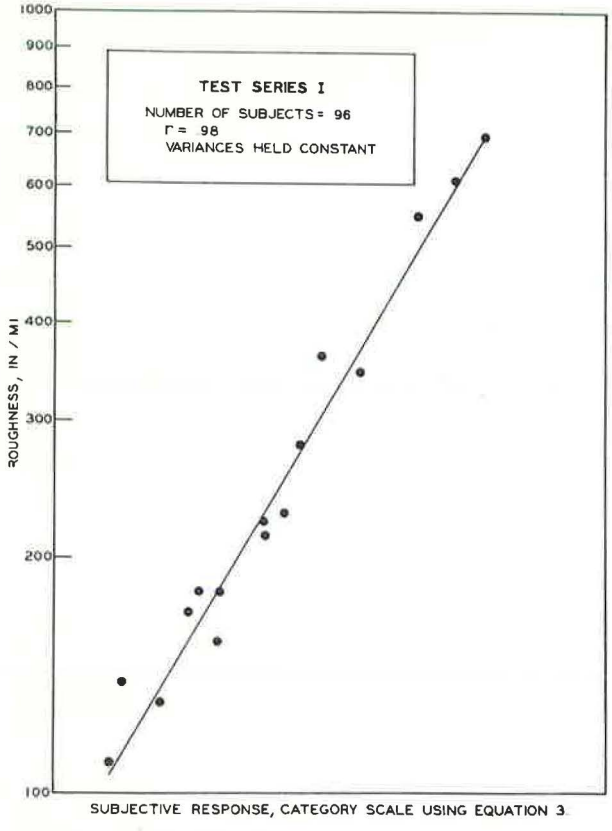

Figure 6. Relationship between roughometer roughness and subjective response as measured by three category scaling methods.

The second test series of this study was designed to contrast the scale produced by magnitude estimation techniques with that of the category methods discussed previously. In this series, 37 test sections were evaluated by 40 observers by requiring them to report the ratio of the riding quality of each section to the preceding one; 20 subjects rated "roughness" and 20 rated "smoothness" in order to remove possible bias associated with the direction of ratio estimation. Because the responses are ratios, they must be multiplied sequentially (the first road is defined as 1.0 on the subjective scale) to generate scale values (16, 17). This procedure, although yielding magnitude estimates, is subject to considerable error in view of the number of multiplications necessary (37 for the last ratio in Test Series II). Randomization of test roads would distribute these errors; however, it was found administratively necessary to present the roads in the same order to each subject. It would not be possible to present all combinations of roads directly without contaminating the ratio judgments with irrelevant intervening roadway. Nevertheless, a large variety of roughness ratios were available from the 37 roads. It has been found (15, 18, 19, 20) that magnitude estimates of subjective response ratios are related to physical input (roughness) ratios by the power law:

$$\frac{S_i}{S_j} = \left(\frac{R_i}{R_j}\right)^{\phi} \tag{5}$$

or in general

$$S = KR^{\phi} \tag{6}$$

where K is a scale factor and ϕ is an exponent related to the type of physical input.

Equation 6 can be used for both estimates of roughness and smoothness ratios. Figure 7 shows the distribution of 36 estimates each of ϕ_S and ϕ_R. Median ϕ_R for "roughness" is 1.10 and median ϕ_S for "smoothness" is -1.10. It appears that there is little, if any, difference in "roughness" rating as opposed to "smoothness" rating, and that the two values can be averaged to provide an overall estimate of 1.10 for roughness. This means that subjective response is directly related to roughness:

$$S = KR^{1.10}$$

$$S \cong R \tag{7}$$

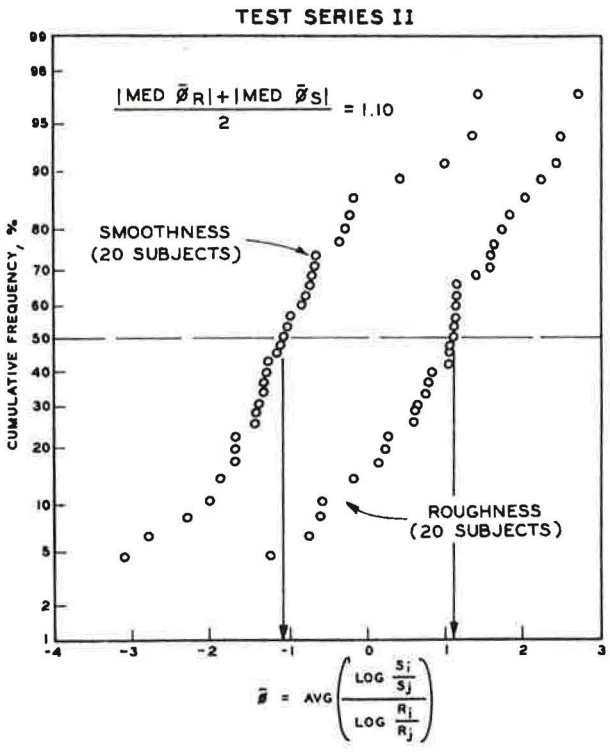

Figure 7. "Smoothness" and "roughness" distribution of ϕ.

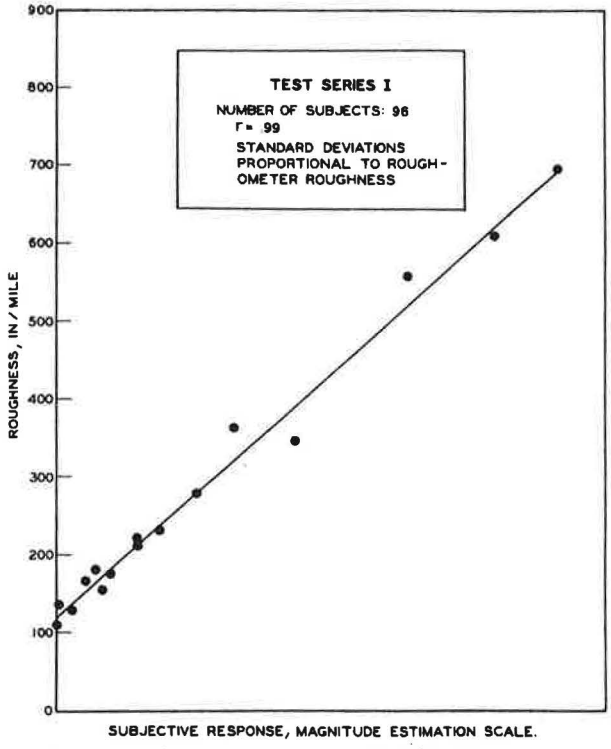

Figure 8. Relationship between roughometer roughness and subjective response as measured by magnitude estimation methods.

This result is contrary to that obtained with linear or category scaling (compare Eq. 4). Although not discussed here, it can be shown that Eq. 1 can reproduce Eq. 7 when the subjective response standard deviations are set equal to the roughness values, i. e.,

$$\sigma_i = R_i \tag{8}$$

Thus, when roughness figures are substituted in Eq. 1, the resulting scale turns out to be of the form S = R (rather than S = log R) as found by ratio scaling. The correlation of this subjective response scale with roughness is shown in Figure 8 and should be compared to the correlation with log roughness shown in Figure 6.

Analog processing of RTP data provided sufficiently filtered profiles to permit computation of power spectral density plots (amplitude variance spectrum). Spectra for each wheel-track profile and its first three derivatives were computed from automatically digitized RTP data. Generally, the two wheel tracks for each road were similar, with the high-frequency amplitude variance always somewhat greater for the outside wheel track.

Wheel-track spectra were averaged and plotted with wavelength (λ) on log-log coordinates as shown in Figure 9. As is generally known, these plots are well approximated by a straight line; hence,

$$AVD = C\lambda^x \tag{9}$$

where AVD is amplitude variance density (power), and C is a constant reflecting the general variance density level (probably the best overall parametric correlate of subjective response). Correlations of AVD parameters with subjective response are C = -0.88, x = 0.54, and multiple of C and x = 0.89. The exponent x, ranging from about 1.5 to 2.5, is essentially unrelated to subjective response. Linear correlations of log AVD

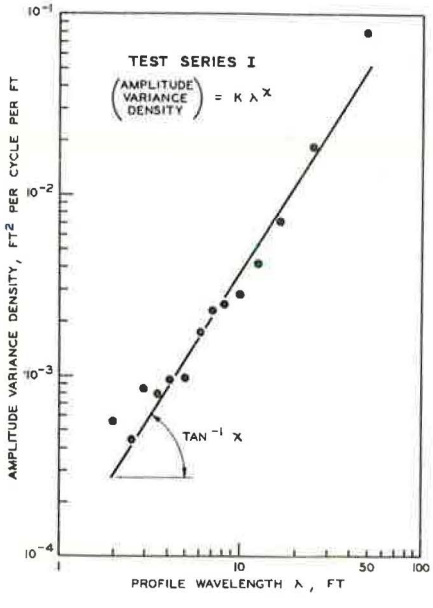

Figure 9. Relationship between profile variance and wavelength.

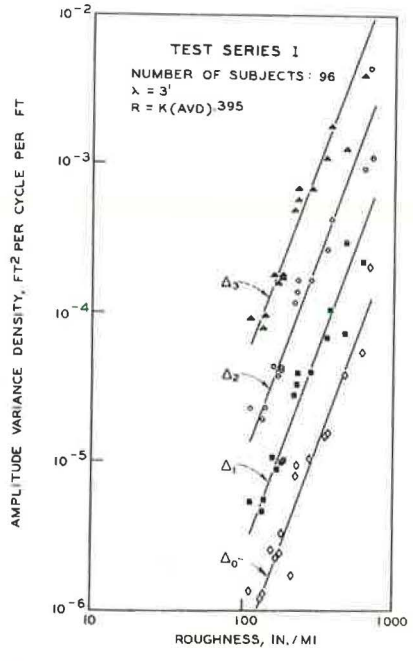

Figure 10. Relationship between profile derivative variance and roughness.

and log λ averaged 0.98 for the 16 roads of Test Series I. Total amplitude variance (within the limits of measurement) of the profile or its derivatives is often used as a ride indicator (1, 5, 9). However, this method ignores the unequal variance contributions of wavelength intervals to subjective response and is therefore an imperfect indicator. Because roughometer measurements correlate well with subjective response (r = 0.98), this instrument can be used to select the wavelengths best relating to ride.

Correlations between roughometer measurements and AVD were poor for low frequencies (1 to 5 cps) and improved to a maximum (r = 0.99) for the 18 to 36 cps range. Because this frequency range (for the vehicle speeds used, 25 to 60 mph) results from a very narrow band of road wavelengths, it was possible to simplify the analysis by relating subjective response directly to the profile.

Figure 10 shows the correlations of the variance contributions of the 3-ft wavelengths for the profile and its first three derivatives with roughometer figures. The lines are parallel and separated roughly by a multiplier of four. Successive differentiation of $(\sin \omega t)^2$ indicates that they should be in the ratio 1 : 3 : 9 : 27 because λ = 3. Moreover, the slopes show the general equation relating amplitude variance to roughness (in./mi) to be

$$R = K\,(AVD)^{0.395} \tag{10}$$

where K depends on the derivative order. The exponent of 0.395 compares with 0.365 given elsewhere (21). At λ = 3, correlations are all high, but this is not true for the greater wavelengths. Figure 11 shows that the fall-off of correlation with subjective response is greatest for the third derivative and least for the first derivative. As far as total variance is concerned, it appears that the slope profile is best suited for ride predictions. However, the best correlations are obtained with the very short wavelengths for all derivatives. There seems to be little point in measuring variance contributions from wavelengths much above approximately 5 ft as far as ride research is concerned.

If graphic or category rating scales are used to measure subjective response, we find (Fig. 12) by substituting Eq. 10 in Eq. 4 that

$$S = K \log (AVD) \tag{11}$$

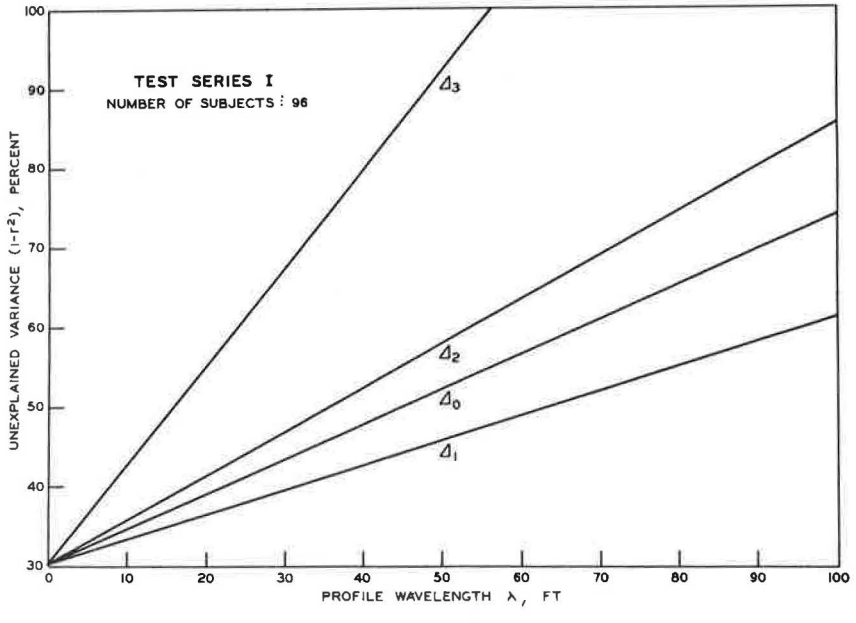

Figure 11. Relationship between profile wavelength and predictability of subjective response.

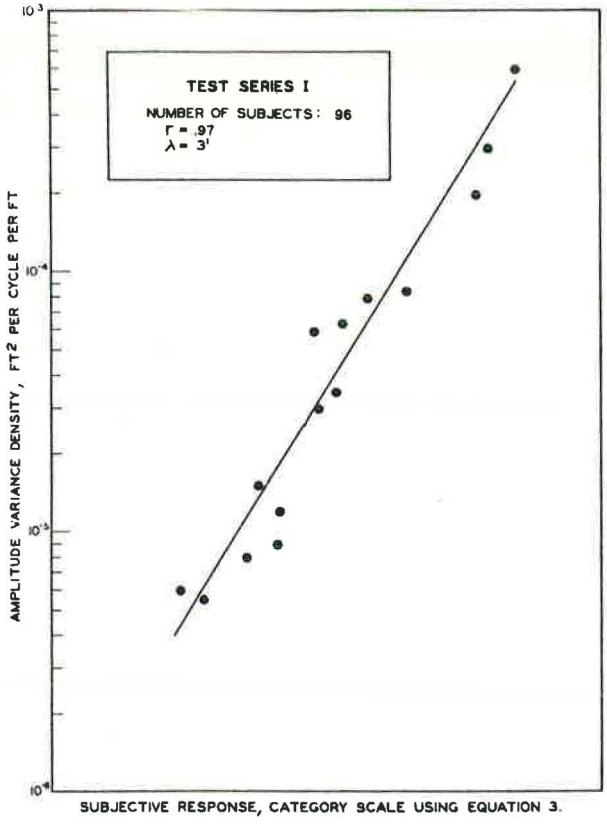

Figure 12. Relationship between profile variance and category scale subjective response.

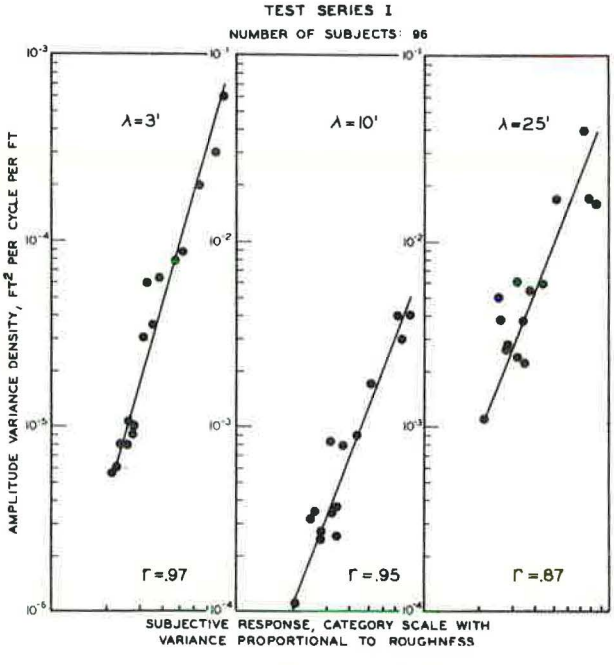

Figure 13. Relationship between amplitude variance and subjective response as measured by magnitude estimation methods.

The log transform of slope variance (of unpublished wavelength composition) appears in the PSI equations and can be expected to appear in any ride or serviceability experiment where category scaling is used. Serviceability is properly introduced into this discussion because it is so highly correlated with roughness (9). When magnitude scaling is used (or category scaling is accomplished with Eq. 1 utilizing the dispersion relationship $\sigma = R$), the results agree with Eq. 7 (i.e., S = R) because $R = K(AVD)^X$ and $S = K(AVD)^X$ (Fig. 13).

At this point the possible reasons for the different functional forms obtained by the two scaling methods will be discussed. Suppose that subjects find it easy to discriminate small roughness differences at the smooth end of the scale and difficult at the rough end. The effect on the category scale will be as follows. At the smooth end where discrimination is best, a large portion of the scale will be used to reflect small but perceivable differences in roughness, whereas at the rough end where discrimination is poorest, the same small roughness differences are less easily detected and will tend to be lumped into a single category or confined to a small scale range. For example, the difference between 100 and 200 in. per mile is easily detected and would, therefore, show up as a sizable scale separation consistently reported. However, the difference between 600 and 700 in. per mile, although arithmetically the same, is more difficult to detect and consequently will show up as a small scale difference not consistently reported (Fig. 14). In addition, if many subjects are used and their judgments combined into a single average for each road, disagreement and hence variance differences may result from differential sensitivity to frequency. For example, subjects might respond similarly to low-frequency vibrations, but differently to high frequencies. The result would be good agreement at one end of the scale and poor agreement at the other. If one of these conditions exists, the resulting category scale will probably not be a linear transform of a scale based on direct estimates of psychological magnitude utilizing ratios. This is because the magnitude methods produce scales whose mathematical properties are free of the effects of subjective response variance.

Because the level of inter- and intra-subjective response agreement determines the disparity between the magnitude and category scales, one can theoretically produce an infinity of category scale transforms by merely controlling the background factors that affect subjective response agreement. For example because one person is usually more consistent than several, a category scale produced from replicated judgments of a single individual would probably not be linearly related to a scale produced from the combined judgments of a group. Consequently, the exact mathematical form of the relationship between subjective response as measured on category scales and physical input may depend on experimental conditions and technology. Should changes in experimental conditions or improvements in technology alter the functional relationship between response agreement and input level, laws depending on the affected variables would have to be updated accordingly. This defines the first disadvantage of measuring subjective response to roughness with category scaling methods.

The second disadvantage of category scales is that measurements based on them will not confirm laws utilizing magnitude scales. The problem is especially acute for laws derived from intuitive formulations. These formulations generally involve variables that are traditionally measured on magnitude scales. To be sure, a logically coherent system of laws based on either scaling system could be evolved; however, those based on category scale measurements would not benefit from intuitions growing out of everyday experience with the magnitude scales.

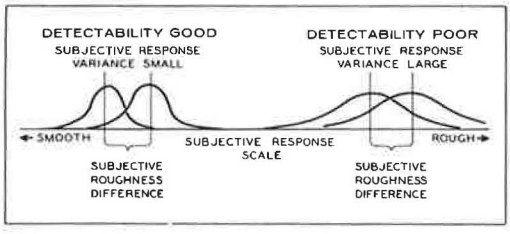

Figure 14. Hypothetical relationship between subjective response variability and response level.

A third disadvantage could occur if, with the use of a group of subjects in a ride experiment, several proved more tolerant of increased amplitudes at all frequencies. This might be due to the ride

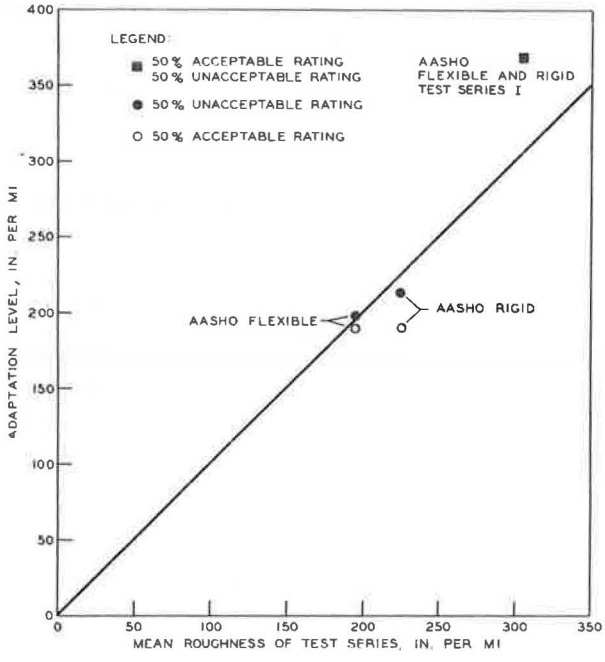

Figure 15. Relationship between adaptation level and test series average.

experience the subject brings with him to the experiment. Thus, if a subject is familiar with only very smooth Interstate roads, he will tend to "down-rate" the rougher roads more than a subject who has encountered the latter in his daily experience. On the other hand, a subject habitually adapted to very rough gravel or secondary roads will necessarily view all primary and Interstate Highways as superior. The full range of test responses for this subject would show a bias toward the high or smooth end of the scale. In addition, experience with the test series of the experiment itself probably affects the distribution of subjective responses as well as their general location bias or "adaptation level" (22, 23, 24, 25, 26, 27, 28).

Adaptation level is defined as a neutral point from which psychological judgments are made, and is defined as the midpoint of the category scale. It has been suggested that as far as a test series is concerned, this point corresponds to the geometric average on the physical scale of all the rated or judged objects in the experiment. Accordingly, the psychological neutral point will follow the mean of the series, which, of course, is a function of the roads selected for test. In ride research one prefers that the psychological neutral point that is marked by the difference between, say, "acceptable" and "unacceptable" be independent of the experimenter's choice of test roads (Fig. 15). It has been argued that the category scaling methods are particularly sensitive to these adaptation level problems.

In the writer's opinion, some magnitude estimation methods are relatively free of adaptation level effects, for it is reasonable to assume that a subject can decide on the ratio of riding quality of two roads without bias caused by other roads in the series.

CONCLUSIONS

1. When measurements of human subjective response to ride were made on category scales (with subjects choosing from categories provided), very little difference was detected between category scale types, automobiles, or perceptual conditions produced by various degrees of sight and hearing restrictions. Not only did subjects rank the test roads about the same for each test condition, but they closely agreed among themselves within each condition. These results are probably due to adaptation level problems often found with category scaling methods.
2. When human subjective response to ride is measured by means of category rating scales, the relationship between subjective response and profile parameters is of the form (Subjective Response) = log (Physical Input). Physical input can be measured by roughometer roughness or the amplitude variance density of any of the commonly used profile derivatives.
3. When human subjective response to ride is measured by means of magnitude estimation methods (subjects reporting ride ratios), the relationship between subjective response and roughometer roughness is of the form (Subjective Response) = (Roughness).

For profile amplitude variance densities, the relationship becomes (Subjective Response) = K (Amplitude Variance Density)^X where K depends on profile derivative order, and x is about 0.4. Slightly better correlation with subjective response is obtained when a small variance band is used rather than the density ordinate at a specific wavelength.

4. The equations predicting ride from physical input by means of magnitude estimation scaling are to be preferred because (a) they give results that are independent of subjective disagreement or error variance; (b) theoretical formulations are generally based on variables measured on magnitude scales; and (c) there is reason to think that magnitude estimation procedures can be administered without adaptation level problems.
5. Profile derivatives (slopes, acceleration, jerk) do not appear to offer any advantage in predicting subjective response over the profile itself. Variance contributions of higher order derivatives tend to become unstable and correlate poorly with subjective response as profile wavelength increases.
6. The best correlations of subjective response with profile variance is obtained for the profile wavelength region under about 5 ft. Little, if any, improvement is obtained from the inclusion of wavelengths greater than this figure.
7. Prediction of subjective response was not significantly improved by utilizing vehicle speed data in a time-frequency analysis. Good results can be obtained from an examination of the road profile alone provided the test vehicle speed range is not large.

ACKNOWLEDGMENTS

I would like to thank the following people for their cooperation in the research program: Mr. Paul Milliman, field measurement and data analysis; Mr. Eric Fisher, computer programming; and Dr. Terry Allen, review of the text.

The opinions, findings, and conclusions expressed in this publication are the author's and not necessarily those of the Bureau of Public Roads.

REFERENCES

1. The AASHO Road Test: History and Description of Project. HRB Spec. Rept. 61A, 1961.
2. Hutchinson, B. G. A Measure of Pavement Unserviceability. Report No. 105, Department of Highways, Ontario, 1965.
3. Hutchinson, B. G. Principles of Subjective Rating Scale Construction. Highway Research Record 46, pp. 60-70, 1964.
4. Darlington, J. R., and Milliman, P. A Progress Report on the Evaluation and Application Study of the General Motors Rapid Travel Road Profilometer. Highway Research Record 214, pp. 50-67, 1968.
5. Hutchinson, B. G. Analysis of Road Roughness Records by Power Spectral Density Techniques. Report No. 101, Department of Highways, Ontario, 1965.
6. Quinn, B. E., and Hagen, K. Problems Encountered in Using Elevation Power Spectra as Criteria of Pavement Condition. Highway Research Record 189, pp. 166-181, 1967.
7. Carey, W. N., Jr., and Irick, P. E. The Pavement Serviceability-Performance Concept. HRB Bull. 250, pp. 40-58, 1960.
8. Manual on Pavement Investigations. Canadian Good Roads Association Tech. Publ. No. 11, 1959.
9. Yoder, E. J., and Milhous, R. T. Comparison of Different Methods of Measuring Pavement Condition—Interim Report. NCHRP Rept. 7, 1965.
10. Versace, J. Measurement of Ride Comfort. Society of Automotive Engineers Publ. 638A, 1963.
11. Guilford, J. P. Psychometric Methods. McGraw-Hill, 1954.
12. Thurstone, L. L. Psychophysical Analysis. Amer. Jour. Psychology, Vol. 38, pp. 368-389, 1927.
13. Thurstone, L. L. A Law of Comparative Judgement. Psychological Review, Vol. 34, pp. 273-286, 1927.
14. Luce, D. On the Possible Psychophysical Laws. Psychological Review, Vol. 66, pp. 81-95, 1959.

15. Stevens, S. S., and Galanter, E. H. Ratio Scales and Category Scales for a Dozen Perceptual Continua. Jour. Experimental Psychology, Vol. 54, No. 6, pp. 377-409, 1967.
16. Comrey, A. L. A Proposed Method for Absolute Ratio Scaling. Psychometrika, Vol. 15, pp. 317-325, 1950.
17. Torgerson, W. S. Theory and Methods of Scaling. John Wiley and Sons, 1967.
18. Stevens, S. S. Ratio Scales, Partition Scales and Confusion Scales. In Psychological Scaling (Gulliksen and Messick, eds.), John Wiley and Sons, pp. 49-66, 1960.
19. Stevens, S. S. The Surprising Simplicity of Sensory Metrics. American Psychologist, Vol. 17, No. 1, pp. 29-39, 1962.
20. Stevens, S. S. The Direct Estimation of Sensory Magnitude-Loudness. Amer. Jour. Psychology, Vol. 69, pp. 1-25, 1956.
21. Hudson, W. R. Special Report, The AASHO Road Test, 1961.
22. Volkman, J., Hunt, W. A., and McGourty, M. Variability of Judgement as a Function of Stimulus Density. Amer. Jour. Psychology, Vol. 53, pp. 277-284, 1940.
23. Rogers, S. The Frame of Reference. Archives of Psychology, Vol. 37, No. 261, Part I, pp. 5-12, 1941.
24. Helson, H. Adaption-Level as a Basis for a Quantitative Theory of Frames of Reference. Psychological Review, Vol. 55, pp. 297-312, 1948.
25. Philip, B. R. The Frame of Reference Concept. Canadian Jour. Psychology, Vol. 3, No. 2, pp. 73-79, 1949.
26. Tresselt, M. E. The Effect of the Experiences of Contrasted Groups Upon the Formulation of a New Scale of Judgment. Jour. Social Psychology, Vol. 27, pp. 209-216, 1948.
27. Sherif, M., and Cantril, H. The Psychology of "Attitudes". Psychological Review, Vol. 53, pp. 1-20, 1946.
28. Helson, H. Adaptation Level Theory. Harper and Row, 1964.

A Comparison of Four Roughness Measuring Systems

M. B. PHILLIPS and GILBERT SWIFT, Texas Transportation Institute, Texas A&M University

•FOUR different measuring devices for use in evaluating highway surface roughness were investigated in this study. Two, the CHLOE profilometer (1) and the Bureau of Public Roads roughometer (2) with mechanical integrator (newer BPR roughometers are equipped with an electronic integrator), are well known and have been compared previously (3). The others, the Portland Cement Association roadmeter (4) and the Mays Road Meter (patent applied for by Ivan K. Mays), are recent developments that warrant some description, especially the latter, because no description has previously appeared in the literature.

The aims of our study of these instruments were (a) to examine the field-worthiness of the several systems; (b) to determine the validity of their respective measurements; and (c) to determine the effects on their results of such variables as operating speed, driver characteristics, operating temperatures, and other factors.

In conducting the tests and interpreting the results, we have adopted a viewpoint that should be explained. We regard all of these instruments as expedient tools that measure, possibly quite imperfectly, one or another aspect of the interaction between a complex, irregular surface and an incompletely specified vehicle that traverses it. However, as imperfect as all may be, each may be employed usefully within its recognized limitations. It is our intent to provide comparative information within this framework whereby, through a better understanding of the various instruments, a user or potential user may be aided in selecting the one best suited to his needs.

The following abbreviations will be used in this report:

1. MAYS 40—Mays Road Meter roughness index (inches per mile) determined at 40 mph.
2. MAYS 50—Mays Road Meter roughness index (inches per mile) determined at 50 mph.
3. PCA 40—Portland Cement Association roadmeter roughness index determined at 40 mph.
4. PCA 50—Portland Cement Association roadmeter roughness index determined at 50 mph.
5. BPR—Bureau of Public Roads roughometer roughness index (inches per mile) determined at 20 mph.
6. CHLOE—Slope variance determined by the CHLOE profilometer at 3 mph.

EXPERIMENT

The road sections used in this evaluation were located in the Texas Highway Department's District 12. This district is located geographically on the east central Gulf Coast. The sections were divided into two groups, 24 sections that comprised the main experiment on which all four instruments were run, and 21 additional sections on which only the Mays Road Meter and the Portland Cement Association roadmeter were run. The sections had an average length of 0.155 miles. The sections in the main experiment were representative of the types of pavement surface found in Texas; there were 14 flexible pavement sections (8 asphaltic concrete and 6 with sur-

Paper sponsored by Committee on Surface Properties—Vehicle Interactions.

Figure 1. The Mays Road Meter installed in trunk compartment of automobile. Note the three cables leading to the left. The top cable is connected to the differential housing; the center cable leads to the front seat and is the on-off control; and the lower cable, which also leads to the front seat, is the event marker control.

face treatment), 7 concrete sections, and 3 concrete sections that had been overlaid with asphaltic concrete. The additional 21-section group had a similar distribution between concrete and flexible surfaces.

The data were taken during the summer of 1968. Replicate measurements were made approximately one week apart. The CHLOE profilometer and the BPR roughometer were operated independently of the Mays Road Meter and the PCA roadmeter. The Mays Road Meter (Fig. 1) and the PCA roadmeter (Fig. 2) were installed in the same vehicle, a 1967 Ford sedan with 20,000 miles of use. It is recommended that only vehicles with coil springs in the rear be used. The controls of the two instruments were situated so that it was possible to operate then simultaneously. Time limitations did not permit investigation of the effect of different vehicles on these instruments.

A 14-member panel, comprised of Texas Highway Department engineers, personnel from the Center for Highway Research, University of Texas, and nontechnical personnel rated the 24 sections in accordance with established procedures. The average of their ratings for each section was used in this report. Their examination of the sections was conducted during July 1968.

The effect of different operators and the effect of varying operating speeds on the Mays Road Meter measurements were also investigated. Three sections near College Station, Texas, each 1 mile in length, were run at speeds of 30, 40, 50, 60, and 70 mph with two operators, each making two runs through the section at each speed. Data taken on these tests indicated that there was negligible effect from changing operators, but that the higher operating speeds (60 and 70 mph) led to increased replication errors, whereas 30 mph was too slow for operation in freeway traffic. Therefore, the two speeds used in the remaining tests were 40 and 50 mph. The slower speed (40 mph) was found to offer more precision with the Mays Meter, but the degree of impairment (as indicated in Table 1) does not prohibit use of this instrument at the higher speed (50 mph).

Early morning and late afternoon runs were made on successive days on a single flexible section for a period of 5 days using the Mays Road Meter and the PCA roadmeter with the object of determining the extent to which temperature influenced these

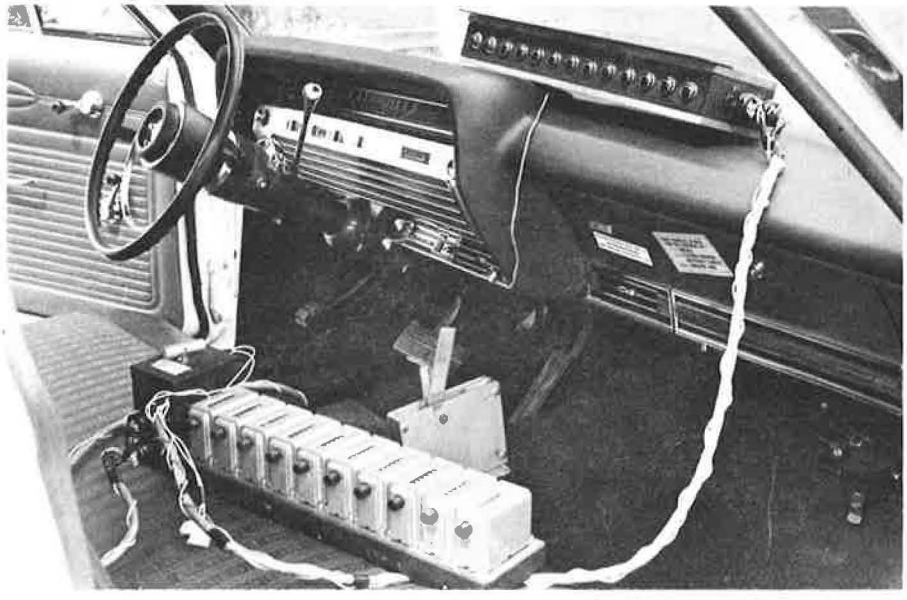

Figure 2. View of the front seat of an automobile showing both the counters and indicator-light panel of the PCA roadmeter and the two controls of the Mays Road Meter (two levers at center of photograph).

instruments. The average temperatures for these runs were 70 F in the morning and 89 F in the afternoon. The effect on the Mays Road Meter appeared to lie within the normal replication error associated with this instrument, whereas the effect on the PCA roadmeter was an unexplained 15 percent increase in its roughness index with the 19 F increase in temperature.

Six sections on a smooth textured road near Llano, Texas, were used to determine how much the Mays Road Meter output was influenced by the texture of the road surface. Four runs were made on each of these sections just prior to resurfacing with a surface treatment, and four runs were again made on each of these sections one week after the new surface was completed. The aggregate used in the treatment had a maximum size of $^3/_8$ in. and a mean size of $^1/_4$ in. On the average, it was found that this surface change increased the Mays Road Meter readings by 10 percent. We believe the increase results from the texture rather than from any decrease in overall smoothness of these sections.

MAYS ROAD METER AND PORTLAND CEMENT ASSOCIATION ROADMETER DESCRIPTION

Both the Portland Cement Association roadmeter and Mays Road Meter systems have been developed with the objective of providing a simple, low-cost instrument for installation in a passenger vehicle and capable of producing a reading acceptably representative of the surface roughness encountered while traversing highway sections at normal vehicle speeds. In one respect these two systems are alike. They both employ the vehicle chassis as their "reference plane", and respond to the variations of vertical distance between the chassis and the rear axle (differential housing) of the car. Because the Mays Road Meter is basically more similar to the familiar Bureau of Public Roads roughometer, it will be described first. A flexible wire cable attached to the differential housing extends vertically upward through a small hole made in the floor of the trunk compartment. Passing over a fixed pulley, this cable is brought

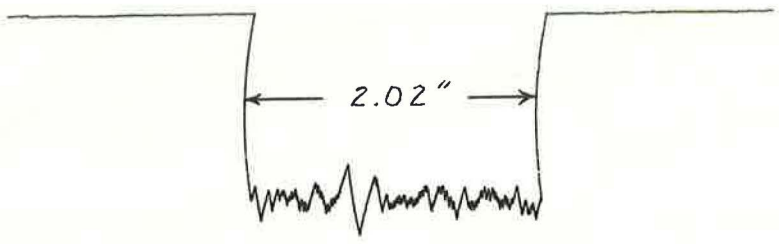

Figure 3. Typical chart produced by the Mays Road Meter on a 0.2-mile section of flexible pavement. The distance between beginning mark and end mark, 2.02 in., when multiplied by 8 and divided by section length, gives a roughness index of 80.8 in. per mile.

horizontally to the instrument where it wraps around a 7.5-in. diameter wheel and continues to an anchored tension spring. Accordingly, relative vertical motion between chassis and axle produces proportional rotation of this wheel; in one direction for upward axle movement, in the other direction for downward movement. The resulting reciprocating motion is linked mechanically to a pen that produces a continuous record on adding machine tape. The same motion, but applied through a nonreversing clutch, is employed to advance the tape. The result is a graphic record on which the magnitude of the individual vertical excursions of the axle relative to the chassis are depicted as proportional excursions of the trace, whereas the length of the record represents the sum of all the upward movements of the axle that have occurred. A marking device controlled by the operator permits the beginning and end of each section to be indicated on the record. Figure 3 shows a typical example of the Mays Road Meter presentation.

The indicated roughness is obtained by measuring the length of the Mays Road Meter record in inches and multiplying by an appropriate constant. This constant is a function simply of the paper drive mechanism and the length of the section. The resulting roughness index is expressed in units of inches per mile, representing the total of the

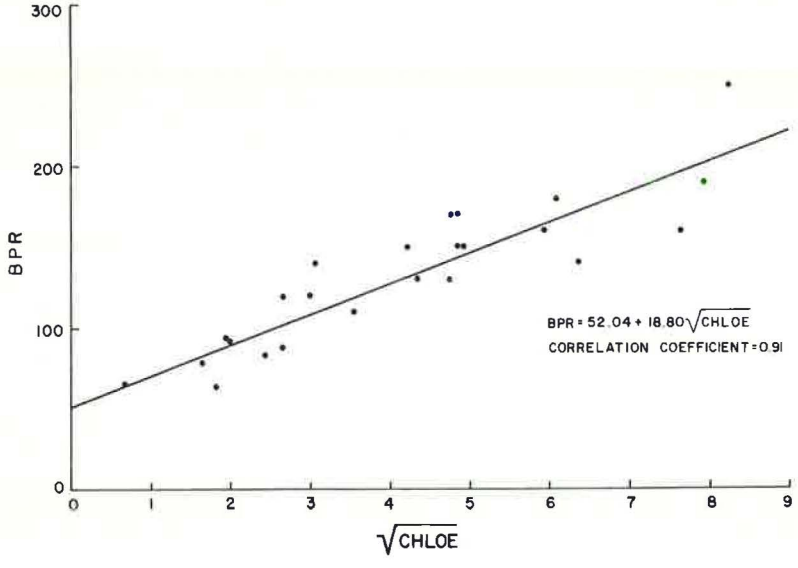

Figure 4. Correlation between square root of CHLOE output and BPR roughometer output.

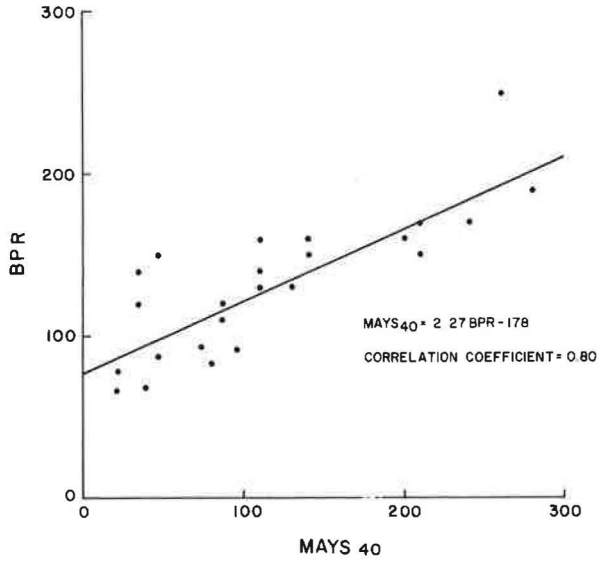

Figure 5. Correlation between Mays Road Meter run at 40 mph and BPR roughometer.

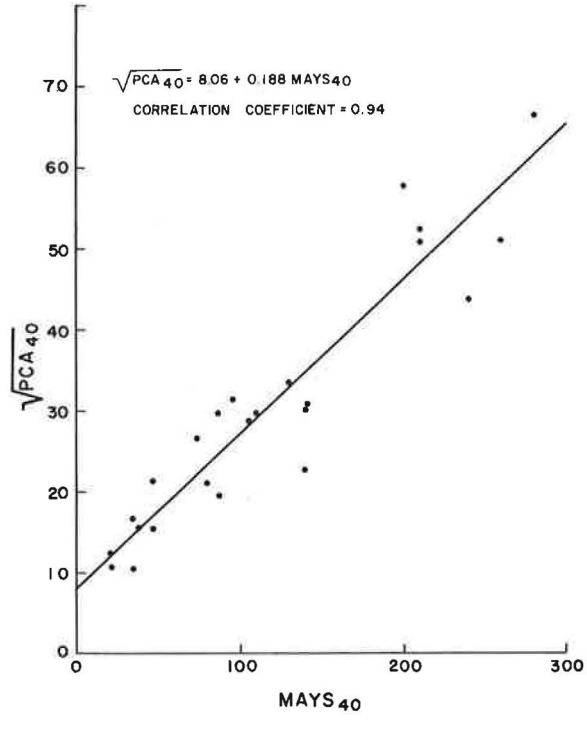

Figure 6. Correlation between Mays Road Meter and PCA roadmeter, both run at 40 mph.

upward excursions (which is necessarily almost exactly half of all the vertical excursions) divided by the distance traveled. The basic similarity of this system to the BPR roughometer will be apparent. However, the additional feature of a pen trace that depicts the magnitude of the separate excursions, coupled with the simplicity of adding only a small recording device inside the car, instead of a trailer, makes it an attractive alternative system.

Likewise, the PCA roadmeter comprises a simple set of components added to a passenger vehicle. Its cable from the rear axle is attached to a switch or commutator so arranged that each successive $\frac{1}{8}$-in. departure from a preselected "zero" or midposition results in energizing a different contact of the switch. A series of electromagnetic counters registers the number of times that the moving arm encounters each particular contact. Thus, in the course of driving over a given section, contacts near the midposition will generally be reached frequently and those farther away will be seldom encountered, because there are ordinarily many small surface irregularities and only a few large ones. Accordingly, at the end of any traverse, the several counters indicate the number of times their respective contacts have been energized. The indication of surface roughness is obtained by multiplying the readings of the individual counters each by an appropriate constant, then summing the resulting numbers. It has been demonstrated (4) that this procedure, which gives greater weight to the larger excursions in proportion to their magnitudes, has a "square law" effect that renders the measurement closely akin to slope variance, the quantity derived by the CHLOE profilometer. The summed PCA roadmeter count (divided by 64 times the section length) represents a measure of roughness in inches-squared per mile of section traversed.

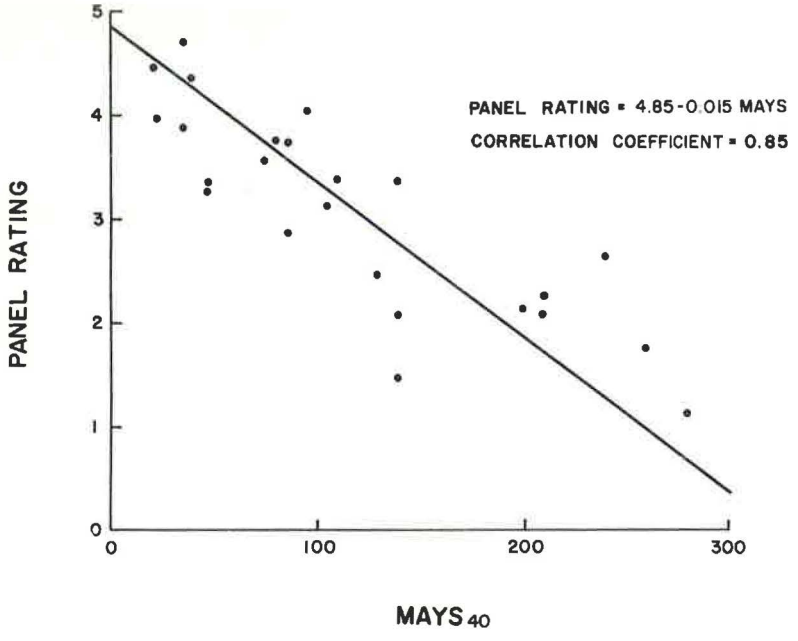

Figure 7. Correlation between Mays Road Meter run at 40 mph and panel ratings.

RESULTS

The correlations shown in Figures 4, 5, and 6 demonstrate that each of the four instruments responds to much the same properties of the surface. As we expected, linear correlations were obtained among the measurements of all the instruments when comparing the square root of the indicated slope variance against the direct readings of the "linear" instruments. Figure 4 indicates that a fixed offset of 52 units per mile exists in the data from the BPR roughometer. This we ascribe to tire or axle eccentricity in the particular instrument we used that introduced an effective motion of the order of 0.07 in. at each revolution of its wheel. A similar effect, on the order of 0.02 in., may exist in the vehicle in which we installed the PCA and Mays devices.

Because all the instruments appear to measure substantially the same thing, the question naturally arises as to which instrument does the best job. If panel ratings could be accepted as being perfect, the most precise instrument would be the one exhibiting the greatest correlation with these ratings. More realistically, however, the panel ratings must be subject to variation, and thus the best correlation may merely

TABLE 1

ANALYSES OF VARIANCE AND CORRELATION COEFFICIENTS

Instrument	Variable Analyzed	F-Ratio		Correlation Coefficient With Panel Ratings, 24 Sections
		24 Sections	45 Sections	
CHLOE profilometer (3 mph)	Square root of slope variance	416.7	—	0.80
Mays Road Meter (40 mph)	Roughness index	192.2	172.2	0.85
Mays Road Meter (50 mph)	Roughness index	82.4	100.0	0.82
PCA roadmeter (40 mph)	Roughness index	61.1	52.5	0.80
BPR roughometer (20 mph)	Roughness index	59.0	—	0.77
PCA roadmeter (50 mph)	Roughness index	27.5	28.9	0.71

indicate which particular instrument exhibits variations most similar to those of the panel. Accordingly, an independent check on instrument precision is very desirable.

A method (5) that can be used to rank each of the instruments in the order of its relative precision consists of comparing the variability of its measurements between sets with the variability of its measurements within sets. Here we use the word "set" to mean a pair of measurements one week apart on the same road section. If the variability between sets is large compared with the variability within sets, it can be said that the instrument is sensitive and precise, and the greater the ratio of these variabilities the greater its relative precision. The ratio of the between-set to the within-set variability is known as the F-ratio.

Because the F-ratio depends on the variabilities between and within sets—which, in turn, depend principally on the physical differences between sections, and principally on the instrument-operator-procedure within sections—it follows that a group of instruments can be ranked with complete fairness by their F-ratios, provided all instruments were used on the same group of sections and all were operated in a consistent manner at nearly the same time of day, and, further, provided linear correlations exist between the data-sets representing each of the instruments. It can be seen from Table 1 and Figures 4, 5, and 6 that these criteria of fairness are satisfied for the four instruments. From the fact that the CHLOE profilometer exhibits the largest F-ratio, whereas the Mays Road Meter (Table 1 and Fig. 7) exhibits the largest correlation coefficient with respect to panel ratings, we conclude that the precision of the CHLOE profilometer is greatest among the four instruments, but that the Mays Road Meter has characteristics that systematically follow departures of the panel from agreement with the CHLOE profilometer. From the reported standard deviations associated with the panel ratings, which averaged 0.66 PSR units, we also conclude that the panel ratings do not constitute a superior set of roughness measurements. In fact, they may, quite possibly, be inferior in this respect to the measurements provided by several of the instruments. However, it is recognized that panel ratings do not depend exclusively on surface roughness. Hence their validity and general utility are not necessarily lessened by failure to correlate with a precise roughness instrument.

To confirm the relative ranking of the Mays Road Meter and PCA roadmeter, their respective F-ratios were determined from a larger number of tests comprising 45 sections. As shown in Table 1, the ranking was unchanged from that derived from the 24 section tests.

CONCLUSIONS

Although the CHLOE profilometer is best with respect to F-ratio, it is not necessarily the optimum choice for all applications. It is desirable in making a choice among instruments to consider numerous additional factors. These include initial cost, operating and maintenance costs, convenience and speed of operation, plus other less tangible factors such as the output data format and its compatability with the user's mental or physical data reduction scheme. Accordingly, each instrument, but most particularly the second most precise one, the Mays Road Meter, warrants careful consideration.

The Mays Road Meter offers several attractive advantages that for many users may more than offset its slightly diminished precision. Specifically, it can be obtained and installed for less than $750. It utilizes an ordinary sedan without trailer. Simple in operation, low in maintenance, it measures while traveling at 40 or 50 mph. In comparison, the CHLOE profilometer may be characterized as precise, but complex, costly, very slow, and, in the experience of these writers, difficult to maintain in operating condition. The BPR roughometer requires a trailer, is somewhat costly, and operates at intermediate speed. The PCA roadmeter matches the Mays Road Meter closely in several basic respects and would provide an attractive alternative if its precision were improved.

It should be understood that different makes and models of cars have different dynamic characteristics. This, coupled with the fact that there may be constructional differences among several Mays Meters and among several PCA roadmeters, presently

TABLE 2

COMPARISON OF ROAD ROUGHNESS DEVICES

Description	CHLOE Profilometer	BPR Roughometer	PCA Roadmeter	Mays Road Meter
1. Apparatus	Trailer and car	Trailer and car	Car only	Car only
2. Basic response	Slope	Height	Height	Height
3. Proportionality	Square-law	Linear	Square-law	Linear
4. Accepted designation of measurement	Slope-variance	Roughness	$\Sigma (D^2)$, sum of road-car deviations squared	Roughness index
5. Speed while measuring	3 to 5 mph	20 mph	40 or 50 mph	40 or 50 mph
6. Speed while traveling to and from sections	Legal limit	Legal limit	Legal limit	Legal limit
7. In-field set-up time	15 minutes	5 minutes	1 minute	None
8. In-field set-up requirements	Unload CHLOE from transport trailer, hook up cables, calibrate	Lower wheel; hook up roughness integrator and counters	Stop vehicle to set to zero	None
9. Maximum section length	Less than 0.5 mile	Limited only by roughness exceeding counter capacity	Limited only by roughness exceeding counter capacity	Unlimited
10. Minimum section length	Not recommended for less than 0.1 mile	Not recommended for less than 0.1 mile	Not recommended for less than 0.1 mile	Not recommended for less than 0.1 mile
11. Data presentation form	Number of 6-in. units traversed, counts and counts squared	Single numerical counter	Plurality of numerical counters	Length of chart record
12. Location of presentation	Adjacent to driver	Adjacent to driver	Adjacent to driver	Adjacent to driver or in trunk
13. Determination of section length	Counter	Counter	Car odometer or roadside marker	Car odometer or roadside marker
14. In-field data requirements (when measuring sections of known lengths	Record three readings	One reading at end of each section	Eight counter readings at end of each section and reset counters	Merely keep track of the sequence in which the sections are traversed
15. In-field adjustments	None required	Frequent check of dash pot fluid level	Frequent zero adjustment recommended—requires vehicle halt	None required
16. At-home data processing to determine roughness	Calculating $\sqrt{\overline{SV}}$ from three readings	Tabulating (may be done in-field)	Summing and tabulating	Measuring chart lengths and tabulating
17. Additional data obtainable from record	None	None	Frequency distribution of roughness heights	Approximate location and heights of roughness within sections
18. Maintenance requirements	Frequent malfunction requiring repairs	Frequent servicing of grease fittings and dash pots	Frequent polishing of commutator to ensure contact	Minimal

necessitates that each unit (vehicle with its Mays Road Meters and/or PCA roadmeter) be correlated with a known unit on a group of sections that have been rated by a panel. Further study may reveal that these differences among units are not of significant magnitude to require extensive correlation effort.

In Table 2 we have endeavored to provide a means for choosing among these four instruments. The potential user may give weight to the various factors in the chart in accordance with his specific needs. Thus different users may arrive at different choices, but we consider the CHLOE profilometer applicable where precision is paramount and the Mays Road Meter most appropriate for general field use.

ACKNOWLEDGMENTS

The authors are deeply grateful to Mr. Ivan K. Mays, Texas Highway Department, Austin, who developed the Mays Road Meter, for furnishing this instrument and valuable knowledge about its operating characteristics. The authors are also indebted to Mr. Phillip Brua of the Portland Cement Association for his assistance in the construction of the Portland Cement Association roadmeter.

Special thanks go to Dr. W. Ronald Hudson and Mr. Freddy Roberts of the Center for Highway Research in Austin, who selected the test sections and provided panel ratings obtained in their Project 73, and to Mr. Janes Bissett of District 12, Texas Highway Department, who provided traffic protection to the field crews. The data were furnished to this study at no cost.

REFERENCES

1. Carey, W. N., Jr., Huckins, H. C., and Leathers, R. C. Slope Variance as a Measure of Roughness and the CHLOE Profilometer. HRB Spec. Rept. 73, pp. 126-137, 1962.
2. Buchanan, J. A., and Catudal, A. L. Standardizable Equipment for Evaluation of Road Surface Roughness. HRB Proc., Vol. 20, pp. 621-638, 1940.
3. Yoder, Eldon J., and Milhous, R. T. Comparison of Different Methods of Measuring Pavement Condition—Interim Report. NCHRP Rept. 7, 1964.
4. Brokaw, M. P. Development of the PCA Road Meter: A Rapid Method for Measuring Slope Variance. Highway Research Record 189, pp. 137-149, 1967.
5. Scrivner, F. H., Poehl, Rudell, Moore, William M., and Phillips, M. B. Detecting Seasonal Changes in Load-Carrying Capabilities of Flexible Pavements. NCHRP Project 1-5(2) (in press).